THE UNIVERSITY OF LIVERPOOL

BI 6727 and Gemcitabine Combination Therapy in Pancreatic Cancer

Thesis submitted in accordance with the requirements of the University of Liverpool for the degree of Doctor of Medicine by

Owain Peris Jones

Summer 2017

Student ID: 200005147

THE UNIVERSITY OF LIVERPOOL

Declaration

I declare that this thesis and the research upon which it is based is the result of my own work. Wherever I have incorporated the work of others, it has been clearly stated.

This work has not been submitted in any substance for any degree, nor is it concurrently being submitted in candidature for this or any other University.

Part of this work has been published in:

Jones OP, Melling JD, Ghaneh P, Adjuvant Therapy in Pancreatic Cancer. World J Gastroenterol. 2014; 20(40): 14733-14746

THE UNIVERSITY OF LIVERPOOL

Acknowledgements

I would like to thank my supervisors, Dr. Bill Greenhalf and Professor Paula Ghaneh for the guidance they have shown me during my time with the School of Cancer Studies at the University of Liverpool. Their input was essential for the completion of this work. Throughout my period of research, I worked alongside many valued colleagues, whose patience and assistance introduced and familiarised me with the alien environment of the research laboratory. In addition to the teaching of laboratory techniques, I would like to acknowledge the multiple members of Dr Greenhalf's and Dr. Eithne Costello's groups for their invaluable peer review at weekly laboratory meetings.

My particular thanks go to both Dr. Melanie Oates and Dr. Asma Salman for patiently processing my Annexin V and FACS samples.

Last, but not least, I would like to thank my wife for her unwavering support and understanding in helping me complete this work during the numerous highs and lows of the past five years.

Abstract

Introduction: Though adjuvant chemotherapy improves survival following surgery, pancreatic cancer carries a poor prognosis. Alternatives are required to the current drug regimens consisting of S-phase dependent drugs such as gemcitabine. PLK1 is a passenger protein involved in G2/M phases which presents a novel target to inhibit in combination with current therapies, which may help overcome inate and acquired resistance.

Aim: To evaluate the potential role of a novel PLK1 inhibitor, BI 6727 in pancreatic cancer – both as monotherapy and in combination with gemcitabine *in vitro*.

Methods: The IC_{50} concentrations of both drugs were established in Suit-2, BxPC-3, Panc-1 and MiaPaCa-2 pancreatic cancer cell lines and isobolar analyses undertaken with a variety of combination therapies. Cell cycle analyses were performed with Flow Activated Cell Sorting, with apoptosis and necrosis quantified on the basis of phosphatidylserine cell surface exposure, propidium iodide staining and cleavage of caspase-3.

Results: IC_{50} ranges for BI 6727 and gemcitabine were 53-77nM and 11-34nM respectively across four pancreatic cell lines. Flow cytometry of MiaPaCa-2 cells demonstrated G2 arrest with BI 6727 and S-phase accumulation with gemcitabine monotherapy. Isobolar analyses showed that when added together the combination of drugs was additive, but BI 6727 pretreatment followed by combination was synergistic. Western blotting for cleaved caspase-3 showed evidence of apoptosis with gemcitabine monotherapy but none with BI 6727 treatment. Although membrane inversion was seen with synergistic drug combinations there was no evidence of cleaved-caspase-3, suggesting a modified form of apoptosis.

Conclusion: BI 6727 is effective against a variety of pancreatic cancer cells *in vitro.* Synergy is demonstrated in MiaPaCa-2 cells when BI 6727 is administered prior to combination therapy with gemcitabine, though mode of cell death does not appear to be caspase-dependent. This supports the concept that PLK1 inhibition can overcome gemcitabine resistance in some cells by allowing resistant cells to initiate gemcitabine induced apoptosis, although this is dependent on drug phasing and the full apoptotic pathway may not be achieved.

Table of Contents

Table of Tables

Table of Figures

List of Abbreviations

5-FU	Fluorouracil
5'-NT	5-nucleotidase
γTuRC	γ-tubulin ring complex
γTuSC	γ-tubulin small complex
ACC	Acetyl-CoA-carboxylase
ADP	Adenosine diphosphase
AIF	Apoptosis-inducing factor
AMPK	AMP-activated protein kinase
APC	Anaphase-promoting complex
ATM	Ataxia telangiectasia
ATP	Adenosine triphosphase
ATR	Ataxia telangiectasia and Rad3-related protein
BAK1	BCL-2-antagonist killer 1
BAX	BCL-2-associated x protein
BCL	B-cell lymphoma
Bid	BH3-interacting domain death agoinist
CDA	Cytidine deaminase
CDK	Cyclin-dependent kinase
CEP192	Centrosomal protein of 192kDA
Chk	Checkpoint kinase
CI	Confidence interval
CLASP	CLIP-associating protein
CNAP1	Centrosome-associated protein 1
CONKO	Charité Onkologie
CRT	Chemoradiotherapy
CT	Computed tomography

CUL	Cullin
DCC	Deleted in colon cancer
dCK	Deoxycytidine kinase
dCTD	Deoxycytidylate deaminase
dFdC	2','-difluoro 2'deoxycytidine (gemcitabine)
dFdCDP	Gemcitabine diphosphate
dFdCMP	Gemcitabine monophosphate
dFdCTP	Gemcitabine triphosphate
dFdU	2'-2'- difluoro-2'-deoxyuridine
dFdUMP	2'-2'- difluoro-2'-deoxyuridine monophosphate
DFS	Disease-free survival
DIABLO	Direct inhibitor of apoptosis-binding protein with low pl/SMAC
DISC	Death-inducing signalling complex
DMSO	Dimethyl sulfoxide
DNA	Deoxyribonucleic acid
DTT	DL-Dithiothreitol
dNTP	deoxynucleotide tri-phosphate
eGFR	Epidermal growth factor
ECL	Enhanced chemiluminescence
EMI	Early mitotic inhibitor
ENDOG	Endonuclease G
EORTC	European organisation for research and treatment of cancer
ERAS	Enhanced recovery after surgery
ERCP	Endoscopic retrograde cholangiopancreatography
ESPAC	European study group for pancreatic cancer
EthD-III	Ethidium Homodimer III
EUS	Endoscopic ultrasound

FACS	Fluorescence-activated cell sorting
FADD	Fas-associated death domain
FAP	Fibroblast Activation Protein
FBS	Foetal bovine serum
FNA	Fine needle aspirate
FOLFIRINOX	Folinic acid, 5-FU, irinotecan, oxaliplatin
GITSG	Gastrointestinal tumour study group
HER2	Human epidermal growth factor
hCNT	Human nucleoside transporter concentrative type
hENT	Human nucleoside transporter equilibrative type
hNT	Human nucleoside transporter
HR	Hazard ratio
HTRA2	High temperature requirement protein A2
ICD	International classification of diseases
INCENP	Inner centromere protein
ISGPS	International study group of pancreatic surgery
IQR	Interquartile range
JASPAC	Japan adjuvant study group of pancreatic cancer
JSAP	Japanese study group of adjuvant therapy for pancreatic cancer
KLH22	Kelch-like protein
KNM	Kinetochore-null protein
KT-MT	Kinetochore-microtubule
LOK	Lymphocyte oriented kinase
NIR	N-terminal domain-interacting receptor
NLP	Ninein-like protein
NUDC	Nuclear distribution protein C
M	Mole(s)

MAPK	Mitogen-activated kinase
MIPD	Minimally invasive pancreaticoduodenectomy
MKLP	Mitotic kinesin-like protein
MRCP	Magnetic resonance cholangiopancreatography
mRNA	Messenger RNA
MST2	See STK
MUC	Mammary-type mucin
NEK	NIMA-related kinase
NLP	Ninein-like protein
nM	Nanomolar
OS	Overall survival
p53BP	p53-binding protein
PanIN	Pancreatic epithelial neoplasia
PBD	Polo-box domain
PBIP1	Polo-box interacting protein 1
PBS	Phosphate buffered saline
Pc	Polo-cap
PCM	Pericentriolar matrix
PCNT	Pericentrin
PCR	Polymerase chain reaction
pHH3	Phosphorylated histone H3
PI	Propidium iodide
PLK	Polo-like kinase
PP	Protein phosphatase
PRC	Protein regulator of cytokinesis
RA21	See Scc
Rb	Retinoblastoma

RNA	Ribonucleic acid
RR	Ribonucleotide reductase
RTOG	Radiation therapy oncology group
SAC	Spindle assembly checkpoint
Scc	Sister chromatid cohesion protein
SCF βTrCP	Skp/Cullin/F-box-β-Trasducin repeat containing protein
SDS	Sodium dodecyl sulfate
Sgo1	Shugoshin
siRNA	Small interfering RNA
SLK	STE20-like kinase
SPARC	Secreted protein acidic and rich in cysteine
STK	Serine/threonine kinase
TBS	Tris-buffered saline
TBST	Tris-buffered saline with tween
T-Effs	T-effector cells
TGF-β	Transforming growth factor β
TNF	Tumour necrosis factor
TNM	Tumour nodes metastases
TPX2	Targeting protein for Xklp2
TRAIL	TNF-related apoptosis-inducing ligand
UICC	Union for international cancer control
UK	United Kingdom
UNC5B	Uncoordinated-5 homolog
VEGF	Vascular endothelial growth factor

Chapter 1 - Introduction

The Pancreas

Structure

The pancreas is an elongated organ measuring 12-15cm which lies horizontally in the retroperitoneum, posterior to the stomach. The gland is broadly anatomically divided into the head, uncinate, neck, body and tail. The widest part - the head, lies in the concavity of the duodenum which has an inferior projection known as the uncinate process. Medial to the head is a constriction described as the pancreatic neck, leading to the body, which represents the mid-portion of the pancreas. Adjacent to the body is the tail which tapers and terminates next to the spleen in the left upper quadrant[1 2 3].

Embryologically, the human pancreas develops from the dorsal and ventral pancreatic buds which fuse at 7-8 weeks. These buds possess two ductal systems which anastomose during fusion with multiple anatomical variants described in the literature[4]. Classically, a main pancreatic duct originates in the tail, draining the gland's secretions medially. This duct then drains into the two ductal systems at the site of their embryological fusion. Firstly, the segment of duct originating from the dorsal bud, named the Accessory duct of Santorini[5] (Giovanni Dominico Santorini 1681-1737, Italian anatomist), drains into the minor papilla. Alternatively, secretions will pass downstream from the main pancreatic duct into the Duct of Wirsung (Johann Wirsung 1589-1643, German anatomist), which originates from the ventral bud and drains into major papilla, where it meets the common bile duct[6 7 8 9]. These two structures drain into the second part of the duodenum via a protrusion of the Ampulla of Vater[10] (Abraham Vater 1684–1751, German anatomist). The secretion of bile and pancreatic juices is controlled by a circumferential smooth muscular layer known as the Sphincter of Oddi[11] (Ruggero Oddi 1864-1913, Italian anatomist and physiologist).

Exocrine and Endocrine Function

Histologically, the pancreatic parenchyma can be grossly divided into its exocrine and endocrine components. The majority of the pancreas is composed of acinar cells, which are arranged in clusters around interlobular ducts that lead to the main pancreatic duct[12]. Acini are exocrine cells which secrete approximately 2.5 litres of bicarbonate-rich fluid per 24

hours. This fluid contains digestive enzymes such as pancreatic amylase and lipase in addition to several proenzymes such as proteases[13].

The endocrine function of the pancreas is dependent on islet cells which group to form the Islets of Langerhans[14] (Paul Langerhans 1847-88, German pathologist). These cells only account for approximately 1-2% of pancreatic mass[15] and secrete hormones including insulin, glucagon, somatostatin and pancreatic polypeptide into the bloodstream[16].

The Incidence of Pancreatic Cancer

Despite accounting for less than 3% of all cancer diagnoses, pancreatic cancer (ICD Code: ICD-10 C25) is now the 4th leading cause of cancer-related deaths in the developed world[17]. In 2014, 8080 people in England were diagnosed with the disease making it the 10th commonest cancer in the country. Incidence of the disease has remained relatively unchanged over the past 40 years. For males and females, current figures suggest an incidence of 10.7 and 8.7 respectively per 100,000, with mortality rates being only marginally lower (Figure 1). Currently, of the 21 most common cancers in the United Kingdom, pancreatic cancer has the lowest life expectancy[18]. Figures for patients diagnosed in England between 2005 and 2009 suggest a 5-year survival rate of only 3.7%[19].

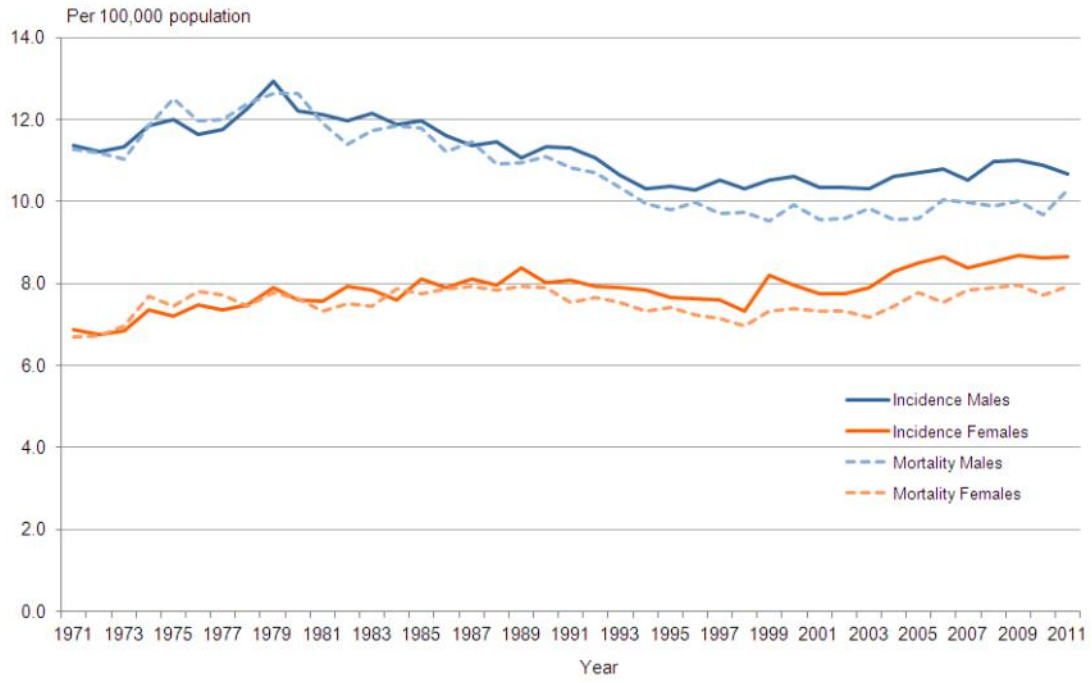

Figure 1: Pancreatic cancer incidence and mortality rates, England, 1971-2011
The incidence of pancreatic cancer has remained relatively unchanged over the past 40 years. Taken without permission from the Office of National Statistics[18]

Risk Factors

In addition to advancing age[18], other recognized risk factors for developing pancreatic cancer include obesity[20 21 22 23] and smoking[24 25 26]. Two meta-analyses also suggest that diabetes mellitus is a risk factor in the development of the disease[27 28]. However, it is now argued that diabetes is a consequence of pancreatic cancer[29], which may be of potential benefit in screening and the early detection of the malignant process[30].

The evidence surrounding the association between alcohol consumption and pancreatic cancer is conflicting. Several case-control and cohort studies have found no association between the two whilst other studies have suggested an increased risk in heavy consumers[31]. Nevertheless, alcohol excess accounts for the vast majority of chronic pancreatitis cases[32], which is now a recognized risk factor in developing pancreatic cancer[33]. A recent meta-analysis declared a thirteen-fold relative risk for developing the disease, with a time course of one or two decades between developing both diseases[34].

Exclusive of lifestyle factors, few other genetic and hereditary factors can increase the risk of pancreatic cancer (Table 1) including hereditary pancreatitis[35 36], cystic fibrosis [37 38 39] and familial pancreatic cancer[40 41 42]. Presently, both European[43] and American[44] registers for familial pancreatic cancer have been established with view to offering screening, surveillance and in extreme cases, prophylactic surgery for high-risk individuals.

Table 1: Related mutational genes and their respective risks in developing pancreatic cancer

Setting of Inherited Pancreatic Cancer	Gene	Pancreatic Cancer Risk until 70 years (%)
Hereditary tumour predisposition syndromes		
Peutz-Jeghers syndrome	*SK11/LKB1*	36
Atypical multiple mole melanoma syndrome	*CDKN2a*	17
Hereditary breast and ovarian cancer	*BRCA1, BRCA2*	3 to 8
Li-Fraumeni	*TP53*	<5
Hereditary nonpolyposis colorectal cancer	*MLH1, MSH2*	<5
Familial adenomatous polyposis	*APC*	<5
Ataxia telangectasia	*ATM*	<5
Tumour syndromes with chronic inflammation/dysfunction of the gland		
Hereditary pancreatitis	*PRSS1, SPINK1*	40
Cystic fibrosis	*CFTR*	<5
Familial pancreatic cancer syndrome	*BRCA2, PALB2, ?*	~40

Several genes are associated with an increased risk of developing pancreatic cancer. Modified from Fendrich et al[45]

Pancreatic Tumours

Pancreatic tumours can be broadly divided into being of exocrine or endocrine origin with further classification with regards to their malignancy.

Endocrine Pancreatic Tumours

Neuroendocrine pancreatic tumours appear to arise from Islet cells and account for <5% of all primary pancreatic malignancies[46]. 'Functional' tumours are associated with a clinical syndrome[47] and are classified according to the hormone that they produce (insulinoma, gastrinoma, glucagonoma, somatostatinoma and Vasoactive Intestinal Peptide [VIP]oma). 'Non-functioning' tumours, typically produce a precursor or negligible quantity of hormone and are most commonly found in the head of the pancreas[48]. Non-functioning tumours have a poorer prognosis, with one large series[49] concluding that individuals with functional tumours survive for twice as long as those with non-functioning tumours (median survival of 54 months vs. 26 months). It must also be noted that long term survival can also be achieved in the metastatic patient with a 5-year survival of 19.5% in the same series. This highlights the importance of distinguishing these rare endocrine tumours from their exocrine counterparts which have a comparably dismal prognosis.

Exocrine Pancreatic Tumours

A wide variety of benign, pre malignant and malignant exocrine pancreatic lesions have been recognised (Table 2). However, ductal adenocarcinoma and its variants represent up to 90% of all pancreatic tumours[50] and is widely what is understood by the term 'pancreatic cancer'.

Table 2: Malignant tumours of the exocrine pancreas

Malignant Exocrine Pancreatic Tumours
Epithelial tumours:
Ductal adenocarcinoma
• Mucinous noncystic carcinoma (Mucinous Adenocarcinoma)
• Signet-ring cell carcinoma
• Adenosquamous carcinoma
• Undifferentiated (anaplastic) carcinoma
• Mixed ductal-endocrine carcinoma
• Osteoclast-like giant cell tumour
Serous cystadeoncarcinoma
Mucinous cystadenocarcinoma
Intraductal papilliary-mucinous carcinoma
Invasive papilliary-mucinous carcinoma
Acinar cell carcinoma
Pancreatoblastoma
Solid-pseudopapilliary carcinoma
Extremely Rare:
Clear cell carcinoma (clear cell adenocarcinoma)
Oncocytic carcinoma (oxyphilic adenocarcinoma)
Choriocarcinoma (NOS)
Non-epithelial tumours
Secondary tumours

There are several subtypes of malignant exocrine pancreatic tumours with pancreatic ductal adenocarcinoma being by far the commonest. Pancreatic intraepithelial neoplasia (PanIN) is now thought to be the precursor to the development of most ductal adenocarcinomas[51].

Pancreatic Cancer in the Clinical Environment

Clinical Presentation

The presenting symptoms and signs of pancreatic cancer are often vague and can be extremely variable. Upper abdominal and back pain can be a feature with patients often complaining of loss of appetite or nausea. Tumours of the pancreatic head commonly lead to obstructive jaundice being the main presenting feature, but such tumours may also cause pancreatitis, gastric outlet obstruction or gastrointestinal bleeding. Individuals with systemic manifestation of the neoplastic process may present with diabetes, venous thrombosis, weight loss or abdominal distension secondary to ascites[52]. Occasionally, asymptomatic patients may be found to have a pancreatic lesion following radiological imaging for unrelated reasons.

Clinical Signs

Signs of the disease may be absent though inspection of the patient may reveal a myriad of signs. The patient may be jaundiced, with evidence of pruritis or dark urine to indicate cholestasis. They may appear pale and cachexic or wear loose fitting clothes indicating recent weight loss. Examination of the abdomen may reveal a palpable abdominal mass, hepatomegaly, abdominal distension with shifting dullness or lymphadenopathy[53].

Imaging in Pancreatic Cancer

The aims when assessing any patient with a possible malignant disease are to alleviate any symptoms, diagnose and stage the disease and finally to determine their treatment options such as potentially curative surgery. Studies have shown that computed tomography (CT) imaging is highly sensitive in detecting pancreatic tumours[54] and has therefore become the imaging procedure of choice for evaluating any suspected pancreatic lesion[55]. An equivocal CT with a continuing suspicion for a pancreatic lesion should lead to an endoscopic ultrasound (EUS), which is superior in detecting early tumours as small as 2-3mm[56].

In addition to revealing any obvious distant metastases, an arterial and portal-phase CT will enable visualisation of the tumour in relation to both the adjacent organs and vasculature. Evaluating a primary pancreatic tumour with regards to local invasion is a critical process, as surgical resection is currently the only potentially curative treatment. On the contrary, it is

not desirable to subject patients with irresectable disease to a trial dissection, as this inevitably leads increased hospital morbidity and mortality[57].

Borderline Resectable Pancreatic Cancer

Radiologically assessing a pancreatic tumour in relation to its adjacent vasculature - the common hepatic artery, coeliac axis, superior mesenteric artery, vein and portal vein is both a critical and challenging process. CT examination has a varied accuracy of 62-92% in assessing vascular involvement[58] in pancreatic cancer, with magnetic resonance cholangiopancreatography (MRCP) adding little in assessing tumour resectability[59]. In the absence of metastatic disease, a clear plane between the tumour and this vasculature indicates a resectable cancer. However, any apparent contact between the two no longer contraindicates curative surgery[60]. The International Study Group of Pancreatic Surgery (ISGPS)[61] have definined 'bordeline resectable' with regards to the arterial and venous involvement of tumours.

Endoscopic Techniques and Obtaining a Definitive Diagnosis

Frequently, tumours of the pancreatic head will obstruct the bile duct leading to jaundice, pruritis and occasionally cholangitis. Biliary drainage can be achieved prior to resection with the endoscopic insertion of a stent. However, an endoscopic retrograde cholangiopancreatography (ERCP) should not be routinely performed on all patients with pancreatic cancer. Obtaining a definitive histological diagnosis is not always necessary prior to resection, especially if there is a history of chronic pancreatitis. However, a definitive diagnosis must be reached if neo-adjuvant or palliative chemotherapy is to be administered. An ERCP with brushings is a notoriously unreliable technique in establishing a diagnosis, with a large meta-analysis determining a sensitivity of 41.6% and a negative predictive value of 58%[62]. For this reason, an expert panel recently strongly recommended that in the absence of jaundice, an endoscopic ultrasound and fine needle aspiration (EUS-FNA) should be the preferred method of obtaining confirmation of malignancy[63].

The Staging of Pancreatic Cancer

The Union for International Cancer Control (UICC) has formulated the 7th Edition staging system for pancreatic cancer[64] (Table 3 and Table 4). Staging of the disease is critical in guiding each patient's treatment and prognosis, in addition to its importance for audit and research purposes.

Table 3: The Union for International Cancer Control (UICC)'s TNM staging of pancreatic cancer

Tumour	
Tx	Primary tumour cannot be assessed
T0	No evidence of primary tumour
Tis	Carcinoma in situ
T1	Tumour limited to the pancreas and <2cm at its greatest diameter
T2	Tumour limited to the pancreas and >2cm at its greatest diameter
T3	Tumour extends beyond the pancreas but not involving the coeliac axis of superior mesenteric artery
T4	Tumour involves the coeliac axis or superior mesenteric artery
Lymph Nodes	
Nx	Regional lymph nodes cannot be assessed
N0	No regional lymph node metastasis
N1	Regional lymph node metastasis
Metastases	
M0	No distant metastasis
M1	Distant metastasis

The TNM classification is widely applied to a spectrum of malignant diseases and has been modified for pancreatic cancer.

Table 4: The UICC TNM staging of pancreatic cancer

Stage	Tumour	Lymph Nodes	Metastasis
0	Tis	N0	M0
IA	T1	N0	M0
IB	T2	N0	M0
IIA	T3	N0	M0
IIB	T1	N1	M0
	T2	N1	M0
	T3	N1	M0
III	T4	Any N	M0
IV	Any T	Any N	M1

The individual components of the TNM classification is then collated to stage the disease, graded from stages 1 to 4.

The Multidisciplinary Team

Multidisciplinary teams were introduced to overcome shortfalls in UK cancer care[65]. All confirmed or suspected cases of pancreatic cancer are now routinely discussed in a multidisciplinary meeting. This usually weekly, collective discussion involves a spectrum of healthcare professionals ensures a timely diagnosis and treatment in accordance with the best available evidence.

The Surgical Management of Pancreatic Cancer

Kausch reported the first successful two-stage pancreatoduodenectomy in 1912[66], which was undertaken for an ampullary cancer. It was not until 1946 that Whipple published his single-stage procedure that it now known by his name[67]. The classic 'Kausch-Whipple' involves excision of the common bile duct, gallbladder, pancreatic head, pylorus and the duodenum. This has been modified over time, with preservation of the pylorus performed if possible – the 'pylorus-preserving Kausch-Whipple'. This avoids the need for a 'Roux-en-Y' reconstruction though no difference in morbidity, mortality or long-term survival is noted[68].

Less common are tumours of the body or tail of the pancreas. These tumours account for approximately a third of all pancreatic tumours[69], but are less likely to be resectable and have a poorer prognosis in comparison to lesions of the head[70]. These distal lesions are

subject to a left/distal pancreatectomy and splenectomy, ensuring the removal of the lymphatic chain adjacent to the splenic vessels.

Morbidity and Mortality of Surgical Resection for Pancreatic Cancer

The first published series of pancreaticoduodenectomies included 12 patients with an operative mortality rate of 43%[71]. With continuing improvements in surgical techniques and perioperative care, this figure has dropped significantly with two series of over 100 patients even reporting no mortality[72 73].

Given the complexity of pancreatic surgery, the National Health Service recommended that specialist pancreatic teams cover a minimum catchment area of a million patients to deliver optimal care[74]. One of the reasons for this is to ensure an adequate case-load for specialist centres. There is plentiful evidence to support that high volume centres reduce surgical mortality rates, and are better equipped to deal with any complications that occur[75 76].

Recent Advances in the Surgical Management of Pancreatic Cancer

The first laparoscopic pancreaticoduodenectomy was reported in 1994[77] and more recent times have seen the advent of a robotic technique[78]. Three recent meta-analyses have compared minimally invasive pancreaticoduodenectomy (MIPD) with open surgery[79 80 81]. All three agreed that though the former procedure takes significantly longer, MIPD leads to less intraoperative blood loss, a shorter hospital stay, comparable oncological results, morbidity and mortality compared to the open technique. However, to date, no randomised study has been published comparing techniques.

Consistent with other surgical specialties, Enhanced Recovery after Surgery (ERAS) guidelines have been published specifically for patients undergoing pancreaticoduodenectomy[82]. These guidelines aim to reduce the length of hospital stay after surgery without compromising morbidity and mortality. A 2013 meta-analysis[83] suggests that this is possible in a range of pancreatic procedures, with lower morbidity rates noted in patients undergoing ERAS compared with standard postoperative care.

New Treatments

The fundamental problem with surgical treatment of pancreatic cancer is that the disease has inevitably spread by the time of detection and so even though the primary can be removed this will only give a temporary benefit unless systemic treatment is applied to

remove the metastatic deposits. In order to understand how current therapies work and how they can be improved it is necessary to understand the molecular basis of the disease.

The Development of Pancreatic Cancer

Though pancreatic cancer can arise from intraductal papilliary mucinous neoplasms or mucinous cystic neoplasms, it is believed that the vast majority will originate from non-invasive precursor lesions called pancreatic intraepithelial neoplasia (PanIN). PanINs are non-invasive and usually less than 5mm in size, therefore being asymptomatic. Though multiple terminologies were initially utilised to describe these lesions, the current PanIN classification in use was introduced in 2001[84 85].

Histology of PanINs

PanINs can be classified into four broad categories depending on their histological appearance. PanIN-1A and PanIN-1B are low-grade lesions displaying only minimal atypia, with the former appearing flat and the latter papilliary in appearance. PanIN-2 are papilliary lesions, showing a greater degree of cytological and architectural atypia compared to lower grade lesions. PanIN-3, often described as 'carcinoma in-situ,' shows severe cytological and architectural atypia[86].

Genetic Alterations in the Development of Pancreatic Adenocarcinoma from PanINs

Pancreatic adenocarcinoma is thought to develop from normal epithelium, which gradually progresses through the histological stages of PanIN described above, before developing invasive properties. Simultaneously, the lesion will undergo a variety of genetic alterations[87] with the most prevalent discussed below (Figure 2).

Telomere Shortening

Telomeres are DNA-protein structures located at the ends of chromosomes, preventing inter or intra-chromosomal adhesion[88]. The shortening of telomeres is a recognised event with ageing[89], with a small portion of DNA lost with each cell division. Shortened telomeres increase the risk of fusion, leading to the instability of chromosomes and carcinogenesis[90]. Evidence of shortened telomeres even in in PanIN-1 suggests that this may be one of the earliest events in pancreatic carcinogenesis[91 92].

KRAS2

A mutation in the *KRAS2* oncogene is seen in over 90% of pancreatic adenocarcinomas and *KRAS2* was the first gene to be studied in detail with regards to its association with the development of the disease. *KRAS2* mutations in pancreatic adenocarcinoma are located at

p.G12 in 98% of cases, with the remaining seen in either p.G13 or p.Q61[93]. Once active, KRAS will stimulate downstream pathways such as the mitogen-activated kinase (MAPK)[94] pathway, encouraging cellular proliferation and evading apoptosis – the hallmarks of cancer[95].

KRAS mutations in healthy control tissue are uncommon, with studies showing a strong correlation between the degree of PanIN dysplasia and frequency of *KRAS* mutations[96]. It is the earliest genetic mutation seen in the PanIN-carcinoma sequence, being a common finding in PanIN-1A lesions[97].

CDKN2A

A further mutation often seen in early PanIN is in the tumour suppressor p16[98]. Its encoding gene, *CDKN2A* is located on the short arm of chromosome 9 and almost all pancreatic adenocarcinoma have lost its function[99]. This can be by mutation of both alleles or by a combination of mutation of one allele and promoter methylation in the other. At the G1-S phase transition, p16 inhibits the phosphorylation of the retinoblastoma tumour suppressor gene (Rb) by cyclin-dependent kinases 4 and 6[100], decelerating the progression of cells into S-phase. This control over Rb phosphorylation is lost when p16 is inactivated, resulting in the loss of control over cell cycle arrest[101], contributing to carcinogenesis[102].

TP53

The *TP53* gene, located on chromosome 17p codes for p53[103]. Described as the guardian of the genome[104], mutations in *TP53* are the commonest known in human cancer[105] and are seen in 50-70% of pancreatic cancers[106]. The tumour suppressor p53 propagates several pathways involving cell cycle checkpoints and apoptosis in response to cellular insults, in addition to multiple other events[107]. The absence of this function leads to malfunctions in cellular processes such as cell division and death[108]. Mutations in *TP53* are usually not seen until PanIN-3 lesions, suggesting that this is a late genetic event in the development of pancreatic cancer[109].

DPC4 (Also known as SMAD4)

The tumour-suppressor gene *DPC4* is located on chromosome 18q and codes for the SMAD4 protein[110]. As with p53, loss of SMAD4 function is a late event in pancreatic carcinogenesis as *DPC4* mutations are absent in PanIN-1 and PanIN-2 lesions, but is seen in around a third

of PanIN-3 and 55% of pancreatic ductal adenocarcinoma specimens[111]. SMAD4 mediates transforming growth factor-β (TGF-β) signalling, which when activated, stimulates other SMAD proteins to form complexes with SMAD4 which translocate to the nucleus[112]. These complexes bind to specific areas of DNA to control the activity of particular genes[113]. This regulates cell proliferation, explaining why SMAD4 is recognised as a tumour suppressor, as loss of its function leads to uncontrolled cellular growth and division.

MUC1 and MUC5AC

Mammary-type mucin 1 (MUC1) is expressed in most human glandular epithelial tissue throughout the gastrointestinal tract[114]. In normal pancreatic tissue, it is expressed by pancreatic ducts and centroacinar cells and works as an anti-adhesive to maintain luminal patency[115]. For reasons currently unclear, MUC1 is almost absent in PanIN-1 and PanIN-2 lesions. However, it is expressed in a large proportion of PanIN-3 lesions and it is almost universally present in invasive pancreatic carcinoma[116] which suggests a significant role in the PanIN-adenocarcinoma sequence.

In contrast to MUC1, there is no expression of MUC5AC by normal pancreatic tissue. However, early-stage PanINs frequently express MUC5AC and is seen in up to 92% of pancreatic adenocarcinoma[117].

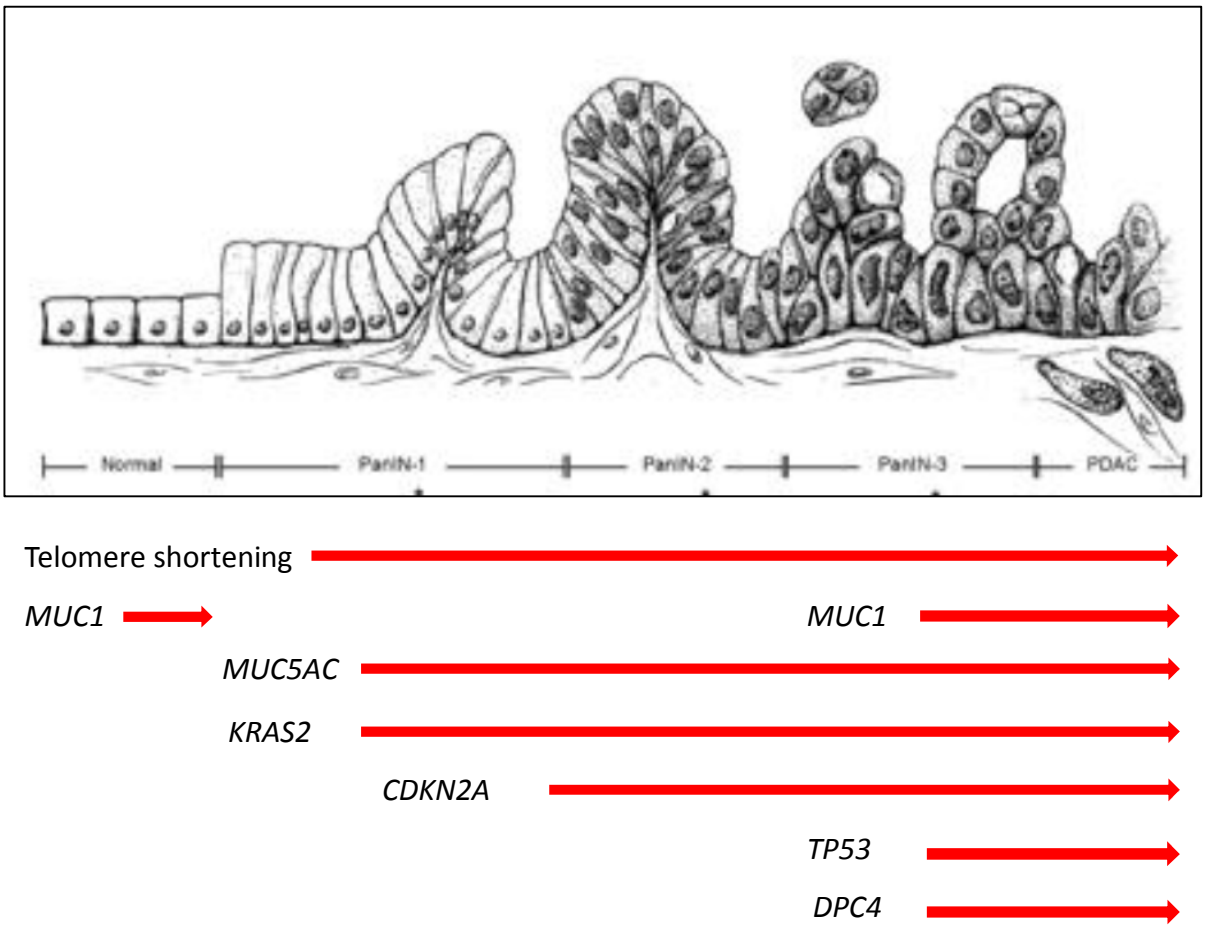

Figure 2: The PanIN to adenocarcinoma pathway with its associated mutations
Early cellular changes in the PanIN to carcinoma sequence include telomere shortening with mutations commonly seen in KRAS2, CDKN2A and MUC5A. Late changes often not seen until PanIN-3 and adenocarcinoma include mutations in MUC1, TP53 and DPC4. Diagram taken without permission from Wilentz et al[118].

Apoptosis

Background

Apoptosis is a mode of programmed cell death characterised by morphological and biochemical changes including cell shrinkage, condensation of chromatin, nuclear DNA fragmentation and the disintegration of the cell into fragments, called 'apoptotic bodies' which can be eliminated by phagocytosis[119] [120]. Classically, two major apoptotic signal transduction pathways exist – the extrinsic or 'death receptor' pathway and the intrinsic or 'mitochondrial' pathway. However, in 2012 The Nomenclature Committee on Cell Death aimed to standardise definitions regarding the modes of cell death. In addition to the plethora of other cell death subroutines, they have further classified apoptosis into four subtypes: extrinsic apoptosis by death receptors, extrinsic apoptosis by dependence receptors, caspase-dependent intrinsic apoptosis and caspase-independent intrinsic apoptosis[121].

Caspases are a family of cysteinyl aspartate–specific proteases, which are divided into two types. First are the initiator caspases (e.g. caspase-2, 8 and 9), which are the apical caspases in the apoptosis cascade. Secondly are the executioner caspases (e.g. caspase-3, 6 and 7), whose activation is usually dependent on the activity of initiator caspases[122].

Extrinsic Apoptosis

Death Receptor Pathway

The death receptor pathway is activated at the plasma membrane when ligands from the tumour necrosis factor (TNF) family, such as CD95 or TNF-related apoptosis-inducing ligand (TRAIL) become bound to their respective death receptors – CD95-ligand (CD95L) and TRAIL receptor 1 and 2 (TRAIL-R1 and TRAIL-R2). This results in the recruitment of adaptor molecules, such as Fas-associated death domain [123] which forms death-inducing signaling complexes (DISC) with procaspase 8[124]. Upon the formation of this complex, caspase-8 oligomerizes and is activated by autocatalysis. Caspase-8 is an initiator caspase, and in its activated form can stimulate apoptosis via two parallel cascades depending on the cell type[125]. In type I cells such as lymphocytes, it can directly cleave and activate caspase-3, an executioner caspase[126] . Alternatively, in type II cells such as hepatocytes or pancreatic β-cells, caspase-8 cleaves a pro-apoptotic Bcl-2 family protein called BH3-interacting domain death agonist (Bid)[127]. This results in a mitochondria-permeabilizing protein, known as

truncated Bid (tBid), which translocates to mitochondria[128]. This loss of membrane integrity of the mitochondria leads to the release of cytochrome c into the cytoplasm, which can be instigated by several factors including cytotoxicity, heat shock, oxidative stress, and DNA damage[129]. In the presence of ATP, cytochrome c forms the 'apoptosome' with APAF1 and caspase-9[130 131]. This functions to cleave and thereby activate effector caspases-3, -6, and -7 to execute apoptosis[132].

Dependence Pathway

The activation of the dependence pathway is reliant on the absence of ligands for dependence receptors such as Patched, DCC and UNC5B. These receptors interact with alternative adaptor proteins, forming complexes to both instigate mitochondrial outer membrane permeabilization and caspase-9 activation[133 134], which in turn will activate caspase-3.

Intrinsic Apoptosis

Caspase-dependent

Intrinsic apoptosis is a mitochondria-centred process which, in addition to engaging pro-apoptotic signalling, involves the anti-apoptotic cascade, enabling cells to tolerate and recover from certain degrees of stress. The pro-apoptotic BCL-2 associated x protein (BAX) and BCL-2 antagonist killer 1 (BAK1), which are members of the B-cell lymphoma 2 (BCL-2) family, causes the mitochondrial membrane to become porous[135]. As a result, DIABLO (direct inhibitor of apoptosis protein-binding protein with low pI/SMAC), cytochrome *c* and high temperature requirement protein A2 (HTRA2) are released into the cytosol. Cytochrome c again activates caspase-3 through forming the 'apoptosome' while DIABLO and HTRA2 promote caspase activation by inhibiting cellular inhibitor of apoptosis proteins (IAPs)[136].

Caspase-independent

Apart from DIABLO, cytochrome c and HTRA2, a further two proteins are released from the mitochondria after the transmembrane potential of mitochondria is overcome. Apoptosis-inducing factor (AIF) and endonuclease G (ENDOG) can both induce caspase-independent apoptosis by their intranuclear translocation to cause DNA fragmentation. HTRA2 can be

both caspase-dependent and independent, and induces the latter by cleaving cytoskeletal proteins[121].

Adjuvant Therapy in Pancreatic Cancer

Major Chemotherapy Trials

In 1993, a Norwegian group[137] was first to publish a randomised study assessing the role of adjuvant chemotherapy in resected pancreatic cancer. Median survival improved to 23 months with adjuvant chemotherapy in comparison to 11 months in those undergoing observation alone (p = 0.04).

The landmark ESPAC-1[138] (European Study Group for Pancreatic Cancer) study was designed to determine whether adjuvant chemoradiotherapy or adjuvant chemotherapy (5-FU and Folinic Acid) alone had a role in improving survival following pancreatic cancer resection. This was the first adequately powered randomised trial to assess adjuvant therapy in pancreatic cancer, recruiting 541 patients over a six-year period in 61 centres internationally. 285 patients were randomised in a two-by-two factorial design to receive chemoradiotherapy alone, chemotherapy alone, both or observation; with a further 256 patients also randomised to receive chemoradiotherapy, chemotherapy, or observation.

The final analysis of the 2X2 ESPAC-1 data[139] was based on 237 deaths in 289 patients with a median follow up of 47 months (IQR 33-62 months). Median survival was 20.1 months (95%CI: 16.5-22.7) amongst patients who had undergone chemotherapy vs. 15.5 months (95%CI: 13-17.7) in those who had not (HR = 0.71, 95%CI: 0.55-0.92, p = 0.009). The estimated two and five year survival was 40% vs. 21% and 21% vs. 8% respectively in those who received chemotherapy against patients which had not. The cohort of 75 patients that received chemotherapy alone fared significantly better than those who underwent just observation (n = 69).

Takada *et al*[140] randomised patients to receive surgery alone or adjuvant chemotherapy with 5-FU and Mitomycin C and showed no significant improvement in 5-year survival or 5-year disease free survival. Unusually, this study utilised oral 5-FU as opposed to the usual intravenous form which may offer a reason for its ineffectiveness. Kosuge and colleagues (JSAP)[141] randomised patients having undergone an R0 resection to either adjuvant cisplatin or 5-FU and found no significant difference in median survival, 5-year survival and 5-year disease-free survival in comparison to patients undergoing surgery alone. As only 89 patients were recruited over 8 years, this resulted in an underpowered study.

In 1997, Burris *et al*[142] published their randomised control trial comparing the nucleoside analogue gemcitabine with 5-FU in advanced pancreatic cancer. In addition to demonstrating a clinical benefit with regards to pain relief, weight and performance status, those receiving gemcitabine achieved a one-year survival rate of 18% as opposed to 2% with 5-FU. These findings resulted in the recruitment of patients for CONKO-001[143] between 1998 and 2004. This study randomised 368 patients to receive either adjuvant gemcitabine or observation alone. Gemcitabine significantly improved disease-free survival following pancreatic cancer resection whether patients had undergone an R0 or R1 resection. With regards median overall survival, the gemcitabine benefit was only marginal in comparison to the observation group (22.8 months vs. 20.2 months, $p = 0.005$)[144]. This minimal difference is potentially explained by the authors by the fact that almost all patients that relapsed in the observation group received gemcitabine or a further line of chemotherapy. However, this study established gemcitabine as the favoured adjuvant chemotherapeutic agent particularly due to its excellent toxicity profile in comparison to 5-FU.

Coincidentally, at the same time as CONKO-001[143], a further study to compare adjuvant gemcitabine and observation was being undertaken. One hundred and nineteen patients were recruited between 2002 and 2005 for JSAP-2[145]. Gemcitabine resulted in a median disease-free survival of 11.4 months (95%CI: 8-14.5) against 5 months (95%CI: 3.7-8.9) in the observation group (HR = 0.60, 95%CI: 0.40-0.89, $p = 0.01$). This however, did not convert to a significant benefit in overall survival as the study was underpowered.

Following on from the ESPAC-1 study, the group undertook another randomised controlled trial, ESPAC-3 to compare 5-FU and folinic acid (as per the ESPAC-1 regime), gemcitabine (as per CONKO-001 regime) and surgery alone in resected pancreatic cancer. During recruitment however, the publication of ESPAC-1 proved the undoubted benefit of adjuvant chemotherapy. This resulted in the observation arm being forfeited and the study was renamed ESPAC-3(v2)[146].

ESPAC-3(v2) was the largest study of its kind, recruiting 1088 patients with pancreatic ductal adenocarcinoma in 159 centres worldwide over a seven year period. With a median follow-up of 34.2 months (range 0.4-86.3, IQR 27.1-43.4), no significant difference was shown in overall survival or progression-free survival between the two treatment groups. However,

gemcitabine halved the number of serious treatment-related adverse events compared to its opposing arm (14% vs. 7.5% of patients, $p < 0.001$). It was also noted a more favourable outcome was achieved in patients with node positive disease or an R1 resection when administered gemcitabine. This firmly established the drug as the current gold standard in the adjuvant treatment of pancreatic cancer.

A meta-analysis in 2009[147] combined data from a subgroup of ESPAC-3(v1) with ESPAC-1 2X2 and ESPAC-1 Plus (a subgroup of 192 patients in a randomised comparison between 5-FU and observation +/- chemoradiation). Chemotherapy improved overall survival at one, two and five years, providing robust evidence for the continued use of 5-FU and folinic acid in the adjuvant setting alongside gemcitabine.

The JASPAC-01 trial[148] enrolled 385 patients between 2007 and 2010 to compare adjuvant gemcitabine with S-1, a combination of the fluorinated pyrimidine Tegafur with 5-chloro-2,4-dihydroxypyridine and oteracil potassium, in resected pancreatic cancer. Promising interim results were presented in 2012[149] with an overall 2-year survival of 53% and 70% in the gemcitabine and S-1 groups respectively (HR = 0.56, 95%CI: 0.42-0.74, $p < 0.0001$). S-1 also proved superior with regards to recurrence-free survival at 2-years with 49% of patients remaining disease-free compared with 29% in the gemcitabine cohort (HR = 0.56, 95%CI: 0.43-0.71, log-rank $p < 0.0001$). S-1's comparatively low toxicity in addition to the fact that S-1 is orally administered, would be partly responsible for the superior quality of life scores in this group ($p < 0.0001$).Though the authors conclude that S-1 should be considered the new standard treatment for resected pancreatic cancer, its efficacy is yet to be investigated in a randomised study in a Western population. It has been stated that due to the metabolic differences between Asian and Caucasian populations, gastrointestinal side effects are far greater in the latter leading to lower tolerated doses of S-1[150].

In recent months, results from the international, multicentre, phase III trial, ESPAC-4 have been presented[151]. Between 2008 and 2014, 732 patients were recruited and randomised to receive either adjuvant gemcitabine or a combination of gemcitabine and capecitabine. This landmark study showed an improved median survival with combination therapy as opposed to gemcitabine alone (28 vs. 25.5 months, $p = 0.032$). This benefit was seen without a statistically significant increase in toxicity related events, suggesting that this drug regime

will soon become the standard of care against, against which all others are to be compared (Table 5).

Table 5: Major adjuvant chemotherapy trials in pancreatic cancer

			Final analysis			Survival (95%CI)					Disease-free survival (DFS)(95%CI)				
Year published	Author/Group	Treatment arms (*n*)	T3 (%)	N+ (%)	R0 (%)	Median survival (months)	1-year survival (%)	2-year survival (%)	3-year survival (%)	5-year survival (%)	Median DFS (months)	1-year DFS (%)	2-year DFS (%)	3-year DFS (%)	5-year DFS (%)
1993	Bakkevold[137]	5-FU/Doxorubicin/ MitomycinC (30)	N/A	N/A	100	23	N/A	70	27	4	N/A	N/A	N/A	N/A	N/A
		Surgery alone (31)				11 (p=0.02)	N/A	45	30	8 (=0.1)	N/A	N/A	N/A	N/A	N/A
2001	ESPAC-1[138] (All patients)	5-FU/Folinic Acid +/- CRT (238)	N/A	53	82	19.7 (16.4-22.4)	N/A	N/A	N/A	N/A	N/A	N/A	N/A	N/A	N/A
		No chemotherapy +/- CRT (235)				14 (11.9-16.5) (HR = 0.66, 0.52-0.83, p=0.0005)	N/A	N/A	N/A	N/A	N/A	N/A	N/A	N/A	N/A
2002	Takada[140]	5-FU/MitomycinC (89)	N/A	85	58	n/a	N/A	N/A	N/A	11.5	N/A	N/A	N/A	N/A	8.6
		Surgery alone (84)					N/A	N/A	N/A	18 (log rank NS)	N/A	N/A	N/A	N/A	7.8 (log rank p=0.84)
2004	ESPAC-1[139] (2x2 final analysis)	5-FU/Folinic Acid (147)	N/A	54	82	20.1 (16.5-22.7)	N/A	40	N/A	21	N/A	N/A	N/A	N/A	N/A
		No chemotherapy +/- CRT (142)				15.5 (13-17.7) (HR = 0.71, 0.55-0.92, p=0.009)	N/A	30	N/A	8	N/A	N/A	N/A	N/A	N/A
2006	JSAP[141] (Kosuge)	Cisplatin/5-FU (45)	N/A	27	100	12.50	N/A	N/A	N/A	26.40	N/A	N/A	N/A	N/A	N/A
		Surgery alone (44)				15.8	N/A	N/A	N/A	14.9 (p=0.94)	N/A	N/A	N/A	N/A	N/A
2007	CONKO-001[143] (Oettle)	Gemcitabine (179)				22.1 (18.4-25.8)	72.5	47.5	34	22.5	13.4 (11.4-15.3)	58	30.5	23.5	16.5
		Surgery alone (175)	86	72	83	20.2 (17-23.4) (p=0.06)	72.5	42	20.5	20.5	6.9 (6.1-7.8) (p<0.001)	31	14.5	7.5	5.5
2008	CONKO-001 Final[144] (Neuhaus)	Gemcitabine (179)				22.8	N/A	N/A	36.5	21	13.4	N/A	N/A	23.5	16
		Surgery alone (175)				20.2 (p=0.005)	N/A	N/A	19.5	9	6.9 (p<0.001)	N/A	N/A	8.5	6.5
2009	JSAP-2[145] (Ueno)	Gemcitabine +/- RT (58)	86	69	84	22.3 (16.1-30.7)	77.6	48.3	N/A	23.9	11.4 (8-14.5)	49	27.2	N/A	N/A
		Surgery alone +/- RT (60)				18.4 (15.1-25.3) (HR = 0.77, 0.51-1.14, p=0.19)	75	40	N/A	10.6	5 (3.7-8.9) (HR = 0.6, 0.4-0.89, p=0.01)	26.7	16.7	N/A	N/A
2009	Collated data ESPAC-1, ESPAC-1 Plus, ESPAC-3(v1)[147]	5-FU/Folinic Acid (233)	N/A	55	75	23.2 (20.1-26.5)	77	49	N/A	24	N/A	N/A	N/A	N/A	N/A
		Surgery alone (225)				16.8 (14.3-19.2) (HR = 0.7, 0.55-0.88, p=0.003)	63	37	N/A	14	N/A	N/A	N/A	N/A	N/A
2010	ESPAC-3(v2)[146]	5-FU/Folinic Acid (551)	N/A	72	65	23 (21.1-25)	78.5 (75-82)	48.1 (43.8-52.4)	N/A	N/A	14.1 (12.5-15.3)	56.1 (51.8-60.3)	30.7 (26.7-34.6)	N/A	N/A
		Gemcitabine (537)				23.6 (21.4-26.4) (HR = 0.94, 0.81-1.08, p=0.39)	80.1 (76.7-83.6)	49.1 (44.8-53.4)	N/A	N/A	14.3 (13.5-15.6)	61.3 (57.1-65.5)	29.6 (25.6-33.5)	N/A	N/A
2013	JASPAC-01[148]	S-1 (187)	87	63	87	46.3	N/A	70	N/A	N/A	23.2	N/A	49	N/A	N/A
		Gemcitabine (191)				25.5 (p<0.0001)	N/A	53 (HR = 0.56, 0.42-0.74, p<0.0001)	N/A	N/A	11.2 (log rank p<0.0001)	N/A	29 (HR = 0.56, 0.43-0.71, log rank p<0.0001)	N/A	N/A
2017	ESPAC-4[151]	Gemcitabine	N/A	80	40	25.5 (22.7-27.9)	80.5 (76-84.3)	52.1 (46.7-57.2)			13.1 (11.6-15.3)			20.9 (16.5-25.7)	11.9 (7.8-16.9)
		Gemcitabine/ Capecitabine				28 (23.5-31.5) (HR 0.82, 0.68-0.98, p=0.032)	84.1 (79.9-87.5)	53.8 (48.4-58.8)			13.9 (12.1-16.1) (HR 0.86, 0.73-1.02, p=0.082)			23.8(19.2-28.6)	18.6 (13.8-24)

Several major studies have investigated the role of adjuvant chemotherapy in resected pancreatic cancer over the past three decades. Table modified from Jones et al[152]

Meta-analysis of Adjuvant Chemotherapy Trials

A meta-analysis assessing adjuvant therapy in pancreatic cancer was published in 2005. Stocken *et al*[153] included five randomised trials (Bakkevold *et al*[137], ESPAC-1[138], Takada *et al*[140], EORTC[154] and GITSG[155 156]) to evaluate the effects of both chemotherapy and chemoradiotherapy in the adjuvant setting (*n* = 939)(Table 6). With the exception of GISTG, the authors collected individual patient data from each of these studies (*n* = 875) to produce as accurate a results as possible. When collating results from the three chemotherapy trials, heterogeneity was affected with the inclusion of the Japanese results, which the authors suggest was due to the large number of R1 resections included in that particular study. Nevertheless, analysis of the dataset both including and excluding this study resulted in reductions of 25% (HR = 0.75, 95%CI: 0.64-0.9, $p = 0.001$) and 35% (HR = 0.65, 95%CI: 0.54-0.8, $p < 0.001$) respectively in the risk of death with adjuvant chemotherapy. Median survival was estimated to be 19 months (95%CI: 16.4-21.1) with chemotherapy and 13.5 months (95%CI: 12.2-15.8) without.

A later meta-analysis[157] included the five randomised trials comparing adjuvant chemotherapy to observation (Bakkevold *et al*[137], ESPAC-1[138], Takada *et al*[140140], JSAP[141] and CONKO-001[143]). Median survival data was available from all studies with the exception of Takada *et al*, with no significant heterogeneity between the remaining four conflicting studies ($p = 0.07$). Meta-analysis indicated a significant survival benefit of 3 months (95%CI: 0.3-5.7, $p = 0.03$) in patients receiving adjuvant chemotherapy as opposed to observation. However, adjuvant treatment translated into only a 3.1% benefit in 5-year survival which proved insignificant.

A third meta-analysis looked specifically at adjuvant therapy in relation to resection margins[158]. This meta-analysis was supportive of adjuvant chemotherapy, indicating a 25% reduction in the risk of death with treatment as opposed to observation (HR = 0.75, 95%CI: 0.64-0.9, $p = 0.001$). Patients undergoing a clear-margin resection benefited from a 7-month survival increase with chemotherapy (median survival of 20.8 months vs. 13.8 months), but the effect was less pronounced in R1 resections (median survival of 15 months vs. 13.2 months). This finding was in agreement with Stocken who noted that chemotherapy was less effective in patients with a positive resection margin.

A published network meta-analysis[159] examined overall survival in patients receiving adjuvant gemcitabine or 5-FU in comparison to observation. Results suggested that adjuvant therapy with either gemcitabine (*n* = 774) or 5-FU (*n* = 876) showed a survival benefit in comparison with observation alone (*n* = 670) with hazard ratios of 0.68 (95%CI: 0.44-1.07) and 0.62 (95%CI: 0.42-0.88) respectively. No significant survival difference was noted in comparing adjuvant gemcitabine and 5-FU, though grades 3-4 non-haematological toxicity was almost four-times as common in patients receiving the latter drug.

Table 6: Meta-analyses of adjuvant chemotherapy trials in pancreatic cancer

			Survival (95%CI)		
Year published	**Author**	**Arm (*n*)**	**Median survival (months)**	**2-year survival (%)**	**5-year survival (%)**
2005	Stocken[153]	CT (348) No CT (338)	19 (16.4-21.1) 13.5 (12.2-15.8)	38 28	19 12
2007	Boeck[157]	CT (482) No CT (469)	3 month (0.3-5.7) survival benefit with CT *vs* no CT (p = 0.03)	_____	3.1% (-4.6-10.8) survival benefit with CT *vs* no CT (p > 0.05)
2008	Butturini[158]		R0 Resections		
		CT (236) No CT (222)	20.8 (17.7-23.2) 13.8 (12.2-16.4)	42 (35-48) 27 (21-33)	22 (17-28) 10 (5-14)
			R1 Resections		
		CT (109) No CT (114)	15 (11.7-18.1) 13.2 (10.5-17.6)	29 (20-38) 31 (22-40)	14 (7-21) 17 (10-24)
2013	Liao[159]		**Hazard ratio for death (95%CI)**		
		Fluorouracil (876) Observation (670)	0.62 (0.42-0.88)		
		Gemcitabine (774) Observation (670)	0.68 (0.44-1.07)		
		Gemcitabine (774) Fluorouracil (876)	1.1 (0.70-1.86)		

CT: Chemotherapy.

A handful of meta-analyses have examined the benefit of adjuvant chemotherapy following a pancreatic cancer resection. Table modified from Jones et al.[152]

Major Chemoradiotherapy Trials in Pancreatic Cancer

The Gastrointestinal Study Group (GITSG) was the first randomised trial evaluating the role of adjuvant therapy in pancreatic cancer[155 156]. In non-resectable patients, previous studies had shown the benefit of both radiotherapy[160] and 5-FU combined with radiotherapy[161] and on this basis GITSG compared adjuvant 5-FU chemoradiation versus no adjuvant therapy. Though the study population was small, final analysis of the data revealed a substantial median survival benefit with treatment and following this evidence, chemoradiotherapy became a standard adjuvant treatment option for pancreatic cancer patients in the United States[162]. A decade later, the findings from GITSG were supported by a prospective, non-randomised study in which Yeo *et al*[163] demonstrated an improved median and one-year benefit with adjuvant chemoradiotherapy in comparison to observation with a median and one-year survival of 19.5 months and 80%, in comparison to 13.5 months and 54% in those undergoing observation alone (p = 0.003).

The EORTC study[154] was undertaken across twenty-nine European centres and included 218 patients who had undergone resection for pancreatic or ampullary lesions. One hundred and fourteen of these were for pancreatic head cancers and those tumours graded as ≥T3 or N1b nodal disease were excluded. Patients were assigned surgery alone or to additionally receive two four-week cycles of adjuvant 5-FU and concurrent radiotherapy. When considering the pancreatic group alone, median two and five-year survival was improved in the treatment group. The pattern of recurrent locoregional and distant metastases was similar in both groups, suggesting that adjuvant radiotherapy is ineffective against pancreatic/ampullary cancer.

ESPAC-1 showed no survival benefit in those receiving chemoradiotherapy. These findings were echoed when evaluating patients in the 2X2 study design alone, comparing those patients receiving chemoradiotherapy alone (median survival of 15.8 months (95%CI: 13.5-19.4) with all others (median survival 17.8 months (95%CI: 14-23.6): this did not reach statistical significance.

Final analysis of the 2X2 data showed that chemoradiotherapy had a negative effect on patient survival with a median survival of 15.9 months (95%CI: 13.7-19.9) in those that received chemoradiotherapy and 17.9 months (95%CI: 14.8-23.6), p = 0.05 in patients that

did not. Estimated 5-year survival was 10% in the chemoradiotherapy cohort in comparison to 20% in those patients who received none. In those patients randomised outside the 2X2 study design, median survival was only 13.9 months (95%CI: 12.2-17.3) amongst the 73 patients who had received chemoradiotherapy. This was in comparison to a median survival of 16.9 months (95%CI: 12.3-24.8) in those who underwent surgery alone and 21.6 months (95%CI: 13.5-27.3) in those who underwent adjuvant chemotherapy without any chemoradiation. Estimated 5-year survival in these individual treatment groups was 7%, 11% and 29% respectively. Though this is strongly suggestive that adjuvant chemoradiation has a negative impact on survival, ESPAC-1 was underpowered to directly assess these smaller cohorts outside the 2X2 design. The authors suggest that the lack of survival benefit with chemoradiation may be due to a delay in administering the treatment to patients who were also receiving chemotherapy. Some have argued that the radiotherapy given during ESPAC-1 was substandard and not subject to rigorous quality control, though the survival rates achieved in the individual groups were similar to those achieved in other major studies[164].

Following the publication of their interim findings in 2008[165], the final 5-year analysis of the RTOG 97-04 study was published in 2011[166]. Patients were stratified to receive either gemcitabine or 5-FU both prior to, and after 5-FU based chemoradiation. No significant difference was identified in overall or disease-free survival in the final analysis. Worth noting, is though completion rates for designated treatments were equally high (87% in the 5-FU group and 90% in the gemcitabine group), those in the latter group experienced greater numbers of haematological ($p < 0.001$) and Grade 4 events ($p < 0.001$) secondary to acute toxicity. A subgroup analysis from RTOG was undertaken observing those with pancreatic head tumours. The difference in median survival between both groups was not statistically significant, being 17.1 months in the 5-FU group and 20.5 months in the gemcitabine group (HR = 0.933, 95%CI: 0.76-1.15, log rank $p = 0.51$). However, following adjustment for stratification variables including nodal status, tumour size and surgical margins, multivariate analysis suggested a benefit with gemcitabine over 5-FU (HR = 0.80, 95%CI: 0.63-1.00, $p = 0.05$).

A Phase III randomised trial published in 2012 compared adjuvant chemoradiation, including 5-FU, cisplatin and interferon α-2b (Group 1) with adjuvant 5-FU and folinic acid without

chemoradiation (Group 2). CapRI[167] followed a similar Phase II trial which reported a promising 5-year survival rate of 55%[168]. Overall survival and disease free survival was not significantly different between the two groups. However, the median survival data from the per-protocol population are amongst the best published, being 32.1 months (95%CI: 22.8-42.2) in group 1, and 28.5 months (95%CI: 19.5-38.6) in group 2 (HR = 1.2, 95%CI: 0.49-2.95, p = 0.49). Selection bias was unlikely, given that 97% of tumours were T3 and above, 79% of patients had nodal disease and only 61% of patients underwent an R0 resection. The authors conceded that these impressive survival figures are unlikely to be due to adjuvant therapy alone, and acknowledge that the vast majority of patients underwent an aggressive soft tissue clearance during their resection in Heidelberg. Nevertheless, these results seem to have been achieved at the expense of very high levels of toxicity, with 85% of patients receiving chemoradioimmunotherapy experiencing grades 3 or 4 toxicity which were mainly haematological in origin. In a separate study[169] this controversial regime led to a 93% grade 3 and 4 gastrointestinal toxicity rate, leading to its abandonment (Table 7).

Table 7: Major adjuvant chemoradiotherapy trials in pancreatic cancer

			Final analysis			Survival (95%CI)				Disease-free survival (95%CI)	
Year published	**Author/Group**	**Treatment arms (*n*)**	**T3**	**N+**	**R0**	**Median survival (months)**	**2-year survival (%)**	**3-year survival (%)**	**5-year survival (%)**	**Median DFS (months)**	**2-year DFS (%)**
1985	GITSG[156 156]	CRT (21) Surgery alone (22)	37	28	100	21 10.9	43 (0.25-0.63) 18 (0.08-0.36)	N/A	N/A	N/A	N/A
1999	EORTC[154]	5-FU/RT (104) Surgery alone (103)	21	46	77	24.5 19 (log rank p = 0.208)	51 (41-61) 41 (31-51)	N/A	28 (17-39) 22 (12-32)	17.4 16 (p = 0.643)	38 (28-48) 37 (27-47) (p = 0.643)
		5-FU/RT (60) Surgery alone (54)	0	51	N/A	17.1 12.6 (log rank p = 0.099)	37 (24-50) 23 (11-35)	N/A	20 (5-35) 10 (0-20)	N/A	N/A
2001	ESPAC-1 (All patients)[138]	CRT +/- 5-FU/Folinic Acid (175) No CRT +/- 5-FU/Folinic acid (178)	N/A	56	82	15.5 (13.5-17.4) 16.1 (13.1-20.1) (HR = 1.18, 0.9-1.55, p = 0.24)	N/A	N/A	N/A	N/A	N/A
	ESPAC-1 (2x2 design only)	CRT +/- 5-FU/Folinic Acid (142) No CRT +/- 5-FU/Folinic acid (143)	N/A	N/A	N/A	15.8 (13.5-19.4) 17.8 (14-23.6) (HR = 1.3, 0.96-1.77, p = 0.09)	N/A	N/A	N/A	N/A	N/A
2004	ESPAC-1 (2x2 final analysis)[139]	CRT +/- 5-FU/Folinic Acid (145) No CRT +/- 5-FU/Folinic acid (144)	N/A	53	82	15.9 (13.7-19.9) 17.9 (14.8-23.6) (HR = 1.28, 0.99-1.66, p = 0.05)	29 41	N/A	10 20	N/A	N/A
	ESPAC-1 (Individual Treatment Groups)	5-FU/Folinic Acid (75) CRT + 5-FU/Folinic Acid (72) Observation (69) CRT (73)	N/A	N/A	N/A	21.6 (13.5-27.3) 19.9 (14.2-22.5) 16.9 (12.3-24.8) 13.9 (12.2-17.3)	N/A	N/A	29 13 11 7	N/A	N/A
2006	RTOG 97-04[165]	CRT + 5-FU (230) CRT + Gemcitabine (221)	75	66	66	No significant difference	N/A	N/A	N/A	N/A	N/A
		CRT + 5-FU (201) CRT + Gemcitabine (187)	N/A	N/A	N/A	16.9 20.5 (HR = 0.82, 0.65-1.03, p = 0.09)	N/A	22 31	N/A	N/A	N/A
2011	RTOG 97-04 (5-year analysis)[166]	CRT + 5-FU (230) CRT + Gemcitabine (221)	75	66	66	No significant difference HR = 0.933, 0.76-1.145, p = 0.51	35 40	23 27	19 19	No significant difference	N/A
		CRT + 5-FU (201) CRT + Gemcitabine (187)	N/A	N/A	N/A	17.1 20.5	34 42	21 28	18 (13-24) 22	N/A	N/A
2012	CapRI (Schmidt)[167] 167	5-FU/Cisplatin/Interferon α-2b → RT → 5-FU (53) 5-FU/Folinic acid (57)	97	79	61	32.1 (22.8-42.2) 28.5 (19.5-38.6) (HR = 1.2, 0.49-2.95, p = 0.49)	N/A	N/A	N/A	15.2 (10.3-24.8) 11.5 (9.8-17.6) (p = 0.61)	N/A

The role of adjuvant chemoradiotherapy in pancreatic cancer is a controversial topic with many conflicting studies. Table modified from Jones et al.[152]

Meta-analysis of Adjuvant Chemoradiotherapy Trials

In addition to the analysis of adjuvant chemotherapy data, Stocken *et al*[153] also pooled individual patient data from ESPAC-1 2X2[138], ESPAC-1 Plus[139] and EORTC[154] to assess the benefit of adjuvant chemoradiotherapy. Despite borderline heterogeneity, no significant difference in the risk of death was observed with chemoradiotherapy. The GISTG trial[155 156] was unfortunately unable to provide individual patient data and therefore summary data was utilised. Though heterogeneity was increased by the addition of the GISTG summary data to the individual data from other studies, the pooled HR again showed no difference in the risk of death between those receiving chemoradiotherapy and those not.

Butturini's meta-analysis[158] on adjuvant therapy and resection margins noted no significant survival advantage with chemoradiation in patients with clear resection margins (HR = 1.19, 95%CI: 0.95-1.49). Though remaining statistically insignificant, there was evidence of a small survival benefit with adjuvant chemoradiation in patients receiving an R1 resection (HR = 0.72, 95%CI: 0.47-1.10).

Liao *et al*'s meta-analysis[159] was the first to directly compare chemoradiation combined with either 5-FU or gemcitabine with each treatment in isolation. No survival advantage was demonstrated by adding chemoradiation to either adjuvant 5-FU or gemcitabine with all hazard ratios approaching 1. However, the addition of chemoradiation to 5-FU (HR = 2.85, 95%CI: 0.15-61.44) or gemcitabine (HR = 36.49, 95% CI: 0.34-3235.7) dramatically increased toxic events in comparison to the use of the chemotherapeutic agent alone. The authors conclude that on the basis of their results, future trials with chemoradiation are not required citing toxicity, resistance and early tumour dissemination as possible reasons why chemoradiotherapy to the tumour bed may be ineffective in pancreatic cancer (Table 8).

Table 8: Meta-analyses of adjuvant chemoradiotherapy trials in pancreatic cancer					
			Survival (95%CI)		
Year published	**Author**	**Arm (*n*)**	**Median survival (months)**	**2-year survival (%)**	**5-year survival (%)**
2005	Stocken[153]	CRT No CRT	15.8 (13.9-18.1) 15.2 (13.1-18.2)	30 34	12 17
2008	Butturini[158]		R0 Resections		
		CRT (188) No CRT (183)	15.9 (14-18.5) 15.8 (13.4-20.1)	30 (23-36) 38 (31-45)	10 (5-15) 20 (13-26)
			R1 Resections		
		CRT (53) No CRT (53)	14.7 (11.5-20.5) 11.2 (9.4-16.7)	30 (17-42) 19 (8-31)	18 (7-29) 8 (0-16)
2013	Liao[159]		**Hazard ratio for death (95%CI)**		
		Chemoradiation (169) Observation (670)	0.91 (0.55-1.46)		
		Chemoradiation + 5-FU (323) 5-FU (876)	0.87 (0.27-2.69)		
		Chemoradiation + 5-FU (323) Chemoradiation (169)	0.59 (0.19-1.74)		
		Chemoradiation + Gemcitabine (221) Chemoradiation + 5-FU (323)	0.82 (0.4-1.71)		

Meta-analyses show no benefit to adjuvant chemoradiotherapy in pancreatic cancer. Table modified from Jones et al.[152]

Treatment of Advanced Disease

Background

For the majority of patients, curative treatment by tumour resection is not an option due to locally advanced or metastatic disease. In such patients, systemic chemotherapy has been shown to prolong survival in comparison to supportive management[170]. Other palliative management options include analgesia, nerve blocks, radiotherapy, surgical bypass and endoscopic stenting to avert biliary and gastrointestinal obstruction.

Gemcitabine

In 1997, the nucleoside analogue, gemcitabine was established as the palliative agent of choice in pancreatic cancer by Burris *et al*[142] who demonstrated a survival benefit in comparison with 5-FU (median survival of 5.6 months vs. 4.4 months). The treatment was generally well tolerated, and though gemcitabine led to an increased risk of toxicity, this was statistically insignificant. Recent chemotherapy trials in pancreatic cancer have been required to demonstrate the superiority of any novel treatment to gemcitabine monotherapy. This could be achieved by either one of two strategies: by combining gemcitabine with a new drug, or by directly comparing a novel monotherapy against gemcitabine.

Erlotinib

The eGFR inhibitor Erlotinib was the first drug to be shown to be of benefit in combination with gemcitabine in patients with advanced pancreatic cancer. In this study (the PA.3 trial), a Canadian group randomised 569 patients with both locally advanced and metastatic disease to receive gemcitabine, or gemcitabine plus erlotinib[171]. Though overall survival was significantly improved with combination therapy (median survival of 6.2 vs. 5.9 months), in real-terms this is only a fortnight's benefit. This marginal benefit also came at the expense of toxicity, with six treatment-related deaths reported during the study – all within the combination therapy group. Eight patients from the study (7 from the erlotinib cohort) also developed interstitial lung disease and the risk-benefit of this drug combination remains a controversial topic[172].

Interestingly, a small subset of patients responded unusually favourably to a combination of erlotinib and gemcitabine. It was noted that some patients developed a rash, with those

individuals with a rash of Grade ≥2 in severity recording s median survival of 10.5 months and 1-year survival of 43% in comparison with 5.3 months and 16% respectively in patients with no rash. This finding was replicated in a further study[173], which led to a dose-escalation study[174] which unfortunately showed no further benefit.

FOLFIRINOX

FOLFIRINOX is a chemotherapy regime consisting of four drugs – Folinic acid, 5-FU, irinotecan and oxaliplatin. This combination of drugs could be justified by preclinical studies, which demonstrated either single agent efficacy against pancreatic cancer, or synergistic activity in combination with a fellow agent. Following promising results from phase I and II trials[175] [176], a large randomised trial was undertaken to compare FOLFIRINOX with gemcitabine monotherapy as the first-line treatment of patients with metastatic pancreatic cancer, with the results published in 2011. This French study (ACCORD-4 Trial) enrolled 342 patients aged between 18 and 75 with a performance status of either 0 (fully active) or 1 (restricted only by physically strenuous activity) with histologically proven metastatic pancreatic adenocarcinoma. Compared with gemcitabine, treatment with FOLFIRINOX resulted in a superior tumour response rate (9.4% vs. 31.6%), median overall survival (6.8 vs. 11.1 months) and one-year survival (20% vs. 48%)[177]. The production of these results during the interim analysis led to the premature termination of the study.

Despite this study's encouraging results, criticisms have been made. The first is its highly exclusive inclusion criteria, selecting only the fittest patients under the age of 76. A Canadian group undertook a retrospective analysis of 100 consecutive patients of theirs with metastatic pancreatic cancer and demonstrated that only 26 of these would have been eligible with nearly two-thirds of patients excluded on the basis of inadequate performance status and over one-fifth excluded due to advanced age[178]. Secondly is the issue of toxicity, with one study reporting that one-third of patients receiving FOLFIRINOX were hospitalised as a direct result[179], with a further paper reporting the discontinuation of treatment in a similar proportion of patients[180]. In contrast to these findings, further data published from the index study[181] disclosed that quality of life impairment was significantly reduced in the FOLFIRINOX group compared to gemcitabine indicating its acceptability to patients. However, it is widely acknowledged that though FOLFIRINOX is viewed amongst the most effective palliative treatments, it is a viable option for only a minority of patients[182]. Its

survival benefit must be balanced against its associated toxicities which is a decision that must be made on a patient by patient basis.

In locally advanced disease, the outcomes of FOLFIRINOX treatment have only been reported in small retrospective series[179 183 184 185]. These studies show that in certain patients, FOLFIRINOX can induce adequate tumour shrinkage to enable an R0 resection, with some studies also administering chemoradiation. However, no long term survival is reported and one study stated that 3 out of 5 patients developed metastatic disease within 5 months of an R0 resection following neoadjuvant FOLFIRINOX[185].

Nab-Paclitaxel (Abraxane®)

In a murine model, albumin-bound paclitaxel demonstrated synergistic anti-tumour activity in combination with gemcitabine[186]. On this basis, the combination was introduced in a phase I-II clinical trial as a first line treatment in patients with metastatic pancreatic cancer. Results showed an acceptable safety profile and an impressive median survival of 12.2 months[187].

In 2013, the results of an international, phase III randomised trial (MPACT) was published, based on 692 deaths in 861 patients[188] with metastatic pancreatic cancer with more mature data published in 2015[189]. In the original paper, median survival for patients receiving gemcitabine alone was 6.7 months, in comparison to 8.5 months in patients receiving a combination of gemcitabine and nab-paclitaxel. One-year survival was also significantly improved with combination therapy (35% vs. 22%), in addition to the drug-response rate (23% vs. 7%), the median time to treatment failure (5.1 vs. 3.6 months) and progression-free survival (5.5 months vs. 3.7 months). Toxicity was generally comparable in both treatment groups and though combination therapy led to an increased risk of myelosuppression and peripheral neuropathy, these were reversible[190].

In contrast to the FOLFIRINOX vs. gemcitabine study, 10% of this study's patients were aged >75 with 8% of its cohort possessing a performance status of >1. On this basis, nab-paclitaxel has been approved in combination with gemcitabine for the treatment of metastatic pancreatic cancer and can be a valuable option in patients deemed unsuitable for FOLFIRINOX.

As with FOLFIRINOX, studies are ongoing in patients with borderline resectable (NCT01470417[191]) and locally advanced disease (NCT02301143[192]) to determine the efficacy of nab-paclitaxel combined with gemcitabine, with some positive anti-tumour findings already reported in patients with resectable disease[193].

Gemcitabine and Capecitabine

Capecitabine is a fluoropyrimidine which has been shown to exert synergistic antitumour activity when combined with gemcitabine[194]. A meta-analysis of three randomised controlled trials (*n* = 935) compared gemcitabine with gemcitabine plus capecitabine (Gemcap) in advanced pancreatic cancer[195]. This showed an overall survival benefit with the latter treatment (HR = 0.86, 95%CI: 0.75-0.98, *p* = 0.02) with no intertrial heterogeneity.

Selected Negative Clinical Studies Utilising Gemcitabine Combination Therapy

Despite promising preclinical early clinical results, a handful of novel agents have been trialled in large randomised phase II and III trials in combination with gemcitabine in metastatic pancreatic cancer. The anti-VEGF agent Bevacizumab[196], the EGFR receptor inhibitor Cetuximab[197], the anti-IGFTR antibody ganitumab, the TRAIL-R2 targeting conatumumab[198] and lastly the tyrosine-kinase inhibitor axitinib[199] have all failed to show any significant survival benefit in this setting.

Selected Ongoing Phase III Trials in Pancreatic Cancer

It is extremely encouraging to see several Phase III trials that, at the time of writing, are recruiting patients to further investigate the role of novel therapies in the various stages of pancreatic cancer.

Adjuvant Therapy for Resected Pancreatic Cancer

Given its promising results in the advanced setting, FOLFIRINOX is currently subjected to a two armed Phase III trial in opposition to gemcitabine in resected pancreatic cancer with the aim of recruiting 490 patients with a primary outcome of disease-free survival at three years (NCT01526135[200]).

One of the more recent Phase III studies to commence recruiting is the 'Apact' study to trial adjuvant gemcitabine vs. gemcitabine plus nabpaclitaxel (NCT01964430[201]). Based on such positive results in the advanced cancer setting, this international trial aims to recruit 800 patients with an estimated completion date in 2020.

After displaying a borderline benefit in overall survival and progression-free survival compared to gemcitabine in advanced pancreatic cancer, the tyrosine-kinase inhibitor erlotinib is being investigated in the adjuvant setting. A Phase II trial[202] combined these two compounds in the adjuvant setting achieving a respectable median disease-free survival of 14 months. Furthermore, a single-institution Phase II trial[203] (*n* = 48) has also shown that erlotinib can be safely utilised alongside capecitabine and chemoradiotherapy. Currently, erlotinib is being trialled both in combination with gemcitabine vs. gemcitabine alone (DRKS00000247[204]) and in a separate trial, this will be followed by a course of either capecitabine or 5FU-based chemoradiotherapy (NCT0103649[205]).

Platinum compounds have previously been safely utilised in various pancreatic cancer trials and particularly encouraging results have been achieved in the neoadjuvant setting[206 207]. On this basis, phase III trials are now incorporating platinum agents into their chemotherapy regimens. The Hyperthermia European Adjuvant Trial (HEAT) study (NCT01077427[208]) will compare adjuvant gemcitabine to adjuvant gemcitabine plus capecitabine plus regional hyperthermia treatment – a regime that has previously been utilised with low reported toxicity. It has been shown that heat can increase the cytotoxicity of certain chemotherapeutic agents[209] including gemcitabine[210] in *in vitro* experiments with pancreatic cancer cell lines. One phase II study[211] combined gemcitabine with regional heat treatment in the treatment of both metastatic and locally advanced disease. Median survival was 8 months in the entire study population, but extended to 17.7 months in those with localised disease. More recently, a retrospective analysis of 23 patients with gemcitabine refractory inoperable disease was published[212] whereby patients received gemcitabine plus cisplatin alongside regional hyperthermia biweekly for four months. Though 21/23 patients suffered from metastatic disease at recruitment, a median overall survival of 12.9 months was achieved.

Lastly, a trial utilising the immunotherapeutic agent algenpantucel-L in the adjuvant setting has recently completed recruitment and is comparing gemcitabine +/- 5FU chemoradiation both with, and without this novel agent (NCT01072981[213]). A phase II trial[214] combining algenpantucel-L with gemcitabine and 5FU-based chemoradiotherapy yielded a 1-year disease-free survival of 62% and a one-year survival of 86%.

Neoadjuvant Therapy for Resectable, Borderline Resectable and Locally Advanced Pancreatic Cancer

The majority of patients with resectable pancreatic cancer will progress immediately to resection followed by adjuvant chemotherapy - commonly gemcitabine. An ongoing study led by the University of Zurich (NCT01314027[215]) is using this as their control arm, with a second cohort of patients receiving neoadjuvant gemcitabine and oxaliplatin prior to resection.

Two phase III trials are currently recruiting to further delineate the role of FOLFIRINOX in the management of locally advanced, unresectable pancreatic cancer. An American study (NCT01926197[216]) will investigate the progression-free survival benefit of combining 5-FU chemoradiation with FOLFIRINOX vs. FOLFIRINOX alone. A German group (NCT01827553[217]) will administer neoadjuvant FOLFIRINOX to all recruited patients. This will be followed by a randomisation to receive either further FOLFIRINOX or gemcitabine-based chemoradiotherapy, with a primary outcome of overall survival.

A further phase III trial (NCT01836432[218]) is inclusive of patients with borderline resectable and unresectable disease. Individuals in the control arm will receive FOLFIRINOX followed by 5-FU chemoradation, with the second arm receiving the immunotherapy algenpantucel-L in combination with FOLFIRINOX prior to the chemoradiation.

Future Directions and Biomarkers in Pancreatic Cancer

Genetic analysis has revealed that, on average, pancreatic cancers possess 63 exomic alterations across a dozen cellular signalling pathways[219]. This vast heterogeneity between tumours goes some way in explaining globally poor responses to current neoadjuvant and adjuvant therapies. There is an urgent need to identify biomarkers to predict patient response to both current and novel treatments in order to personalise therapy to each patient and tumour. The identification of such a biomarker in breast cancer (HER2[220]) has dramatically improved survival with the development of specifically targeted therapies. For this reason, current and future studies in pancreatic cancer are strongly advised to include biomarkers as an element of their trials[221].

Some progress has already been made in this regard with the secreted protein acidic and rich in cysteine (SPARC). Tumour SPARC expression has been shown to have no correlation

with the efficacy of nab-Paclitaxel plus gemcitabine or gemcitabine monotherapy in metastatic cancer[222]. On the other hand, elevated tumour levels of the gemcitabine-transporter, human nucleoside transporter equilibrative type 1(hENT1) has been associated with improved survival in ESPAC-3 patients administered adjuvant gemcitabine[223]. This was not supported by data from a cohort of patients with metastatic disease[224], though a later publication raised concerns regarding the antibody used (SP120 rabbit monoclonal antibody)[225].

Immunotherapy

Checkpoint inhibitors and other form of immunotherapy promise much for the future treatment of pancreatic cancer, but as yet there have been no successful trials. In mouse models, depletion of macrophages or fibroblasts expressing Fibroblast Activation Protein (FAP) restores immune control[226]. FAP positive fibroblasts express CXCL12 which can form a dimer with HMGB1 (expressed by pancreatic cancer cells) to activate the suppressor CXCR4 on T-Effs (T-effector cells). In mouse models, inhibition of CXCR4 using AMD3100 (Plerixafor) allowed accumulation of T-Effs in the tumour[227].

Gemcitabine

Background

The development of gemcitabine (2','-difluoro 2'deoxycytidine or dFdC) in the 1980s at Lilly Research Laboratories (Eli Lilly and Co., USA)[228], has arguably been the single most important step in the improved survival of patients with pancreatic cancer. Interestingly, the drug was originally developed as an antiviral but showed such impressive anti-tumour activity in the preclinical setting that it was developed as a chemotherapeutic agent.

Cellular Transport of Gemcitabine

Gemcitabine is an intravenously delivered drug and its intracellular delivery is dependent on human nucleoside transporters (hNTs), which are split into two distinct types – the sodium-dependent concentrative type (hCNT) and the sodium independent equilibrative type (hENT)[229]. Both hNT types are involved in the transport of gemcitabine into cells, including two of the three former type (hCNT1 and hCNT3), and two from four (hENT1 and hENT2) of the latter. The majority of gemcitabine uptake is dependent on hENT1 with the remaining three contributing to a lesser extent[230 231]. hENTs differs from hCNTs on the basis that the former can pump gemcitabine in both directions across the cell membrane[232].

The Activation of Gemcitabine Metabolites

Gemcitabine is a prodrug, which requires intracellular phosphorylation into its active metabolites. It is first phosphorylated by deoxycytidine kinase (dCK) to gemcitabine monophosphate (dFdCMP), which is recognised as the rate-limiting step in producing gemcitabine metabolites (Figure 3). Further phosphorylation of dFdCMP to gemcitabine diphosphate (dFdCDP) is undertaken by pyrimidine nucleoside monophosphate kinase (UMP-CMP kinase)[233]. Gemcitabine triphosphate (dFdCTP) results from a final phosphorylation[234]. Though it remains unclear which enzyme is responsible, nucleoside diphosphate kinase has previously been implicated in this step[235].

The Inactivation of Gemcitabine Metabolites

Gemcitabine and its individual metabolites can be inactivated at various stages, though the resulting compounds may exert further toxic effects. dFdC deamination by cytidine deaminase (CDA), produces 2'-2'- difluoro-2'-deoxyuridine (dFdU). In addition to being itself cytotoxic, dFdU also regulates multiple gemcitabine activities. dFdU monophosphate

(dFdUMP) has been shown to inhibit thymidylate synthase[236] which causes imbalances in the deoxynucleotide tri- phosphate (dNTP) pool[237], leading to DNA damage[238].

Gemcitabine's monophosphate form (dFdCMP) can be inactivated by either deamination by deoxycytidylate deaminase (dCTD) or by de-phosphorylation by 5-nucleotidases (5'-NTs)[239]. 5'NTs catalyse the conversion of nucleotides to nucleosides, are also therefore involved in maintaining dNTP pools.

The Mechanism and Effects of Gemcitabine

Masked Chain Termination

Gemcitabine has several intracellular targets, of which many inhibit the synthesis of DNA. DNA polymerase, which assembles nucleotides into DNA, is inhibited by dFdCTP[240], which itself is also incorporated into DNA. The addition of this extra nucleotide into the DNA chain results in the termination of its elongation, a process described as 'masked chain-termination[241]'. Due to dFdCTP's non-terminal position in the chain, it will elude any DNA repair mechanism[242]. A gemcitabine metabolite, again thought to be dFdCTP also incorporates into RNA, though its effects are unclear at present[243].

The Self-potentiating Effects of Gemcitabine

Gemcitabine metabolites exhibit inhibitory effects on several enzymes, resulting in feedback loops to enhance its own actions. dFdCDP inhibits ribonucleotide reductase (RR), resulting in a reduction in the dNTP pool and therefore a drop in dCTD and dCTP levels[244]. dCTP is a potent inhibitor of dCK, and it has been shown that this enzyme's phosphorylation of dFdC is the rate-limiting step in the production of gemcitabine metabolites[245]. Therefore, the inhibition of RR by dFdCDP results in the increased action of dCK in phosphorylating gemcitabine.

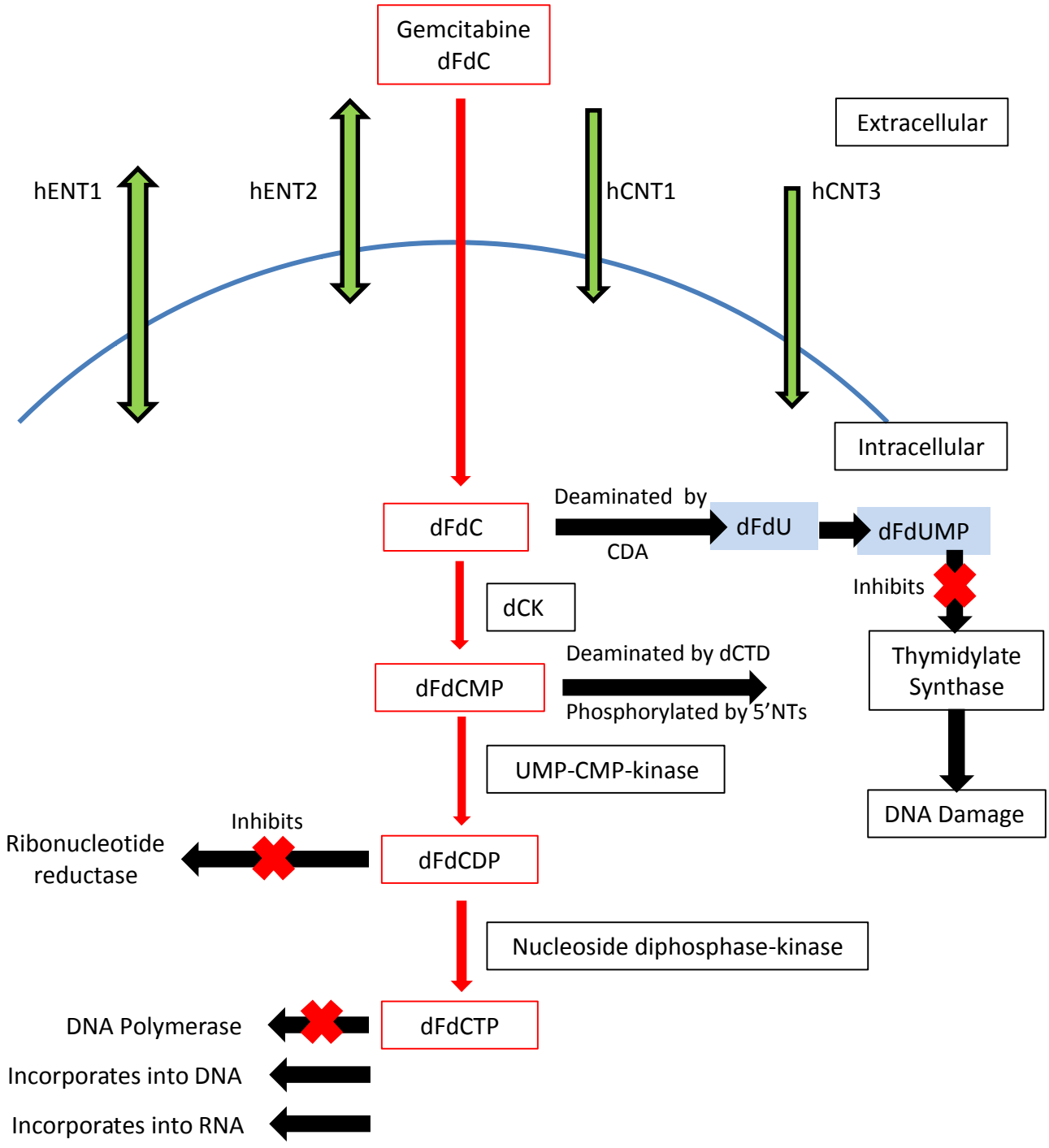

Figure 3: Gemcitabine metabolism

A schematic diagram exhibiting the transport mechanisms of gemcitabine, its intracellular metabolism and key downstream effects.

The Cell Cycle Effects of Gemcitabine

As a result of its DNA damaging effects, gemcitabine has been previously shown to induce the S-phase cell cycle checkpoint[246]. Mammalian cellular stress during S-phase activates Chk1 and Chk2 through the ATM (Ataxia Telangiectasia) pathway[247], activating both the G1 and G2/M checkpoints and causing cell cycle arrest[248]. In addition to the S-phase checkpoint, gemcitabine has also been shown to induce the G1 and G2/M checkpoints in pancreatic cancer cells via the Chk1 and Chk2 pathways. Downstream effects of these pathways result in cdc25A degradation and cell cycle arrest[249].

Multiple publications involving a variety of malignant cell lines show that gemcitabine causes a transient S-phase arrest at lower concentrations, with higher drug concentrations leading to the termination of cell cycle progression[250 251 252].

The Induction of Apoptosis by Gemcitabine

Though gemcitabine is an S-phase specific agent[253], its effects in killing cells is not confined to this. Loss of viability has been demonstrated in cells incubated with gemcitabine for only 4 hours, indicating that its metabolites are retained for several hours, allowing for the majority of the cell population to proceed through the cell cycle[241]. In addition, the drug's destructive effects have been shown to be effective in cell populations undergoing log-phase growth and in confluence[254]. Several pathways have been implicated in gemcitabine-induced apoptosis[255] and it has been demonstrated that this process is caspase-dependent in pancreatic cancer[256 257]. The activation of the p38 mitogen-activated protein kinase (MAPK) pathway, which interacts closely with the tumour-suppressor p53, has also been shown to be involved[258].

Gemcitabine Resistance and Combination Therapies

As with many chemotherapeutic agents, gemcitabine resistance can either be predetermined or acquired[259]. In accordance with gemcitabine's mechanism of action, diminished levels of hENT1[223 260], hCNT1[261] and dCK[262], and elevated expression of both RR subunits, RRM1[263] and RRM2[264] have all been proposed as markers of gemcitabine resistance.

Due to the high prevalence of gemcitabine resistance in pancreatic cancer patients, the development of novel agents to be utilised as an alternative monotherapy or in combination

with gemcitabine is imperative. Gemcitabine lacks cross-resistance with other chemotherapy drugs and is therefore an ideal option for combination therapy. Both *in vivo* and in *vitro*, it has already demonstrated synergy with several other drugs including cisplatin, taxanes, antifolates and trastuzumab[243].

Polo-like kinases

Background

Polo like kinases (PLKs) are a family of serine/threonine kinases. First to be discovered was 'polo' in *Drosophila melanogaster*[265] during a screen for mutants affecting spindle pole behaviour in the 1980s[266]. With the exception of plants and apicomplexans, polo-like kinases are found in all eukaryotes, and in humans are simply recognised numerically as PLK1-5.

Based on phylogeny, three subfamilies of Polo-like kinases are now recognised – PLK1, PLK2 (originally known as Snk) and PLK4 (originally known as SAK - Snk akin kinase[267]). Differing orthologs of PLKs are seen in various species, such as plo1, Cdc5 and polo as variants of PLK1 and zyg-1, sak and Plx4 as variants of PLK4. The PLK2 subfamily, which in humans includes PLK2, PLK3 (previously known as Fnk or Prk) and PLK5, is only seen in vertebrates and in some bilaterians (animals with bilateral symmetry such as the sea urchin). Though *Xenopus* contains an ortholog (Plx5), PLK5 is only seen in the mammalian genome, with neither variant seen in birds or fish[268].

PLK1 localizes to chromosomes during early mitosis, before transferring to the spindle midzone during late mitosis[269]. Such proteins, which also include Aurora and inner centromere protein (INCENP), are proposed to control mitotic events, including chromosome segregation and cytokinesis and are referred to as passenger proteins[270].

Structure and Function of Polo-like kinases

Brief Structure

Polo-like kinases are proteins that broadly consist of an N-terminal serine/threonine kinase catalytic domain and a C-terminal, which encompasses either one or two Polo-box domains (PBDs)[271]. Adjoining the kinase and polo-box domains is a linker region and a small segment known as the polo-box cap[272 273]. Utilising ATP; an active serine/threonine kinase phosphorylates the hydroxyl group from the side chain of serine or threonine amino acid residue present on a protein or substrate. This produces ADP and a phosphorylated protein.

The Kinase Domain

Kinase domains consist of two lobes made of polypeptide chains, connected by a 'hinge region' to allow rotation[274]. These chains accommodate ATP molecules for binding in a cavity between both limbs. This ATP-binding pocket structure is highly conserved among all

PLKs[275], with the ATP-binding site motif being Gly-X-Gly-X-Phe-Ala (where X represents any amino acid) in comparison to Gly-X-Gly-X-X-Gly commonly encountered in other kinases[276]. As similar ATP-binding pockets are exhibited by all protein kinases[277], this can provide a challenge in developing highly specific kinase inhibitors[278].

The kinase domains are conserved among all PLKs with the exception of PLK5. Due to a stop codon in exon 6, human PLK5 only possesses a short form of the kinase domain compared to its murine equivalent which contains a complete kinase domain[268]. This has led human PLK5 being described in the literature as 'kinase-dead'[279] or possessing a 'pseudokinase'[280].

The first step in the activation of the kinase domain is the cessation of the Polo-box's inhibitory effect upon the kinase. This is achieved by a phosphopeptide ligand occupying the PBD which leads to the release of the catalytic domain. Like many other kinases, PLKs are activated through phosphorylation by specific proteins. In PLKs, this process requires the phosphorylation of a threonine on a short segment of the catalytic kinase domain. This region is known as the T-loop, alternatively named the activation loop[281].

The Polo-box Domain

The Polo-box is a conserved amino-acid motif which both regulates the function of the kinase domain and dictates its substrate specificity[272 282]. PLKs 1, 2, 3 and 5[279] each have two Polo-boxes at their C-terminus with PLK4 only possessing one[283]. Alternatively, PLK4 has an additional 'crypto Polo-box' which has weaker homology with the Polo-box domain[283 284 285] and for this reason does not form a Polo-box domain binding pocket like other PLKs[278]. The region containing both Polo-boxes is jointly known as the Polo-box domain[286].

Polo-boxes function by folding on each other to create a 'pincer' which contains a phosphopeptide-binding motif[281]. This motif has a strong affinity for the Ser-pSer/pThr-Pro-X sequence[268 272 273] present on targeted substrates, suggesting that other kinases such as cyclin-dependent (CDK) and mitogen-activated protein kinases (MAPKs) primarily phosphorylate substrates prior to docking in PLKs[271].

The first known function of the PBD is to be auto-inhibitory with respect to its dependant kinase domain[287]. Following the binding of a phosphorylated target-protein to the Polo-box domain, the inhibitory effects of the PBD on the kinase domain is ceased[288]. Its second

dominant role is in the subcellular localisation of PLKs[289]. This crucial function distributes PLKs to locations within the cell to execute vital processes at various stages of the cell cycle.

Polo-like kinase 1

The Crystal structure of the PLK1 Kinase domain

Kothe *et al*[290] recently established the crystal structure of a p.T210V mutant of the human Plk1 kinase domain complexed with an ATP analogue and a pyrrolo-pyrazole inhibitor. The structure consists of 9 β strands and 6 α-helices. Their structure displays a typical kinase fold which accommodates an ATP-binding site within. This binding site is located in a cleft formed by a β-sheet from the N-terminal lobe and an α-helix from the C-terminal lobe. Both these lobes are related by a hinge region which interacts with bound ligands (Figure 4).

The activation loop within the kinase domain assumes a structure similar to other active kinases[291] and consists of residues 194-221. Both Thr210 and Ser137 have also been associated with the activation of PLK1 and are later discussed further.

The Crystal structure of the PLK1 Polo-box domain

Polo-like kinase 1 possesses two Polo-boxes, the first consisting of residues 411-489 and the second 511-592. Each PBD has been shown to comprise a six-stranded β-sheet and one α-helix. These are respectively recognised as β1-6 and αB in Polo-box 1 and β7-12 and αD in Polo-box 2 (Figure 5). Though the two PBDs are structurally similar, they show low homology, exhibiting only 12% sequence identity[273].

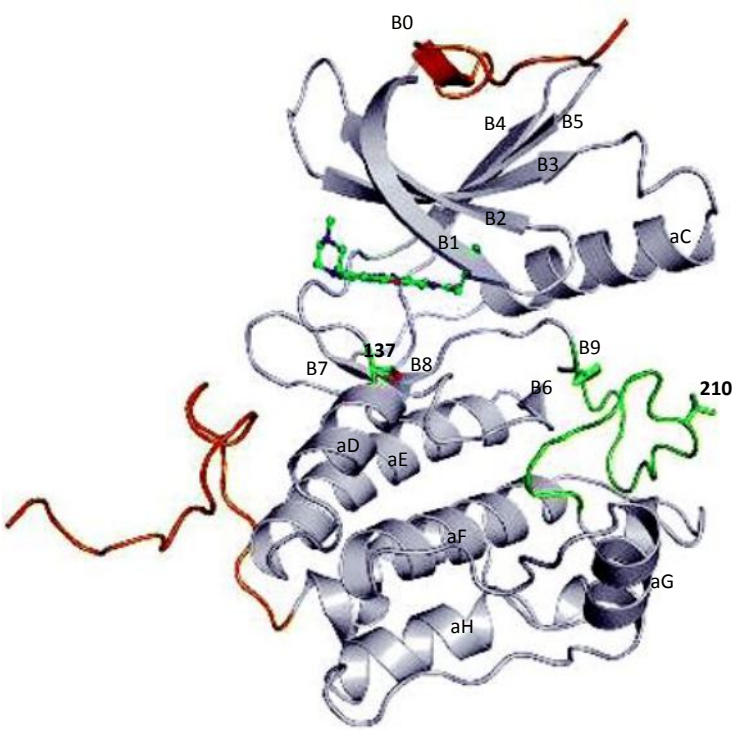

Figure 4: The crystal structure of the kinase domain of PLK1

Crystal structure of the kinase domain of PLK1 consisting of 9 β strands and 6 α-helices. Residue 210 is highlighted within the activation loop, with residue 137 also highlighted due to its association with PLK1 activation. Taken from Kothe et al[290] without permission.

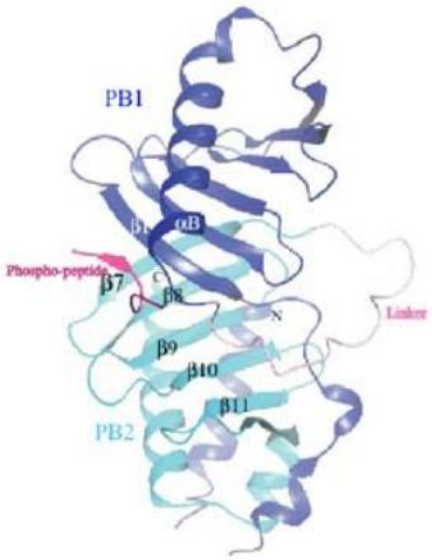

Figure 5: The crystal structure of the polo-box domain of PLK1

Crystal structure of the polo-box domain of PLK1. Both polo-box domains consist of a six-stranded β-sheet and one α-helix.Labelled is the linker region and the phosphopeptide binding site between both polo-boxes. Taken without permission from Cheng et al[273].

The Crystal Structure of the PLK1 Polo-cap and the Linker regions

Elia *et al*[272] determined the boundaries of the PBD by digesting the entire C-terminal with a protease and trypsin which indicated that the last 40 or so residues of the linker between the kinase domain and first Polo-box were part of the PBD. This additional region was named the Polo-cap (Pc).

The Polo-cap consists of a single α-helix, αA and a short 3_{10} helix which connects to the first β-strand of Polo-box 1 via a linker region (L1). The Pc envelops Polo-box 2 harnessing it to Polo-box 1, and these two Polo-boxes are further connected by a second linker region (L2) which assists in orientating the entire domain[272]. Similar to the polo-boxes' β-sheets, both linker regions run antiparallel to each other (Figure 6).

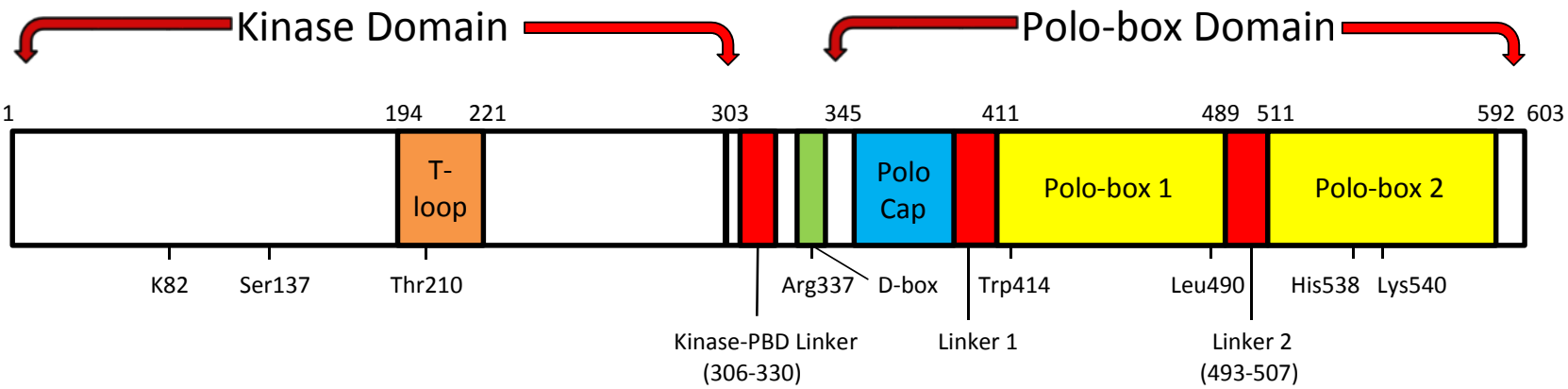

Figure 6: The protein structure of PLK1

Schematic representation of PLK1 with its key residues highlighted – based on Cheng[273], Kothe[290] and Elia[272]. The kinase domain (Residues 1-303) contains K82 responsible for ATP-binding and the activation loop (T-loop) at 194-221. Phosphorylation of both Ser137 and Thr210 have been implicated in kinase activation. Between the kinase and PBD there is a short linker region (306-330) and the D-box which is responsible for the destruction of PLK1 at the completion of mitosis. Cheng identified the polo-box domain as residues 345-603 but electron density at residues 345-372 and 593-603 were absent. The polo-cap joins to the first polo-box by Linker 1 and has been demonstrated to tether both polo-boxes together in 3D. Polo-box 1 (411-489) and polo-box 2 are joined by a linker region (493-507). Within the PBD, residues 414, 490, 538 and 540 have all been identified as important for phosphoselectivity and phosphopeptide binding.

Phosphopeptide binding to the Polo-box domain

The first step in kinase activation consists of the attachment of a phosphopeptide to the PBD which occurs in a cleft between both Polo-boxes involving αB, β1, β7, β9 and β10. The binding peptide makes several specific contacts with PBD residues[273] as a result of the second polo-box's His-538(β9) and Lys-540(β10) side-chain 'pincer'[271]. The significance of these two residues in phosphospecific binding was demonstrated by their mutation to Alanine, which prohibited this process[282].

The contact between the binding peptide and PBD is both non-polar and polar in nature, with residues Leu490 and Trp414 dominating the latter. In addition to being in direct contact, the phosphate component also interacts with the PBD through a complex network of organised hydrogen-bonded water molecules[273 282].

Activation of the PLK1 Kinase Domain

It has been shown that deletion of the C-terminus of PLK1 significantly increased kinase activity[287 292] and it is now widely accepted that the PBD has an inhibitory effect on the kinase domain in PLKs. Occupancy of the PBD by a phosphorylated ligand seems to relieve this inhibitory effect upon the kinase domain, enabling its activation through phosphorylation. However, the precise mechanism of this process remains unclear at present.

Following the termination of the PBDs inhibitory effect on the kinase domain, it is required to be phosphorylated to become active. This process occurs in the T-loop, on the evolutionary conserved Thr210 residue (Figure 7)[293].

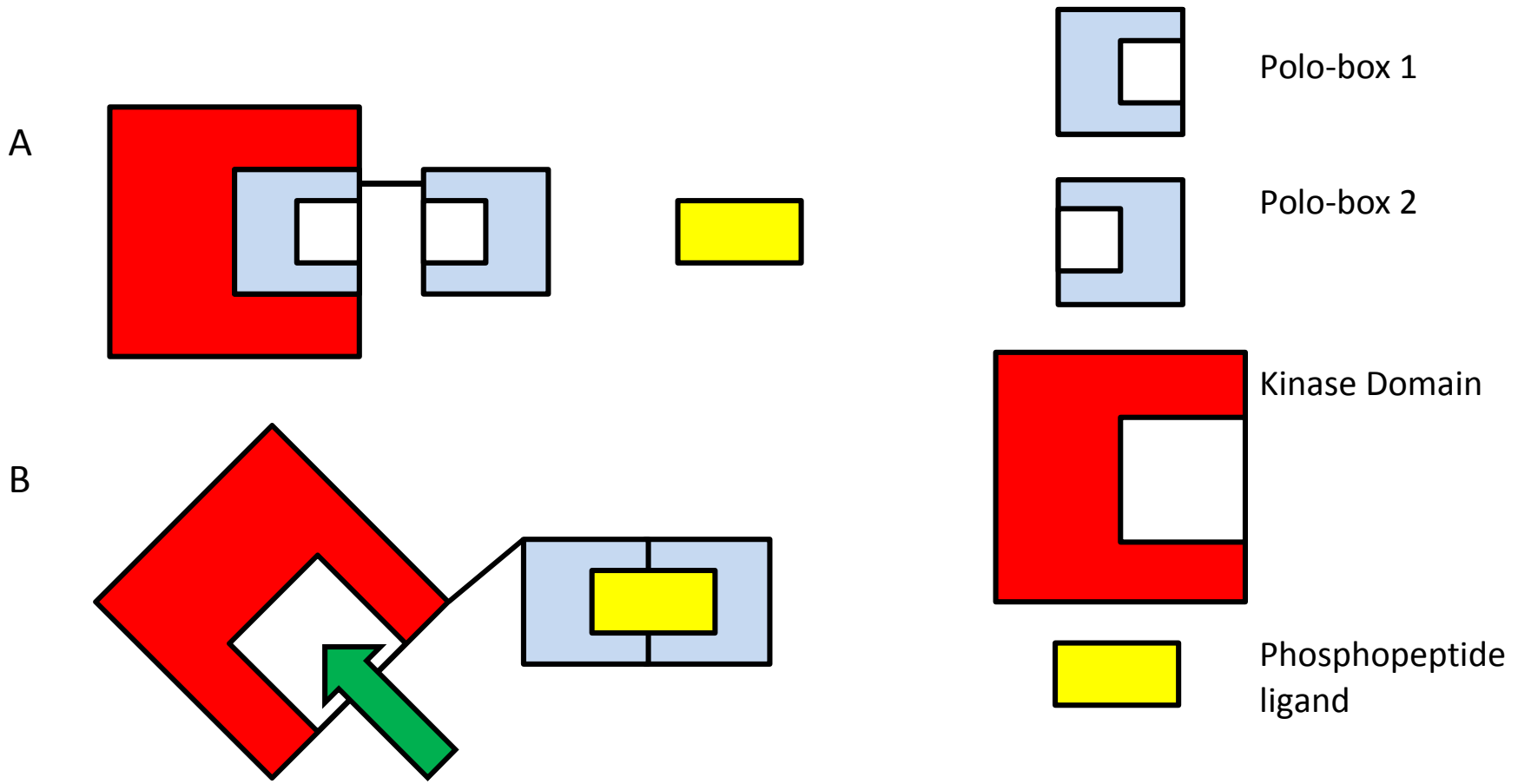

Figure 7: The polo-box domain's inhibitory effect upon the kinase domain

(A) The polo-box prevents phosphopeptide binding to the ligand. (B) A phosphopeptide ligand occupies a cleft between both polo-boxes, releasing its inhibitory effects upon the kinase domain. The kinase domain is now free to bind to ligands, but will require phosphorylation to become active.

Other modes of PLK1 activation

Exclusive to the conventional mode of activation described above, mutations in PLK1 have also been shown to activate its own kinase domain. In HeLa cells, a mutation in Thr210 to aspartic acid mimics phosphorylation of the T-loop, resulting in kinase activity[287 294]. Further to this, a similar mutation in Ser137, located at the end of the hinge region outside of the T-loop also leads to kinase activation[294 295]. Initial doubts as to whether this site was phosphorylated *in vivo*[296] have now been resolved, when it was demonstrated that phosphorylation of both Thr210 and Ser137 residues occurs in mitosis[297].

The mutual inhibitory effect between the kinase and polo-box domains

Interestingly, the PBDs inhibitory effect upon its kinase seems mutual. Elia *et al*[282] showed that an isolated PBD bound with high affinity and specificity to pSer/pThr-containing peptides, but this reduced ten-fold in the presence of full-length PLK1. They then progressed to compare kinase activity in the presence of both the optimal PBD phosphopeptide and non-phosphorylated peptide. Kinase activity more than doubled in the presence of the optimal phosphopeptide, with no change seen with the latter. This suggests that the PBD's binding to phosphorylated proteins not only serves to relieve its auto-inhibitory effect upon its kinase, but also direct its kinase partner towards target substrates.

Further information has been gathered about this mutual inhibitory effect through the recently published crystal structure of *Danio rerio* (Zebrafish) kinase-PBD complex together with a PBD-binding motif of *Drosophila melanogaster* microtubule-associated protein 205 (Map205)[298 299]. Various methods of kinase inhibition have been suggested, including structural changes within the kinase-PBD complex which prevents access to the Thr210 and Ser137 phosphorylation sites. A third pathway suggests that the binding of the PBD to Map205 stabilized this auto-inhibitory relationship and isolated the inactive kinase away from its substrate.

Cessation of the mutual inhibitory effect between the kinase and polo-box domains

Phosphorylation of Map205 or the Ser137 site of PLK1 disrupts the inhibitory relationship between the kinase and PB domains. This effect, which is replicated by the binding of a substrate to the PBD, ceases the isolation of the Thr210 residue on the T-loop enabling it to interact with activating kinases[280].

Stimulation of PLK1 activity

PLK1 activity is stimulated via two main pathways – firstly by the phosphorylation of Thr210 or Ser137 in the kinase domain[280] and secondly, by phosphopeptide binding of the PBD.

Aurora A and Bora are the main activating kinases of PLK1 in mitosis

Phosphorylation of the Thr210 residue commences in G2, leading to a gradual increase in PLK1 activity which peaks at mitosis[300]. Initial phosphorylation is undertaken by Aurora A kinase – a process which is also dependent on its cofactor, Bora[301]. Chan *et al*[302] states that the Bora-PLK1 interaction is likely to be initiated by the CDK1-dependent phosphorylation of Bora, suggesting that CDK1 is required for the activation of PLK1 in G2. In turn, this feedback loop ensures that PLK1 activation is necessary for the subsequent activation of cyclin B/CDK1[300] (Figure 8).

At the onset of mitosis, when PLK1 activity peaks, Bora is degraded in a PLK1-and Skp/Cullin/F-box-β-Trasducin repeat containing protein(SCF βTrCP)-dependent manner[303], leaving Aurora A to interact with other co-activators. However, the continued activity of PLK1 is dependent on the ongoing phosphorylation of Thr210[304] and until recently this mechanism was poorly understood. It has now been demonstrated that the continued phosphorylation of Thr210 remains Bora-Aurora-A dependent, with only minimal Bora-Aurora-A activity necessary to maintain PLK1 activity. Therefore, the inactivation of PLK1 during mitosis requires the complete absence of both Bora and Aurora-A[301], which raises the possibility that they are responsible for the majority, if not all of the Thr210 phosphorylation in mitosis (Figure 9).

Aurora A-independent regulation of PLK1

As Bora is degraded, another cofactor, targeting protein for Xklp2 (TPX2) becomes responsible for the regulation of Aurora A[305]. At this time, regulation of PLK1 becomes Aurora A-independent, though the mechanism of this change is not currently known[306].

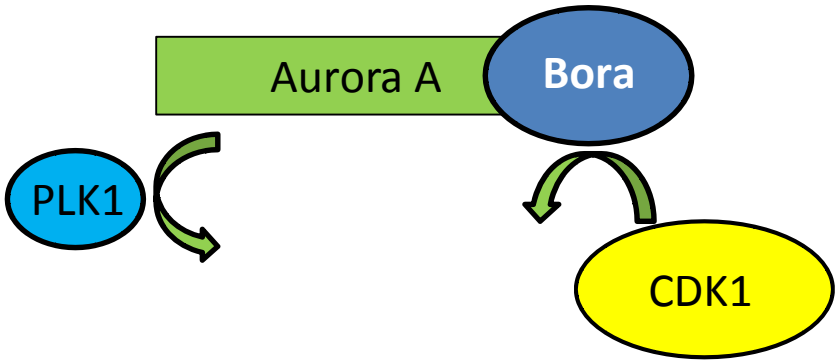

Figure 8: The activation of PLK1 activity in G2
Phosphorylation of the Thr210 residue of PLK1 is undertaken by Aurora A kinase, though this can only occur in conjunction with its cofactor, Bora. The Bora-PLK1 interaction is likely to be initiated by the CDK1-dependent phosphorylation of Bora, suggesting that CDK1 is necessary for activation of PLK1 in G2.

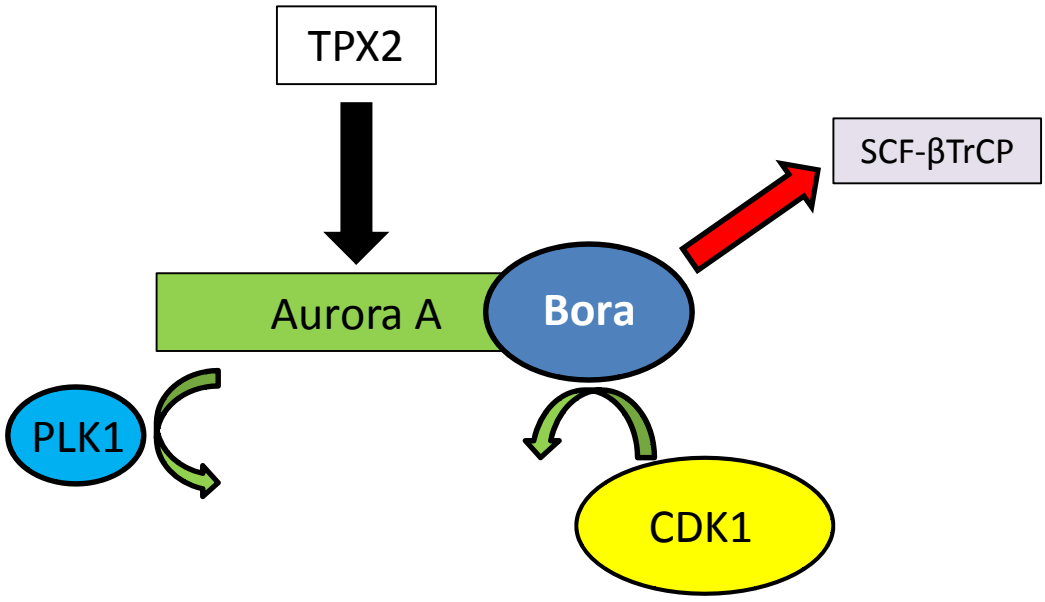

Figure 9: The maintenance of PLK1 activity at mitotic entry
Bora is degraded in a SCF-βTrCP-dependent manner. The maintenance of PLK1 activity requires the continued phosphorylation of its Thr210 residue and only requires minimal Aurora A-Bora activity. As Bora is degraded, another cofactor, targeting protein for Xklp2 (TPX2) becomes responsible for the regulation of Aurora A. At this point, PLK1 activity becomes independent of Aurora A, though this mechanism is not currently understood.

Other activating kinases of PLK1

Though Aurora A in combination with Bora are the main activating kinases of PLK1, other proteins have been shown to phosphorylate Thr210 and stimulate kinase activity including serine/threonine kinase 10 (STK10), Human STE20-like kinase (SLK)[307] and lymphocyte oriented kinase (LOK)[308]. However, it has already been shown that siRNA knockdown of SLK and LOK is not reflected by a fall in Thr210 phosphorylation during interphase or mitosis, suggesting that their effects are marginal[301].

Priming Kinases for PBD phosphopeptides and the subcellular localization of PLK1

The optimal binding peptide for the PBD contains the Ser-[pSer/pThr]-[Pro/X] motif, suggesting that other kinases may act as 'primers' by phosphorylating target proteins in preparation for preferential binding to PBD docking sites. Elia *et al*[272]showed that this optimal phosphoprotein will be favoured by the PBD over binding to centrosomes. Further evidence was presented[282] displaying how mutations in the PBD could hinder cellular localization of PLK1 in centrosomes. This all strongly suggests that the PBDs phosphopeptide binding characteristics plays a key role in the subcellular localisation of PLK1 and therefore in cell cycle progression[271].

Priming kinases are also likely to function as signposts, attracting PLK1 to various cellular locations at predetermined time points in the cell cycle. Examples include the CDK1-primed inner centromere protein (INCENP)[269] and PLK1-primed protein regulator of cytokinesis 1 (PRC1)[309] which binds to PLK1 and localises to the kinetochores and central spindle at key points during mitosis.

Priming Kinases for PBD binding

Kinases known to be responsible for 'priming' target proteins for PBD binding include Cyclin-dependent kinase 1 (CDK1), MAPKs[271 280] and ATR[310]. Self-priming of substrates by PLK1 has also been recognised[280 311].

Phosphorylation of Downstream Targets by PLK1

The preferred substrate epitope for phosphorylation by PLK1 has been reported as Glu/Asp-X-Ser/Thr-Θ, where Θ is usually hydrophobic[312]. Verified *in vivo* substrates of PLK1 include cyclin B[313 314 315], cdc25[315 316], Wee1[317 318], BRCA2[319], Myt1[320], Nlp[321], NudC[322], TCTP[323], Grasp65[324 325], MKlp1[326 327] and MKlp2[328]. However, very few of these substrates have PLK1-

specific sites for PBD-binding or kinase phosphorylation, with many also being targets for phosphorylation by CDK1 and other mitotic kinases[329].

Cellular roles of PLK1

A complex picture of the cellular roles of PLK1 has developed over the past decade, involving several signalling pathways. Though PLK1 commences expression in G2, its kinase activity is not seen until the G2/M transition. Peak levels of PLK1 are achieved during mitosis[330], though it is subsequently degraded by the time this phase is complete[331].

PLK1 in G2

Though PLK1-inhibited cells will eventually progress to mitosis, their entry will be delayed and cell cycle arrest will later ensue. In late G2/prophase[332], a plentiful supply of stable cyclin B is available as it is net exported from the nucleus into the cytoplasm[333]. This enables its binding to CDK1 to create a cyclin B/CDK1 complex (also known as the M-phase promoting factor (MPF))[334] which, in eukaryotes, drives mitosis[335]. In G2, the cyclin B/CDK1 complex remains largely inactive due to the ongoing phosphorylation of residues Thr14 and Tyr15 of its kinase component by Wee1 and Myt1, preventing ATP-binding[336 337] (Figure 10).

PLK1 at mitotic entry

For mitotic entry, cyclin B/CDK1 must be activated, meaning that the inhibitory effects described above need to be terminated. This is instigated in several ways through PLK1, which is located at the centrosomes throughout interphase and prophase[275].

Firstly, CDK1 residues Thr14 and Tyr15 are both dephosphorylated by cdc25A, cdc25B and cdc25C, to enable CDK1-ATP binding. cdc25C is directly phosphorylated by PLK1[315 338 339]. However, it is cdc25B that has been proposed as the 'stimulus phosphatase' for the activation of cytoplasmic cyclin B/CDK1[340]. Secondly, Wee1 and Myt1 are both phosphorylated by PLK1, ceasing their inhibitory effects upon CDK1. Cyclin B/CDK1 activity is also dependent on the phosphorylation of Thr161 located on the T-loop of its kinase domain by the CAK complex (CDK7, cyclin H and MAT1)[341 342], resulting in increased kinase activity.

Once stimulated, cyclin B/CDK1 ensures mitotic commitment by self-promoting its further activation via a positive feedback loop, by phosphorylating both Wee1[343] and cdc25C[344] (Figure 11). The former will later be further phosphorylated by PLK1 again suggesting a 'priming' relationship between PLK1 and other kinases. Wee1 is then degraded through SCF

βTrCP[343]. PLK1 also phosphorylates the cyclin B/CDK1 complex in addition to both cdc25C and cyclin B[315] which stimulates the entry of cells into mitosis which further promotes cyclin B/CDK1 at the centrosome. For a timely mitotic entry, it is necessary for the activated protein-kinase complex to translocate from the cytoplasm to the nucleus[288] as the inability of either cyclin B[345] or active CDK1[346] to enter the nucleus will block or delay this event. PLK1 has previously been implicated in the subcellular localization of cyclin B/CDK1 by phosphorylating Cyclin B's Ser133[313]. However the deletion of this phosphorylation site failed to prevent the nuclear migration of the complex, suggesting that several factors influence its intracellular movement (Figure 11).

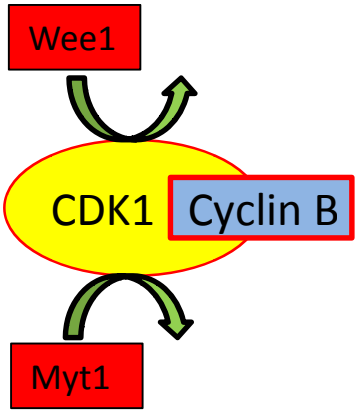

Figure 10: CDK1/Cyclin B in G2
Cyclin B is net exported into the cytoplasm from the nucleus and binds to CDK1. The cyclin B/CDK1 complex remains largely inactive due to the phosphorylation of Thr14 and Tyr15 by Wee1 and Myt1, preventing ATP binding.

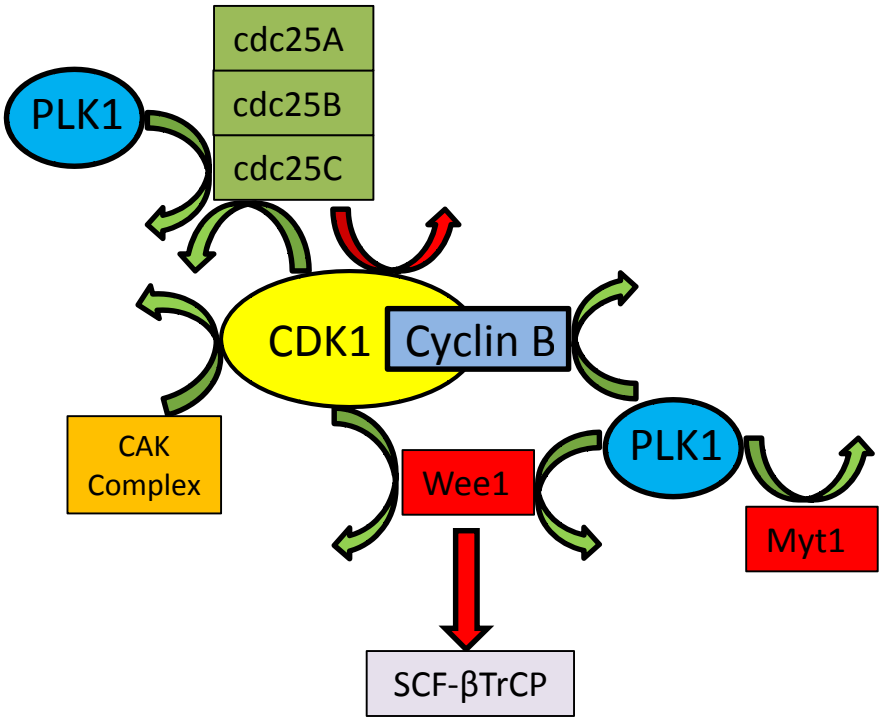

Figure 11: PLK1 at mitotic entry

cdc25A, B and C dephosphorylate CDK1 residues Thr14 and Tyr15. Cdc25C is phosphorylated by PLK1. Both Myt1 and Wee1 are also phosphorylated by PLK1, ceasing their inhibitory effects upon cyclin B/CDK1. This complex can then be activated by the phosphorylation of Thr161 by the CAK complex.

Once stimulated, cyclin B/CDK1 ensures mitotic commitment by self-promotion via a positive feedback loop. This involves the phosphorylation of cdc25C and Wee1 by the complex prior to the degradation of Wee1 by SCF-βTrCP. Cyclin B/CDK1 is phosphorylated by PLK1, which also stimulates the entry of cells into mitosis by phosphorylating cdc25C and cyclin B. For a timely mitotic entry, cyclin B/CDK1 translocates from the cytoplasm into the nucleus.

PLK1 and the G2 DNA Damage Checkpoint

As a consequence of DNA damage in G2, the phosphatase cdc14B activates the anaphase-promoting complex (APC)[347]. The purpose of this DNA damage checkpoint is to enable cells to repair damaged DNA, by inhibiting cyclin B/CDK1 to cease entry into mitosis[348]. Induction of the APC leads to the inactivation and degradation of PLK1[349], and though PLK1 is not usually essential for mitotic entry, this changes once the DNA checkpoint has been activated in G2[350].

Double strand DNA-breaks activates the checkpoint kinase ATM (ataxia telangiectasia mutated), with single stranded breaks activating ATR (ataxia telangiectasia and Rad3-related proteins)[280]. These kinases phosphorylate checkpoint kinases 2 and 1 (Chk2 and Chk1) respectively[351]. Phosphorylation of Chk1 by ATR requires the presence of the adaptor protein Claspin to fuse both proteins together[352]. This protein will later play an important role alongside PLK1 in checkpoint recovery.

Chk1 and Chk2 both inactivate cdc25C which in its active state promotes CDK1. Chk1 also activates Wee1 which, in turn phosphorylates CDK1 on residues Thr14 and Tyr15 to inhibit substrate binding and cell cycle progression[280 288]. Inhibition of the cyclin B/CDK1 complex causes a G2 arrest (Figure 12).

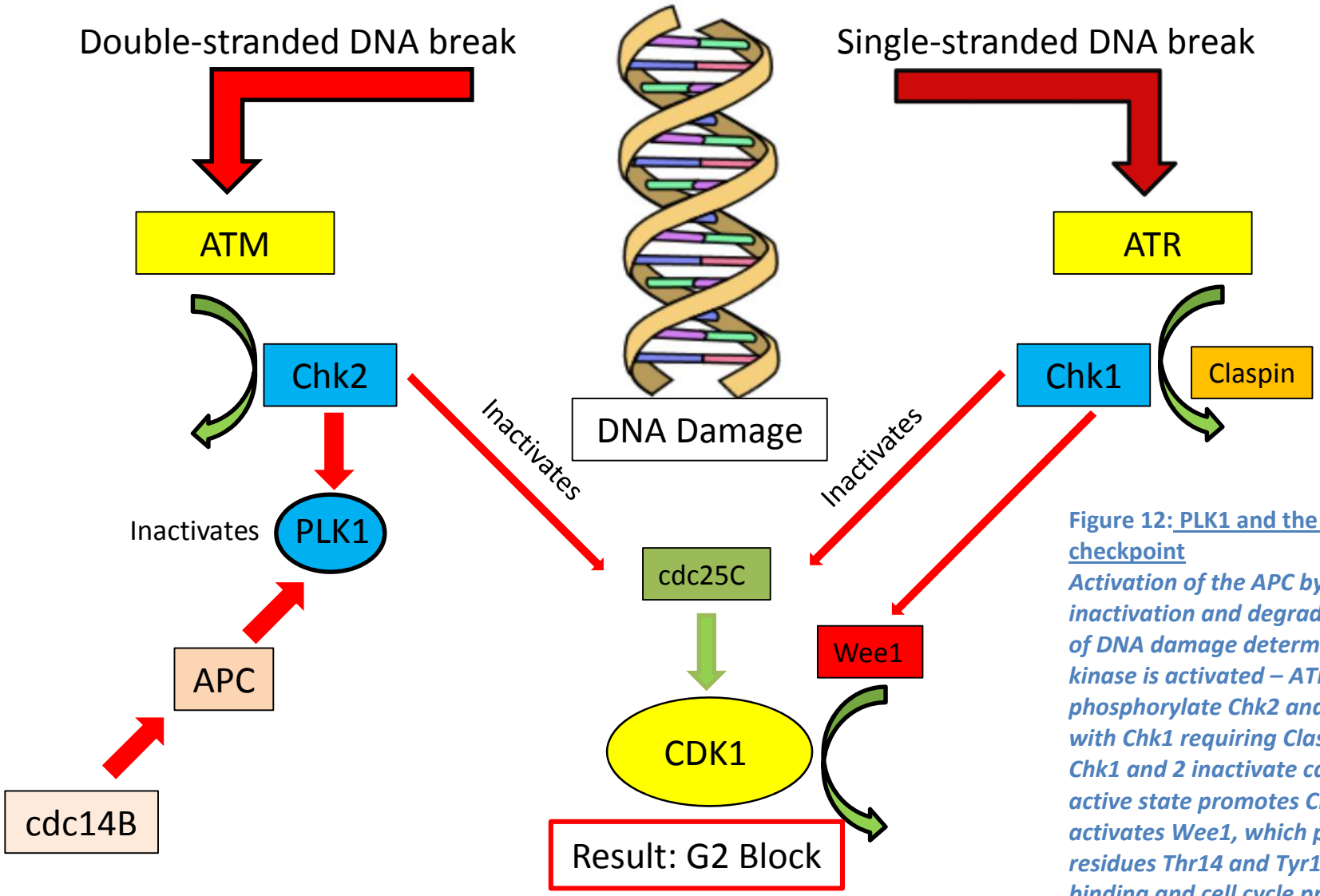

Figure 12: PLK1 and the DNA damage checkpoint

Activation of the APC by cdc14B leads to the inactivation and degradation of PLK1. The scale of DNA damage determines which checkpoint kinase is activated – ATM or ATR. These kinases phosphorylate Chk2 and Chk1 respectively, with Chk1 requiring Claspin for this to occur. Chk1 and 2 inactivate cdc25C, which in its active state promotes CDK1. Chk1 also activates Wee1, which phosphorylates CDK1 on residues Thr14 and Tyr15 to inhibit substrate binding and cell cycle progression.

DNA damage prevents phosphorylation at Thr210 and Ser137

PLK1 activity is inhibited in the event of DNA damage during mitosis[353]. Tsvetkov *et al*[297] treated cells with a combination of nocodazole, a mitosis arresting agent and adriamycin, a DNA damaging agent. Their results suggest that there are two mechanisms for PLK1 inhibition: the first prevents the phosphorylation of Ser137 and Thr210 in G2, while the second operates independently in mitosis.

PLK1 and Cell Cycle Recovery Following the DNA Damage Checkpoint

PLK1 initiates the repair of damaged DNA and subsequent recovery from the DNA damage checkpoint in several ways. Firstly, the adapter protein claspin is phosphorylated by PLK1 which leads to its degradation by SCF-βTrCP[354]. The presence of any nondegradable claspin inhibits a cell's recovery from the DNA checkpoint arrest, emphasising the importance of PLK1 in DNA checkpoint recovery[300] (Figure 13). In addition to this, PLK1 inactivates the DNA damage checkpoint by phosphorylating the tumour suppressor p53-binding protein 1 (p53BP1) and Chk2. p53BP1 is firstly primed by Cyclin B/CDK1, before phosphorylation by PLK1 promotes its self-dissociation from DNA[300] and negative regulation of Chk2, preventing its binding to substrates[355]. PLK1 also promotes the repair of damaged DNA by phosphorylating RAD51 homologue 1 (RAD51) on Ser14, which is later phosphorylated again on Thr15 by casein kinase. This subsequently promotes the accumulation of p53BP1 at the site of damage[356], promotes degradation of Wee1 and inactivates both Chk1 and Chk2.

As DNA is repaired, CDK1 is reactivated to enable the cell cycle to progress. It has been suggested that Wee1 degradation is dependent on phosphorylation by both PLK1 and cyclin B/CDK1 after DNA damage[356]. These observations are consistent with findings made in yeast where active cyclin B/CDK1 is required for cell cycle re-entry after checkpoint arrest[357] (Figure 14).

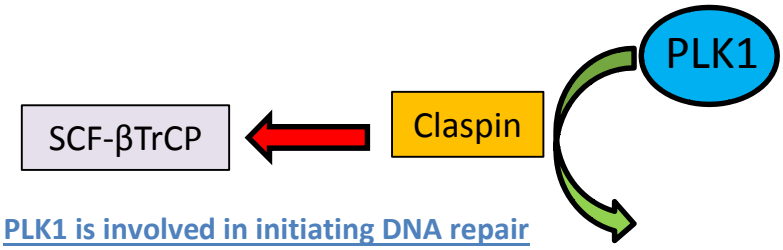

Figure 13: PLK1 is involved in initiating DNA repair

To initiate DNA repair, claspin is phosphorylated by PLK1, prior to its degradation by SCF-βTrCP. The presence of any nondegradable claspin inhibits a cell's ability to recover from a DNA checkpoint arrest.

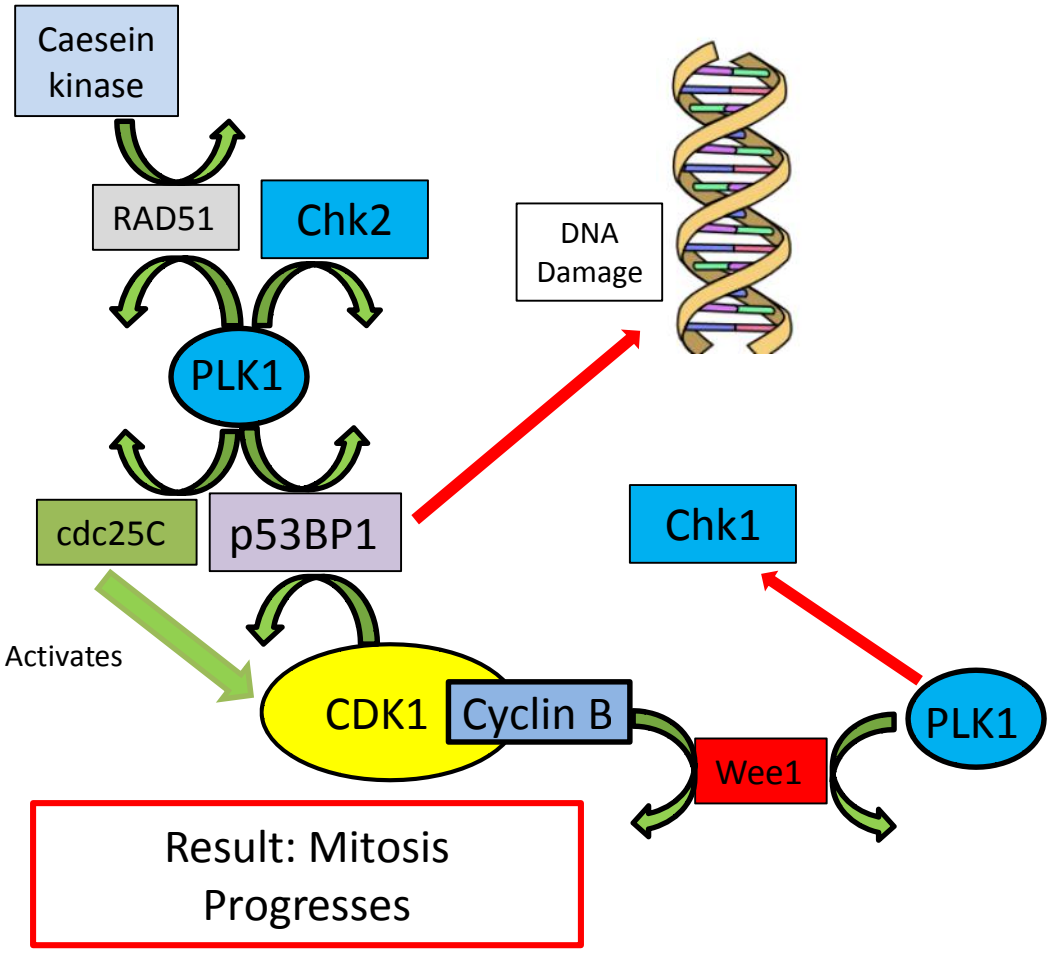

Figure 14: Cell cycle recovery following DNA damage checkpoint arrest

PLK1 inactivates the DNA damage checkpoint by phosphorylating p53BP1 and Chk2. p53BP1 is firstly primed by cyclin B/CDK1, before phosphorylation by PLK1. PLK1 also promotes the repair of damaged DNA by phosphorylating RAD51 on Ser14, which is later phosphorylated again on Thr15 by casein kinase. This promotes the accumulation of p53BP1 at the site of DNA damage, promotes degradation of Wee1 and inactivates both Chk1 and Chk2. As DNA is repaired, CDK1 is reactivated to enable the cell cycle to progress. Wee1 degradation is dependent on phosphorylation by both PLK1 and cyclin B/CDK1 after DNA damage.

PLK1 and the Centrosomes

The centrosome consists of two centrioles positioned in a pericentriolar matrix (PCM). In G2, PLK1 localizes to the centrosomes where it recruits pericentriolar material and enables the centrosome to become a microtubule-nucleating centre[358]. Regulatory factors such as γ-tubulin are activated and arranged into complexes such as γ-tubulin ring complexes (γTuRCs) and γ-tubulin small complexes (γTuSCs) which are incorporated into the cytoskeleton[280]. During cell division, the two centrosomes migrate to establish the poles of the bipolar mitotic spindle that controls the equal division of chromosomes[359].

PLK1 phosphorylates two proteins which play a key role in centrosome maturation. Firstly, ninein-like protein (NLP) is phosphorylated by PLK1 which disturbs the protein's interaction with both the centrosome and γTuRC leading to its exit from the centrosome and promotion of microtubule nucleation[321]. The second protein, pericentrin (PCNT) has only recently been identified as a PLK1 target at the centrosome. Phosphoresistant PCNT mutants lose the ability to attract essential PCM ingredients such as PLK1, Aurora A, γ-tubulin and centrosomal protein of 192kDA (CEP192) to the centrosome which again prevents centrosome maturation[360].

PLK1 also promotes the disengagement and separation of mature centrosomes. A linker protein containing centrosome-associated protein (CNAP1 or CEP250) and rootletin tethers the two dividing centrioles together[361]. This connection is broken by the phosphorylation of both linker proteins by the serine-threonine kinase NIMA-related kinase (NEK2A), resulting in their dissociation from the centrioles. The activation of NEK2A is positively regulated by Serine/Threonine protein kinase 3 (MST2 or STK3) and human Salvador homolog 1 (nSAV1)[362], with a further protein, Serine/Threonine phosphatase PP1γ rendering it inactive[363]. The phosphorylation of MST2 by PLK1 inhibits PP1γ from binding to NEK2A, therefore enhancing NEK2A activity. These intricate interactions explains how increased PLK1 activity in G2/prophase initiates centrosome disjunction.

A further pathway, exclusive to NEK2A also implicates PLK1 with EG5 (also known as KIF11) in the disjunction of centrosomes. Bertram *et al*[364] and Smith *et al*[365] have both shown that the phosphorylation of NEK9 is PLK1- and CDK1-dependent, which in turn activates NEK6 and NEK7 leading to the phosphorylation of EG5. Phosphorylation of EG5 leads to its

accumulation at the centrosomes in prophase and this protein has been shown to be responsible for the full separation of the centrosomes during this phase[366].

PLK1 in Sister Chromatid Separation

As DNA replication occurs, cohesin is recruited to chromosome arms and to the centromeres[288]. Cohesin binds together two newly divided chromatids until M-phase when it is mostly removed[280] via a CDK1-mediated pathway.

During prophase, PLK1 is drawn to chromosome arms through the CDK1-dependent phosphorylation of both soronin and condensin 2 complex subunit D3 (CAPD3)[367]. The former of which acts as a docking protein for PLK1 to phosphorylate the cohesion complex subunit SA2, leading to the removal of cohesion complexes[368] (Figure 15). PLK1 also encourages the release of cohesin from chromosome arms by phosphorylating early mitotic inhibitor 1 (EMI1), leading to its degradation. This contributes to the activation of the anaphase-promoting complex (APC)-cdc20 which promotes cohesin breakdown and chromatid separation[369].

Nevertheless, the divided chromatids will remain linked until the remaining cohesin is also freed from the centromeres[370] . Cohesin complexes are protected during prophase by protein phosphatase 2A (PP2A) and Shugoshin (sgo1) as they dephosphorylate SA2[371]. PLK1 is recruited to both the kinetochore[372] and centrosome by its PBD, where it both binds and phosphorylates polo-box interacting protein 1 (PBIP1)[373]. At the centrosome, the cohesion subunit sister chromatid cohesion protein 1 (Scc1 or RAD21 in vertebrates), is phosphorylated by PLK1, facilitating its cleavage by the protease separase[374].

Just prior to the commencement of the separation of sister chromatids, PLK1 is released from the kinetochores via its monoubiquitation by the ubiquitin ligase cullin 3 (CUL3) – Kelch-like protein 22 (KLH22)[375] (Figure 16).

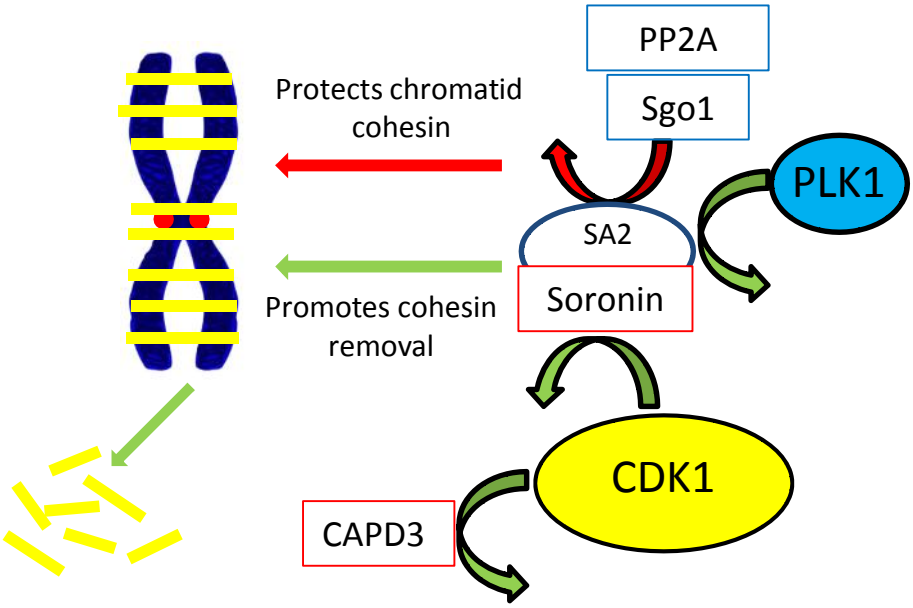

Figure 15: PLK1 in sister chromatid separation - prophase

During prophase, PLK1 is drawn to chromosome arms through the CDK1-dependent phosphorylation of both soronin and CAPD3. The former of which acts as a docking protein for PLK1 to phosphorylate the cohesion complex subunit SA2, leading to the removal of cohesion complexes. Cohesin complexes are usually protected by PP2A and Sgo1 as they dephosphorylate SA2.

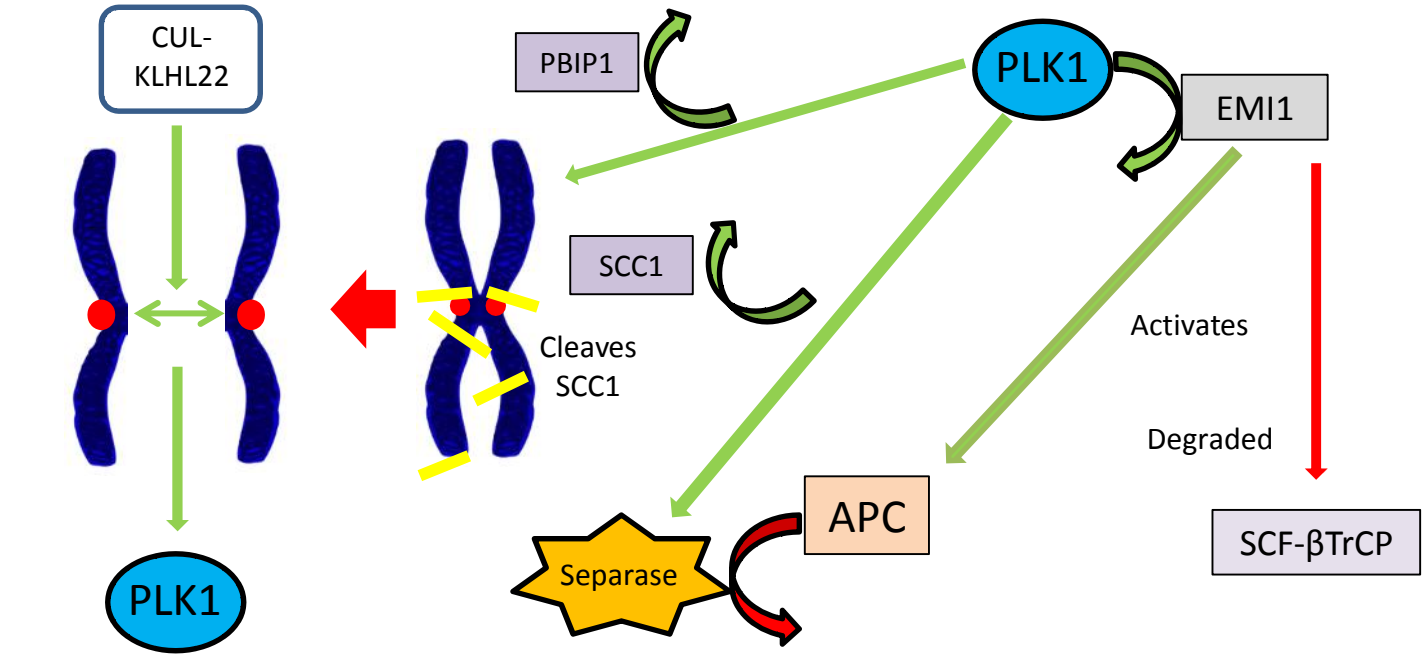

Figure 16: PLK1 in sister chromatid separation – prometaphase and metaphase

During prometaphase and metaphase, PLK1 is recruited to both the kinetochore and centrosome by PBIP1. PLK1 promotes the release of cohesin from chromosome arms by the phosphorylation of EMI1. Activation of the APC promotes cohesin breakdown and chromatid separation. At the centrosome, Scc1 (or RAD21 in vertebrates), is phosphorylated by PLK1, facilitating its cleavage by the protease separase. During anaphase, prior to the separation of sister chromatids, PLK1 is released from the kinetochores via its monoubiquitation by CUL3-KLH22 Both figures are based on Zitouni et al[280]

PLK1 and Activation of the Anaphase-Promoting Complex

In addition to other spindle assembly checkpoint proteins, the activation of the APC-promoter, cdc20, is regulated by EMI1. The phosphorylation of this mitotic inhibitor by PLK1 leads to its degradation by SCF-βTrCP[376], enabling the activation of the APC. PLK1 inhibition has been demonstrated to delay EMI1 degradation, though this isn't a prerequisite for APC activation at mitotic onset[377].

PLK1 in Kinetochore-microtubule Attachment

Kinetochores and spindle microtubules assemble on the centromeres in mitosis and are critical for accurate chromosomal alignment and separation[280]. Despite the degradation of PBIP1 in early mitosis[372], PLK1 remains at the centrosomes and kinetochores following nuclear envelope breakdown to regulate the kinetochore-microtubule (KT-MT) attachment[378]. This is thought to be due the actions of BUBR1 and the inner centromere protein (INCENP) which have both been shown to contribute to the localisation of PLK1[379] [380] [381].

CLIP-associating protein 2 (CLASP2), which is primed by CDK1 in preparation for phosphorylation by PLK1 increases PLK1 recruitment to the kinetochore and stabilises the attachment to the microtubule[382]. Incorrectly attached spindle microtubules will be destabilised by the chromosomal passenger complex (Aurora B, INCENP, survivin and borealin) which also regulates the spindle assembly checkpoint (SAC). CDK1 and PLK1 regulate the kinase haspin, which promotes the phosphorylation of histone H3 which attracts Aurora B to the centromere for this passenger complex[383].

During metaphase, PLK1 has been shown to phosphorylate BUBR1[381] and CAP-Gly domain-containing linker protein 1 (CLIP170)[384], which has been shown to regulate KT-MT attachment and SAC signalling[280]. These attachments are further stabilised[385] by the activation of PLK1 by Aurora B and INCENP at the centrosomes[386]. The later phosphorylation of BUBR1 by PLK1, promotes its binding to the B56α regulatory subunit of PP2A which dephosphorylates Aurora B and regulates mitotic progression[387] [388]. B56α-PP2A also dephosphorylates the KNM network (kinetochore-null protein, MIS12 complex and kinetochore protein NDC80 homologue complex), which is responsible for the initial attachment of microtubules to the kinetochore[280].

PLK1 and Cytokinesis

During cytokinesis, sister chromatids separate into two cells resulting in the formation of two physically separate cells. As these chromatids part, PLK1 translocates to the central spindle and the midzone in anaphase and telophase respectively[389]. This localization of PLK1 is dependent on several substrates including mitotic kinesin-like protein 1 (MKLP1), MKLP2, golgi-associate protein (PYK2), N-terminal domain-interacting receptor 2 (NIR2), dynein-associated nuclear distribution protein C homologue (NUDC), CEP57 and the protein regulator of cytokinesis (PRC1)[280]. PRC1 is an antiparallel microtubule-bundling protein which plays a key role in organizing the spindle midzone and is negatively regulated by both CDK1[390] and PLK1[391]. PLK1 self-primes PRC1 prior to its phosphorylation on Thr602 in metaphase. This process not only inhibits PRC1 activity and therefore prevents premature midzone formation, but also targets PLK1 to the midzone by creating docking sites for the protein to bind[390].

PLK1 and AMPK

AMP-activated protein kinase (AMPK) is a multifunctional fuel-sensing enzyme, involved in the regulation of protein, lipid and glucose metabolism. Vasquez-Martin *et al*[392 393] has shown that its active form, PP-AMPKα^{Thr172}, shares both temporal and spatial similarities to PLK1 during mitosis and cytokinesis and that PLK1 inihbition extinguishes the mitotic activation of AMPKα.

AMPK is an inhibitor of acetyl-CoA carboxylase 1 (ACC), which is the rate-limiting enzyme involved in fatty acid synthesis. AMPK's activity towards ACC is high at the commencement of mitosis and decreases towards its termination – consistent with the rate of fatty acid synthesis. The continued expression of AMPK has been shown to cause mitotic arrest, suggesting that AMPK also plays a key role in the final stages of mitosis[394 395].

PLK1 and p53

The tumour suppressor p53 is intricately involved in several events essential for cell survival including DNA repair, cell cycle arrest and apoptosis[396]. These p53-dependent events ensure the repair and continuing survival of healthy cells or alternatively, programmed cell death. This should result in the prevention of tumour formation, which explains why the loss of p53 function is commonly seen in various human cancers[397].

Studies have demonstrated a mutual negative regulatory relationship between PLK1 and p53. The phosphorylation of p53 by PLK1 has been shown to result in the inhibition of its pro-apoptotic characteristics[398], while depleting PLK1 in HeLa cells has been shown to increase the stability of p53[399]. In addition, a further study proposes the negative influence that p53 imposes upon PLK1[400].

Several pathways have been proposed to explain the negative influence of PLK1 upon p53. Firstly, PLK1 inhibits the phosphorylation of p53 on Ser15, leading to its nuclear export and degradation[401]. Secondly, PLK1 phosphorylates topoisomerase I-binding protein (Topors) at Ser78 which enhances this process[402]. Lastly, is a pathway involving the largely nuclear protein, GTSE1 (G2 and S phase-expressed-1). PLK1 phosphorylates GTSE1 and endorses its transportation of p53 from the nucleus to the cytoplasm for degradation during the G2 checkpoint recovery[403].

The evidence surrounding PLK1 inhibition and p53 status in the treatment of cancer is conflicting. Sanhaji *et al*[404] utilized PLK1 siRNA in addition to both a kinase- and polo-box domain-targeting PLK1 inhibitor in HCT116 (colonic cancer) cells of varying p53 status. With PLK1 knockdown, though the difference was minimal, results showed greater induction of apoptosis and reduced cell proliferation in p53 proficient cells compared with $p53^{(-/-)}$ cells. The PLK1 kinase domain-targeting agents BI 2536 and BI 6727 showed contrasting results with regards to cell proliferation, with BI 2536 slightly more effective in $HCT116p53^{(-/-)}$ cells and BI 6727 showing the opposite. However BI 6727 inhibited cell proliferation with greater potency than BI 2536.

In addition to causing a host of other cell cycle disturbances, the polo-box domain-targeting agent Poloxin has been shown to induce apoptosis in a variety of cell lines[405 406]. The agent caused significant apoptosis in both $HCT116p53^{(-/-)}$ and $HCT116p53^{(+/+)}$ cell lines, but was slightly more effective in the latter. The experiment was repeated in other cell lines with PLK1 inhibition induced by the same agents but in combination with and without p53 siRNA. More apoptosis was evident in MCF (breast cancer), A549 (non-small cell lung cancer) and HeLa (cervical cancer) cells with a functional p53 as opposed to without. Overall, these results strongly suggest that a preserved p53 status could be a predictor of a cell's susceptibility to the inhibition of PLK1.

However, as other studies proposed the opposite of these findings[407 408 409], Sanhaji and colleagues set out to determine whether mitotic stress, as commonly seen in cancer cells, would affect a cell's susceptibility to PLK1 inhibition dependent on their p53 status[410]. PLK1 inhibition was again instigated by the same compounds as previously used with mitotic stress induced by pretreating HCT116 cells with the microtubule destabilizers nocodazole and vincristine, the microtubule stabilizer paclitaxel and the kinesin Eg5 inhibitor monastrol.

Results suggest that by inducing PLK1 inhibition in cells undergoing mitotic stress, those cells with a functional p53 will trigger a strong apoptotic response whereas p53 null cells will arrest in mitosis with less apoptosis. Interestingly, this was despite the fact that HCT116p53$^{(-/-)}$ cells showed evidence of greater DNA damage than HCT116p53$^{(+/+)}$ cells after treatment, but these DNA-damaged cells survived longer in comparison. Proliferation and colony-formation assays showed that HCT116p53$^{(+/+)}$ cell growth was better inhibited than HCT116p53$^{(-/-)}$ cells and these observations were further strengthened when it was shown that p53 knockdown in HCT116 and U2OS (osteosarcoma) cells led to less apoptosis, suggesting that apoptosis is p53-dependent in PLK1 inhibited cells. The authors conclude that based on their results and the available published literature, that loss of p53 is not directly the cause of increased PLK1 toxicity. It is suggested that the efficacy of PLK1 inhibitors is enhanced by an active p53. This may be due to its stimulation of other signalling pathways and its prevention of genome instability, which has been previously described as a result of PLK1 inhibition[411].

The identification of tumour biomarkers is a critical step in the treatment of any malignancy and the hunt for a predictive biomarker for PLK1 inhibition is ongoing. Retrospective immunohistochemical analysis of 215 breast cancers found that 11% expressed PLK1, with its presence significantly associated with mutant p53[412]. The survival of individuals with both a mutated *TP53* and 'high' PLK1 expression was significantly poorer than in individuals possessing only one of these prognostic factors. PLK1 expression was also significantly associated with aggressive triple-negative tumours (p=0.01) and MDM2, a negative regulator of p53 (p=0.04). Overall it could be argued that breast tumours with raised PLK1 expression in association with a *TP53* mutation is a promising target for PLK1 inhibitors.

Sur and colleagues[413] developed a series of matched colorectal cancer cell lines that differed only in their endogenous p53 status. They then progressed to impose DNA damage to these cells through ionising radiation. Their first discovery was the elevated expression of PLK1 in p53 mutant cells in comparison with wild-type p53 cells, suggesting that the ongoing survival of mutant p53 cancer cells may be PLK1-dependent. Ionising radiation was found to cause G1 arrest in p53-proficient cells, but showed no PLK1-inhibition-related effect, likely as a result of the cells not entering mitosis. However, similarly treated, matched, p53-null cells entered mitosis and succumbed to PLK1 inhibition.

PLK1 and KRAS

KRAS mutations are known to be amongst the earliest in the development of pancreatic cancer. Importantly, oncogenic *KRAS* has been shown to be necessary for both the initiation and maintenance of pancreatic cancer in mice[414]. Though direct *KRAS*-targeting is yet to be successful[415], this finding still has treatment implications in emphasising the importance of its downstream proteins as potential targets[416].

Luo *et al*[417] utilised retroviral short hairpin RNAs to target over 30 000 transcripts to identify vulnerabilities in RAS-mutated cancers. The group then progressed to treating both mutant and wild-type RAS tumour cells with a polo-like kinase inhibitor, BI 2536 and PLK1 siRNA. Mutant RAS cells were highly sensitized to treatment, with evidence suggesting that these cells were unable to recover from even transient exposure to BI 2536. Given the prevalence of *KRAS* mutations in pancreatic ductal adenocarcinoma this seems particularly promising.

This suggests that PLK1 is essential to the survival of RAS-driven cells exposed to mitotic stress, suggesting that such cells may be particularly sensitive to PLK1-inhibition. Moreover, this raises the question whether PLK1 inhibitors should be specifically targeted towards patients with tumours that are both mutant *KRAS* and overexpress PLK1[418] - an area that is yet to be explored in any great detail.

PLK1 and Cancer

In keeping with its role in promoting cell proliferation, PLK1 is overexpressed in a variety of tumours[419 420] and this has been suggested to contribute to carcinogenesis by causing chromosome instability[421] and other mitotic defects[422]. Malignancies thus far associated with overexpression of PLK1 include pancreatic[423], hepatocellular[424], hepatoblastoma[425], oesophageal[426], gastric[427 428 429], colorectal[430 431 432], breast[433 434], prostate[435], head and neck[436], thyroid[437], gliomas[438], non small-cell lung[439], melanoma[440] and cutaneous T-cell lymphoma[441]. In addition to this, elevated levels of the protein has been shown to be a poor prognostic indicator in the majority of these cancers, including hepatocellular carcinoma[423], hepatoblastoma[424], oesophageal[426], gastric[428 429], prostate[435], urothelial[442], head and neck[436], non small-cell lung cancer[439 443], non-Hodgkins lymphoma[444 445], myeloma[446], melanoma[440 447], ovarian[448 449], endometrial[450] and cervical[451] (Figure 17).

Though some argue that this overexpression is simply a reflection of rapidly proliferating cells in tumours, there is plentiful evidence to support PLK1 as a potentially valuable anti-cancer target[452]. One of the earliest publications to support this theory was Smith *et al*[453] who showed that by constitutively expressing PLK1 in NIH3T3 fibroblasts the cells became transformed, enabling the cell line to grow in soft agar and induce tumour growth when injected into nude mice. A second example is that PLK1 expression has already been shown to be a predictor of response of rectal cancer to radiotherapy[454].

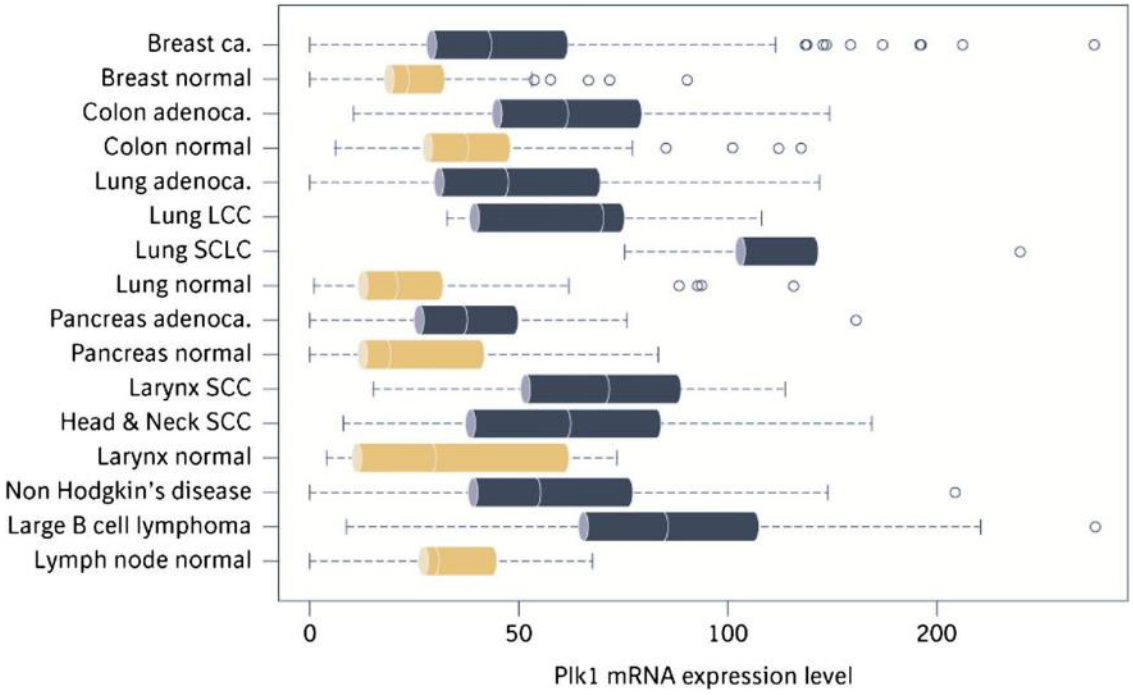

Figure 17: mRNA expression profile of PLK1 in normal and malignant human tissue
This panel shows whisker-box plots for normal tissues (yellow/brown) and malignant lesions (blue). The vertical lines in each box indicate median values, and box limits represent the first and third quartiles; the whiskers extend to 1.5 times this interquartile range. The circles represent outliers. Abbreviations : LCC, large-cell carcinoma; SCLC, small-cell lung carcinoma; SCC,squamous-cell carcinoma. The number of samples for each tissue from top to bottom is n = 278, 84, 95, 215, 73, 10, 5, 134, 66, 51, 11, 27, 6, 175, 64, and 14, respectively. Taken without permission from Steegmaier[455].

PLK1 and Pancreatic Cancer

Gray *et al*[423] assessed the suitability of PLK1 as a potential therapeutic target in pancreatic cancer. PCR demonstrated the upregulation of PLK1 in 9 of 10 pancreatic cancer cell lines examined, in comparison to HPDE6c7, a non-transformed pancreatic epithelial cell line. Genetic overexpression ranged from 8-fold in Panc-1 cells, to 58-fold, seen in MiaPaCa-2. mRNA isolated from 4 tumours revealed up-regulation of PLK1 signal in all samples with one tumour expressing a 20-fold increase compared with normal pancreatic tissue. To delineate whether overexpression at the RNA level led to an increase in protein levels, a tissue microarray of 35 pancreatic adenocarcinoma samples from their facility was examined. 74% of tumours stained positively for PLK1 with 31% demonstrating high staining. Overall, this suggests vastly heterogenous behaviour between tumours with regards to PLK1 expression.

PLK1 Inhibition

Inhibiting *PLK1* Gene Expression

Germline knockout of *PLK1* result in embryos that failed to survive past the 8-cell stage demonstrating the vital function of PLK1 in early development[456]. Furthermore, inhibiting PLK1 at a translational level has been extensively described in the literature. One method is RNA interference, which involves the enzymatic cleavage of 21-nucleotide siRNA fragments into single RNA strands, which when bound to complementary mRNA leads to its degradation. Secondly are single-stranded DNA antisense oligonucleotides, which can also reduce the genetic expression of PLK1 by binding to complementary mRNA[275].

Studies have already described successfully utilising *PLK1* siRNA to inhibit PLK1 in cancer cells, leading to mitotic arrest and apoptosis[457] [458], suggesting that cancer cells may not possess an alternate signalling pathway to overcome PLK1 inhibition.

Attaining RNA interference *in vivo* is challenging, though this was successfully achieved by Strebhardt[459], who demonstrated the survival of normal cells in the presence of cancer-cell death. The exact mechanism of this finding is a mystery though it is proposed that *PLK1* siRNA may leave enough residual PLK1 activity to ensure the continued viability of normal cells. Another potential explanation would be that cancer cells lose a mechanism to bypass the absence of PLK1, which is conserved in normal cells. A final suggestion is that this finding is exclusive to *PLK1* siRNA-treated cells, as both cancer and normal cells have been to respond in a similar manner when treated by PLK1 inhibiting compounds as opposed to being impeded on a genetic basis[275].

Functional PLK1 Inhibitors

Detailed knowledge regarding the structural configuration of PLK1 is imperative in order to manufacture specific inhibitors. Current compounds can be divided into two distinct classes: ATP-competitive, which target the kinase domain, and Non-ATP-competitive which target the PBD. A single compound possessing both these characteristics is yet to be developed[460].

ATP-Competitive Inhibitors

ATP-competitive PLK1 inhibitors target the ATP-binding site on the kinase domain of PLK1. However, developing a highly specific PLK1 inhibitor is extremely challenging, given that the kinase component of PLK1 shares a sequence identity of 53%, 54% and 37% with PLK2, PLK3

and PLK4 respectively. The residues comprising the ATP-binding pockets are more greatly conserved, with PLK1 sharing 90%, 86% and 60% sequence homology with PLK2, 3 and 4[461]. It is therefore unsurprising to discover that the ATP-competitive inhibitors PHA-680626 and BI 2536 interferes with PLKs1-3 with little difference in selectivity[290 455 462].

Non-ATP-Competitive Inhibitors

Despite the protein kinase family consisting of over 2000 members[463], PLKs are unique in containing a PBD. Therefore, the PBD's potential as a target to develop a highly specific polo-like kinase inhibitor is unrivalled. Non-ATP competitive PLK1 inhibitors function by inhibiting the protein-protein interactions of the PBD and the first compound of this nature to be developed was Poloxin.

PLK1 Inhibitors – Preclinical Findings and Results of Early Clinical Trials in Solid Tumours

Non-ATP Competitive Inhibitors

Poloxin

Preclinical Findings with Poloxin

Poloxin is a small molecule that impairs the PBDs interaction with its binding peptide. It was the first non-peptidic inhibitor that prevents the inter-protein reactions of PLK1's PBD. Poloxin arrests cells in mitosis with phenotypic changes including dissociated centrosomes, misaligned chromosomes and abnormal spindles noted[464]. In contrast to ATP-competitive inhibitors, peptidic PBD inhibitors cause bipolar, as opposed mono or multipolar spindles. Though poloxin assisted in the understanding of PLK1 it was weakly potent and non-specific[465].

ON 01910.Na

Preclinical Findings with ON 01910.Na

The substrate-dependent PLK1 inhibitor ON 01910.Na inhibits the PLK1 pathway activity at 9-10nM in addition to inhibiting other kinases such as PLK2. The compound induces a G2-M phase arrest with phenotype abnormalities including multipolar spindles, centrosome fragmentation and chromosomal misalignment noted, leading to apoptosis. In xenograft models this ATP-independent drug was found to be highly efficacious both as a single agent and in combination with established chemotherapeutic agents, including gemcitabine[466].

Clinical Studies with ON 01910.Na

The first Phase I study investigating the effects of ON 01910.Na on solid tumours revealed rapid distribution and slow elimination of the drug, with lower haematological toxicity compared with other PLK1 inhibitors[467]. One patient with ovarian cancer remained progression-free for 2 years, though this finding was not replicated in a later Phase I trial in solid tumours[468]. The current development of ON 01910.Na now seems focused on myelodysplastic syndrome.

ATP-Competitive PLK1 Inhibitors

GSK461364A

Preclinical Findings with GSK461364A

The thiophene derivative GSK461364A has been shown to have a 1000-fold greater selectivity for PLK1 compared to nearly 50 other examined kinases[469]. *In vitro*, GSK461364A has demonstrated antiproliferative activity in over 120 cancer cell lines, with its effects shown to be concentration-dependent. Low nanomolar concentrations cause moderate mitotic effects and the inhibition of cytokinesis with moderate to high concentrations leading to abnormal mitotic spindles, misaligned chromosomes and mitotic arrest[470] [471]. One in vitro study suggested that cells possessing a TP53 mutation may be more sensitive to GSK461364A with cells exhibiting increased chromosome instability[472], though this effect is yet to be replicated *in vivo*. Intravenous infusion of the compound in xenograft tumour models reported successes ranging from tumour growth inhibition to tumour shrinkage[473] [474].

Clinical Studies with GSK461364A

A phase I study of GSK461361364A in 40 patients with solid tumours showed dose-proportional pharmacokinetics and anti-cancer activity with increased phosphorylated histone H3 (pHH3) seen in circulating tumour cells[475] [476]. Only 15% of patients showed stable disease at 4 months and it was concluded that the drug should be administered in conjunction with anticoagulation in future due to the significantly increased risk of venous thrombosis (20%). A further trial to ascertain the efficacy of GSK461364A in the prevention of large brain metastases in breast cancer yielded more positive results, though further investigation is required[477].

HMN-214 and HMN-176

Preclinical Findings with HMN-214 and HMN-176

HMN-214 is an orally administered prodrug of the active agent HMN-176[478]. HMN-214 interferes with the subcellular distribution of PLK1 as opposed to directly inhibiting the kinase. This results in G2-M phase arrest, abnormal spindle polar bodies and DNA destruction[479]. *In vivo*, HMN-176 has shown potent anticancer activity against a spectrum of human tumour xenografts, including pancreatic cancer[480].

Clinical Studies with HMN-214 and HMN-176

Phase I studies of HMN-214 in patients with advanced solid malignancies resulted in 24%[478] and 9%[481] of patients achieving stable disease respectively. However, these studies were not specifically targeted at tumours with PLK1 overexpression, suggesting this may be an area for further development[482].

TAK-960

Preclinical Findings with TAK-960

TAK-960 (Takada Pharmaceuticals) in an orally administered pyrimidodiazepinone with potent PLK1 inhibitory properties[483]. The drug has been shown to induce the accumulation of cells in G2-M phase in addition to causing a 'polo' arrest and increased level of pHH3 in treated cells. In a mouse xenograft, TAK-960 inhibited the growth of the colorectal cancer HT-29 with good tolerance of the drug[484].

Clinical Studies with TAK-960

Unfortunately, a recent trial investigating TAK-960 in non-haematological malignancies (NCT01179399) was terminated early by the sponsor due to business reasons[485] and its development was ceased in 2013[486].

NMS-P937

Preclinical Studies with NMS-P937

The pyrazolo-quinazoline derivative NMS-P937, also recognised as NMS-1286937, is an ATP-competitive, orally administered PLK1 inhibitor. In keeping with other PLK1 inhibitors, the agent has been shown to induce a G2-M phase arrest and shown antiproliferative activity against over a hundred haematological and solid malignant cell lines[487]. In a xenograft model, NMS-P937 has demonstrated synergy in inhibiting tumour growth, in combination

with irinotecan[488]. This provides further weight to the argument that PLK1 inhibitors' future may be in combination with other anticancer agents, as opposed to monotherapy.

Clinical Studies with NMS-937

NMS-937 is currently being evaluated in a Phase I trial in adult patient with advanced or metastatic solid tumours (NCT01014429[489]), though the results are yet to be published.

BI 2536

Preclinical Findings with BI 2536

The dihydropteridnone derivative BI 2536 was the first-in-class prototype PLK1 inhibitor developed by Boehringer Ingelheim. It showed high selectivity for PLK1 (IC_{50} 0.83nM) but was also potent in inhibiting both PLK2 (IC_{50} 3.5nM) and PLK3 (IC_{50} 9nM)[455].

In vitro, BI 2536 was demonstrated to block the proliferation of multiple human cancer-cell types at concentrations of 2-25nM. Further work with HeLa cells, revealed the accumulation of treated cells with a 4*N* DNA content, indicative of a G2 or mitotic block. Phenotypic observation revealed monopolar spindles, described as 'polo' spindles surrounded by a ring of chromosomes, similar to those seen in *PLK1* siRNA-treated samples[490 491 492]. Synchronised HeLa cells released into BI 2536-containing media arrested in G2/M phase, with evidence of apoptosis at 24-48 hours[455 493]

Intravenous BI 2536 is highly efficacious in inhibiting tumour growth in several xenograft models including colonic, pancreatic and non-small-cell lung cancer. *In vivo* results indicated that tumour regression was induced by a mitotic arrest within the tumour leading to cell death[455].

Clinical Studies with BI 2536

Unfortunately, BI 2536's initial promise in the preclinical setting failed to translate into the clinical environment. A multitude of phase I and II trials[494 495 496 497 498] showed no clinical benefit in BI 2536 monotherapy, including in patients with advanced pancreatic cancer[499]. These results, coupled with the emergence of BI 6727, a second dihydropteridinone derivative with an improved safety profile and PLK1 specificity, terminated the further development of BI 2536[500].

BI 6727

Preclinical Findings with BI 6727

BI 6727 (molecular weight 728.21 g/mol), also known as Volasertib, is the second dihydropteridinone derivative developed by Boehringer Ingelheim. Compared to the previous generation, it has a large volume distribution and long half-life in mouse models enabling the drug to be administered both intravenously and orally[501]. The drug is highly potent and is currently the most specific ATP-competitive Plk1 inhibitor commercially available, with an IC_{50} of 0.87nM. It has also been shown to inhibit PLK2 and PLK3 at IC_{50} values of 5nM and 56nM respectively, but is ineffective against 64 other known kinases at concentrations of up to 10μM[502].

BI 6727 functions by attaching to the ATP binding pocket of PLK1 resulting in abnormal monopolar mitotic spindles and 'polo-arrest' in mitosis due to the cell's inability to separate their chromosomes. Flow cytometry of such cells shows a prominent G2-M block, a picture consistent with that caused by *PLK1* siRNA[490] and this prolonged mitotic arrest will eventually lead to cell death by apoptosis.

In preclinical studies, BI 6727 demonstrated *in vitro* efficacy against cervical cancer[503] and prostate cancer[504], in addition to showing anti-tumour activity in numerous xenograft models of human cancers, including taxane-resistant colonic, breast, lung, haemopoetic[490] [502], pancreatic[293] and a variety of paediatric tumours (Rhabdoid and Wilms renal tumours, Ewings and osteosarcomas and a variety of neurological tumours)[505].

Clinical Studies with BI 6727 Monotherapy

An initial Phase I trial was undertaken in 65 patients with advanced solid tumours[500], with the final results later presented at the American Society of Clinical Oncology[506]. The Caucasian cohort's malignancies included soft tissue sarcoma, melanoma, non-small cell lung, colorectal, urothelial and prostate cancers, with 28% classified as 'other'. BI 6727 was confirmed to have al ong half-life of 100 hours and was administered intravenously every three weeks to a maximum tolerated dose of 400mg per infusion. However, due to the frequency of dose reductions in later courses, adverse events and dose-limiting toxicities, 300mg per dose was chosen for further development.

Overall, the drug was well tolerated with the main side-effects encountered being haematological, with thrombocytopenia, neutropenia and febrile neutropenia becoming dose-limiting. These toxicities were reversible with no evidence of cumulative toxicity. Clinical outcomes were favourable with 48% of patients experiencing stable disease. Partial response was seen with a variety of tumour types with a further six patients remaining progression-free for over 6 months.

A second phase I trial in 59 Asian patients with advanced solid tumours[507] included patients with soft tissue sarcoma, melanoma, colorectal, urothelial, oesophageal, liver and biliary, lung and head and neck cancers. This trial compared two infusion regimes: BI 6727 every three weeks vs. BI 6727 on day 1 and day 8 of a three week cycle. The mean tolerated dose was similar to the first trial, being 300mg per 3-weekly infusion and 150mg in the opposing arm. Haematological and dose-limiting toxicities were seen in both treatment arms but were much less prevalent in those patients receiving the drug in two infusions. As in the first Phase I trial, clinical outcomes were favourable with 44.1% of patients showing stable disease and two patients with urothelial cancer and melanoma displaying a partial response.

A Phase II trial in advanced urothelial cancer[508] reported a 14% partial response and 26% with stable disease in patients undergoing three weekly infusions of BI 6727, which was deemed insufficient to justify further trials in the disease.

A further Phase II trial (NCT01121406[509]) compared BI 6727 with the investigator's choice of alternative monotherapy, as 3rd or 4th line treatment in advanced ovarian cancer. In summary, outcomes were similar in both groups, with fewer adverse events noted in patients receiving BI 6727. The investigators conclude that the identification of a biomarker to predict response to BI 6727 would be the next step.

Clinical Studies with BI 6727 in Combination with other Compounds

Combining novel agents with established drugs has the potential to improve efficacy and given the relatively poor results thus far achieved with BI 6727 monotherapy this may be where this drug's future lies. In a Phase II trial, Ellis *et al*[510] combined BI 6727 with the established agent for non small-cell lung cancer, pemetrexed, and compared responses to those receiving pemetrexed monotherapy. However, no improvement in progression-free or overall survival was seen.

BI 6727 was combined with platinum agents (cisplatin and carboplatin) in a Phase I study of 61 patients with advanced solid tumours[511 512], with 44% achieving either stable disease or a partial response. Though the cohort had already previously been heavily pretreated, combination therapy was well tolerated, suggesting that BI 6727 can be administered in combination with cytotoxic agents at full monotherapy dose[513].

Other studies combined BI 6727 with kinase inhibitors afatinib[514] and nintedanib[515] in patients with advanced solid tumours. Though results were generally poor with only 2/29 and 2/30 patients respectively showing any response, one patient with breast cancer showed a complete response in the latter study, suggesting that a specific cohort of patients could benefit from such treatment.

With regards to haematological malignancy, a Phase II trial combined BI 6727 with low-dose cytarabine (LD-AraC) versus cytarabine alone in the treatment of acute myeloid leukemia (AML) in 87 frail elderly patients. Preliminary results from this randomised trial showed a significant benefit with combination therapy with a median event-free survival of 5.6 months compared to 2.3 months (HR: 0.57, 95%CI 0.35-0.92, p=0.021) and a median overall survival of 8 months compared with 5.2 months (HR 0.63, 95% CI 0.4-1, p=0.047)[516]. On this basis, BI 6727 in combination with LD-AraC was granted 'breakthrough status' by the FDA in 2013, with the aim of expediting the development of BI 6727 as a potential therapy for AML.

Current Trials with BI 6727

At the time of writing, a few trials remain ongoing with BI 6727 as both monotherapy and in combination[517]. The overwhelming majority of these trials are understandably focused on haematological malignancies where BI 6727 shows most promise.

Chapter 2 – Materials and Methods

Materials

Chemical or Reagent and Supplier

Albumin from Bovine Serum	Sigma Chemical Co, Poole, Dorset
BI 6727	Boehringer Ingelheim, Germany
β-actin Primary Antibody	Cell Signalling, Hitchin, Hertfordshire
Bradford dye reagent	BioRad, Hemel Hempstead, Hertfordshire
Bromophenol blue	Sigma Chemical Co, Poole, Dorset
Caspase-3 Primary Antibody	Cell Signalling, Hitchin, Hertfordshire
Cell lines: Suit-2, MiaPaCa-2, Panc-1, BxPC-3	American Type Culture Collection (ATCC), Rockville, MD, USA
Dimethyl Sulfoxide (DMSO)	Fisher Scientific, Loughborough, Leicestershire
Distilled water	University of Liverpool stores
DL-Dithiothreitol (DTT)	Sigma Chemical Co, Poole, Dorset
Ethanol	University of Liverpool stores
EZ4U Assay	Biomedica, Austria
Foetal Bovine Serum (FBS)	Life technologies, Paisley, Renfrewshire
Gemcitabine	Eli-Lilly, Basingstoke, Hampshire
Glycerol	Sigma Chemical Co, Poole, Dorset
Glycine	Fisher Scientific, Loughborough, Leicestershire
Goat anti-rabbit Immunoglobulin HRP	Dako Ltd, High Wycombe, Buckinghamshire
Hydrochloric acid	University of Liverpool stores
L-glutamine	Life technologies, Paisley, Renfrewshire

Non fat Dry Milk – Blotting Grade	BioRad, Hemel Hempstead, Hertfordshire
Nonidet P-40	Abcam, Cambridge, Cambridgeshire
Restore™ Western Blot Stripping Buffer	Thermo Scientific, Loughborough, Leicestershire
Phosphate Buffered Saline (PBS) Tablets	Fisher Scientific, Loughborough, Leicestershire
Pipettes - 5, 10, 25ml	Corning Inc., New York
Pipette tips - 10, 200 and 100µl	Starlab, Milton Keynes, Buckinghamshire
Penicillin-streptomycin	Sigma Chemical Co, Poole, Dorset
Phosphate Buffered Saline (PBS)	Sigma Chemical Co, Poole, Dorset
Propidium Iodide	Sigma Chemical Co, Poole, Dorset
Protease inhibitor tablets, EDTA-free	Roche, Welwyn Garden City, Hertfordshire
Protein ladder	Life technologies, Paisley, Renfrewshire
RNAse A	Thermo Scientific, Loughborough, Leicestershire
RPMI-1640 Media	Sigma Chemical Co, Poole, Dorset
Sodium chloride	Sigma Chemical Co, Poole, Dorset
Sodium deoxycholate	Sigma Chemical Co, Poole, Dorset
Sodium Dodecyl Sulfate (SDS)	Fisher Scientific, Loughborough, Leicestershire
Sodium hydroxide pellets	VWR, Lutterworth, Leicestershire
Tris Base	EMD Chemicals, San Diego
Tris HCL	Sigma Chemical Co, Poole, Dorset
Triton X-100	Sigma Chemical Co, Poole, Dorset
Tween® 20	Sigma Chemical Co, Poole, Dorset
Trypsin	Sigma Chemical Co, Poole, Dorset

Virkon	Antec International, Sudbury, Suffolk
Western Lightning Plus ECL	PerkinElmer, Cambridge, Cambridgeshire

Equipment

0.5 and 1.5ml microcentrifuge tubes	Eppendorf, Stevenage, Hertfordshire
96-well plates	Corning Inc., New York
Annexin Apoptosis and Necrosis Quantitation Kit	Biotium, Wembley, Middlesex
Axiovert 40C Microscope	Zeiss, Cambridge, Cambridgeshire
Branson Sonicade	Branson Ultrasonics Co, Shangai, China
Cell Counting Slides	BioRad, Hemel Hempstead, Hertfordshire
Cell scrapers	Corning Inc., New York
DC126291 Camera	Canon
FACSDiva Software	Beckton Dickinson, Oxford, Oxfordshire
FACS Tubes	Beckton Dickinson, Oxford, Oxfordshire
Falcon Tubes - 15 and 50ml	Corning Inc., New York
Mr. Frosty™ freezing container	Thermo Scientific, Loughborough, Leicestershire
Photograph film	Kodak
Heraeus Biofuge Primo Centrifuge	Thermo Scientific, Loughborough, Leicestershire
Heraeus Pico17 Mini Centrifuge	Thermo Scientific, Loughborough, Leicestershire
Procell Incubator	Jencons Scientific Ltd, Leighton Buzzard, Bedfordshire
JB Aqua 26 Plus Water Bath	Grant, Shepreth, Cambridgeshire
Kodak GBX Developer and Fixer	Kodak
LSRFortressa™ Flow Activated Cell Sorter	Beckton Dickinson, Oxford, Oxfordshire

Mini Protean® Tetra System/AnyKD gels	BioRad, Hemel Hempstead, Hertfordshire
Multiscan Ex Plate Reader	Thermo Scientific, Loughborough, Leicestershire
Seven Compact pH Meter	Mettler-Toledo, Beaumont Leys, Leicestershire
QBTP Heat Block	Grant, Shepreth, Cambridgeshire
Reagent Resevoirs	Thermo Scientific, Loughborough, Leicestershire
Sonicade	Branson Ultrasonics, Connecticut
TC10™ Automated Cell Counter	BioRad, Hemel Hempstead, Hertfordshire
Trans-Blot® Turbo™ Transfer System	BioRad, Hemel Hempstead, Hertfordshire
T25 and T75 Flasks	Thermo Scientific, Loughborough, Leicestershire
Vortex Genie 2	Scientific Industries, New York
Weighing Scales	VWR, Lutterworth, Leicestershire

Preparation of Solutions

1M DL-Dithiothreitol (DTT)

0.154g DTT

1ml distilled water

Storage: Aliquoted and stored at -20°c

1M Tris

30.29g Tris HCl

200ml distilled water

pH as required

Storage: Room temperature

RNAse (10mg/ml)

100mg RNAse

10ml PBS

Storage: Aliquoted and stored at -20°c

Propidium iodide (1mg/ml)

10mg Propidium iodide

10ml PBS

Storage: Aliquoted and stored at -20°c

Running Buffer x10

50ml 20% Sodium dodecyl sulphate (SDS)

144g Glycine

30g Tris Base

Make up to 1L with distilled water

Storage: Room temperature

PBST x1

10 phosphate buffered saline (PBS) tablets

1L distilled water

1ml Tween per 0.1% concentration desired

Storage: Room temperature

TBST x10

87.66g Sodium chloride

121g Tris Base

1L distilled water

pH to 7.5 with sodium chloride and/or sodium hydroxide

Titrate to x1 with distilled water, then add 1ml Tween per 0.1% concentration desired

Storage: Room temperature

Reducing Sample Buffer x5

1g Sodium dodecyl sulphate (SDS) powder

3ml 1M Tris HCl pH 6.8

5ml Glycerol

2ml distilled water

0.05g bromophenol blue

Storage: Aliquoted and stored at -20°c

RIPA Buffer

50nM Tris HCL pH 8

150mM NaCl

1% NP-40

0.5% Sodium deoxycholate

0.1% SDS

Storage: Stored at 4°c. 10ml aliquoted when required with a protease inhibitor tablet added

Freezing Media

90% Foetal bovine serum

10% DMSO

Storage: Aliquoted and stored at -20°c

Methods

Drugs

BI 6727

BI 6727 was provided by Boehringer Ingelheim. The powdered agent was stored away from light at room temperature. Dimethyl sulfoxide (DMSO) was utilised to formulate a 10millimolar (mM) stock solution and kept in 100µl aliquots at -20°C. Further dilutions were formulated from the stock solution with 0.1% DMSO-containing RPMI-1640 tissue culture media.

Gemcitabine

Powdered gemicitabine was purchased from Eli lilly Ltd. A stock solution of 0.05molar (M) was formulated in PBS and stored at -20°C in 1ml aliquots. Further dilutions were made with RPMI-1640 tissue culture media.

In Vitro Cell Work

Cell Lines

The pancreatic cell lines utilised in this research are detailed below (Table 9).

Table 9: The names and origins of pancreatic cell lines utilised in this research

Cell Line	Origin
Suit-2	Liver metastasis from a 73-year old male secondary to pancreatic ductal adenocarcinoma
BxPC-3	61-year old female with adenocarcinoma of the pancreatic body
MiaPaCa-2	65-year old male with an adenocarcinoma of the pancreatic body and tail
Panc-1	56-year old male with an adenocarcinoma of the head of the pancreas

The cell lines in this research have diverse characteristics but all are pancreatic in origin.

All cell lines were sourced from the stores in the Department of Molecular and Clinical Cancer Medicine. Their genetic alterations have been characterised and are well documented in the literature (Table 10).

Table 10: The genetic mutations and tumour marker expression of the pancreatic cell lines utilised in this research

Cell Line	*KRAS* alteration	*TP53* alteration	*CDKN2A* alteration	*DPC4* alteration	Tumour Marker Expression
Suit-2	p.G12D	p.R273H	p.E69*	Wt	CA 19-9 CEA
BxPC-3	Wt	p.Y220C	Homozygous deletion	Homozygous deletion	CA 19-9 CEA
MiaPaCa-2	p.G12C	p.R248W	Homozygous deletion	Wt	____
Panc-1	p.G12D	p.R273H	Homozygous deletion	Wt	____

The genetic mutations and tumour marker expression varied widely between the pancreatic cell lines

Authentication and Mycoplasma Testing

Cell lines were verified as the specified type by genotyping via PCR. Cells were regularly screened for mycoplasma by Departmental technical services using Hoechst 33258 or by PCR.

Risk assessment and Universal precautions

Universal precautions were taken at all times including Howie coat and gloves and a face mask when necessary. Good clinical practice course, induction procedures and risk assessments were completed in accordance with University policy on working with clinical samples.

Tissue Culture

All tissue culture work was undertaken in a containment level class II hood with laminar flow which was cleaned with 70% ethanol both prior to, and after use. Tissue culture reagents were all stored at 4°C and warmed to 37°C before use. All bottles and materials were cleaned with 70% ethanol prior to transfer to the hood, with an aseptic technique.

Defrosting Cell Stocks

Cryotubes were defrosted in a waterbath and the contents pipetted into tissue culture media to a total volume of 10ml. The flask was incubated for 24 hours at 37°C (5% CO_2) prior to changing the media to eliminate the DMSO from the freezing media.

Sub-culturing

Tissue culture media was removed and the cells washed with PBS. Trypsin was added until the cells were no longer adhered to the base of the flask (Table 11). The trypsin was neutralised with FCS in culture media to make a total volume of 10ml. The desired concentration of cells was then returned to the flask (with the addition of further culture media) and the remainder either discarded, or harvested for experiments.

Table 11: The routine trypsin time and sub-culture split ratios of pancreatic cell lines

Cell Line	Trypsin Time (minutes)	Routine sub-culture split (Cells:Media)
Suit-2	3	1:10
BxPC-3	5	1:5
MiaPaCa-2	3	1:10
Panc-1	2	1:5

The times taken to routinely remove adherent cell from incubated flasks and their respective sub-culture split rations when transferred into fresh media

Freezing Cell Stocks

The cell-containing media mixture was spun at 200g for 5 minutes prior to the media being extracted and PBS added to agitate the cell pellet. This was followed by a further centrifuge prior to the PBS being removed. Freezing media was added and the cell pellet agitated. This was aliquoted into cryotubes and placed in a 'Mr. Frosty™' freezing container to be stored at -80°C for 24 hours, prior to transfer to long term storage in liquid nitrogen (<-150°C).

MTS Assay

Cell pellets were washed in PBS prior to being dissolved in culture media. 10µl of this solution was inserted into a cell counter to calculate the concentration of cells and the dilution required to attain a desired final concentration for a MTS Assay at 100µl per well in a 96-well plate. All cell lines - Suit-2, Panc-1, BxPC-3 and MiaPaCa-2 cells were seeded at 2.0 $x10^4$/ml (2000 cells per well).

The plates were incubated at 37°C to enable the cells to adhere. After 24 hours, the culture media was removed and the required drug(s) concentrations administered at 100µl per well. A typical MTS plate is shown below (Figure 18).

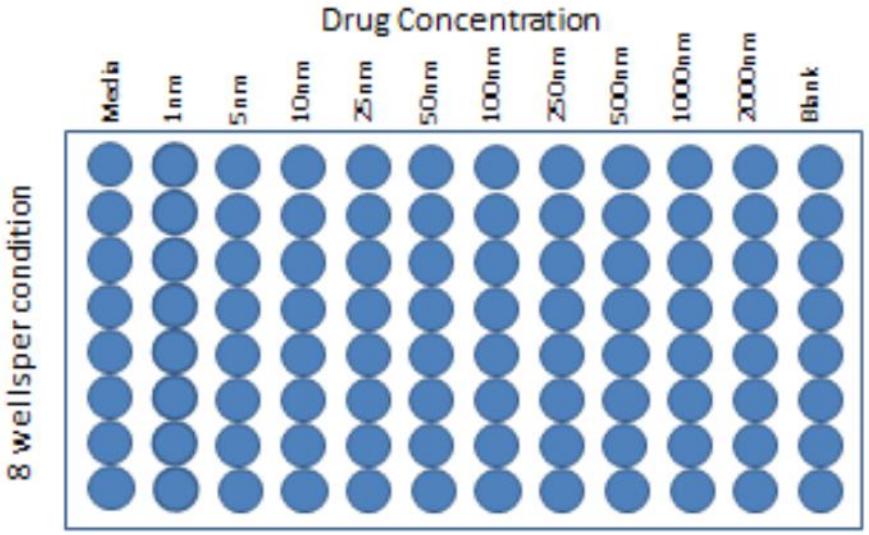

Figure 18: A typical example of a 96-well plate when undertaking a MTS assay
Rows of wells with increasing drug concentrations were established, in addition to a media-only and a blank/empty row for control purposes.

Drug treatments were undertaken for 24, 48 and 72 hours prior to the MTS assay. One plate was required per time point and all time points were repeated in triplicate.

Determination of IC_{50}

EZ4U substrate was dissolved in 2.5ml of activator and warmed to 37°C. This was added to 22.5ml of tissue culture media and mixed. The drug-containing media was extracted from the 96-well plates and replaced with 100µl of the EZ4U reagent mixture prior to the plate being incubated.

Isobolar Analysis of Drug Combinations

The concentrations of both drugs to be utilised during this analysis was determined from their respective IC_{50} readings from previous single-agent MTS assay results. The typical distribution of drug concentrations for an isobolar analysis 96-well plate is displayed below (Figure 19) with the IC_{50} of each drug equating to the highest concentrations utilised. MiaPaCa-2 cells were seeded at 2000 cells per well for 24 hours prior to the removal of the media and the commencing of drug treatment.

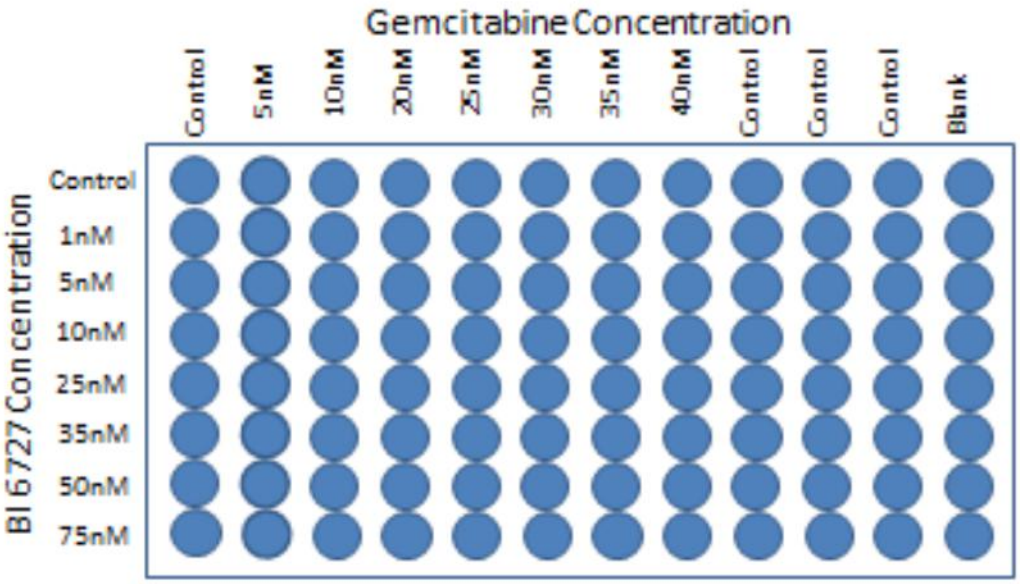

Figure 19: A typical example of a 96-well plate when undertaking an isobolar analysis
The rows of cells were treated in accordance with the seven regimes below. As previously mentioned, both media-only and blank/empty rows were established for control purposes.

Seven isobolar experiments were undertaken in total to ascertain the effects of adding both drugs together and sequentially, as demonstrated in (

Table 12).

Table 12: The isobolar analyses undertaken and their respective timing protocol

Experiment	Day 1	Day 2	Day 3	Day 4	Day 5	Day 6
1	Seeding Cells	Drug 1 added	Drug 1 added			MTS assay (72 hours)
2	Seeding Cells	Drug 1 added	Drug 2 added			MTS assay (72 hours)
3	Seeding Cells	Drug 2 added	Drug 2 added			MTS assay (72 hours)
4	Seeding Cells	Drug 2 added	Drug 1 added			MTS assay (72 hours)
5	Seeding Cells	Drug 1+2 added			MTS assay (72 hours)	
6	Seeding Cells	Drug 1 added	Drugs 1+2 added			MTS assay (72 hours)
7	Seeding Cells	Drug 2 added	Drugs 1+2 added			MTS assay (72 hours)

Timing protocol for isobolar analyses of combination drug therapy with BI 6727 and gemcitabine

Plate Reading for IC_{50}s, MTS Assays and Isobolar Analyses

As cell lines vary in their metabolic capacity, readings were taken at hourly intervals after incubation from 1 to 4 hours as necessary to ascertain a control reading close to 1. The plate was re-incubated between readings. Absorbance was measured at a wavelength of 450nm, with a further reading at 620nm as a reference to correct for nonspecific background or other potential interferences.

Western Blotting

Preparation of Cell Lysate for Western Blotting

The culture media was collected prior to twice washing the adherent cells with PBS which was also collected. The adherent cells were trypsinised and reincubated before further culture media was added to neutralise the trypsin and all contents harvested. These were

spun for 2 minutes at 1000g and the media removed. The formed cell pellet was suspended in PBS prior to being re-spun at 1000g for 2 minutes. The cell pellet was re-suspended in 200-600µl of RIPA buffer, sonicated at 13amps for 10 seconds and stored at -20°C.

Following the first thaw, the sonicated mixture was centrifuged at 1000g for 5 minutes. The resulting cell lysis supernatant was then aliquoted and stored at -20°C and the debris discarded.

Bradford Protein Assay

The Quick Start Bradford dye reagent was left to reach room temperature prior to use. A stock solution of BSA was formulated by dissolving 0.005g of bovine albumin in 1ml of distilled water. Five standard concentrations were made as detailed in (Table 13).

Table 13: The composition ratios for BSA standards

Concentration	BSA Stock Solution (µl)	Distilled Water (µl)
10	100	0
7	70	30
5	50	50
2	20	80
1	10	90

The formulation of BSA standards for the purpose of producing a standard curve, utilised in determining the protein concentration of samples.

The spectrophotometer was calibrated and zeroed by utilising a blank curvette containing 800µl of Bradford Reagent and 200µl of distilled water. Standards were made by adding 2µl of each concentration to 798µl of Bradford reagent and 200µl of distilled water. Prior to analysis, each microcentrifuge tube of Bradford-Protein combination was briefly vortexed and left at room temperature for a minimum of five minutes as instructed by the manufacturer's protocol. This process was done only once for each standard, but repeated in triplicate for each sample of cell lysate to obtain a mean reading. The standard readings were utilised to produce a standard curve, with a formula applied to calculate the volume of each sample required to include 20µg of protein.

Preparation of Samples for Western Blotting

The representative volume from each sample to include 20µg of protein (as previously determined by a Bradford assay) was aliquoted into a microcentrifuge tube. Reducing sample buffer and 1M DL-Dithiothreitol were combined at a volume ratio of 3:2 and an equal volume of this solution added to each sample to a maximum volume of 50µl in each microcentrifuge tube. To ensure that each final sample were of equal volume, the necessary volume of reducing sample buffer and water (to a ratio of 1:4) was added to each sample. Due to the capacity of each well on the precast gels, sample volumes did not exceed 50µl. Each sample was warmed on a hotplate for 15 minutes at 96°C and then spun at 1000g for 20 seconds in preparation for loading onto a gel.

Running Western Blotting Gels

BioRad 10-well Any kD Mini-PROTEAN TGX Precast Gels were placed into the negative electrode chamber with the wells facing inwards, prior to being placed into the tank which was then filled to the desired level with running buffer. Any air bubbles trapped in the running chambers were removed with a syringe and a 25 gauge needle.

The protein ladder was pipetted into the leftmost lane of each gel prior to the running lanes being filled with the required volume of samples. The gels were run at 300 Volts until the dye front had run to the bottom of the gel.

The gel cassettes were removed, trimmed and then sandwiched within two ion reservoir stacks containing a PVDF blotting membrane (BioRad Trans-Blot Turbo Transfer Pack). This was carefully rolled to remove any trapped air bubbles, prior to being placed within a locked cassette and the Trans-Blot machine programmed to run on a low molecular weight setting. The PVDF blotting membrane was then placed into a tray containing the desired blocking agent and then placed on a rocker.

Antibody Probing for Caspase-3

After blocking the membrane for the desired period, the blocking agent was replaced like-for-like but with the addition of a caspase-3 antibody at a concentration of 1:1000 (Table 14). Optimal antibody probing for caspase-3 was concluded to be overnight for 16 hours at 4°c.

This was followed by three, ten minute washes with 10mls of 0.1% TBST, with the liquid discarded after each wash. A secondary antibody was than added, diluted to the necessary concentration in 10mls of 5% Milk in 0.1% TBST (Table 15). Optimal conditions for probing for secondary antibody (Table 15) was for an hour and a half at room temperature. This process was again followed by three, ten minute washes, after which membrane was immersed in 4mls of enhanced chemiluminescence (ECL) for 2 minutes. The membrane was then removed from the rocker and taken to the dark room for developing.

Stripping Membranes

After probing for the caspase-3 antibody as described and after the film was developed, the membrane was repositioned in a tray containing 10ml of stripping buffer and placed on a rocker at room temperature for 10 minutes. The stripping buffer was then discarded and three, five-minute washes with 10mls of 0.3% TBST undertaken.

Beta Actin

The stripping and washing of the membrane was followed by blocking with 5% milk in 0.1% TBS for 30 minutes on the rocker followed by a the addition of 10mls of 5% Milk in 0.1% TBST containing 1:10 000 monoclonal anti-beta-actin antibody produced in mouse for a further 30 minutes (Table 14). Three 0.3% TBS wash were then repeated prior to the addition of 10mls 5% Milk in 0.1% TBST with 1:3000 anti mouse secondary antibody for 30 minutes. The membrane then underwent a final round of 0.3% TBST washes prior to the addition of ECL in preparation for developing as previously described.

Table 14: Primary antibodies utilised in Western Blotting

Antibody	Manufacturer	Molecular Weight	Code	Source	Dilution	Incubation and Blocking Agent
Caspase-3	Cell Signalling	17, 19 and 35 kDa	#9662	Rabbit	1:1000	5% Milk in 0.1% TBST
Beta Actin	Cell Signalling	45kDa	#4967	Rabbit	1:10 000	5% Milk in 0.1% TBST

A table of the primary antibodies utilised, in addition to their optimal concentration and dilutent.

Table 15: Secondary antibody utilised in Western Blotting

Antibody	Manufacturer	Code	Source	Dilution	Incubation and Blocking Agent
Anti-Rabbit IgG HRP	Dako	P0448	Goat	1:3000	5% Milk in 0.1% TBST

A table of the secondary antibody utilised, in addition to its optimal concentration and dilutent.

Freezing Membranes

Membranes were wrapped in cling film and stored at -80°C. To re-use the membrane, it was quickly defrosted at room temperature and stripped. The membrane could then be washed, blocked and re-probed with a further antibody if required. No membrane was frozen or stripped more than once.

FACS Analysis

At time of cell harvest the media was removed and discarded to exclude floating cells. Further media was added to the culture flask and a cell scraper utilised to release all adherent cells. These were spun for 5 minutes at 1000g at 4°C and the resulting supernatant aspirated. The cells were then re-suspended in PBS and re-centriguged. All but a few drops of the supernatant was then aspirated and the microcentrifuge tube vortexed to commence re-suspension of the cell pellet. 1ml of cold 70% ethanol was then added drop-wise to each tube during a further vortex, prior to storage at 4°C for a minimum of 16 hours to fix the cells.

When ready to undertake FACS analysis, the microcentrifuge tubes were spun at 1000g for 5 minutes at 4°C and the alcohol discarded. PBS was added to re-suspend the cell pellet and a cell count performed. 150 000 cells per sample was transferred to a microcentrifuge tube, re-spun as previously described and the supernatant aspirated. 350µl of 50µg/ml propidium iodide containing 0.2% triton was added to each sample, along with 50µl of 10mg/ml RNAse. The samples were vortexed and transferred to BD FACS tubes prior to being stored on ice in the dark room for 15 minutes. FACS analysis was kindly undertaken by on Dr. Asmaa Salman and Dr. Melaine Oates on LSRFortressa™ Flow Activated Cell Sorter and the data analysed with FACSDiva Software.

Annexin V Apoptosis and Necrosis Assay

An Annexin Apoptosis and Necrosis Quantification Kit (Biotium) was stored at 4°C in the dark. This kit contained:

- FITC-Annexin V stain
- Ethidium Homodimer III (EthD-III) stain
- X5 Annexin V binding buffer

Floating and adherent cells were harvested and spun for 5 minutes at 1000g at 4°C with the resulting supernatant aspirated. Cells were re-suspended in 1ml of PBS, and again spun at 1000g. The supernatant was aspirated and discarded and the remaining cell pellet processed immediately. Cell pellets were re-suspended at 2-3 x 10^6 cells/ml in X1 binding buffer (diluted in distilled water) with 5µl of both FITC-Annexin V and EthD-III added. Samples were incubated at room temperature in the dark room for 15 minutes prior to the addition of a further 400µl of X1 binding buffer to each sample. Flow cytometric analysis to measure fluorescence in FITC and propidium iodide channels was kindly undertaken by Dr. Melanie Oakes within an hour of staining, using LSRFortressa™ Flow Activated Cell Sorter, with the data analysed by BD FACSDiva 7.0 Software.

Hypothesis

PKL1 inhibition arrests cells in G2 and gemcitabine requires dividing cells to work optimally. Combining both BI 6727 and gemcitabine will therefore not be as effective as gemcitabine monotherapy in pancreatic cancer cells *in vitro*.

Aim

In vitro evaluation of the potential role of a novel PLK1 inhibitor, BI 6727, in pancreatic cancer – both as monotherapy and in combination with gemcitabine.

Objectives

1. Establish the IC_{50} concentrations of both BI 6727 and gemcitabine in pancreatic cancer cell lines.
2. Establish an optimal drug sequencing and combination regime for BI 6727 and gemcitabine in pancreatic cancer cells *in vitro.*
3. Identify the mode of cell death when BI 6727 and gemcitabine are utilised in combination in pancreatic cancer cells *in vitro.*

Chapter 3 – Results

Cell-Line Experiments

The aim of this thesis is to examine the role of a novel PLK1 inhibitor, BI 6727 in pancreatic cancer. According to the World Medical Association's revised Decleration of Helsinki, clinical trial participants in every country are entitled to the best standard of care[518]. As gemcitabine is an established chemotherapeutic agent in the treatment of the disease and any new drug should arguably be tested in combination with gemcitabine: therefore, BI 6727 was also investigated in combination with this drug.

Tissue culture is the most convenient way of investigating the efficacy of a novel drug with the National Cancer Institute recognising that *in vitro* evaluation utilising cell lines is an appropriate method of developing chemotherapeutic agents[519]. Following the drug discovery and development pathway, successful *in vitro* results with a chemotherapeutic agent may progress to human tumour xenograft models and eventually, clinical trials. Taking into account the massive failure rate of novel anticancer agents[520], the estimated cost of developing a new drug to attain market approval currently exceeds $2.5 billion and takes over a decade[521].

These results must be appreciated and interpreted within the limitations of cell culture. Cancer cells growing in a culture plate will not behave as tumour cells *in situ*. Over time, cell lines often acquire additional mutations and adapt to growth in culture media. Given the absence of a heterogenous cell population and lack of tissue architecture such as stroma, some cell characteristics will be lost or altered[522].

Single Drug Experiments

Establishing the IC_{50}s of BI 6727 and Gemcitabine

The first step in assessing the properties of BI 6727 was to establish the IC_{50} concentration of the drug in four pancreatic cancer cell lines: MiaPaCa-2, Suit-2, Panc-1 and BxPC-3 - a task which was replicated with gemcitabine. The IC_{50} is universally recognised as half maximal inhibitory concentration, which is the concentration of a specified drug which halves the number of viable cells in comparison to a control containing no drug[523]. This was done by treating the various cell lines with increasing concentrations of the drug for 24, 48 and 72 hours prior to undertaking a viability assay with a spectrophotometer (Figure 20) with the

mean 'blank' reading subtracted from the final values. A curve was plotted against the control which was standardised as 100% at the plateau (the highest point on the curve) and 0% at the lowest point. The concentration at the midpoint of the curve was then determined at the IC_{50} concentration. Each cell line was repeated in triplicate with a mean reading across the three experiments declared as the IC_{50}.

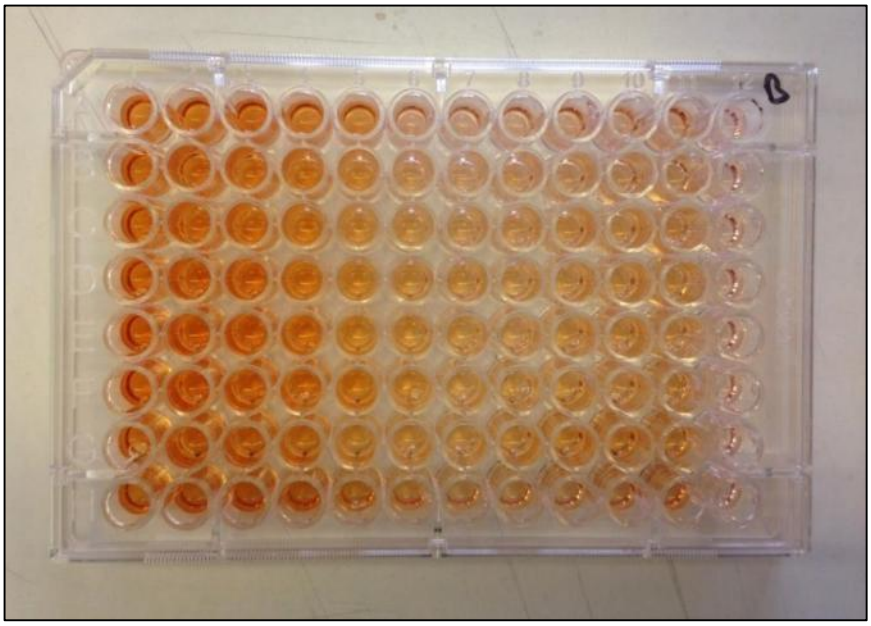

Figure 20: A photograph of an MTS experiment to determine an IC_{50} in a 96-well plate
An example of a typical MTS plate prepared for the plate reader with eight rows prepared per condition/drug concentration. The EZ4U reagent has already been added to each well. The control lane (pure media with no drug) is the left-most column. From left to right the concentration of drug increases, reflected in a paler orange colour indicating a lower number of viable cells. The right-most column in this example is left blank.

The IC_{50} Concentration of BI 6727 in Pancreatic Cancer Cell Lines

In the literature, the IC_{50} concentration of BI 6727 in cell lines is widely variable. Most cell lines are declared in the low nanomolar range with one prostate cancer cell line, PC3 reported as having an IC_{50} as high as 600nM[504]. Plasma levels established in patients safely treated with BI 6727 far exceeds this level[507].

Pancreatic cancer cell lines MiaPaCa-2 (Figure 21), Suit-2, Panc-1 and BxPC-3 exhibited similar IC_{50} readings of 53-77nM during our experiments (Table 16) Their response to increasing concentrations of BI 6727 was similar, in being able to maintain near control level number of viable cells at the lower nanomolar concentrations, before exhibiting a sharp drop in cell numbers in comparison to the control, as the IC_{50} concentration was

approached. Complete IC_{50} graphs at the 72 hour time point, repeated in triplicate for all pancreatic cancer cell lines treated with BI 6727 can be seen in Appendix B

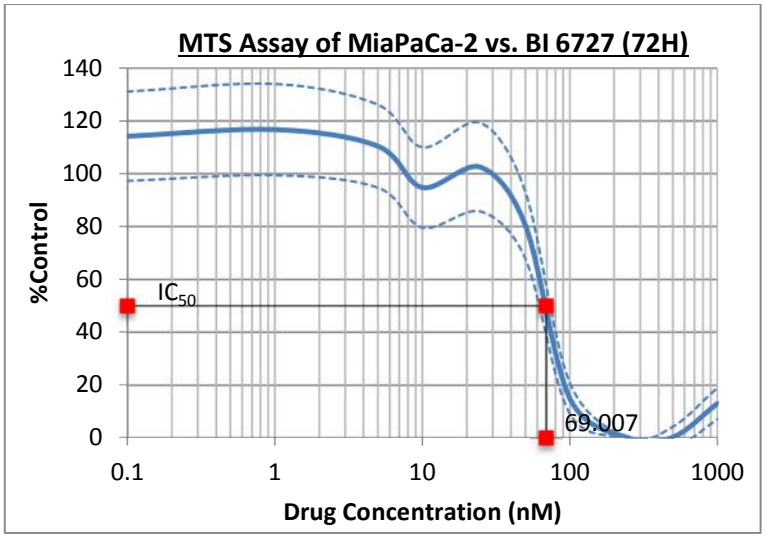

Figure 21: Determining the IC_{50} concentration of BI 6727 in MiaPaCa-2 cells
A graph displaying how the IC_{50} of BI 6727 was determined in the MiaPaCa-2 cell line. This is a typical appearance of a dose-response curve with BI 6727 across all the studied pancreatic cancer cell lines. MiaPaCa-2 cells seem resistant to BI 6727 at low nanomolar concentrations. All cell line experiments were repeated in triplicate with a mean reading calculated to determine a final IC_{50} concentration.

BI 6727's Antiproliferative Effect on Pancreatic Cancer Cells

In order to compare data across cell lines MTS assays were standardised to a control reading with no drug (100%) at 24, 48 and 72 hours. The 'blank' absorbance reading was universally subtracted prior to standardisation and the results plotted on a line graph (Figure 22).

As early as 24 hours, BI 6727 can be seen to reduce viable cell numbers in all pancreatic cancer cell lines in comparison to an untreated control, even at very low nanomolar concentrations. The only exception to this statement seems to be with concentrations of up to 10nM in Panc-1 cells, which generally is the most resistant of the cell lines at 24 hours. MiaPaCa-2, BxPC-3 and Suit-2 show similar sensitivity at concentrations below 10nM and above 250nM with some disparity between these concentrations. Notably, BxPC-3 seems to have two phases of MTS reduction, one at below 10nM and one at above 100 nM.

At 48 hours, all cell lines show sensitivity to BI 6727 with prolonged exposure and display a linear response to increasing drug concentrations. Suit-2 and MiaPaCa-2 exhibit marginally greater sensitivity than BxPC-3 and Panc-1, though MiaPaCa-2 plateaus at a slightly lower drug concentration than other cell lines. As noted at the 24 hour timepoint, there appears to be no further benefit in exposing any of the aforementioned cell lines to concentrations of BI 6727 in excess of 250nM.

At 72 hours, the plotted graph from each cell line becomes strikingly similar. A sharp drop in viable cell number is seen between 50 and 100nM of BI 6727, which is echoed in their respective IC_{50} readings. Interestingly, the lower concentrations (<50nM) of BI 6727 seem increasingly ineffective in pancreatic cancer cells as time progresses suggesting that its effects can be transient at low doses. However, at higher concentrations (>250nM) where a plateau is reached by all cell lines, BI 6727's efficacy in maintaining cell populations at under 20% of control level is maintained.

Given how genetically diverse cell lines responds in such a similar fashion to BI 6727, it could be argued that genetic background (e.g. *KRAS, TP53, CDK2A* or *DPC4* status) has little impact on pancreatic cancer cell resistance to BI 6727, although it could also be argued that this is absence of evidence rather than evidence of absence.

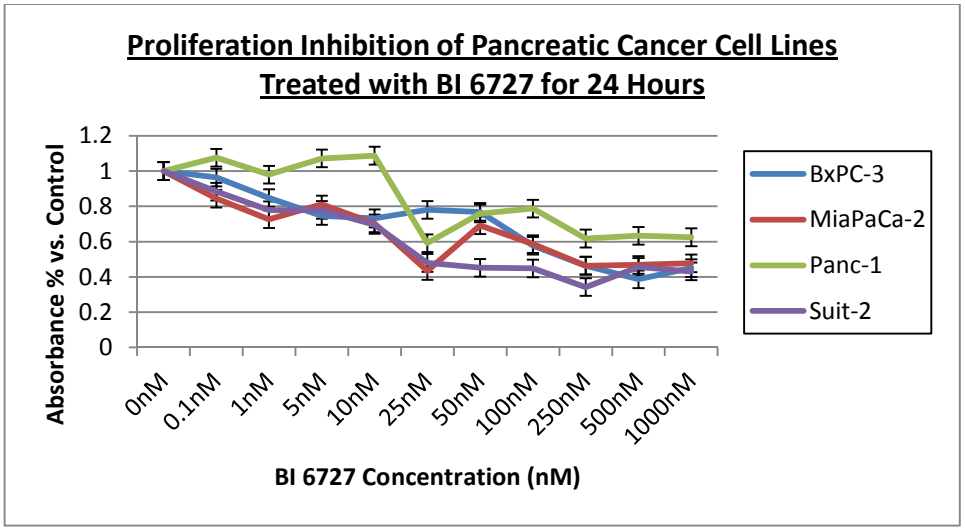

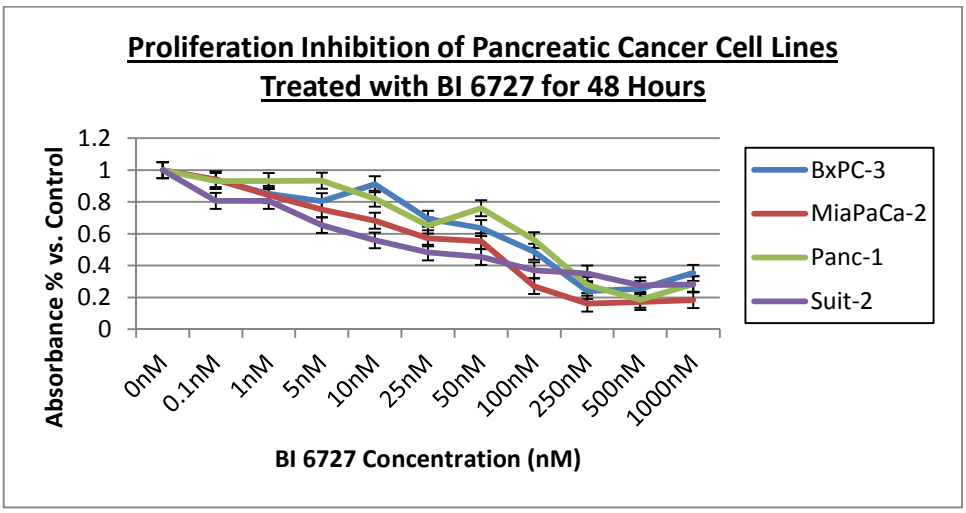

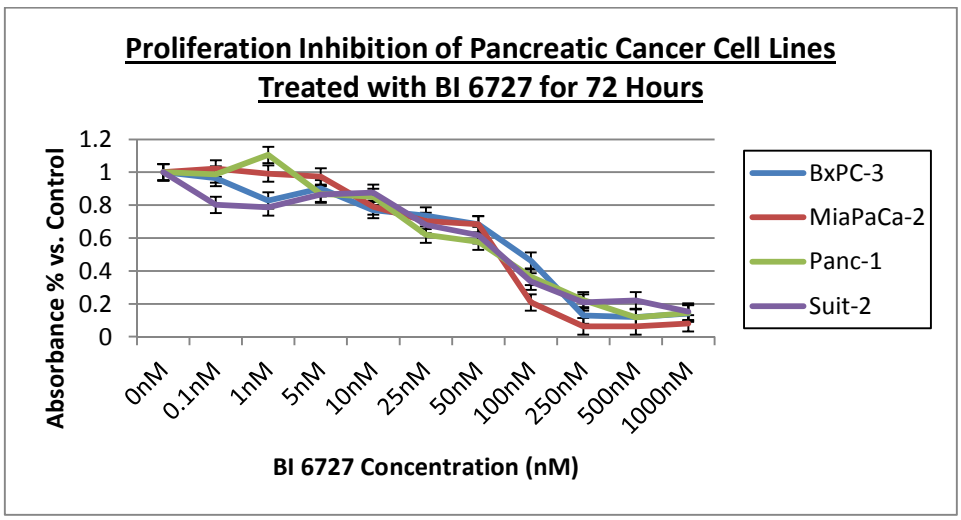

Figure 22: BI 6727 displays antiproliferative action against pancreatic cancer cells
Graphs comparing pancreatic cancer cell line response to BI 6727 across 24, 48 and 72 hours of exposure. Their dose-response curves show remarkable similarity at 72 hours. All cell lines achieve a plateau at concentrations of 250nM and above, with viable cell numbers being at least 80% lower than in controls.Full MTS readings in Appendix A.

The IC_{50} Concentration of Gemcitabine in Pancreatic Cancer Cell Lines

To evaluate the cytotoxicity of gemcitabine, the same pancreatic cancer cell lines were continually exposed to various concentrations of the drug for 72 hours prior to undertaking a viability assay. The concentration-dependent cytotoxicity of gemcitabine in pancreatic cancer cell lines has been widely published over the last quarter-century. These experiments and resulting IC_{50} concentrations vary considerably not only between relative degree of sensitivity exhibited between individual cell lines, but also for the same cell lines between studies. Each cell line was investigated in triplicate, with a final IC_{50} determined as a mean of the three IC_{50} readings. Our results suggest that Suit-2 and Panc-1 exhibit similar sensitivity to gemcitabine with IC_{50} of 11.1-13.8nM with MiaPaCa-2 (Figure 23) and BxPC-3 showing greater resistance with IC_{50} concentrations above 20nM. These low nanomolar concentrations fall safely below the serum concentration of 20-60µM achieved with a standard 30-minute intravenous infusion of 1,000–1,200 mg/$m^2$of gemcitabine[524]. Complete IC_{50} graphs at the 72 hour time point, repeated in triplicate for all pancreatic cancer cell lines treated with BI 6727 can be seen in Appendix C.

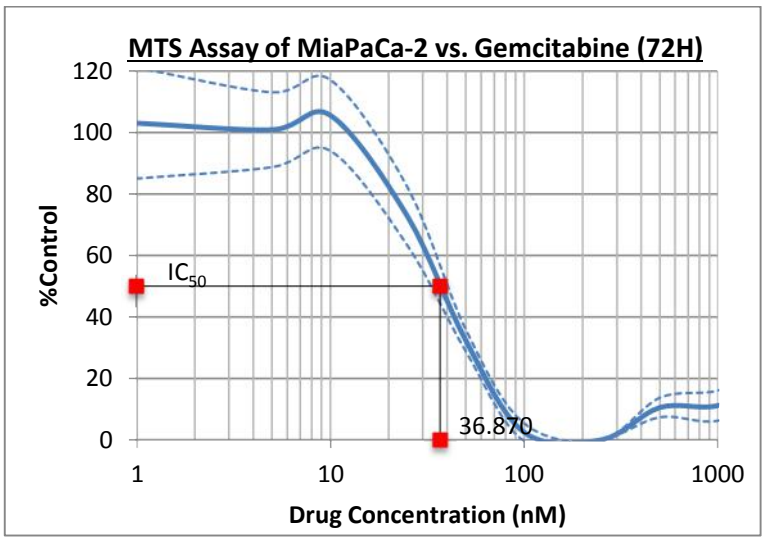

Figure 23: Determining the IC_{50} concentration of gemcitabine in MiaPaCa-2 cells
A graph displaying how the IC_{50} of gemcitabine was determined in the MiaPaCa-2 cell line. This dose-response curve is representative of gemcitabine's effect on the pancreatic cancer cell lines studies achieving IC_{50} values in the low nanomolar range.

Table 16: Complete IC_{50} results of BI 6727 and gemcitabine in pancreatic cancer cell lines

	Experiment	BI 6727 IC_{50} at 72h (95% CI) (nM)	Mean (nM)	Gemcitabine IC_{50} at 72h (95% CI) (nM)	Mean (nM)
BxPC-3	1	85.659 (68.311-110.024)	77.483	14.149 (12.28-15.924)	22.102
	2	84.357 (53.753-136.301)		39.562 (36.445-42.413)	
	3	62.434 (56.511-68.233)		12.595 (11.114-14.206)	
MiaPaCa-2	1	71.681 (66.954-76.022)	68.362	36.870 (32.580-40.420)	34.47
	2	69.007 (61.693-75.573)		27.812 (24.750-30.920)	
	3	64.398 (61.388-67.198)		38.740 (34.904-41.861)	
Panc-1	1	58.058 (36.848-76.465)	63.514	9.407 (7.16-11.669)	13.797
	2	74.98 (67.304-81.954)		15.598 (13.511-17.687)	
	3	57.505 (40.076-74.999)		16.385 (14.84-17.944)	
Suit-2	1	53.629 (49.593-57.911)	53.527	10.943 (9.815-12.034)	11.084
	2	61.911 (54.508-70.461)		13.760 (10.798-16.746)	
	3	45.037 (36.755-53.02)		8.550 (6.935-10.127)	

The IC_{50} concentrations of BI 6727 and gemcitabine were largely reproducible in all four cell lines investigated. Some variation in results within certain cell lines were occasionally encountered. Individual IC_{50} graphs can be seen in Appendix B and C.

Gemcitabine's Antiproliferative Effect on Pancreatic Cancer Cells

To delineate further the effects of gemcitabine on pancreatic cancer cells, MTS data was again extracted and processed as described for BI 6727.

From the data displayed in Figure 24, it can be argued that 24 hours of gemcitabine exposure, even at concentrations of up to 2M, has little effect on the proliferation of pancreatic cancer cells. This statement certainly seems applicable to BxPC-3, MiaPaCa-2 and Panc-1 cells though in comparison, Suit-2 cells seem to display slightly greater sensitivity at this early time point. This marked lack of gemcitabine activity at 24 hours is explained by the requirement of active cell division for the drug to be incorporated into DNA and exert its cytotoxic properties. At 24 hours, it is likely to be too early to observe these effects, as most cells will not yet have completed a full cell cycle. Panc-1 cells are reported to possess a doubling time of 52 hours[525], which is slightly slower in comparison to Suit-2 at 38 hours[526], MiaPaCa-2 at 40 hours[527] and BxPC-3 at approximately 48 hours[528].

At 48 hours' gemcitabine exposure, all cell lines show a degree of sensitivity to gemcitabine, even at a low nanomolar concentration. BxPC-3, MiaPaCa-2 and Suit-2 exhibit a similar response, showing at best a 60% reduction in viable cell numbers compared to an untreated control. Panc-1 cells are more resistant however, showing only a 40% reduction compared to a control, which is possibly explained by their comparatively slower doubling time.

By 72 hours of drug exposure it becomes apparent that the IC_{50} of all cell lines is between 10 and 50nM with a marked drop in viable cell numbers between these concentrations. As noted for 24 hours, Panc-1 cells seem more resistant to gemcitabine than the remaining cell lines investigated, with little reduction In MTS values. Though all cell lines show progressively diminished cell numbers compared to an untreated control, it is unclear whether this is due to increased drug toxicity or solely explained by the exponential proliferation of control cells.

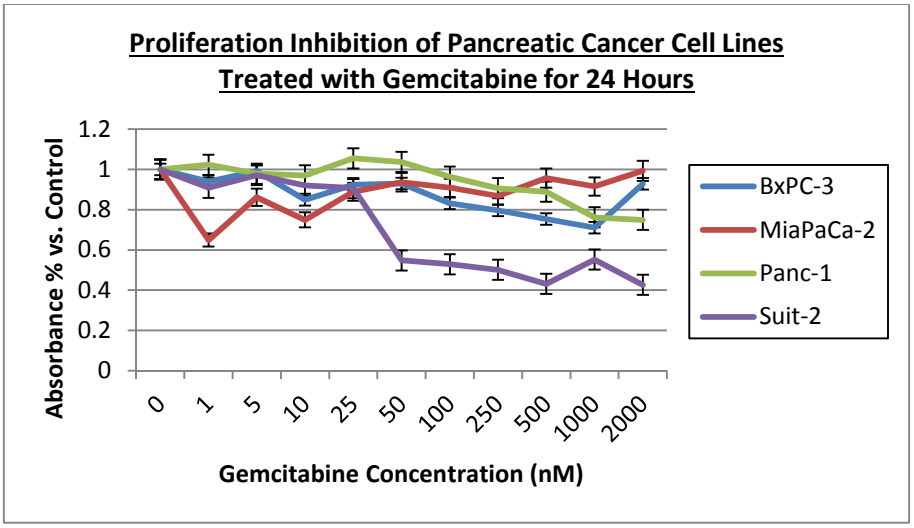

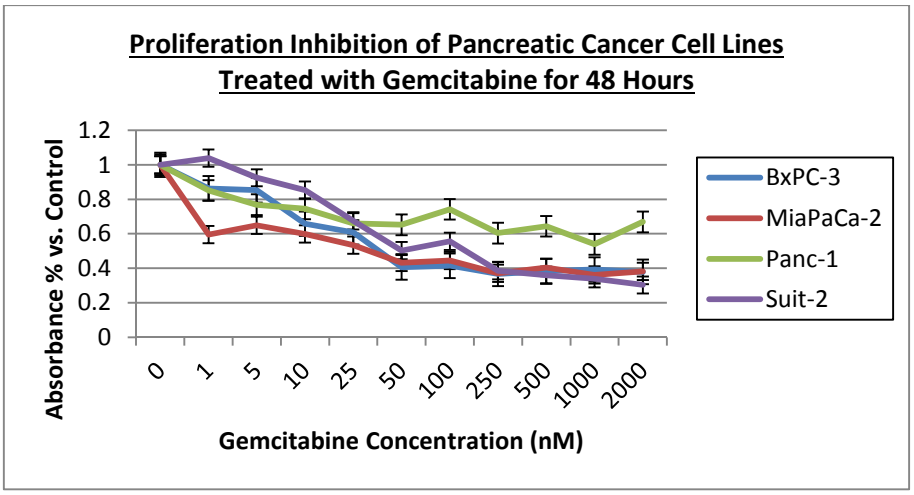

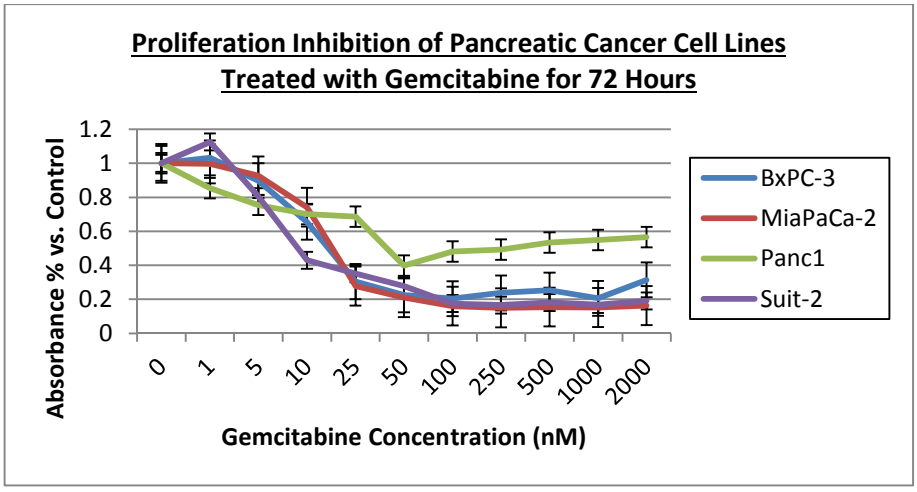

Figure 24: Gemcitabine displays antiproliferative activity in pancreatic cancer cells
Gemcitabine has minimal effect on pancreatic cancer cell lines within the first 24 hours of exposure. BxPC-3, MiaPaCa-2 and Suit-2 cells exhibit similar responses and sensitivity to the drug over time with Panc-1 cells being comparatively resistant to even high drug concentrations. Full MTS readings can be seen in Appendix D.

The Selection of MiaPaCa-2 Cells for Further Experiments

Due to pressures on time and resources, it was decided to utilise only one cell line for further experiments. Due to a relatively rapid doubling time and its reproducible behaviour with both gemcitabine and BI 6727, MiaPaCa-2 cells were selected. This cell line also possesses several common mutations seen in pancreatic cancer, with mutations in KRAS, p16 and p53.

BI 6727's Effects on MiaPaCa-2 Cells

MiaPaCa-2 proliferation data was extracted from MTS assay results by utilising the readings taken an hour following the application of EZ4U assay to cells at the 24, 48 and 72 hour time points with the 'blank' absorbance reading universally subtracted as previously described.

Figure 25 shows that continued MiaPaCa-2 cell exposure to concentrations of up to 5nM of BI 6727 does not seem to affect viable cell numbers at 72 hours. Though at the 24 and 48 hour time points cell numbers gradually fall at increasing drug concentrations, exponential cell growth does seem to continue at concentrations of up to 50nM. However, this growth seems delayed at concentrations in excess of 5nM in comparison to lower concentrations.

The IC_{50} concentration of BI 6727 (68nM) can be identified as being 50-100nM from this graph due to the sharp drop in the number of viable cells between these concentrations. At 100nM it can be said that cell proliferation is minimal after 24 hours with very little increase in cell numbers with continued exposure to BI 6727.

It is not possible to state from this experiment whether the gradual decrease in viable cell number at the 24 hour time point with increasing drug concentration is a result of delayed cell division, by cell death or a combination of both effects. However what can be stated is at concentrations of 250-1000nM we see a marginal fall in the number of viable cells as time progresses. This is a clear indication that at high concentrations of the novel PLK1 inhibitor, cell death may occur, possibly as a result of polo arrest (spindle malformation) and apoptosis.

Despite BI 6727 having previously been shown to possess a half-life of approximately 110 hours[529] it was observed that recovery was seen much earlier than this under certain conditions. To delineate this further, absorbance data from an MTS experiment with MiaPaCa-2 was converted to a percentage of the control reading from each time point as

seen previously in Figure 22. From this data (Figure 26) we can clearly see that even as early as 24 hours, MiaPaCa-2 proliferation in general is reduced in comparison to control with rising drug concentrations. The effects of low BI 6727 concentrations (<25nM) seem to diminish as time progresses, with cells being able to almost recover completely at concentrations of up to 5nM. However, at higher concentrations (>100nM), cells seem unable to recover, with proportionally fewer viable cells at 48 and 72 hours in comparison to earlier time point. Nevertheless, on the basis of this data there seems to be no benefit in utilising concentrations above 250nM as a plateau effect is observed.

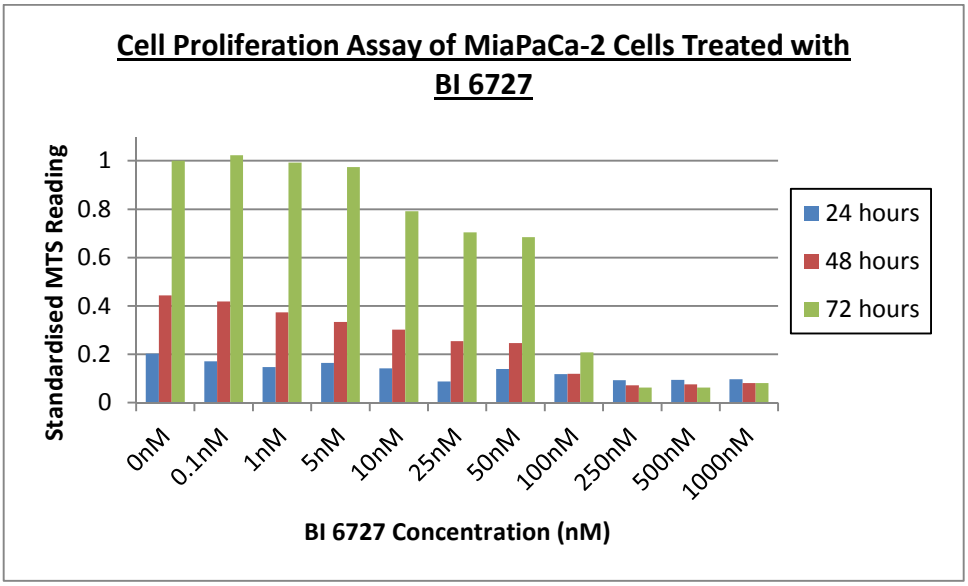

Figure 25: BI 6727's effect on the proliferation of MiaPaCa-2 cells

BI 6727 has limited effect on MiaPaCa-2 proliferation at concentrations of up to 5nM. Cell division seems restricted at concentrations of up to 50nM with the IC_{50} likely to be between 50 and 100nM on the basis of this graph. Cell death is likely at concentrations of 250nM and above with progressive time points showing less absorbance. Full MTS readings can be seen in Appendix E.

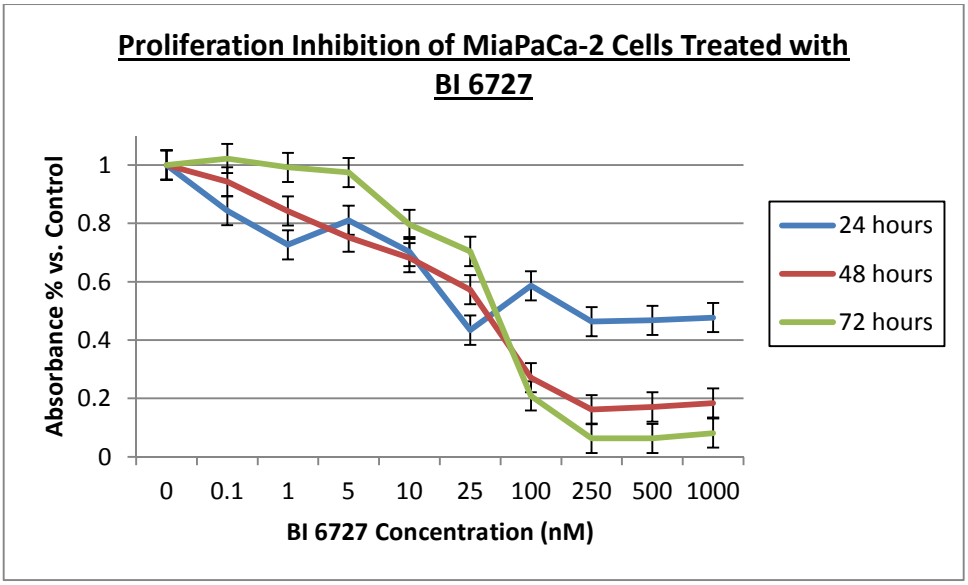

Figure 26: BI 6727's effect on viable cell numbers vs. untreated control

Low concentrations (0.1-25nM) of BI 6727 seem to be effective in reducing MiaPaCa-2 proliferation only in the short-term. Its effects are likely to have expired by 72 hours at concentrations of up to 5nM. Full MTS readings ican be seen in Appendix F.

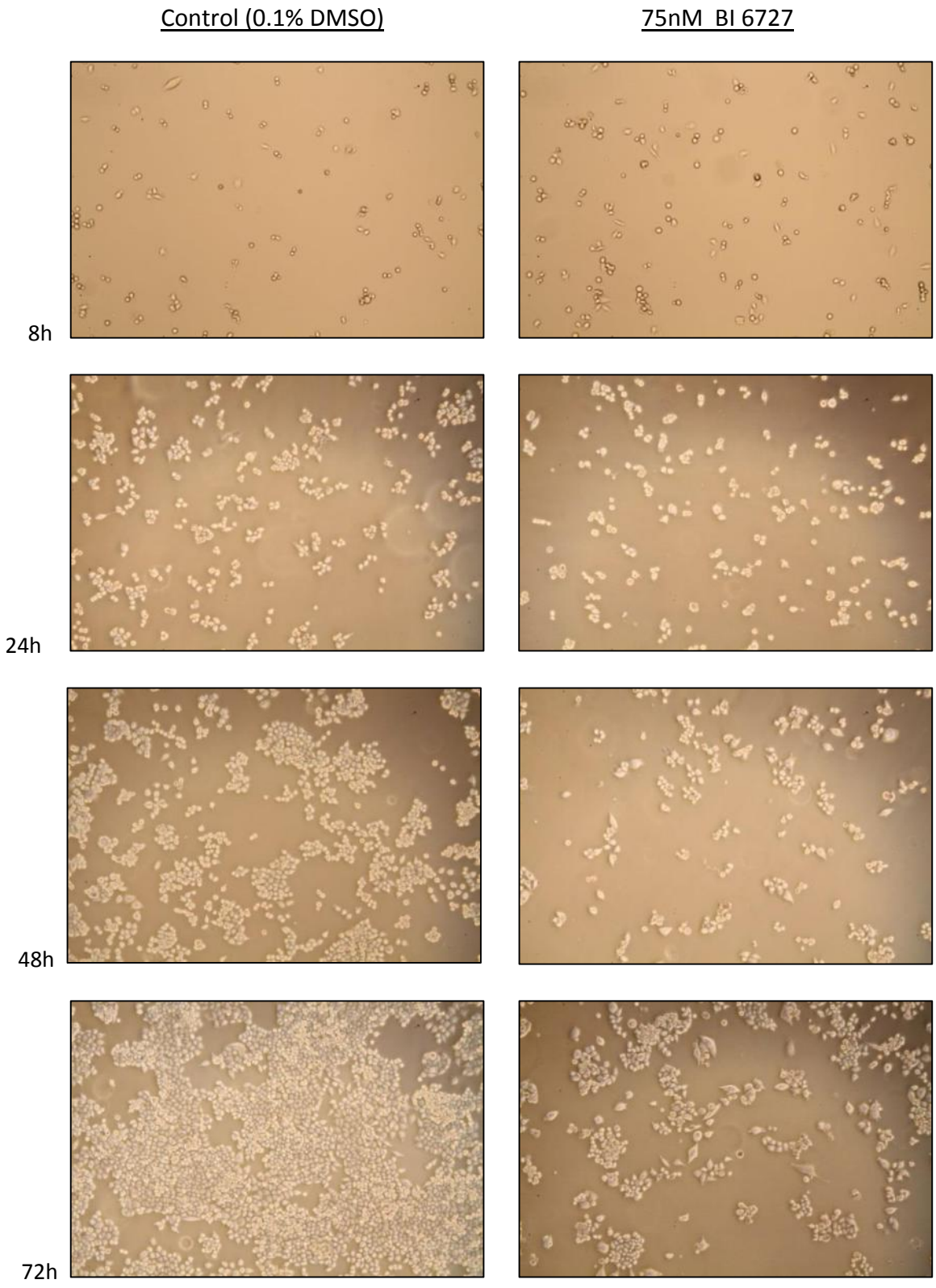

Figure 27: Photographs of BI 6727 vs. control (0.1% DMSO) in MiaPaCa-2 cells
x25 000 magnification photographs showing MiaPaCa-2 cell growth at 8, 24, 48 and 72 hours at 0.1% DMSO/untreated control condition (left column) and 75nM BI 6727 (right column) treatment. Exponential cell growth is seen under control conditions with cell division vastly reduced in comparison when treated with BI 6727.

Gemcitabine's Effect on MiaPaCa-2 Cells

It is seen in Figure 28 that viable cell numbers at 24 hours seems generally unaffected by gemcitabine - a phenomenon likely to be explained by MiaPaCa-2's doubling time of approximately 40 hours as previously discussed. However, by 48 hours, evidence of gemcitabine activity can be seen. At increasing drug concentrations up to 50nM, a gradual reduction is seen in the number of viable cells to under half of that seen in controls. A plateau is seen at a concentration of above 50nM suggesting that gemcitabine saturation may have been achieved.

At 72 hours of exposure, very low levels of gemcitabine (<5nM) seems only marginally effective in restricting logarithmic cell division, before the IC_{50} landmark which is evident after the 25nM point. At concentrations above this, viable cells drop dramatically in number. It is probable that cell death is occurring at concentrations above 25nM due to the observed fall in viable cell numbers as time progresses. In comparison to BI 6727, this discrepancy in cell numbers between the specified time points is vast, suggesting a more toxic drug, whose effect in killing cells remains active for at least 72 hours with its continued exposure. Unlike the results summarised in Figure 25 for BI 6727, Figure 28 demonstrates that at higher doses of gemcitabine there is a decrease in cell number between 24 and 72 hours.

When the MTS readings were standardised versus control (Figure 29), it becomes even more evident that gemcitabine's properties are such that it has a limited effect on MiaPaCa-2 cells at 24 hours exposure. On the basis of this data it seems that at concentrations of gemcitabine of 10nM and under, MiaPaca-2 cells may be able to recover, with the proportion of viable cells versus the untreated control having increased by 72 hours. However, we must be open to the possibility that these readings may be anomalous. As with BI 6727, it also seems that a saturation point can be reached with gemcitabine, with this data suggesting a concentration of approximately 100nM. Very little benefit is seen in increasing the drug concentration beyond this.

When looking at both BI 6727 and gemcitabine monotherapies, the graphs in Figure 26 and Figure 29 show that both drugs can independently reduce MiaPaCa-2 populations by over 80% at 72 hours with continued drug exposure at adequate concentrations. Comparison of

Figure 27Figure 30 also shows that neither drug results in resistant colonies but in both cases the inhibitory effect seems to be fairly uniform (most cells at 72 hours existing in small colonies or even remaining as single entities). However, there is an impression that colonies appear smaller at 72 hours with gemcitabine than with BI 6727 and perhaps there is an indication that colonies regress with gemcitabine between 48 and 72 hours rather than just not forming.

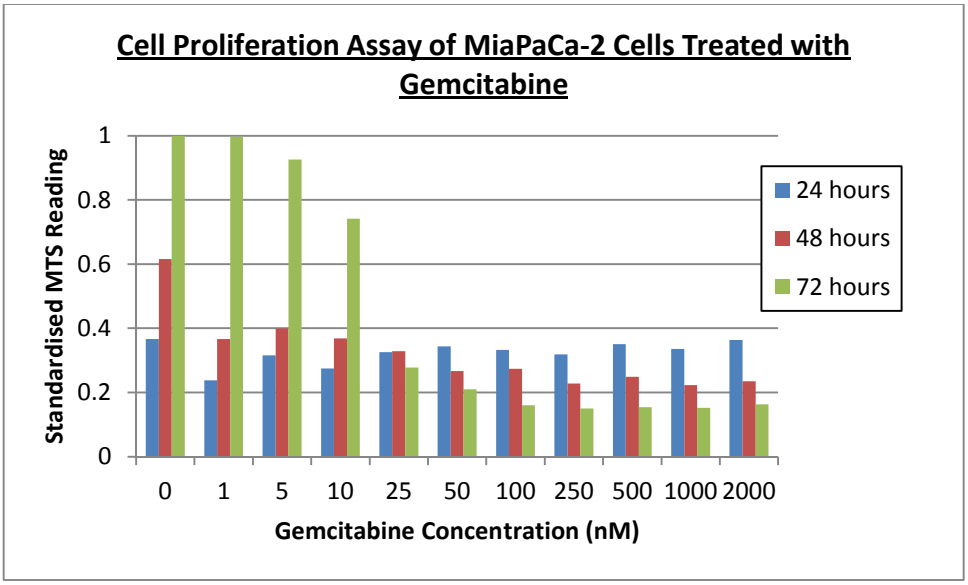

Figure 28: Gemcitabine's effects on the proliferation of MiaPaCa-2 cells
Gemcitabine has limited effect on MiaPaCa-2 proliferation at 24 hours of exposure. Cell death is evident at concentrations of 50nM and above with progressive time points showing less absorbance indicating a fall in the number of living cells. Full MTS readings can be seen in Appendix G.

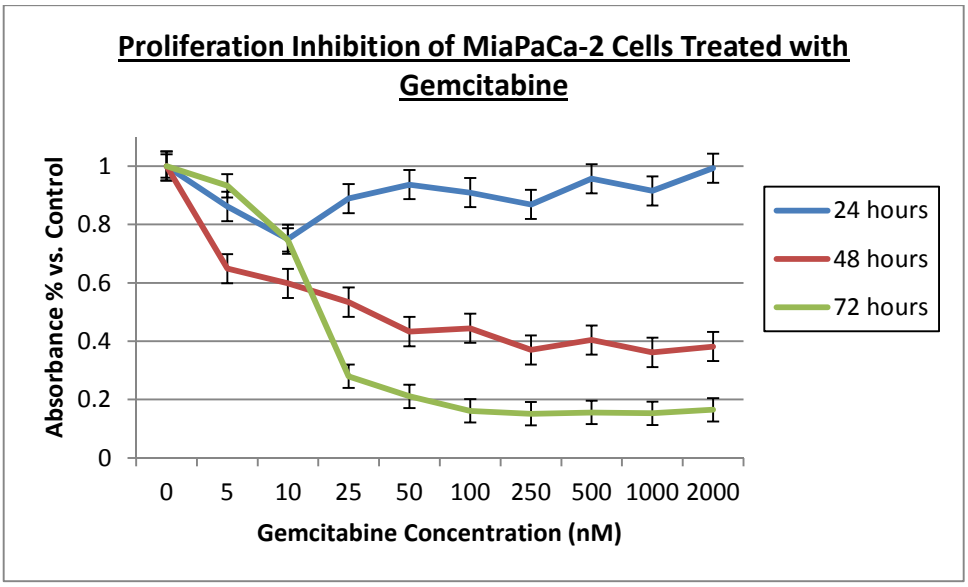

Figure 29: Gemcitabine maintains its toxic properties for at least 72 hours
At 24 hours treatment, gemcitabine seems to have a limited effect on MiaPaCa-2 cell population though continued exposure drastically reduces viable cell numbers in comparison to control. There seems to be little to no benefit in utilising concentrations of gemcitabine in excess of 100nM.Full MTS readings can be seen in Appendix H.

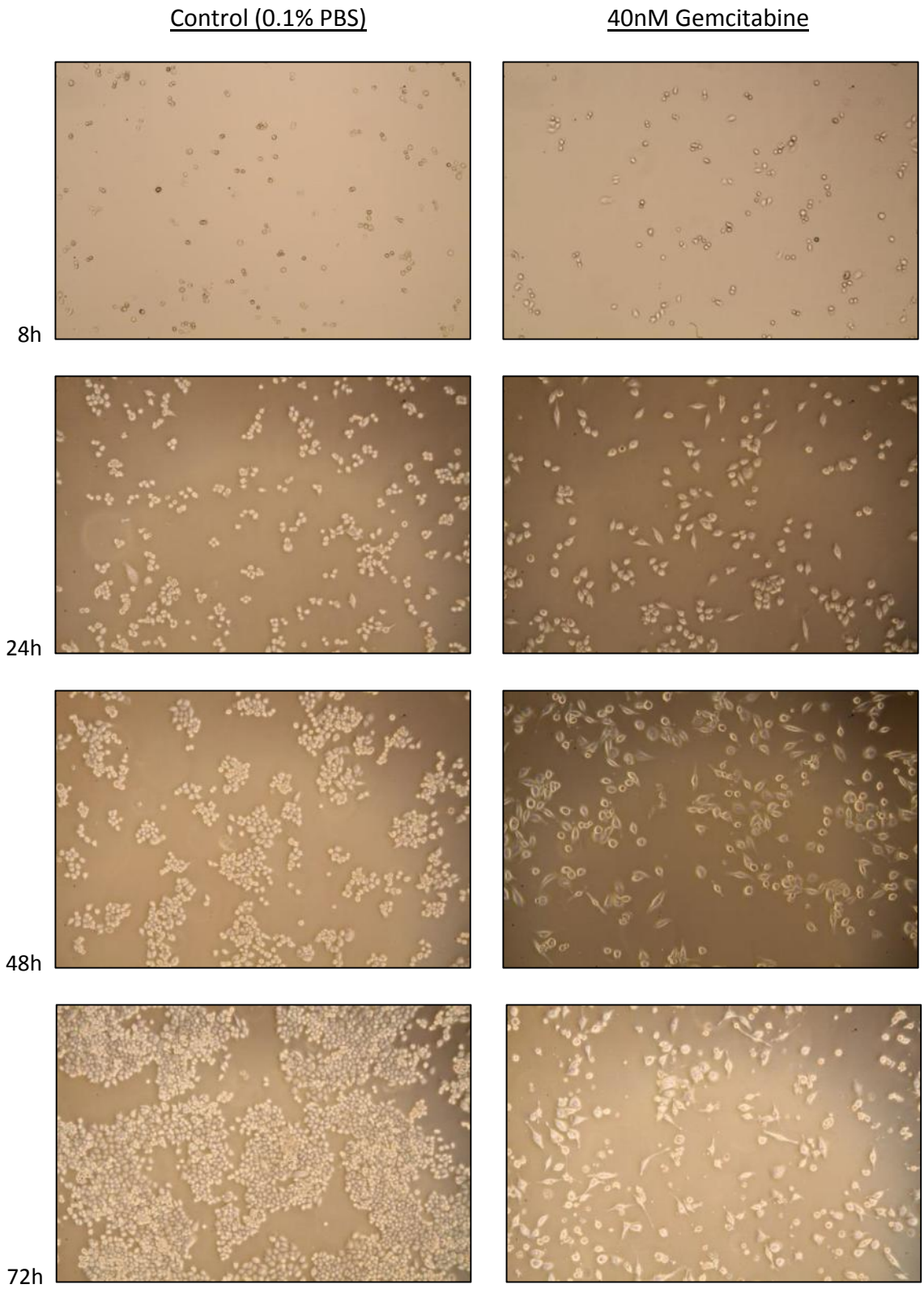

Figure 30: Photographs of gemcitabine vs. control (0.1% PBS) in MiaPaCa-2 cells
x25 000 magnification photographs showing MiaPaCa-2 cell growth at 8, 24, 48 and 72 hours at both 0.1% PBS/control (left column) and 40nM gemcitabine (right column) conditions. Exponential cell growth is seen in the control condition with evidence of cell death and debris, likely to be secondary to apoptosis, when treated with gemcitabine.

Flow Cytometry

Background

To establish the cell cycle effects of BI 6727 and gemcitabine, MiaPaCa-2 cells were treated at the IC_{50} concentration of the drugs for the desired amount of time, and harvested alongside an equivalent untreated control. Samples were stained with propidium iodide and then fixed in ethanol for at least 24 hours prior to FACS analysis. Though 10,000 events were analysed and gated in the vast majority of samples during this project, a small number of samples were subject to an error therefore this number was not always reached.

Flow Cytometry in Untreated Control MiaPaCa-2 Cells

Looking at the control condition, the typical prominent cell cycle G1 peaks is noted. Cells spend most of their life in the G1/G0 phase containing what is recognised as the 2N amount of DNA, representing the two copies of each chromosome in the nucleus of each cell.

As a cell prepares to divide, it first duplicates its DNA so that when division occurs, each daughter cell has the same amount of DNA as the parent cell. This duplication of the DNA is called the S-phase for synthesis of the DNA.

Once the duplication of DNA has been completed, it has double the DNA content of the original cell so contains 4N of DNA. This stage of the cell cycle is called the G2/M and is represented by the second peak on the histogram. Next, the cell undergoes mitosis which divides the 4N amount of DNA back into 2N and the cell returns to G1/G0.

Almost all cell or nuclear suspensions analysed by DNA content flow cytometry contain some damaged or fragmented nuclei (debris). Apoptotic cells often contain fractional DNA content, with some cells also losing chromatin by shedding apoptotic bodies. As these cells no longer possess the expected 2N quantity of DNA, these events are usually visible to the left of the diploid G1 (pre-G1).

Flow Cytometry in MiaPaCa-2 Cells Treated with BI 6727

As expected with a polo-like kinase 1 inhibitor, a large increase in the number of cells accumulating in G2/M is seen in comparison to controls. This is most noticeable at the earliest timepoints of 8 and 24 hours where 50.6% and 56.3% of cells are gated within G2, as opposed to 30.7% and 32.8% in untreated MiaPaCa-2 cells (Table 17). The proportion of G2

cells falls by 48 hours – a trend that continues towards the 72 hour point. The increase in G2 cells seems to be reflected by an almost equivalent fall in the percentage of G1 cells, with the proportion of S-phase cells remaining comparatively constant. This suggests that MiaPaCa-2 cells maintain the ability to duplicate its DNA when exposed to BI 6727, but is then unable to undergo mitosis and divide into two daughter cells.

As the purpose of this experiment was to delineate the cell cycle effects of BI 6727 and not to establish cell death, MiaPaca-2 cells floating in culture media in addition to the PBS used to wash the adherent cells was discarded. This was done with the aim of excluding the majority of dead cells, for the same reason pre-G1 cells were excluded from gates applied for counting and therefore were not included in Table 17. Small numbers of cells can be expected pre-G1 even under control conditions, which is reflected in the resulting histograms. However, also of note is the large number of pre-G1 MiaPaCa-2 cells seen at the 24 hour, and to a lesser extent, the 48 hour timepoint when treated with BI 6727. The reason for this is unclear, and is confused even further by the near-absence of these fragmented cells at 72 hours. It could be argued that if these were true apoptotic cells as a direct result of BI 6727, a substantial presence would be maintained at 72 hours. However, it could also be argued that these cells are dying and are not yet dead. Dead cells and even their fragments could also possibly remain adhered to the surface of a culture flask for a short period of time but would eventually detach. It is quite possible that a proportion of cells seen in the most prominent G2 arrests, seen at 8 and 24 hours, had moved into pre-G1 by 24 and 48 hours respectively. The less prominent G2 peak at 48 hours may then explain why very few events are recorded pre-G1 at 72 hours, as all the cells pre-G1 during the earlier timepoints may now have detached and therefore been discarded.

These results suggest that BI 6727 is most effective in arresting MiaPaCa-2 cells in G2 within the first 24 hours of exposure. There is already a 65% increase in G2 (compared to control) by 8 hours, rising to a 72% increase by 24 hours, but falling back to just 35% by 72 hours. Conclusions regarding cell death cannot be made based on these flow cytometry results alone due to the exclusion of floating cells from the experiment.

Table 17: The distribution of MiaPaCa-2 cells when treated with BI 6727 for 72 hours

	Time Point and Condition							
	8h (Figure 31)		24h (Figure 32)		48h (Figure 33)		72h (Figure 34)	
Phase	0.1% DMSO	BI 6727	0.1% DMSO	BI 6727	0.1% DMSO	BI 6727	0.1% DMSO	BI 6727
G1	50.9%	31.3%	51.5%	30.9%	52.4%	40.5%	56.9%	43.9%
S	18.4%	18.1%	15.7%	12.8%	20.5%	13.3%	12.8%	15.2%
G2	30.7%	50.6%	32.8%	56.3%	27.1%	46.2%	30.3%	40.9%

BI 6727 causes a large increase in the proportion of cells in G2 within the first 24 hours of exposure (56 vs. 33%) before returning to being similar to the control by 72 hours. The increase in G2 cells seems to be at the expense of G1 cells where numbers fall significantly while the proportion of S-phase cells remains comparatively static. Each phase has been gated as a percentage of the total number of cells seen in G1, S and G2 phases.

Table 18: The distribution of MiaPaCa-2 cells when treated with gemcitabine for 72 hours

	Time Point and Condition							
	8h (Figure 35)		24h (*Figure 36*)		48h (Figure 37)		72h (Figure 38)	
Phase	0.1% PBS	Gemcitabine	0.1% PBS	Gemcitabine	0.1% PBS	Gemcitabine	0.1% PBS	Gemcitabine
G1	51.1%	60.8%	48.4%	43.6%	55%	28.9%	61.4%	32.2%
S	14.6%	20.1%	16.3%	38.1%	15.5%	47%	10.7%	47.7%
G2	34.3%	19.1%	35.3%	18.3%	29.5%	24.1%	27.9%	20.1%

In comparison to an untreated control, gemcitabine causes an increase in the proportion of MiaPaCa-2 cells in S-phase, which is most prominent after at least 48 hours of exposure. This seems to mainly be at the expense of G1 cells suggesting that cells are unable to advance any further. Each phase has been gated as a percentage of the total number of cells seen in G1, S and G2 phases.

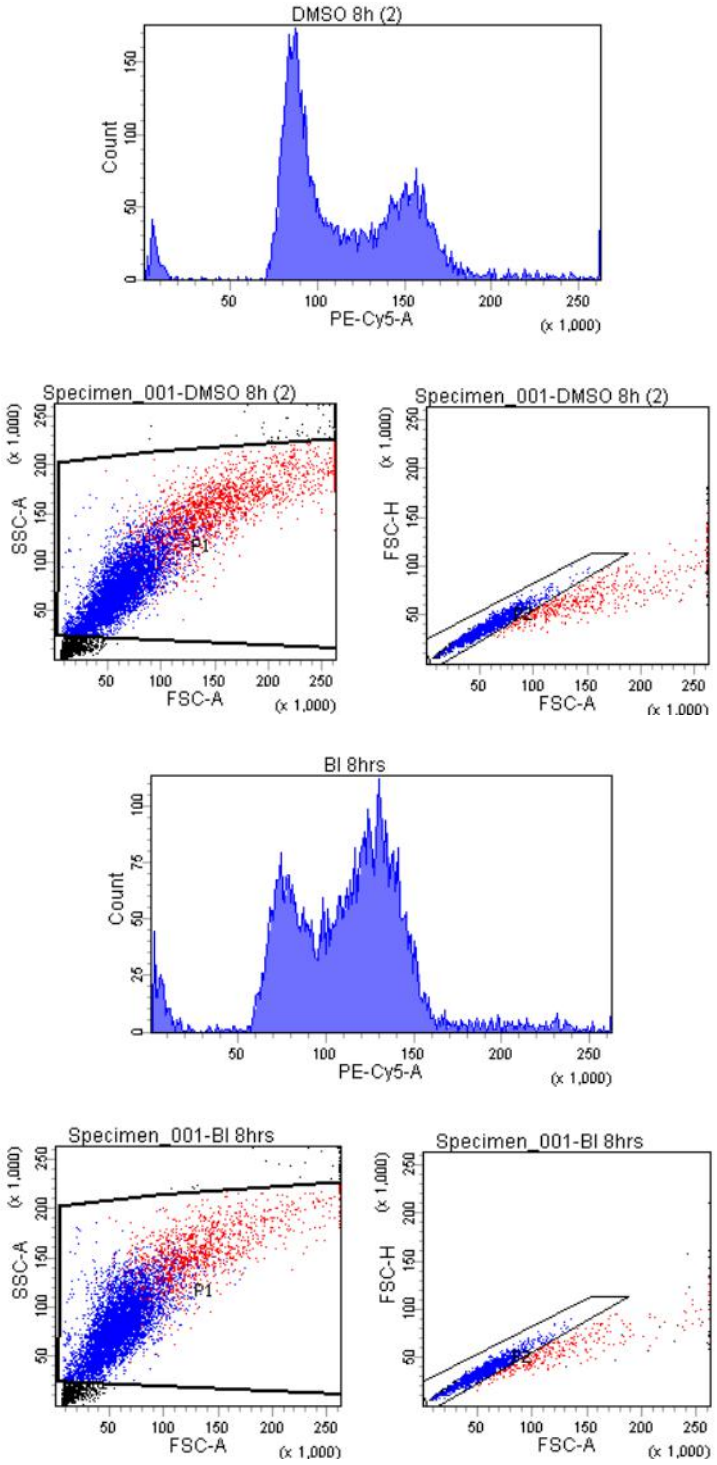

Figure 31: Flow cytometry of MiaPaCa-2 cells treated with 75nM BI 6727 for 8 hours vs. control

Treating MiaPaCa-2 cells at the IC_{50} concentration of BI 6727 (lower histogram) causes a prominent increase in G2 cells after 8 hours in comparison with untreated control (upper histogram). Control 10,000 events, BI 6727 8,600 events.

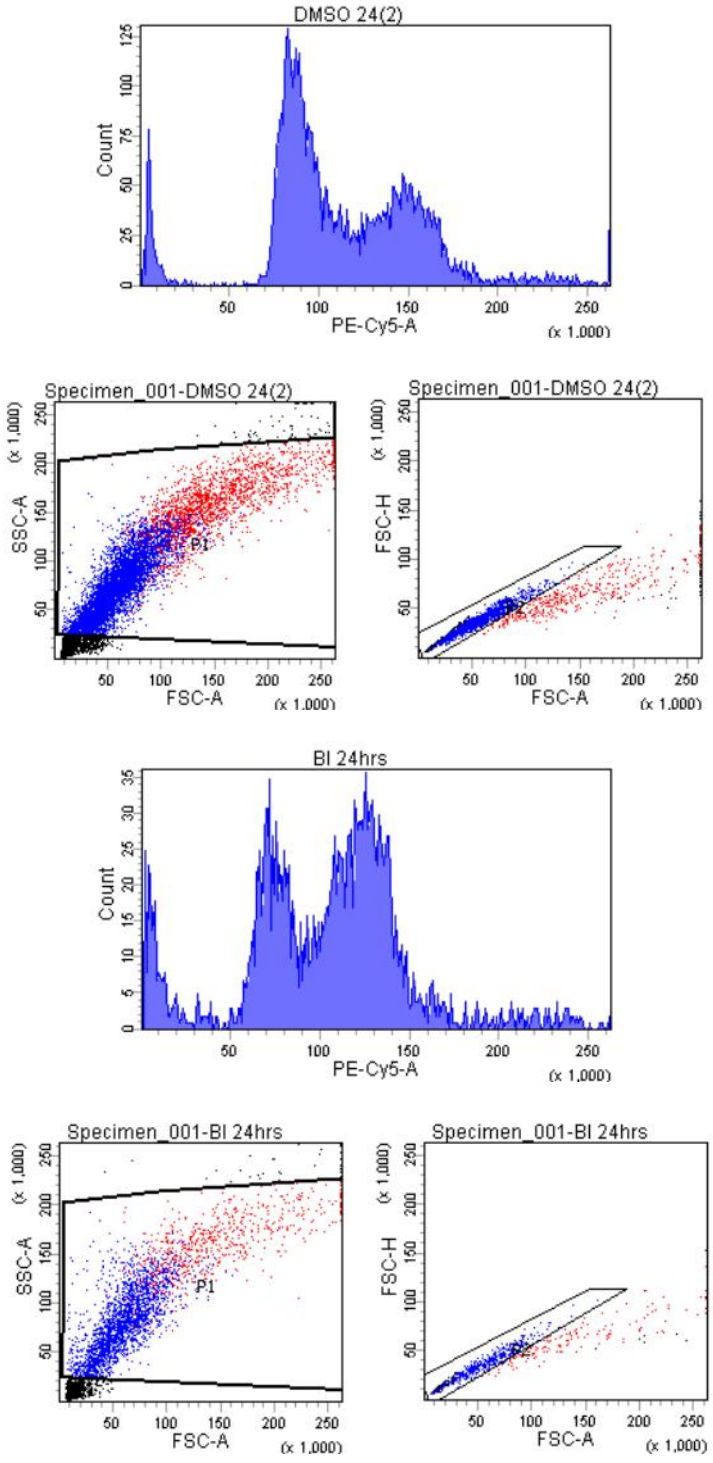

Figure 32: Flow cytometry of MiaPaCa-2 cells treated with 75nM BI 6727 for 24 hours vs. control

The proportion of MiaPaCa-2 cells seen in G2 peaks in the first 24 hours with BI 6727 treatment. Though this experiment was undertaken on adherent cells, a large number of pre-G1 cells are seen which possess subnormal DNA levels. Control 10,000 events, BI 6727 4,600 events.

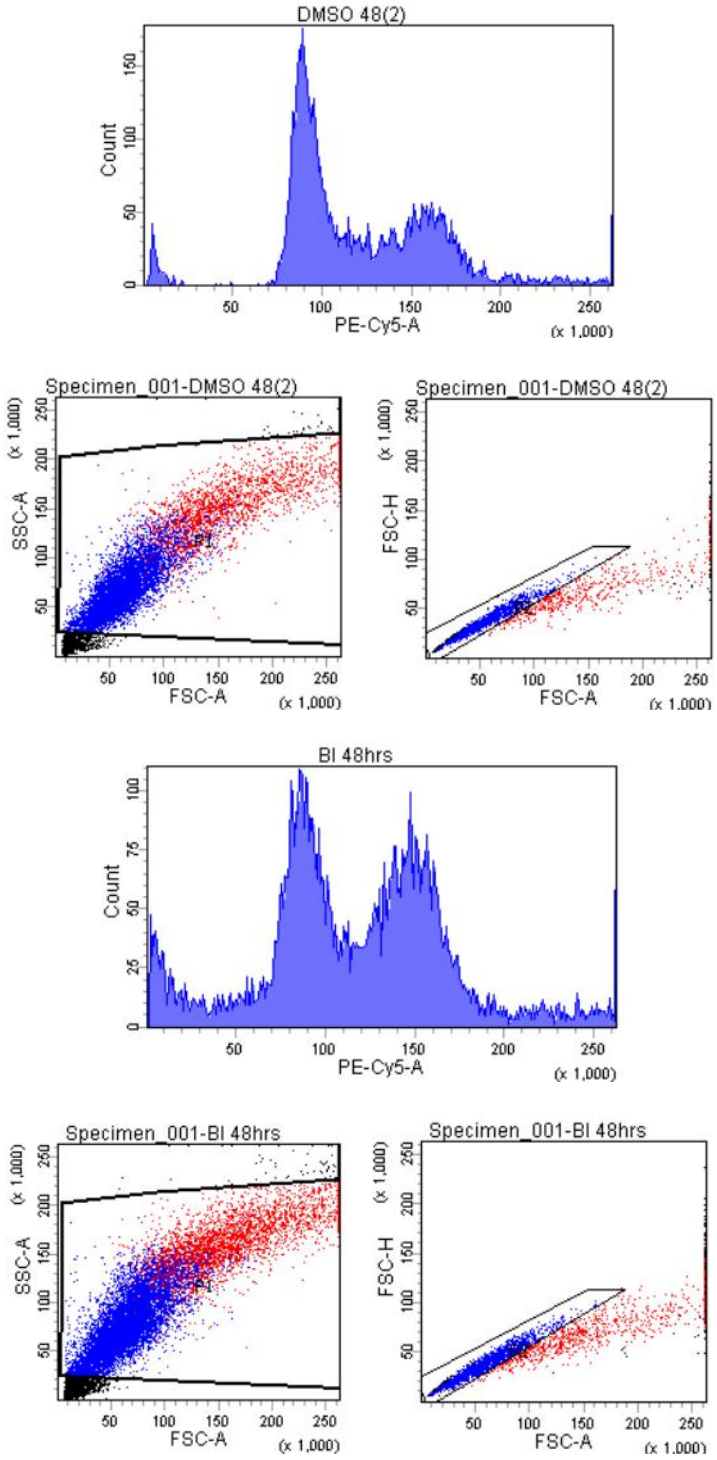

Figure 33: Flow cytometry of MiaPaCa-2 cells treated with 75nM BI 6727 for 48 hours vs. control

Though the G2 peak remains prominent after 48 hours' exposure to BI 6727, its population has now been overtaken in size by G1. Pre G1 cells are again seen in significant numbers in comparison to the untreated control. Control 10,000 events, BI 6727 16,800 events.

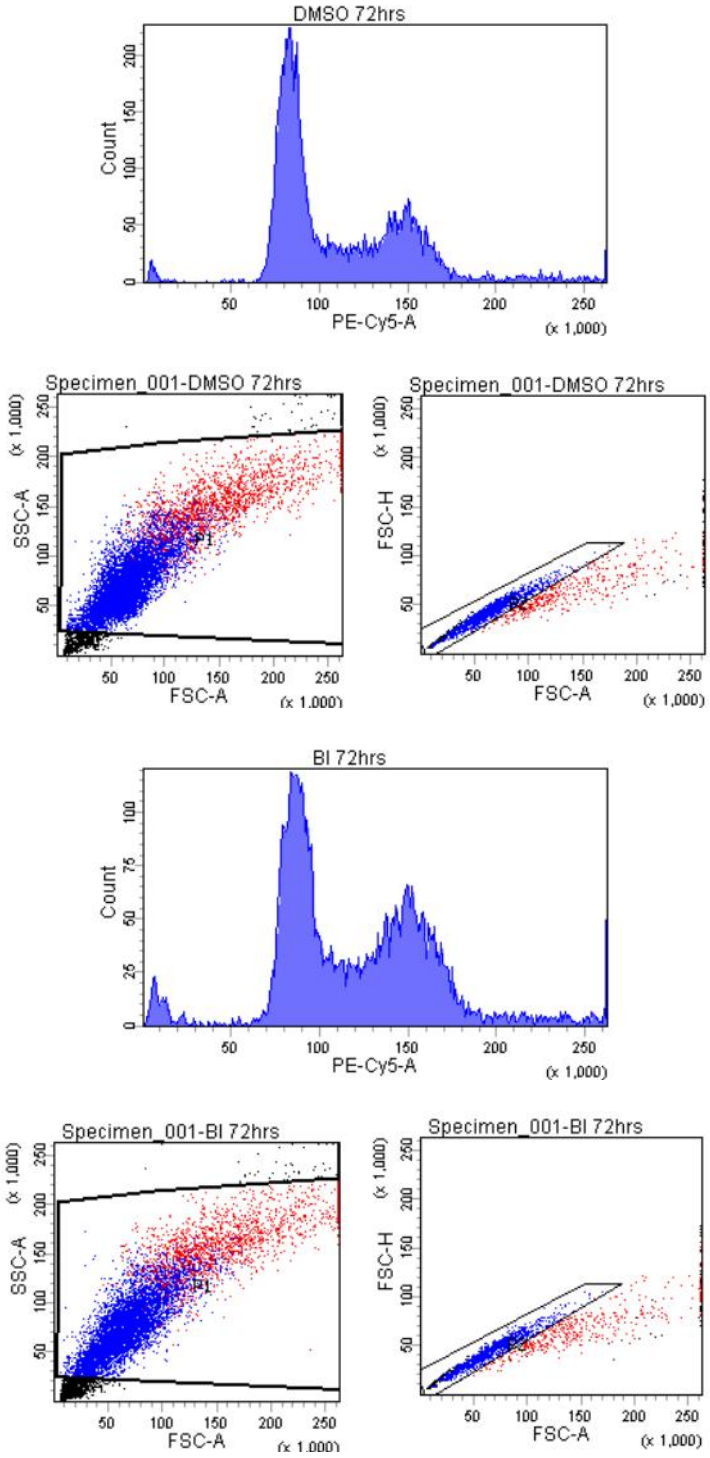

Figure 34: Flow cytometry of MiaPaCa-2 cells treated with 75nM BI 6727 for 72 hours vs. control

The proportion of MiaPaCa-2 cells in G2 phase has returned to near-control levels by 72 hours of exposure to BI 6727. The pre-G1 peak seen at 24 and 48 hours has also largely disappeared, suggesting that these cells may by now have detached and have been discarded. Control and BI 6727 experiments both included 10,000 events.

Flow Cytometry in MiaPaCa-2 Cells Treated with Gemcitabine

Gemcitabine's metabolites have several intracellular targets, of which many affect the synthesis of DNA. It is therefore not surprising that the main cell-cycle-related change seen in gemcitabine-treated cells is the accumulation of cells in S-phase. Though relatively unchanged at 8 hours, data after 1-3 days of gemcitabine exposure shows an S-phase population size two to three-fold that seen in control samples (Table 18).

The proportion of MiaPaCa-2 cells in G1 remains comparable to control-levels during the first 24 hours. This is likely to be a reflection of the cell's doubling time, which takes a while longer. By 48 hours and beyond, these cells should be expected to have completed a full cell cycle. However, instead of progressing through mitosis and restarting another cycle, the cells seen in G1 at 8 and 24 hours have accumulated in S-phase. This fall in G1 cells is also reflected in a fall in G2 cells, which is evident as early as 8 hours and is seen across the duration of the experimental data.

As mentioned when discussing the flow cytometry data of BI 6727-treated cells, this experiment was not planned to directly observe the cell killing effects of drugs as all floating cells were discarded. Nevertheless, it is prudent to observe that the histograms of gemcitabine-treated cells all exhibit ungated pre-G1 events indicative of cell death. As gemcitabine inhibits DNA synthesis, MiapaCa-2 cells will be killed either by the induction of apoptosis or from necrosis which could also result from from mitotic catastrophe in cells that lack the ability to undergo programmed cell death. Up to 24 hours, these pre-G1 peaks are comparable in size to those seen in control conditions. A time-dependent significant increase is then seen in this population up to 72 hours, likely to be secondary to prolonged gemcitabine exposure and subsequent toxicity.

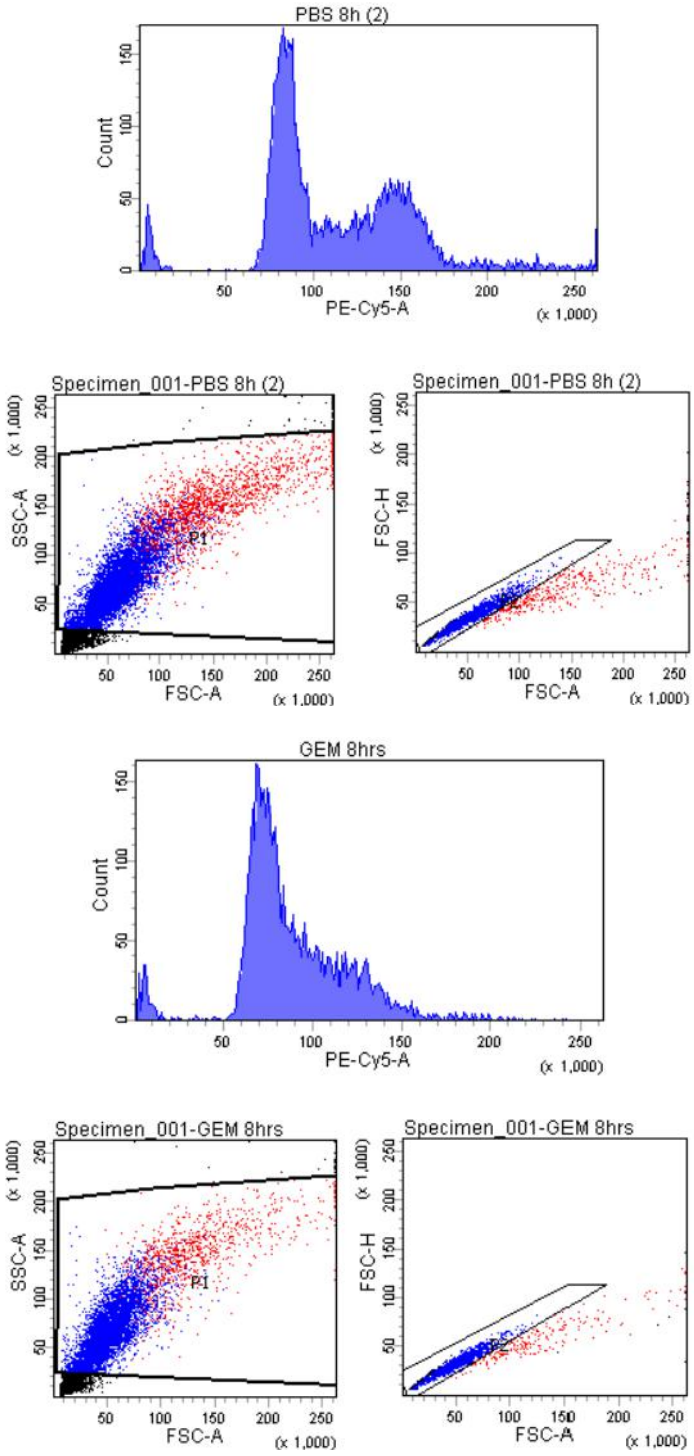

Figure 35: Flow cytometry of MiaPaCa-2 cells treated with 40nM gemcitabine for 8 hours vs. control

After as little as 8 hours of gemcitabine treatment, MiaPaCa-2 cells are already accumulating in both G1 and S-phases. Control 10,000 events, gemcitabine 7,800 events.

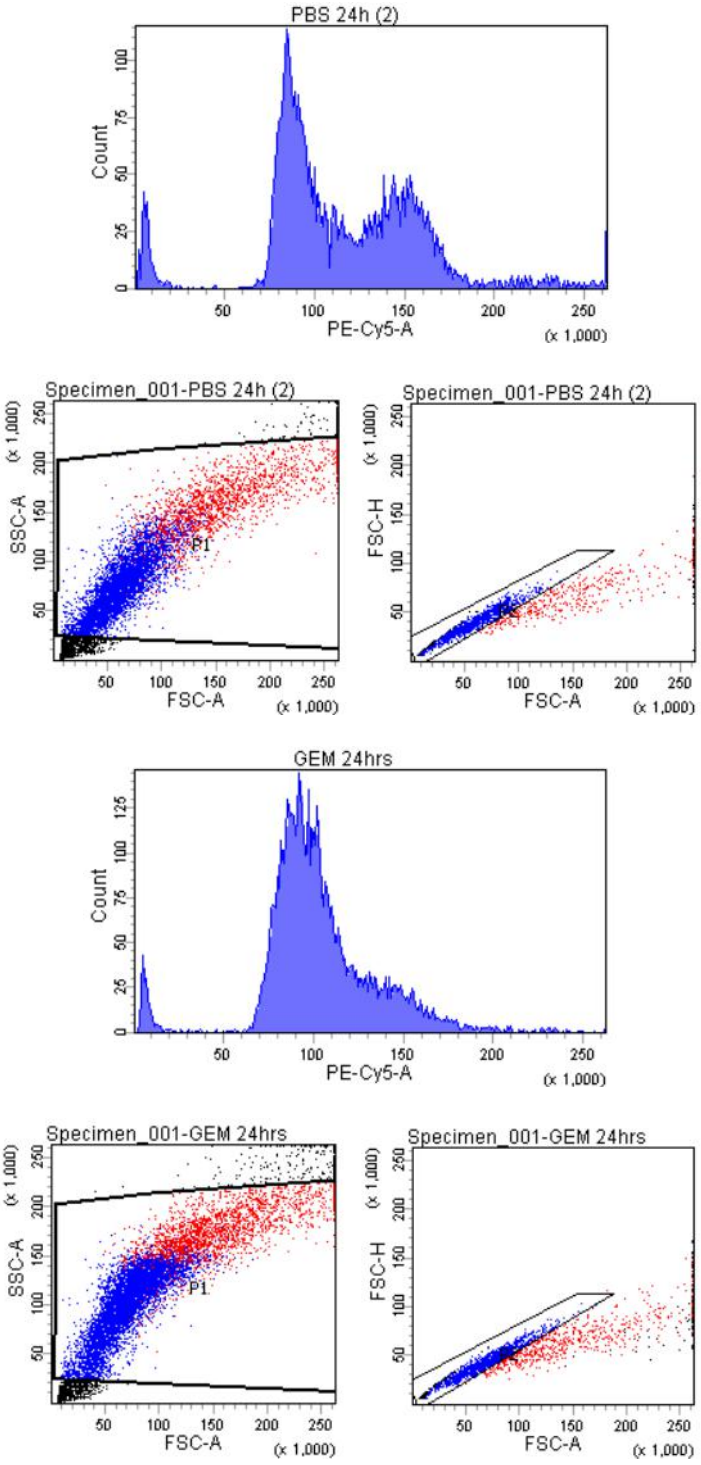

Figure 36: Flow cytometry of MiaPaCa-2 cells treated with 40nM gemcitabine for 24 hours vs. control

Following 24 hours of exposure to gemcitabine, cells previously seen in G1 are collecting in S-phase. Proportionally, the S-phase population is now double the size in gemcitabine-treated cells compared to control. Control 8,200 events, gemcitabine 10,000 events.

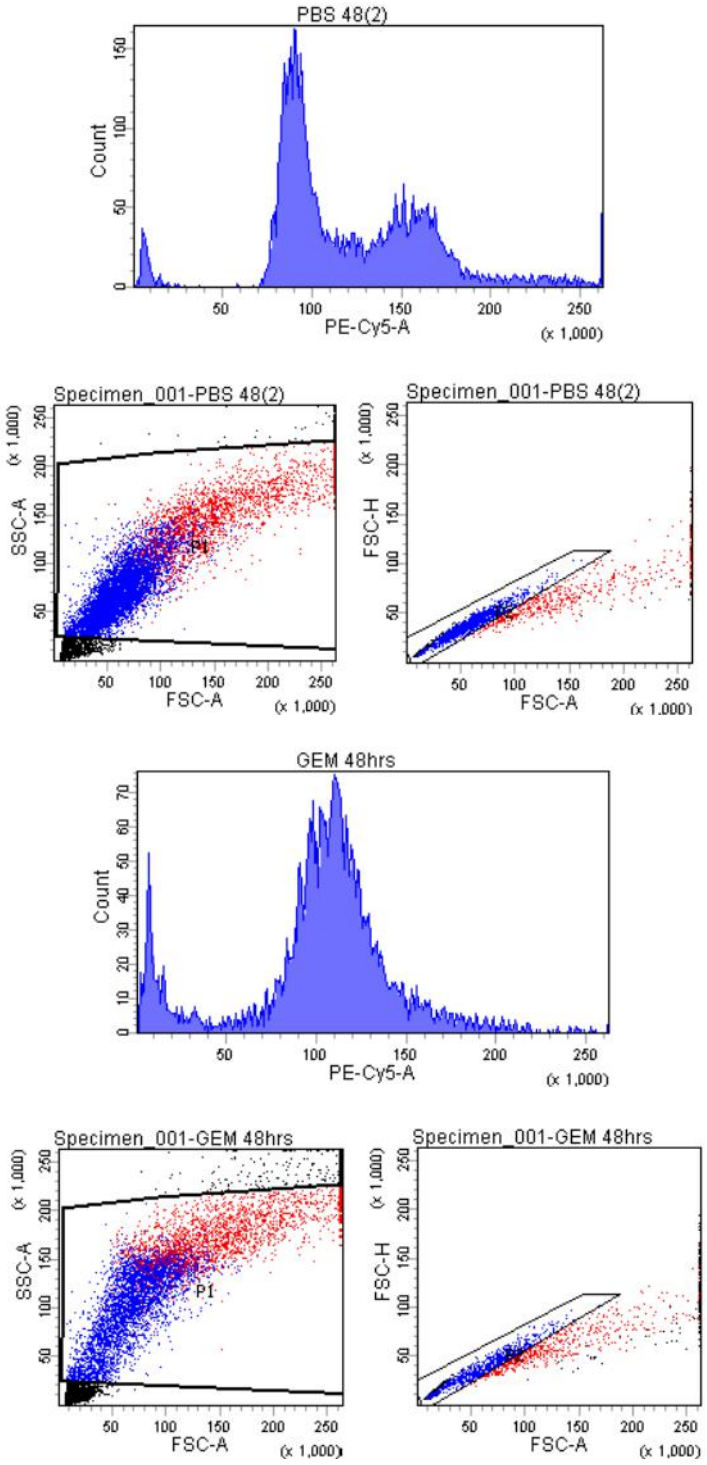

Figure 37: Flow cytometry of MiaPaCa-2 cells treated with 40nM gemcitabine for 48 hours vs. control

After 48 hours of gemcitabine exposure, the G1 population is half of that seen under control conditions, with the S-phase population now being thrice the size. Control and gemcitabine experiments both included 10,000 events.

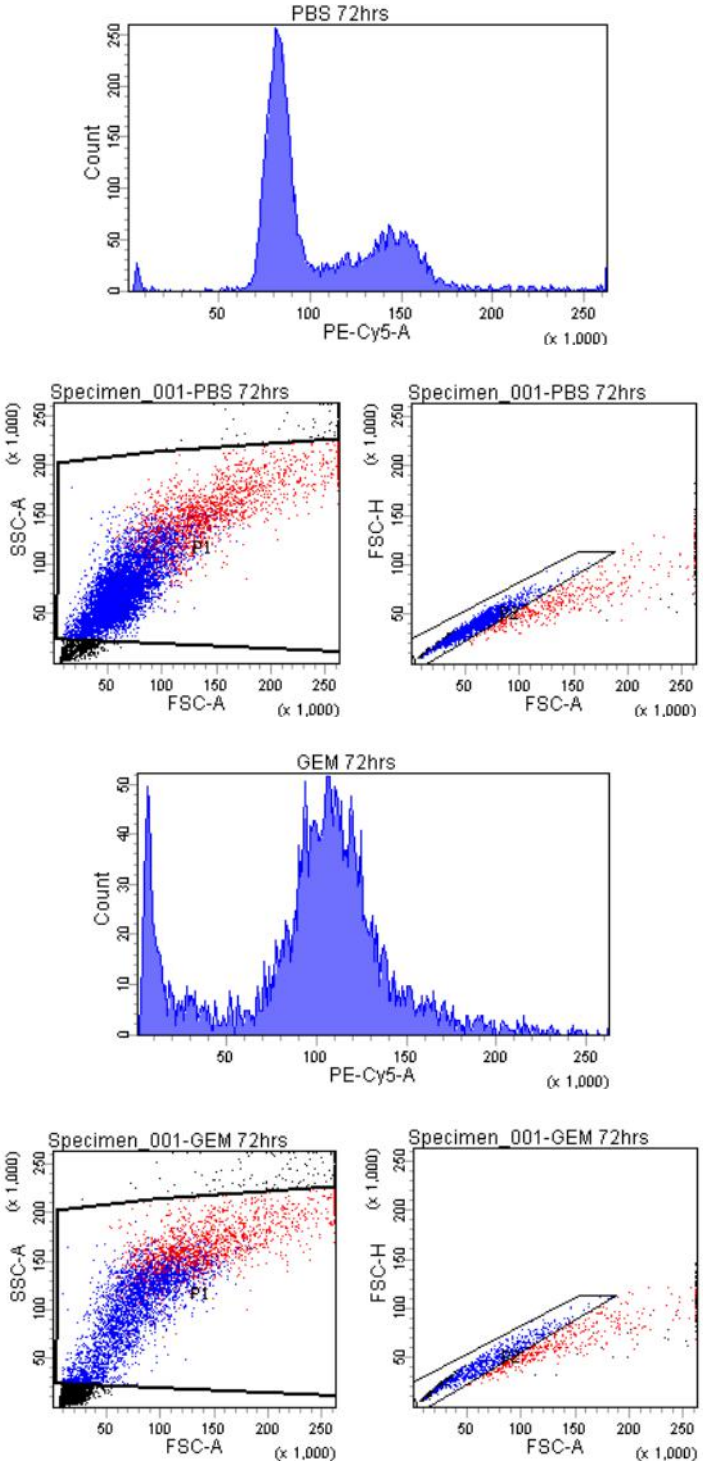

Figure 38: Flow cytometry of MiaPaCa-2 cells treated with 40nM gemcitabine for 72 hours vs. control

A similar pattern as seen at 48 hours is seen with gemcitabine treatment with almost half the total of gated cells now in S-phase. A progressively large pre-G1 peak is seen indicative of dead cells. Control and gemcitabine experiments both included 10,000 events.

Dual Drug Experiments

Isobolar Analysis of Drug Combinations

To delineate the effects of combining both BI 6727 and gemcitabine on MiaPaCa-2 cells, both drugs were administered simultaneously in concentrations ranging from zero, up to the IC_{50} of each agent. Following 72 hours of combination therapy, an MTS assay was undertaken with the mean blank reading deducted from each well. The concentrations of each drug when used in combination that gave the equivalent inhibition of the drugs used in isolation (IC_{50} or other fixed point) were plotted against each other in order to compare the combinations with an additive line that would imply the drugs acted independently.

When plotting an isobologram the doses of drugs A and B give abscissa and ordinate, with the effect of combining the drugs plotted as a graph. In the example overleaf (Figure 39), the IC_{50} of each drug in isolation can be read from the axes – 500nM for drug A and 50nM for drug B. For two drugs to be additive, their simultaneous combined effect would equate to the effects of both drugs in isolation. For example, for these two drugs to be additive, a combination of 250nM of drug A and 25nM of drug B should equate to the same effect of either 500nM of drug A or 50nM of drug B as single agents. Should the IC_{50} effect be achieved at lower concentrations of the two drugs - for example 150nM of drug A and 20nM of B, the drugs would show synergy. If the observed inhibition by the drug combination was less than 50 %, the graph's plots would be located above the additive line and would indicate antagonism.

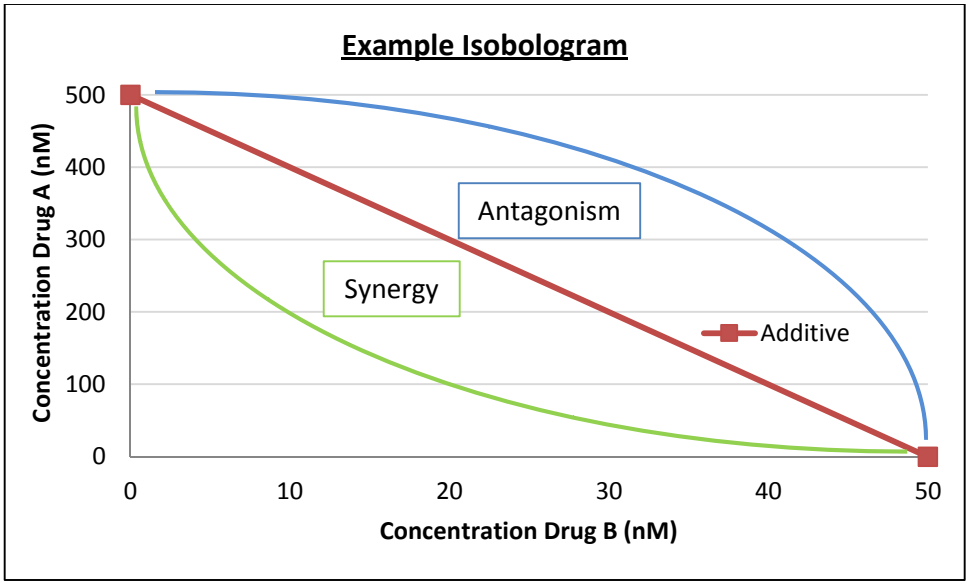

Figure 39: Example isobologram to demonstrate drug interaction
The additive line joins both the drugs' IC_{50} lines. The plotted curve falling below this line indicates synergy, with the opposite indicating antagonism.

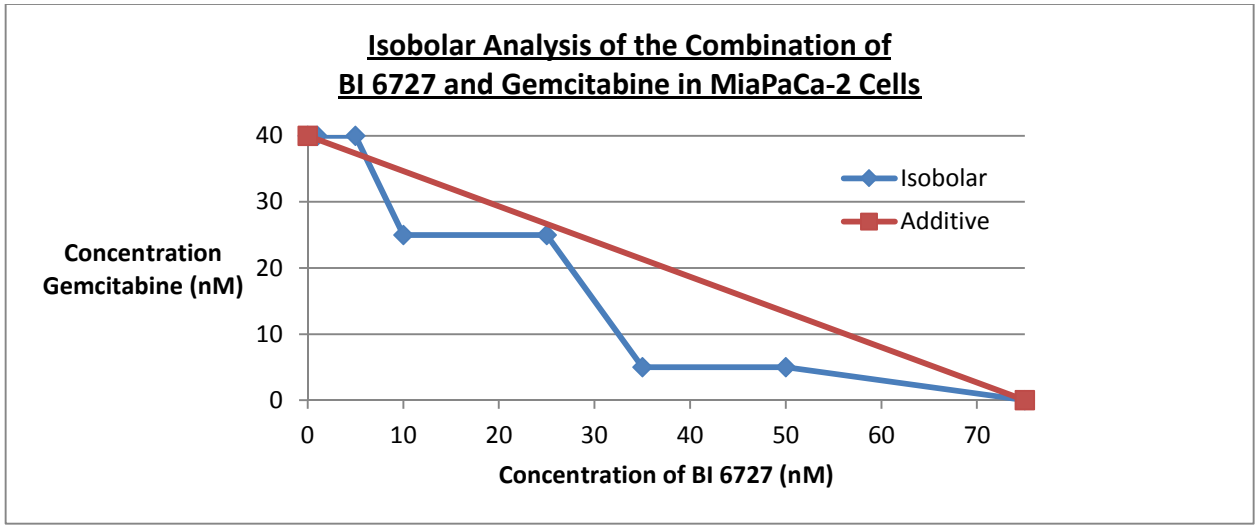

Gemcitabine Concentration (nM)	BI 6727 Concentration (nM)											
	0	1	5	10	25	35	50	75	Control	Control	Control	Blank
0	1.101	1.094	0.909	0.846	0.682	0.624	0.616	0.556	1.257	1.274	1.273	0.036
5	0.981	1.081	0.959	0.62	0.597	0.55	0.556	0.5	1.236	1.255	1.265	0.035
10	0.806	0.759	0.988	0.703	0.575	0.497	0.5	0.444	1.179	1.181	1.216	0.036
20	0.948	0.772	0.988	0.566	0.607	0.506	0.483	0.441	1.14	1.192	1.228	0.035
25	0.844	0.691	0.787	0.539	0.445	0.527	0.434	0.439	1.187	1.263	1.295	0.036
30	0.753	0.773	0.806	0.426	0.465	0.407	0.373	0.383	1.068	1.129	1.139	0.037
35	0.631	0.644	0.625	0.383	0.489	0.373	0.402	0.432	1.241	1.274	1.062	0.035
40	0.46	0.471	0.359	0.343	0.344	0.354	0.409	0.445	1.332	1.337	1.106	0.037

Figure 40: Isobolar analysis of combination therapy with BI 6727 and gemcitabine in MiaPaCa-2 cells for 72 hours

Isobolar analysis of utilising a combination of BI 6727 and gemcitabine in MiaPaCa-2 cells seems generally additive, though a degree of synergy could be argued. Both drugs were administered together, with cells treated for 72 hours.

Isobolar Experiment of the Combination Treatment of MiaPaCa-2 Cells with BI 6727 and Gemcitabine

When looking at the isobolar analysis in

Figure 40 the first aspect to note is that both extremities of the blue isobolar plot (i.e. the individual drug IC_{50}s) is matched to the red additive line as should be expected in this instance.

The isobolar line plotting the effect of combining BI 6727 and gemcitabine on MiaPaCa-2 cells crosses the additive line at one point, and with one only notable exception, all plots are either on, or very near to the additive line. The point representing the combination of 35nM of BI 6727 and 5nM gemcitabine gives the impression of a strong degree of synergy, but whether this is an anomalous reading or not is difficult to ascertain. However, when examining the numerical readings gathered from the MTS assay, the logical progressive reduction in the MTS readings with the increased drug concentrations is lost at this particular point. This certainly raises the suspicion of an anomaly and may be giving the impression of a more impressive result than is true. In excluding this point on the plotted graph, it is the author's opinion that this isobolar graph demonstrates a largely additive effect between the combination of BI 6727 and gemcitabine with no overwhelming evidence of synergy and no evidence of antagnonism.

The Additive Effect of Combining BI 6727 and Gemcitabine

Prior to undertaking this isobolar analysis, it was hypothesised that the combination of a PLK1 inhibitor and gemcitabine would be antagonistic. This was based on the simplistic theory that BI 6727 is a mitotic inhibitor arresting cells in G2 (Table 17) and gemcitabine requires dividing cells to be at its most effective in incorporating into DNA.

By moving from left to right along the isobolar line their combined effects may be hypothesised.

- 40nM gemcitabine + 0nM BI 6727: It has already been demonstrated in Table 18 that gemcitabine causes a surge in the S-phase population, which takes approximately 24 hours to come to prominence on flow cytometry. A fall in the MiaPaCa-2 cell population number will be seen with continued exposure of 40nM of gemcitabine, with cells being terminated either by apoptosis or possibly mitotic catastrophe.

- 25nM gemcitabine + 10nM BI 6727/25nM gemcitabine +25nM BI 6727: Lower concentrations of BI 6727 in isolation has already been shown to reduce the rate of MiaPaCa-2 proliferation in comparison to untreated controls as early as 24 hours (Figure 26). Flow cytometry has revealed that its mechanism of action in causing a G2 block is most prominent at this early timepoint, however, cells seem able to overcome the effects of this low drug concentration by 72 hours of exposure (Table 17). Administering 25-30nM of gemcitabine alone would result in no great effect to cell numbers at 24 hours though fewer viable cells would be seen in comparison by 72 hours (Figure 29). By combining the two drugs, the early effects of BI 6727 is added to the later effects of gemcitabine resulting in a prolonged period of cellular stress.
- 5nM gemcitabine + 50nM BI 6727: At a concentration of 5nM, gemcitabine has been previously shown to marginally reduce MiaPaCa-2 proliferation in comparison to untreated control (Figure 28), though no evidence is yet presented to support cytotoxicity at this concentration. The same cytostatic effect has been observed at 50nM of BI 6727 (Figure 25), though it is seen earlier than with gemcitabine. It could therefore be hypothesised that the additive effect of combining both drugs at these concentrations may be cytostatic in nature, but again a contributory factor may be the extended period of cellular stress
- 0nM gemcitabine + 75nM BI 6727: Effective by causing a G2 arrest and inhibits daughter cellular division following DNA synthesis. No evidence is yet presented to indicate cell death, though proliferation is dramatically reduced in comparison to control (Figure 25).

In summary, the hypothesised antagonism between BI 6727 and gemcitabine is not seen, with an additive effect seen at worst. It is a possibility that the varied concentration combinations of the two drugs may result in a differing mechanism in cellular insult. This may involve, to varying extents, a prolonged period of cellular stress, increasing cytostatic properties with resultant mitotic catastrophe or an increase in apoptotic cell death.

Isobolar Experiments of the Consecutive Treatment of MiaPaCa-2 Cells with BI 6727 and Gemcitabine

To delineate the effects of the consecutive treatment of pancreatic cancer cells with the two compounds, four isobolar analyses were undertaken. This involved treating cells with compound 1 in isolation for 24 hours, followed by compound 2 alone for a further 72 hours prior to a viability assay.

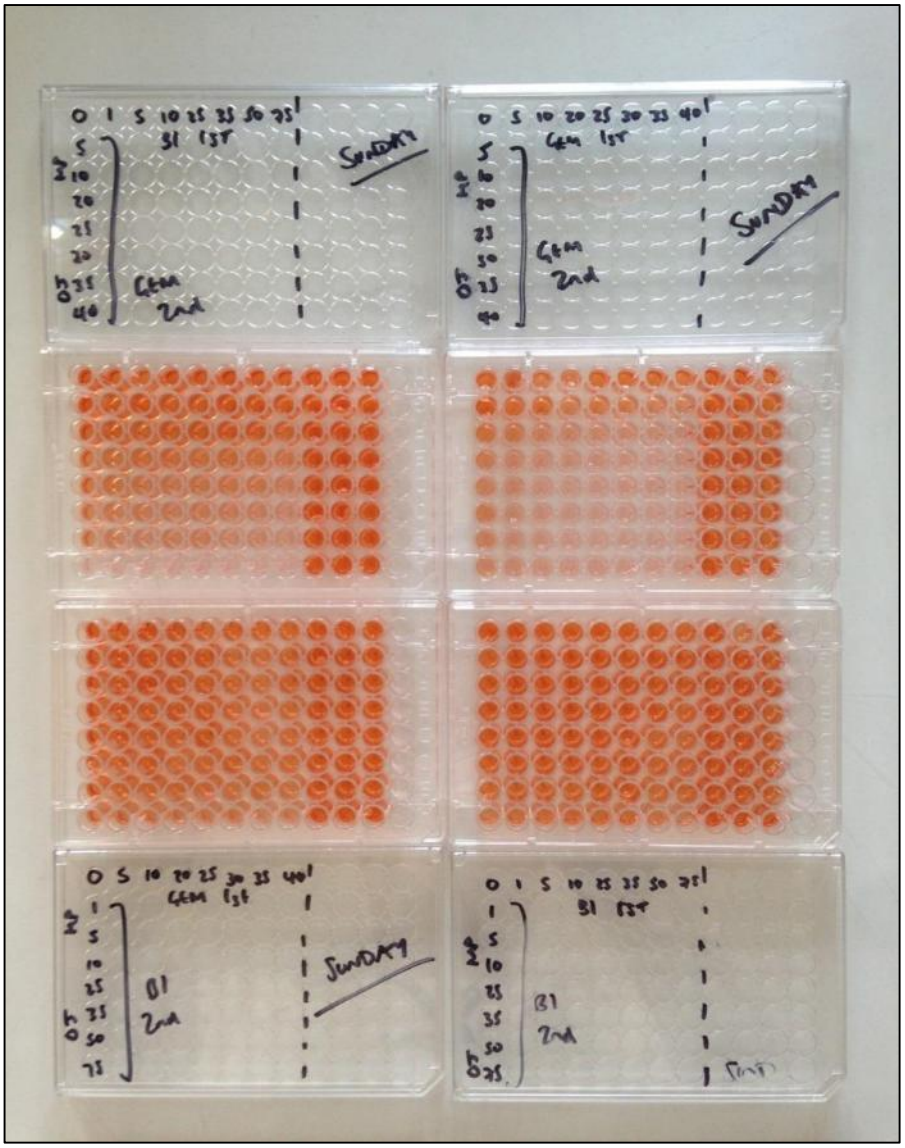

Figure 41: Photograph of isobolar experiments on 96-well plates with the sequential addition of each drug

A photograph of isobolar experiments on 96-well plates following consecutive drug treatment. Viable cells convert the EZ4U assay into an orange colour with decreasing density of colour indicating a fall in the number of viable cells in the well. The rightmost row in each plate is left blank, with the three adjacent rows including untreated control cells.

Following the administration of the EZ4U assay, inspection of the four plates (Figure 41) suggest that MiaPaCa-2 cells were most sensitive to two consecutive treatments with gemcitabine (right upper plate) and least sensitive to two treatments with BI 6727 (right lower plate). Interestingly, the initial administration of BI 6727 followed by gemcitabine (left upper plate) seemed more effective in reducing viable cell numbers than vice versa (left lower plate).

Although the experiment was only undertaken once, the results are strengthened by the fact that all four drug combinations experiments were undertaken concurrently and could simply be directly visually compared to ascertain superiority.

Isobolar Analyses with Gemcitabine as the Initial Drug

Gemcitabine followed by Gemcitabine

As is apparent from the photograph in Figure 41, two consecutive doses of gemcitabine within 24 hours of each other is highly effective in reducing cell viability. The isobolar graph in Figure 42 shows that this phasing is more effective than simply treating the cells with gemcitabine once, though doubts must be raised as to the clinical relevance of this regime, given gemcitabine's recognised toxicity.

Of note from the MTS readings seen in Figure 42 and later in Figure 43, is that the administration of up to 40nM of gemcitabine for 24 hours, followed by its replacement with un-drugged media for 72 hours, seems to only have a modest effect on MiaPaCa-2 viability. Though some cell death will inevitably have occurred, it seems that this transient period of drug exposure is inadequate to cause significant harm to the cell population. Importantly, for this very reason, in this series of isobolar analyses, the plot representing the IC_{50} concentration of the first drug administered, which should correspond to the x-axis extremity of the additive line, is often not reached.

Despite the minimal effect of transient gemcitabine exposure, initial treatment with a moderate to high concentration of gemcitabine followed by continued exposure to a very low concentration i.e.5nM seems very effective, supporting the theory that the length of gemcitabine exposure is an important factor in its toxicity. Initial viability assays with gemcitabine (Figure 29) suggests that MiaPaCa-2 cells are only slightly affected by 5nM of gemcitabine at 72 hours, supporting synergy when combined with pre-exposed cells. Despite there being no doubt as to this drug regime being the most effective, it must be argued that this demonstrated synergy may be due to the fact that what is being compared is 96 hours of gemcitabine treatment against 72 hours – i.e the leftmost plot on the graph represents MiaPaCa-2 cells that were untreated for 24 hours, followed by 72 hours of gemcitabine. It is also of interest in these MTS results that the apparent IC_{50} of gemcitabine is 25-35nM as half the control reading (0.809) is reached at this point in the first vertical column.

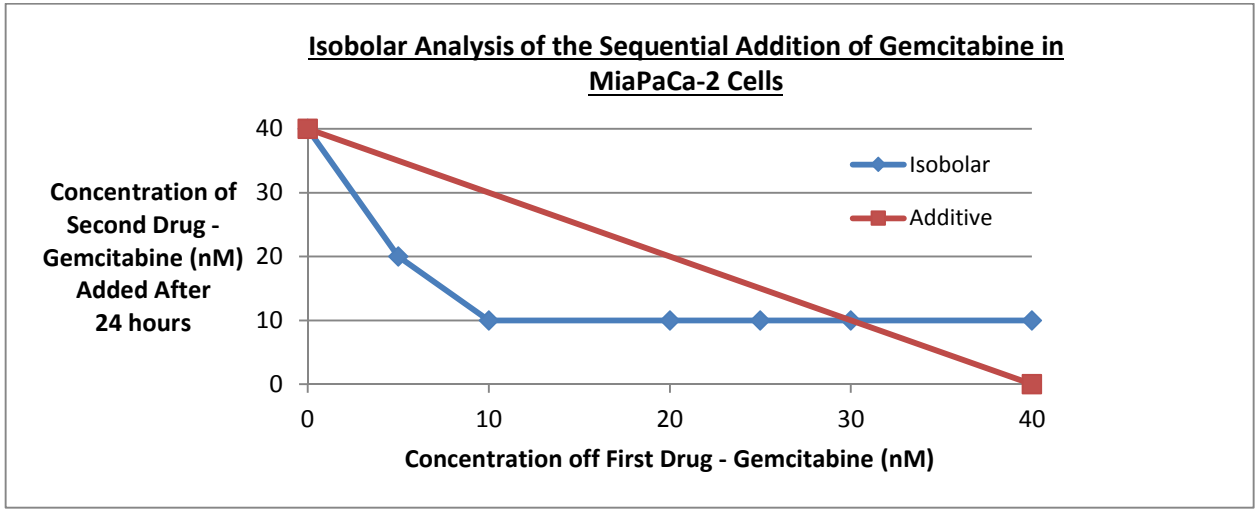

Concentration of Second Drug Added (Gemcitabine) (nM)	Concentration of First Drug Added (Gemcitabine) (nM)											
	0	5	10	20	25	30	35	40	Control	Control	Control	Blank
0	0.809	0.799	0.751	0.745	0.733	0.769	0.725	0.641	0.968	0.965	1.064	0.035
5	0.896	0.678	0.671	0.426	0.521	0.478	0.39	0.37	0.943	0.938	0.961	0.037
10	0.471	0.427	0.328	0.291	0.266	0.291	0.235	0.237	0.936	0.858	0.919	0.05
20	0.364	0.296	0.258	0.236	0.254	0.252	0.19	0.196	0.873	0.908	0.999	0.041
25	0.329	0.293	0.22	0.193	0.203	0.212	0.2	0.177	0.997	0.917	0.916	0.041
30	0.413	0.275	0.23	0.214	0.2	0.216	0.186	0.207	0.915	0.869	0.931	0.049
35	0.346	0.253	0.226	0.193	0.177	0.181	0.176	0.16	0.959	0.783	0.782	0.034
40	0.34	0.281	0.242	0.211	0.215	0.196	0.196	0.189	1.001	0.848	1.029	0.034

Figure 42: Isobolar analysis of the sequential addition of gemcitabine in MiaPaCa-2 cells

This isobolar analysis suggests that administering gemcitabine to MiaPaCa-2 cells for 24 hours, followed by a second dose for a further 72 hours, is synergistic.

Gemcitabine followed by BI 6727

Figure 41 clearly shows the superiority of two consecutive treatments with gemcitabine, in comparison with gemcitabine followed by BI 6727. The isobolar graph in Figure 43 suggests that the effect of pre-treating MiaPaCa-2 cells with gemcitabine for 24 hours prior to 72 hours of BI 6727 exposure is additive.

As previously described, the effects of transiently treating MiaPaCa-2 cells for 24 hours with gemcitabine is moderate at best by 96 hours (Figure 42 Figure 43). However, sequentially adding only a very small concentration i.e. 1-5nM of BI 6727 for 72 hours following gemcitabine exposure seems to greatly decrease cell viability in comparison. This benefit seems concentration dependent up to the maximum dose of 75nM of BI 6727 utilised in this experiment. At this point it must be remembered that previously discussed data in Figure 25 Figure 26 suggest that such low concentrations of BI 6727 as a monotherapy has little to no effect on cell numbers compared to control at 72 hours. This supports the conclusion that there is some benefit in combining gemcitabine with this novel PLK1 inhibitor.

On the other hand, this isobolar curve suggests that there is little benefit in pre-treating MiaPaCa-2 cells with a low concentration (5-10nM) of gemcitabine prior to PLK1 inhibition. Continued exposure to such low concentrations have previously been shown to reduce cell viability, however it could again be argued that transient exposure to gemcitabine is ineffective in killing cells in comparison to continuing treatment.

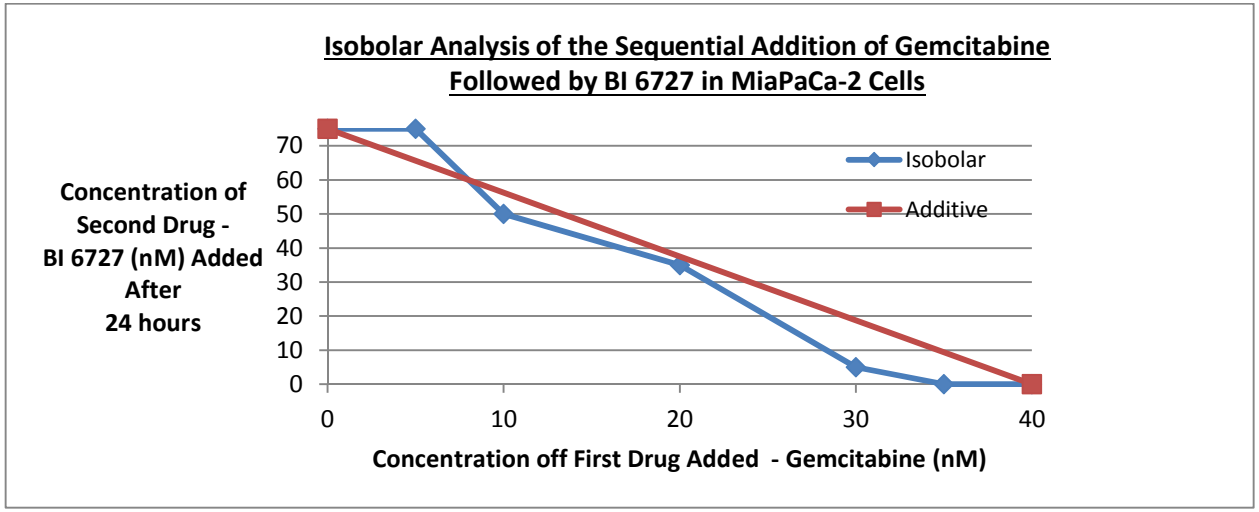

Concentration of Second Drug Added (BI 6727) (nM)↓	Concentration of First Drug Added (Gemcitabine) (nM)										
	0	5	10	20	30	35	40	Control	Control	Control	Blank
0	0.938	0.892	0.924	0.784	0.689	0.64	0.64	0.924	0.913	0.94	0.033
1	0.886	0.85	0.725	0.743	0.499	0.557	0.478	1.093	0.925	0.962	0.032
5	0.888	0.725	0.922	0.621	0.513	0.605	0.448	0.86	0.861	0.925	0.034
10	0.897	0.772	0.646	0.64	0.509	0.491	0.433	0.84	0.864	0.884	0.033
25	0.828	0.781	0.658	0.645	0.518	0.529	0.393	0.872	0.884	0.948	0.034
35	0.757	0.643	0.697	0.463	0.621	0.528	0.462	0.838	0.881	0.901	0.035
50	0.749	0.653	0.593	0.585	0.442	0.429	0.498	0.937	0.913	0.922	0.033
75	0.47	0.463	0.41	0.367	0.394	0.331	0.306	0.932	0.934	1.063	0.035

Figure 43: Isobolar analysis of the sequential addition of gemcitabine for 24 Hours, followed by BI 6727 for 72 hours in MiaPaCa-2 cells
This *isobolar analysis of treating MiaPaCa-2 cells with BI 6727 for 72 hours following 24 hours of gemcitabine exposure suggests an additive effect.*

Isobolar Analyses with BI 727 as the Initial Drug

BI 6727 followed by BI 6727

Administering BI 6727 on consecutive days seems to be of no benefit with a strong suggestion of antagonistic behaviour, which is challenging to explain. Nevertheless, on superficial inspection of the isobolar plates in Figure 41, it was already apparent that this treatment regime is the most ineffective of the four investigated.

As noted with gemcitabine, the transient exposure of cells for 24 hours to the IC_{50} concentration of BI 6727 followed by its removal seems to have only a slight effect on cell viability by 96 hours. This suggests that MiaPaCa-2 cells can recover from a short period G2 arrest, and that prolonged exposure is necessary to be effective.

From earlier results (Figure 25Figure 26) it is already shown that concentrations of up to 5nM of BI 6727 are ineffective against MiaPaCa-2, even with 72 hours of treatment. Higher concentrations of up to 50nM reduces the viable cell population to around 70% of control levels by 72 hours, as is also evident in this isobolar experiment (Figure 44, MTS reading of 0.757 vs. 1.166 in control).

What is evident from the MTS readings in Figure 44, is that administering an initial concentration of up to 50nM of BI 6727 is irrelevant, and that any reduction in cell viability seems entirely dependent on the second 'hit' being at a concentration of 35nM or higher. When the initial concentration administered is at the IC_{50} concentration of 75nM, this seems to sensitize cells to concentrations as low as 10nM as the second dose. Interestingly, previous results in Figure 25 Figure 26 demonstrate that concentrations this low of BI 6727 are ineffective when administered in isolation.

In summary, it can be concluded that if two consecutive doses of BI 6727 are to be administered, utilising concentrations below the IC_{50} are generally ineffective.

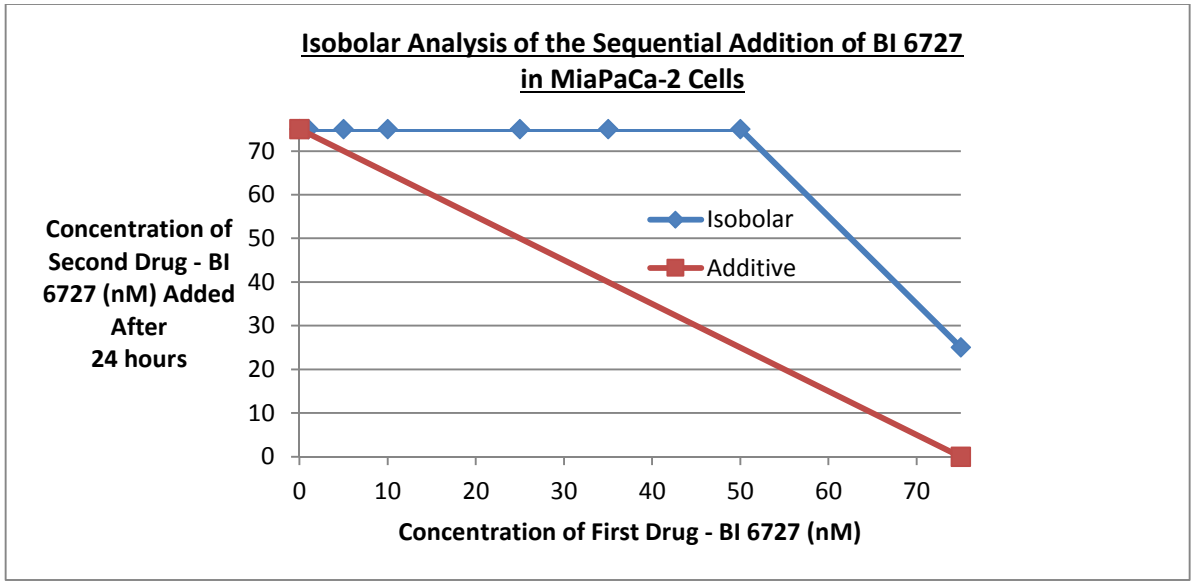

Concentration of Second Drug Added (BI 6727) (nM)↓	Concentration of First Drug Added (BI 6727) (nM)											
	0	1	5	10	25	35	50	75	Control	Control	Control	Blank
0	1.166	1.247	1.041	1.241	0.908	0.891	1.01	0.895	1.005	1.117	0.731	0.034
1	1.165	1.26	1.204	1.226	1.154	1.183	1.158	0.892	0.967	1.078	1.116	0.032
5	1.225	1.268	1.187	1.211	1.108	1.12	1.086	0.934	1.105	1.11	1.198	0.041
10	1.088	1.23	1.179	1.109	1.122	1.139	1.03	0.788	0.965	1.144	1.171	0.033
25	1.122	1.303	1.128	1.144	1.221	0.844	1.005	0.559	1.048	1.15	1.056	0.035
35	0.815	0.96	1.042	0.973	0.749	0.703	0.719	0.487	1.018	0.926	0.874	0.035
50	0.757	1.046	1.12	1.053	1.075	0.899	0.86	0.577	0.932	0.94	0.916	0.033
75	0.687	1.067	0.796	0.921	1.133	0.53	0.507	0.361	1.123	1.095	0.448	0.041

Figure 44 : Isobolar analysis of the sequential addition of BI 6727 in MiaPaCa-2 cells
The addition of BI 6727 to MiaPaCa-2 cells for 72 hours, treated with the same drug only 24 hours earlier seems antagonistic with all plots being above the additive line.

BI 6727 Followed by Gemcitabine

It is apparent from Figure 41 that administering BI 6727 prior to gemcitabine is more effective than vice versa, however, the benefits when examining the isobolar graph in Figure 45 seems marginal with evidence of synergy at high gemcitabine concentrations and low BI 6727 concentrations, but antagonism when these concentrations are reversed.

A closer look at the MTS readings reveals that partly responsible for this confusion is the fact that 50% inhibition point (IC_{50}) seems to have been achieved by a far lower concentration than the gemcitabine concentration previously demonstrated. The first column in Figure 45 shows that this point has been reached at 10-25nM of gemcitabine as opposed to the expected 40nM and the reason for this is unclear.

Secondly, a further anomaly seen on these results is that there was a clear technical error with the multipipette with the bottom row of the plate, likely meaning that possibly no cells or indeed very few cells were seeded. For this reason, the MTS reading for the 0nM BI 6727/40nM gemcitabine well on which the graph is based, has been estimated.

Though difficult to draw conclusions from this experiment it could be argued that low-dose BI 6727 helps sensitize MiaPaCa-2 cells to moderate-high concentrations of gemcitabine. Gemcitabine exposure in isolation for 72 hours has already been shown to be cytotoxic, and this is again evident with these results, particularly at concentrations of 20nM and higher. However, pre-treating these cells with as little as 1-5nM of BI 6727 prior to gemcitabine therapy improves its efficacy in comparison to gemcitabine monotherapy.

In contrast, pre-dosing with the PLK1 inhibitor seems ineffective when followed by a low concentration of gemcitabine, as is evident by the blue isobolar line crossing the red additive line into the antagonistic zone of the graph. By looking at the MTS readings which the graph interprets as antagonism, it should be noted that cell viability continues to decrease with increasing BI 6727 concentration, though this fall is only marginal. What skews the graph somewhat is both the artificially low MTS readings from the 0nM BI 6727 column, in addition to the negligible effect that transient BI 6727 exposure has on MiaPaCa-2 cells. These two circumstances have influenced the results by pulling the isobolar curve to the right, perhaps giving a more negative result than is merited result than otherwise.

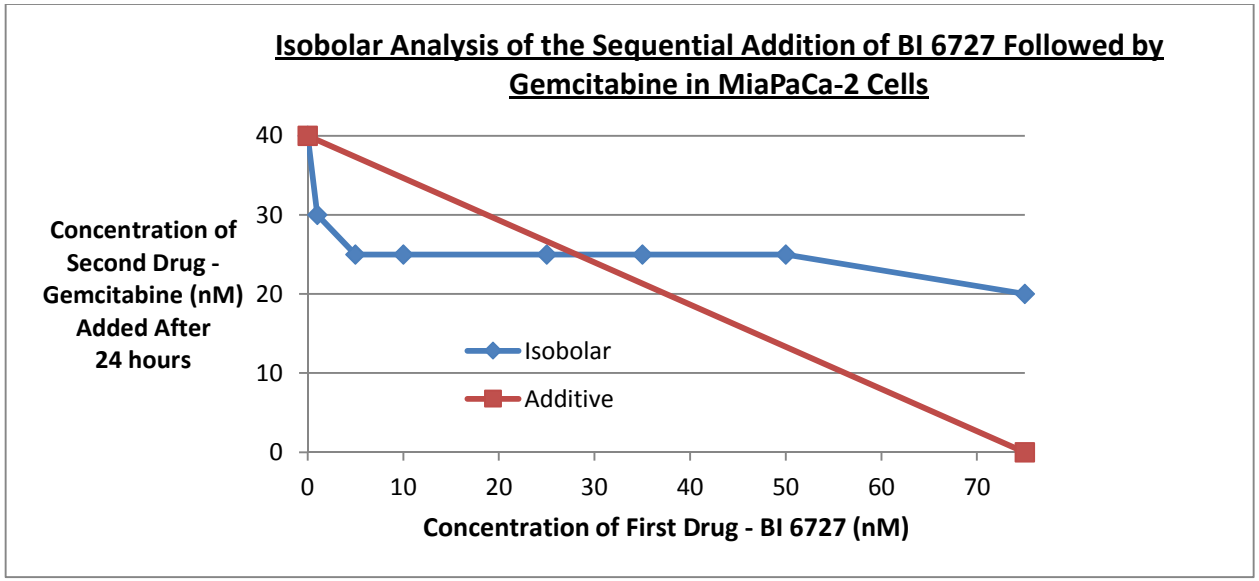

Concentration of Second Drug Added (Gemcitabine) (nM) ↓	Concentration of First Drug Added (BI 6727) (nM)											
	0	1	5	10	25	35	50	75	Control	Control	Control	Blank
0	1.041	0.87	0.676	0.917	0.833	1.017	0.926	0.865	1.044	1.036	1.051	0.034
5	1.114	0.817	0.895	0.735	0.741	0.907	0.877	0.815	1.064	1.419	1.03	0.035
10	0.752	0.739	0.626	0.701	0.74	0.767	0.713	0.603	1.064	0.968	1.026	0.035
20	0.511	0.467	0.532	0.501	0.442	0.504	0.458	0.386	0.964	0.999	1.071	0.033
25	0.504	0.468	0.383	0.348	0.394	0.386	0.387	0.311	0.99	1.159	1.13	0.034
30	0.436	0.372	0.35	0.326	0.356	0.338	0.308	0.253	1.264	0.846	0.991	0.035
35	0.425	0.359	0.286	0.346	0.365	0.267	0.295	0.23	0.99	1.021	1.029	0.034
40	0.125	0.124	0.124	0.125	0.125	0.126	0.122	0.125	0.126	0.128	0.124	0.036

Figure 45: Isobolar analysis of the sequential addition of BI 6727 for 24 hours followed by gemcitabine for 72 hours in MiaPaCa-2 cells
The treatment of MiaPaCa-2 cells with BI 6727 for 24 hours prior to gemcitabine for a further 72 hours seems synergistic at high gemcitabine and low BI 6727 concentrations, with the opposite becoming apparent when these concentrations are reversed.

Pretreatment of MiaPaCa-2 Cells Prior to Combination Drug Therapy

Thus far, it has been both demonstrated that combination therapy with BI 6727 and gemcitabine is at least additive in nature and that the sequential treatment with both drugs is arguably more effective when BI 6727 precedes gemcitabine administration. It was therefore decided to proceed to investigate the efficacy of pretreating MiaPaCa-2 cells for 24 hours with monotherapy, prior to the administration of combination therapy.

Both isobolar experiments (monotherapy followed by combination therapy), were attempted in triplicate, with the mean MTS readings taken to produce a final isobolar analysis. Complete results can be seen in Appendix I and J.

Pretreatment with Gemcitabine Prior to Combination Therapy with BI 6727 and Gemcitabine

As is evident in Figure 46, the exposure of MiaPaCa-2 cells to gemcitabine prior to combination therapy produces an isobolar graph similar to that seen with both combination therapy alone. Figure 46 suggests additive-synergystic behaviour when the two compounds are administered in this sequence. However, as previously noted, the clinical application of administering two consecutive doses of gemcitabine only 24 hours apart seems unrealistic, and it was therefore decided to proceed to repeating this experiment with BI 6727 as the primary drug.

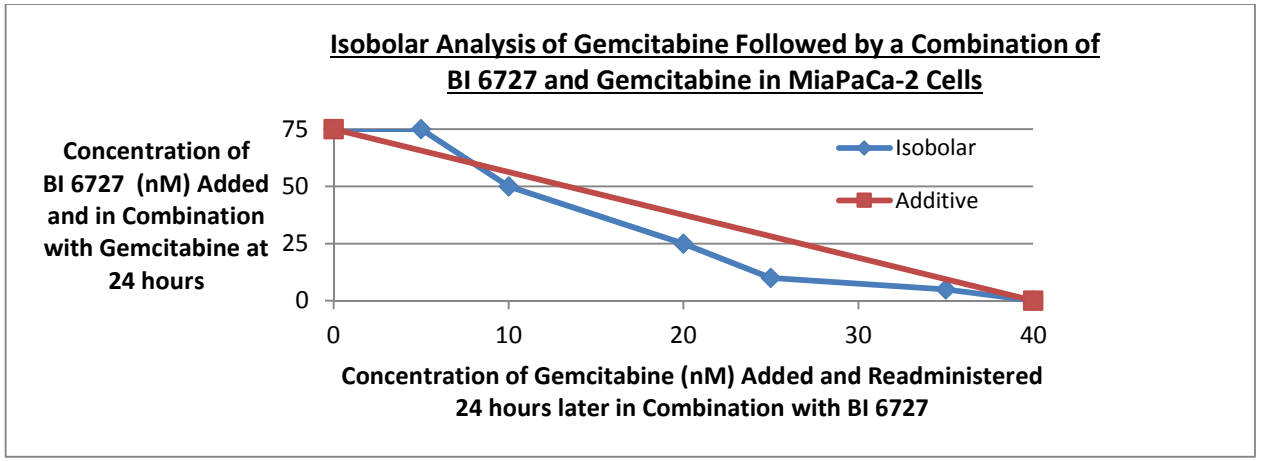

Concentration of BI 6727(nM) Added In	Concentration of Gemcitabine Added and Readministered 24 Hours later in Combination with BI 6727(nM)										
Combina on with Gemcitabine at 24 hours↓	0	5	10	20	25	35	40	Control	Control	Control	Blank
0	0.636	0.609	0.623	0.573	0.487	0.461	0.388	0.544	0.473	0.42	0.062
1	0.616	0.674	0.678	0.653	0.511	0.493	0.442	0.692	0.681	0.693	0.061
5	0.635	0.65	0.607	0.566	0.495	0.424	0.41	0.674	0.685	0.708	0.062
10	0.591	0.64	0.584	0.469	0.299	0.381	0.379	0.661	0.676	0.706	0.061
25	0.584	0.612	0.597	0.414	0.389	0.37	0.369	0.663	0.685	0.724	0.065
50	0.508	0.578	0.262	0.271	0.181	0.296	0.231	0.707	0.712	0.717	0.062
75	0.405	0.225	0.204	0.18	0.169	0.126	0.134	0.683	0.488	0.677	0.064

Figure 46: Isobolar analysis of the sequential addition of gemcitabine for 24 hours, followed by a combination of gemcitabine and BI 6727 for 72 hours in MiaPaCa-2 cells (mean readings taken from three experiments)

Exposure of MiaPaCa-2 cells to gemcitabine for 24 hours prior to combination therapy for a further 72 hours seems additive-synergystic, and produces a graph similar in appearance to both combination therapy alone. Triplicate results can be seen in Appendix I.

Pretreatment with BI 6727 Prior to Combination Therapy with BI 6727 and Gemcitabine

This experiment was performed in triplicate, but one set of data was lost. Therefore, Figure 47 is based on two experiments as opposed to the planned three.

When looking at Figure 47, it can be reasonably concluded that exposing MiaPaCa-2 cells to BI 6727 prior to a second dose combined with gemcitabine demonstrates synergy. An anomaly has to be noted here: the point at which the blue curve of synergy hits the zero gemcitabine concentration is at 50 and not 75nM of BI 6727. This suggests that treating MiaPaCa-2 with either concentration (50 or 75nM) of BI 6727, followed by a second identical dose is synergistic – a claim that is contradicted by Figure 44 which even suggests that this may even be antagonistic. It is not clear why this anomaly exists between the two experiments, but this may reflect undefined variations in experimental conditions (e.g. difference in growth phases of the cells when drugs were added, note these experiments were not undertaken with synchronised cells).

Line of Best Fit for Further Experiments

For further experiments, a line of best fit was established to demonstrate this synergy that is seen in Figure 48. For the remaining experiments – namely an Annexin V apoptosis and necrosis assay and Western blotting – the drug concentrations were established from various plots from this line.

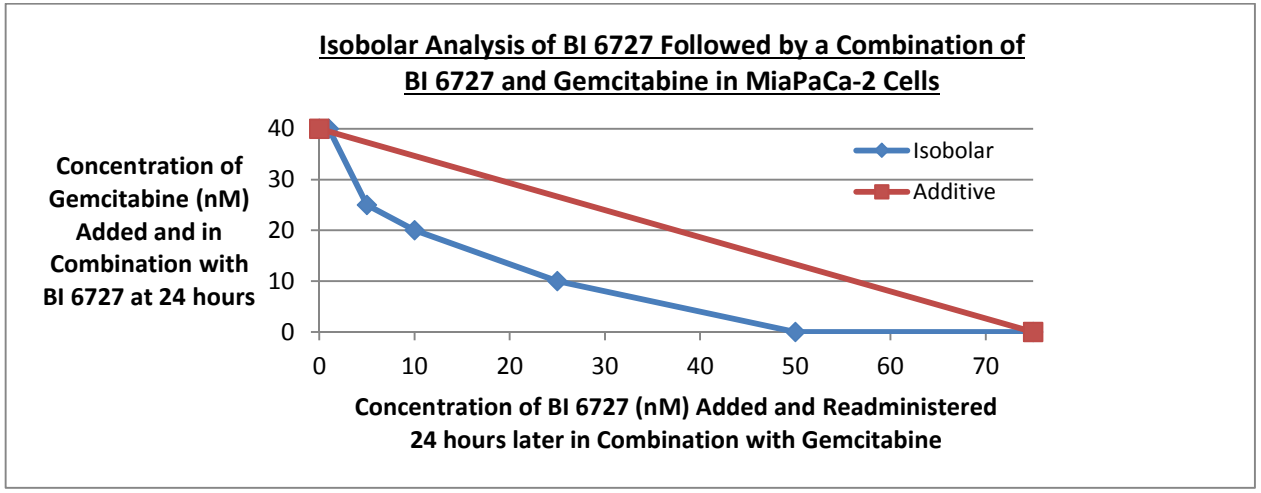

Concentration of Gemcitabine(nM) Added	Concentration of BI 6727 Added and Readministered 24 Hours later in Combination with Gemcitabine(nM)										
In Combination with BI 6727 at 24 hours ↓	0	1	5	10	25	50	75	Control	Control	Control	Blank
0	0.687	0.616	0.543	0.5	0.54	0.47	0.475	0.703	0.709	0.703	0.108
5	0.693	0.557	0.565	0.548	0.541	0.46	0.475	0.669	0.679	0.688	0.109
10	0.672	0.609	0.56	0.477	0.46	0.465	0.474	0.641	0.627	0.692	0.107
20	0.642	0.575	0.508	0.438	0.474	0.429	0.423	0.601	0.623	0.681	0.11
25	0.633	0.481	0.463	0.443	0.454	0.412	0.409	0.607	0.64	0.707	0.112
40	0.427	0.421	0.419	0.407	0.42	0.235	0.248	0.697	0.713	0.725	0.116

Figure 47: Isobolar analysis of the sequential addition of BI 6727 for 24 hours, followed by a combination of BI 6727 and gemcitabine for 72 hours in MiaPaCa-2 cells (mean readings taken from two experiments)

Treating MiaPaCa-2 cells with BI 6727 for 24 hours, followed by a combination of BI 6727 and gemcitabine for a further 72 hours seems to demonstrate synergy. Duplicate results can be seen in Appendix J.

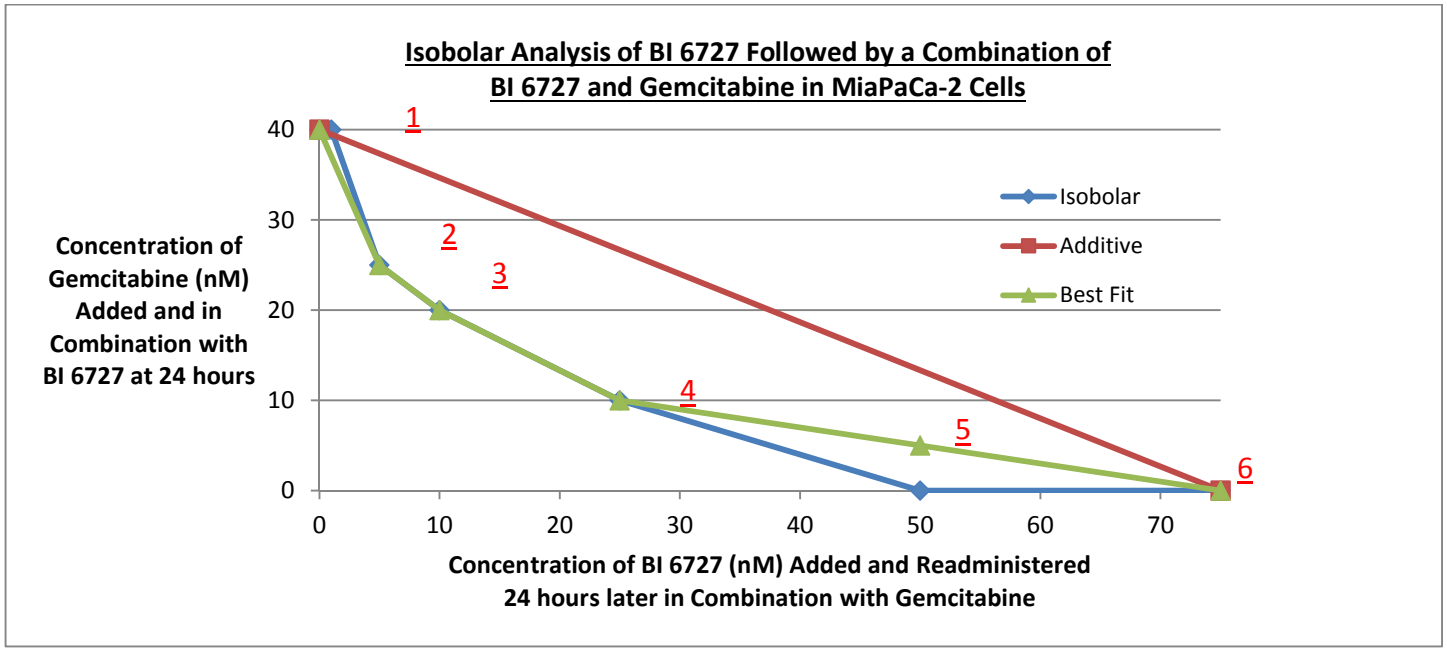

Figure 48: : Isobolar analysis of the sequential addition of BI 6727 for 24 hours followed by a combination of BI 6727 and gemcitabine for 72 hours in MiaPaCa-2 cells

The line of synergy from the previous figure has now been adapted with a line of best fit. Numbers 1-6 indicate points along the line of best fit that further experiments have been based upon (See Annexin Apoptosis and Necrosis V Assay and Westerns Blot).

Annexin V Assay for Apoptosis and Necrosis

During apoptosis, various morphological changes occur within the cell. In addition to the loss of plasma membrane attachment, changes include blebbing of the plasma membrane, cytoplasmic and nuclear condensation and DNA cleavage. An early event in this process includes the translocation of phosphatidylserine from the inner side of the plasma membrane to its exposed outer surface. The phospholipid-binding Annexin V is a 35-36kDa, calcium-dependent protein with high affinity for phosphatidylserine which can be utilised for the detection of exposed phosphatidylserine using flow cytometry.

This early translocation of phophatidylserine occurs prior to the cessation of membrane integrity, which signals the later stages of cell death from either apoptosis or necrosis. For this reason, Annexin V is typically used in conjunction with a further stain such as propidium iodide (PI). In this experiment, Ethidium Homodimer III (EthD-III) was utilised to identify both early and late apoptotic cells as an alternative to PI. According to the manufacturer's information, EthD-III is a superior alternative to PI due to its greater affinity for DNA and higher fluorescence quantum yield.

Figure 49 shows that live cells with intact membranes exclude EthD-III, as opposed to the dead or damaged which are permeable and allow its entry. For this reason, viable cells are negative for both Annexin V and EthD-III, whilst early apoptotic cells are Annexin V positive but EthD-III negative. Late apoptotic or dead cells may stain positively for both Annexin V and EthD-III, whilst necrotic cells are identified by EthD-III positivity in isolation.

For Annexin V experiments, a minimum of 30,000 events were recorded per condition, with P1 cells excluded in all experiments. On the scatter plots, Annexin V conjugated with fluorescein isothiocyante (FITC) is represented on the Y-axis, with the bright red staining of Ethidium Homodimer III represented on the x-axis. For each scatter plot, two histograms representing both stains can also be seen.

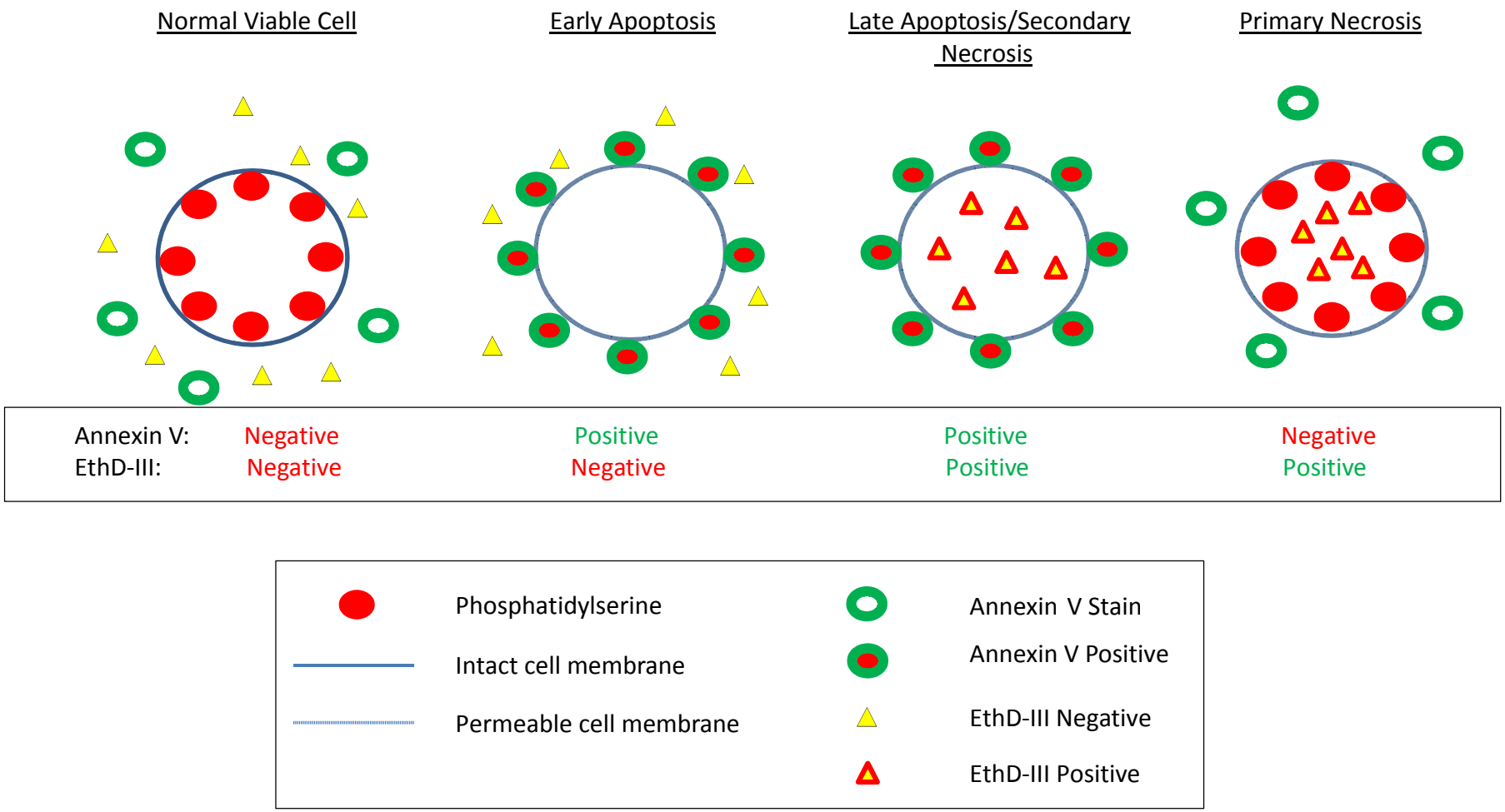

Figure 49: Annexin V apoptosis and necrosis assay with propidium iodide staining

Viable cells will be negative for both Annexin V and EthD-III stains but will progress to become positive for both by the later stages of apoptosis and subsequent secondary necrosis. Cells staining solely for EthD-III may have died from primary necrosis.

Annexin V Results With Synergystic Drug Combinations

Untreated Control

With the untreated control, both the Annexin V and EthD-III histograms display a single, normally distributed population of MiaPaCa-2 cells in the centre of the graph. These populations were gated as negative for both stains for the purpose of comparing histograms between conditions. On this control scatter plot, a small number of cells is in the right upper quadrant is seen, representing a proportion of cells in various stages of apoptosis or necrosis, as can be expected in any colony of cells.

The remaining Annexin V experiments discussed below are based on and represent the red numbered points along the line of synergy on the graph seen in Figure 48.

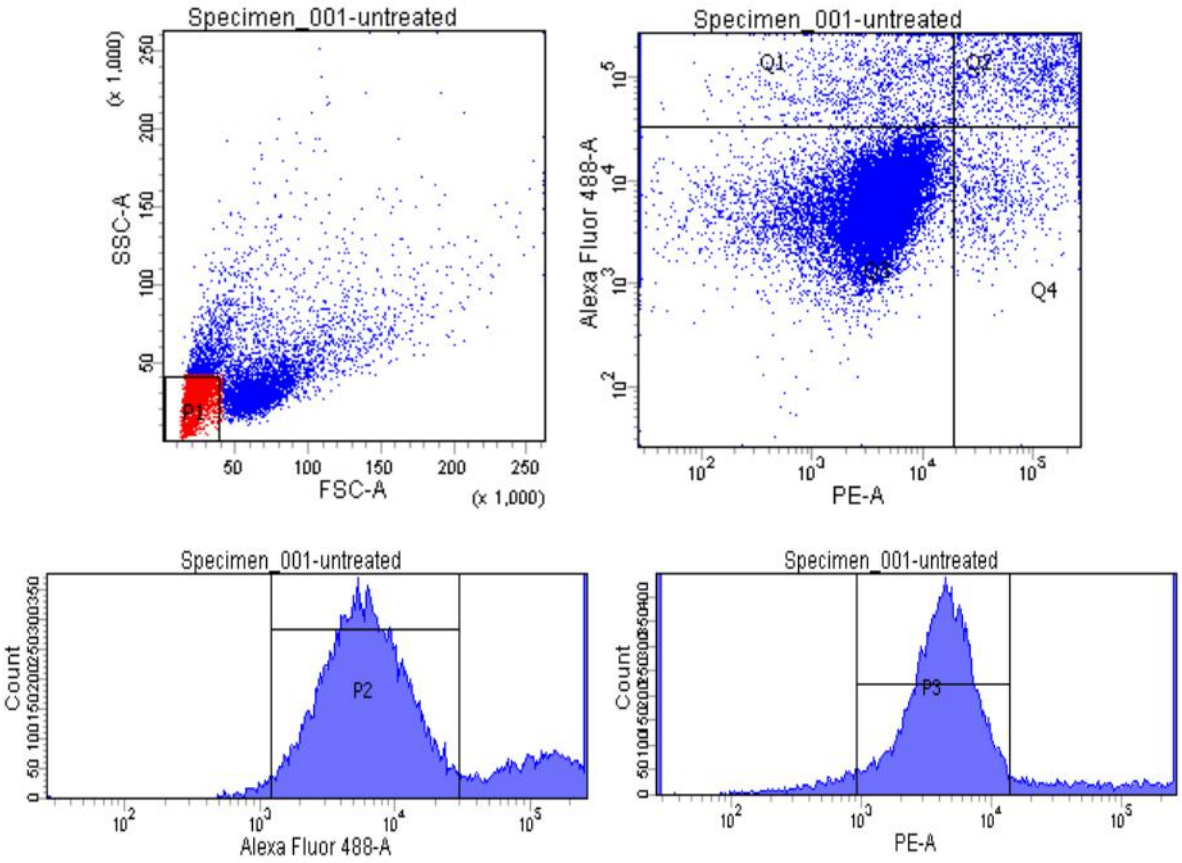

Figure 50: Annexin V assay of MiaPaCa-2 cells under control conditions
Histograms for both Annexin V (bottom left) and EthD-III stains (bottom right) show a largely normally distributed pattern. This is reflected in a single large cellular population in the scatter plot, with only very few dead/dying cells as expected in any cell population.

1) 40nM Gemcitabine 0nM BI 6727 (30 000 events)

There is a definite shift towards increased positive staining on the Annexin V histogram. However, by comparison there is a dramatic increase in EthD-III positivity with the majority of cells staining positively. Though only two very distinct cell populations are visible on the scatter graph, based on the histograms, the cell population on the right of the scatter plot can be further subdivided into two further populations. In the right upper quadrant a large number of cells are seen in late apoptosis or necrosis and have stained positively for both Annexin V and EthD-III (Q2). The second population, located in the right lower quadrant (Q4) have stained positively solely for EthD-III and is therefore likely to represent primary necrotic cells. Though these cells are not also positive for Annexin V stain, it is clear is that this population of cells have had their cellular membrane compromised as the red-fluorescent EthD-III stain binds to intracellular nucleic acid.

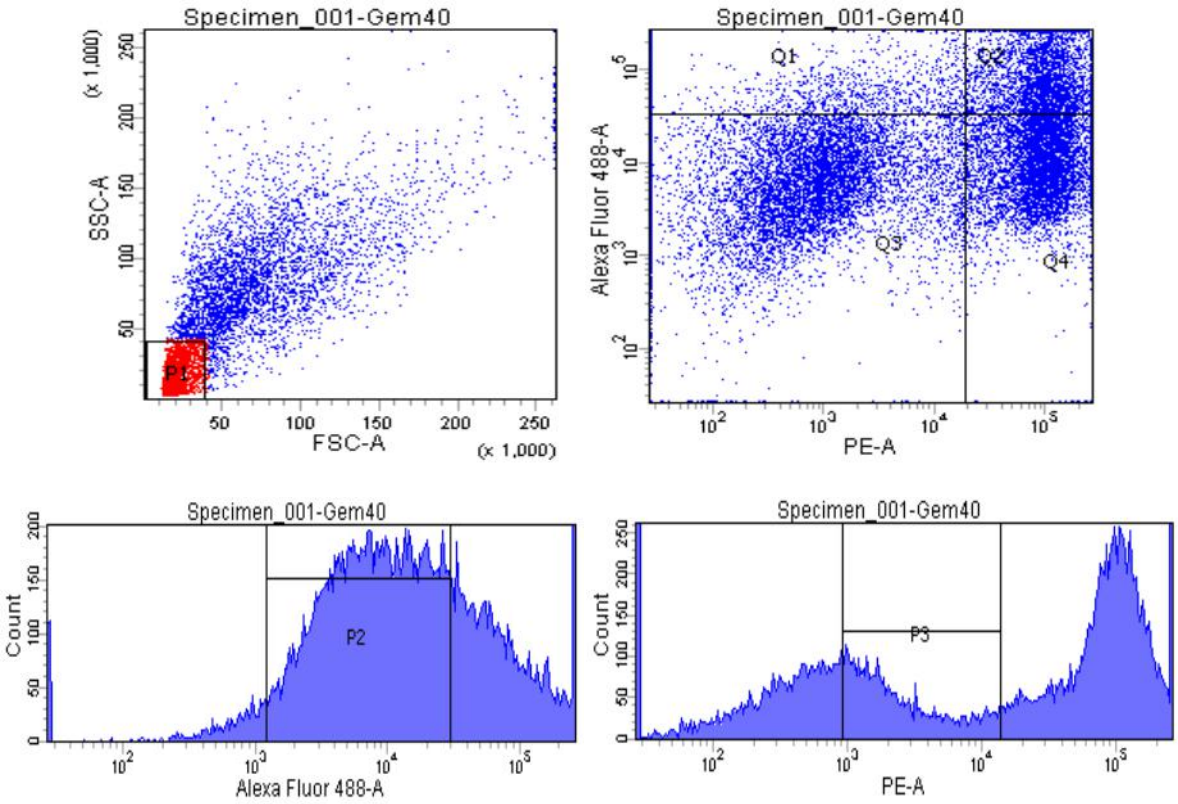

Figure 51: Annexin V assay of MiaPaCa-2 cells left untreated for 24 hours, followed by 40nM of gemcitabine for 72 hours

Gemcitabine causes an increase in both Annexin V and EthD-III staining, represented by a right shift in both histograms. This is reflected in a significant cell population on the right side of the scatter plot with its upper pole indicative of dually stained calls and its lower pole indicating EthD-III stained cells only.

2) 25nM Gemcitabine 5nM BI 6727 (30 000 events)

Though still present, a lesser shift towards positive Annexin V staining is again seen in comparison to with 40nM gemcitabine alone. With regards to EthD-III staining, we see two separate cell populations represented by two peaks, one marginally shifted to the left of the control peak, and the second shifted dramatically to the right compared to the control, indicative of a pronounced positive EthD-III staining. The left shift may represent nuclear changes (possibly resulting from spindle malformation early in G2 preventing nuclear membrane breakdown) causing exclusion of the DNA binding agent or it may represent chromatin chages induced by gemcitabine, although both these hypotheses are highly speculative.

Again two distinct cell populations are seen on the scatter plot, with the right sided population being loaded primarily towards the lower as opposed to the upper quadrant. In comparison to 40nM of gemcitabine in isolation, this data suggest that though a proportion of cells treated with this drug combination undergoes apoptosis, the majority of cell death seems to be as a result of primary necrosis (Q4).

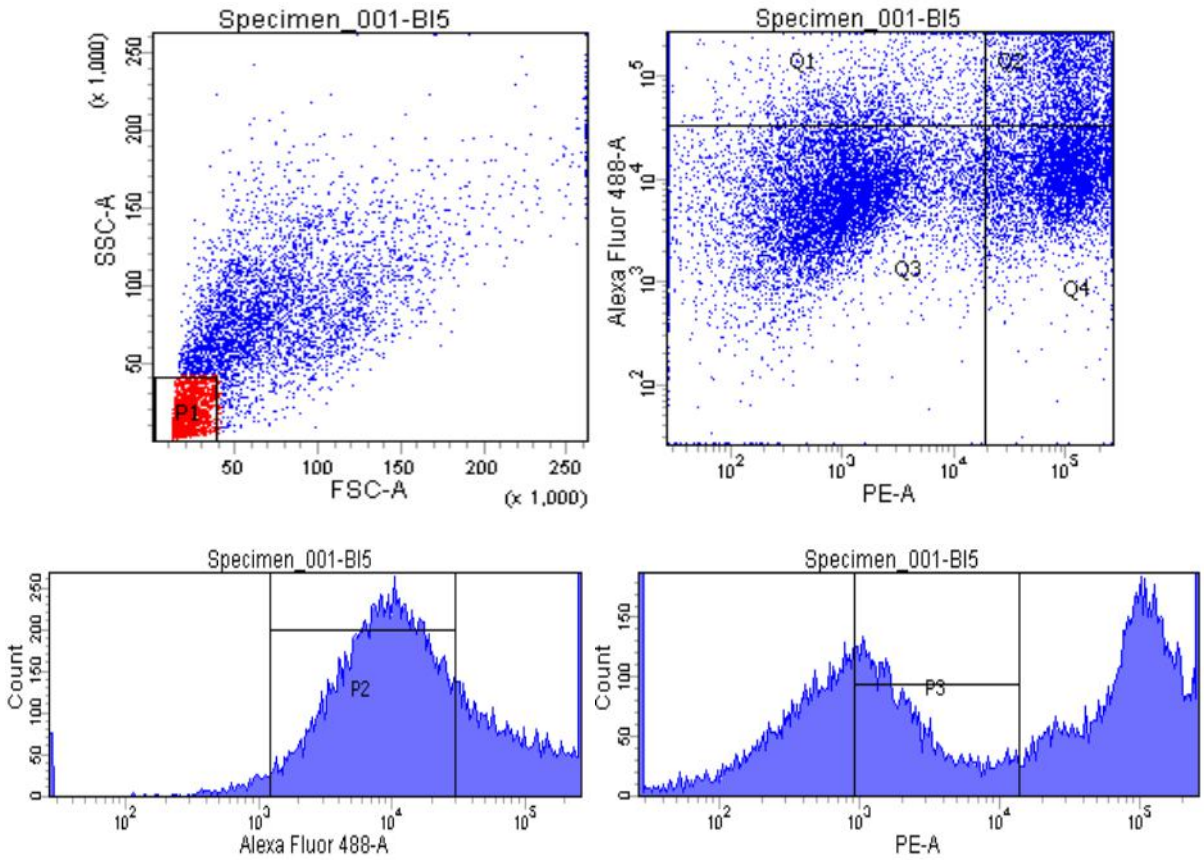

Figure 52: Annexin V assay of MiaPaCa-2 cells treated with 5nM of BI 6727 for 24 hours, followed by 5nM BI 6727 and 25nM gemcitabine for 72 hours

Though less than with 40nM of gemcitabine, a right shift is seen in Annexin V positivity compared to the untreated control. The mismatch betwween the EthD-III and Annexin V histograms suggests that the main mode of death may be primary necrosis.

3) 20nM Gemcitabine 10nM BI 6727 (30 000 events)

The right shift in Annexin V staining is minimal in comparison to an untreated control and is certainly less pronounced than the two previous treatments discussed. The bi-peaked pattern seen with EthD-III staining is very similar to that seen with 25nM gemcitabine and 5nM BI 6727. Graphically, this suggests a similar pattern of MiaPaCa-2 cell distribution as that seen with the previous treatment, though the comparative drop in positive Annexin V staining (Q1 and Q2) suggests that a greater number of cells are dying of a primary necrotic pathway as opposed to apoptosis with possible subsequent secondary necrosis.

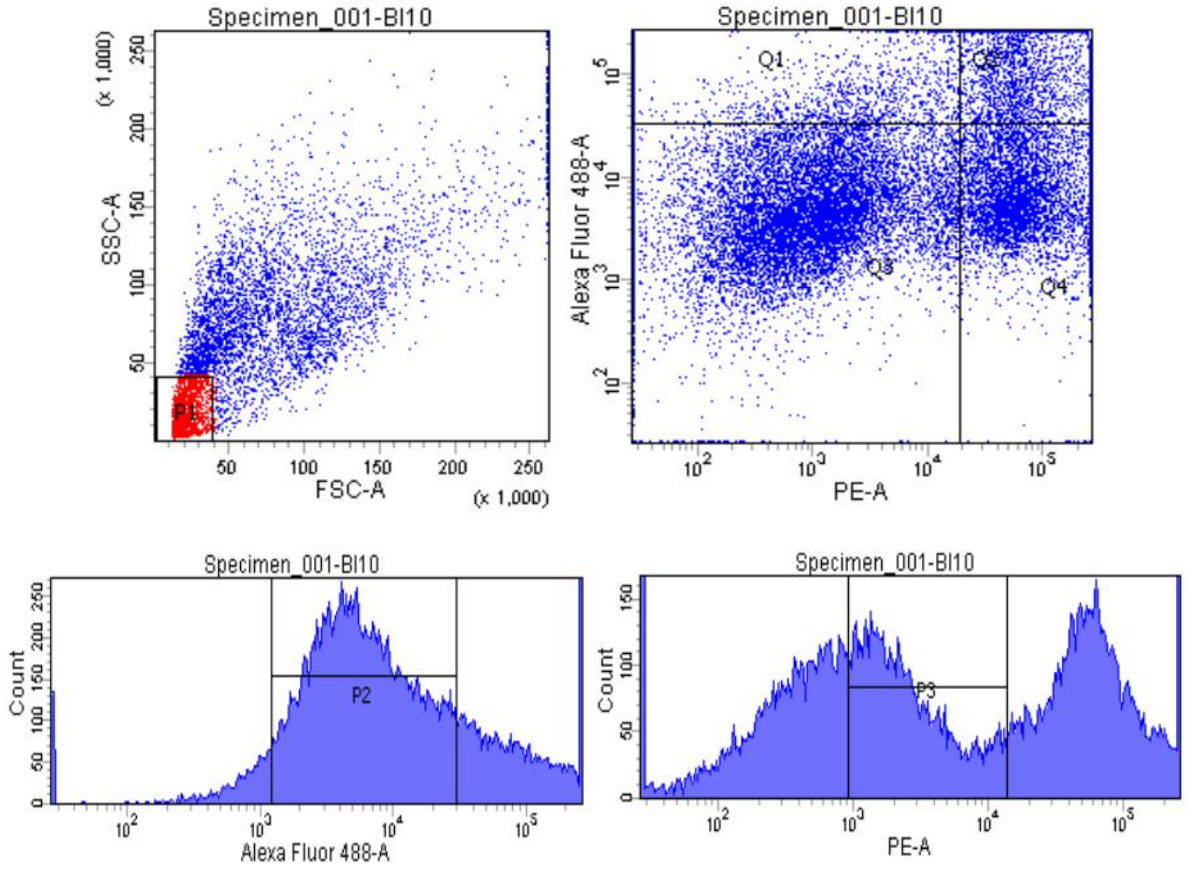

Figure 53: Annexin V assay of MiaPaCa-2 cells treated with 10nM BI 6727 for 24 hours, followed by 10nM BI 6727 and 20nM gemcitabine for 72 hours

Though the right shift in Annexin V staining is slightly decreased compared to the previous condition discussed, the twin peaked appearance in EthD-III staining is similar. The right-sided population on the scatter plot is again loaded at its inferior end suggestive of primary necrosis, as opposed to apoptosis and subsequent secondary necrosis.

4) 10nM Gemcitabine 25nM BI 6727 (30 000 events)

Interestingly, this is the only Annexin V histogram in this experiment that demonstrates a twin-peaked appearance. The fact that the EthD-III histogram also demonstrates two peaks, with the rightmost indicating positivity, has resulted in two very distinct cell populations on the scatter graph. Discounting the main Annexin V negative/EthD-III negative population, the well-defined second population accounts for the vast majority of the remaining cells and is located in the contrasting bi-positive sector. This indicates that these MiaPaCa-2 cells are either in late apoptosis or secondary necrosis. Interestingly, very few cells are seen to be in early apoptosis (solely Annexin V positive, Q1) or having died of primary necrosis (solely Eth-III positive, Q4).

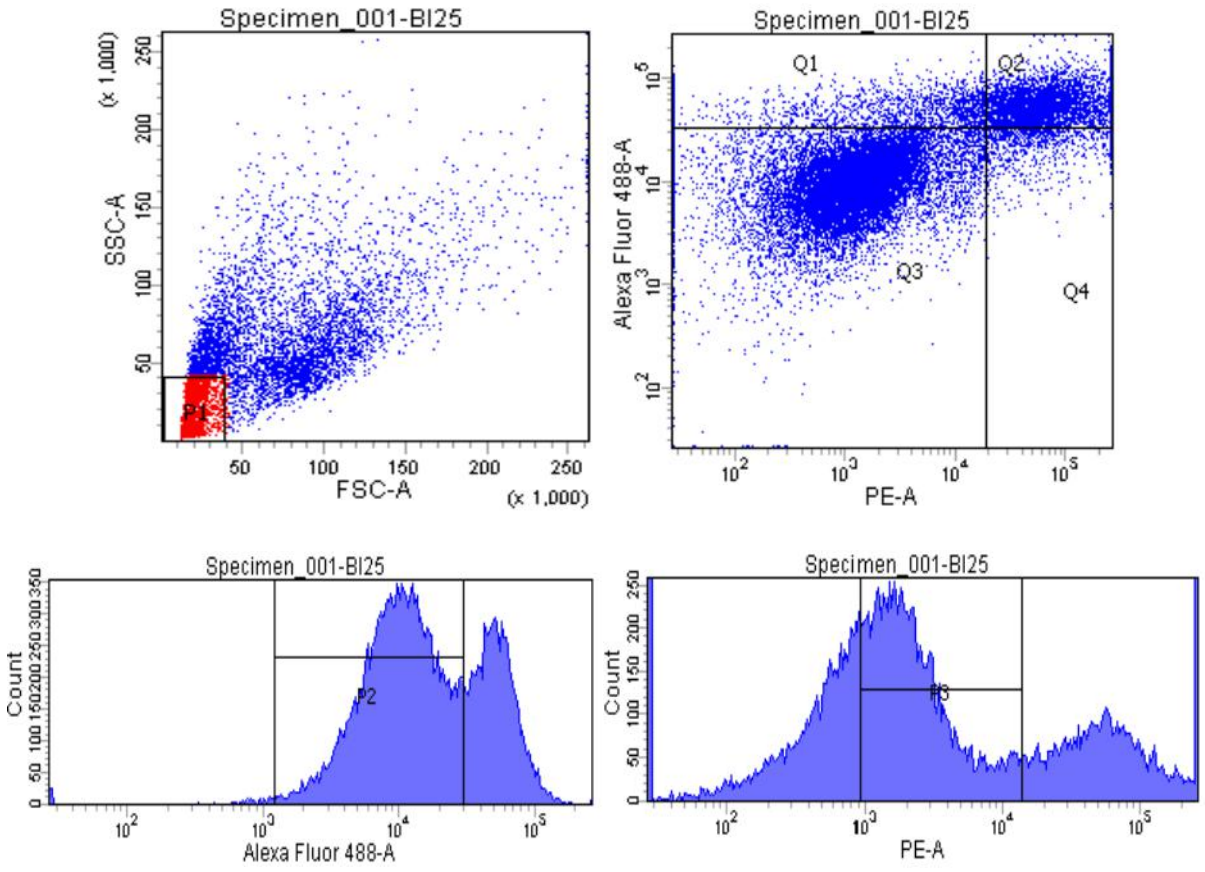

Figure 54: Annexin V assay of MiaPaCa-2 cells treated with 25nM BI 6727 for 24 hours, followed by 25nM BI 6727 and 10nM gemcitabine for 72 hours

Two distinct cell populations are seen on the scatter plot, with the population based in the right upper quadrant indicating cells staining positively for both Annexin V and EthD-III, indicating cells in late apoptosis. Very few cells seem to stain for only a single stain.

5) 5nM Gemcitabine 50nM BI 6727 (30 000 events)

A strong right shift is again seen with the Annexin V histogram, though this is represented by a single, as opposed to a twin peak as seen previously. Looking across each of the Annexin V histograms, it seems that an increase in BI 6727 and fall in gemcitabine concentrations respectively causes a greater right shift in the histogram's peak, though this only applies when both drugs are utilised in combination. In contrast, the ever-present bi-peaked appearance seen across the EthD-III histograms reveals the constant location of the negatively-stained left-shifted peak. The right-shifted EthD-III-positive peak decreases in size with a fall in gemcitabine concentration and increasing PLK1 inhibition. This fall in EthD-III staining has resulted in a scatter plot which has fewer cells on its right side. However, the global right shift in the single-peaked Annexin V histogram has mobilized the main cell population upwards, indicating a strong presence in early apoptosis.

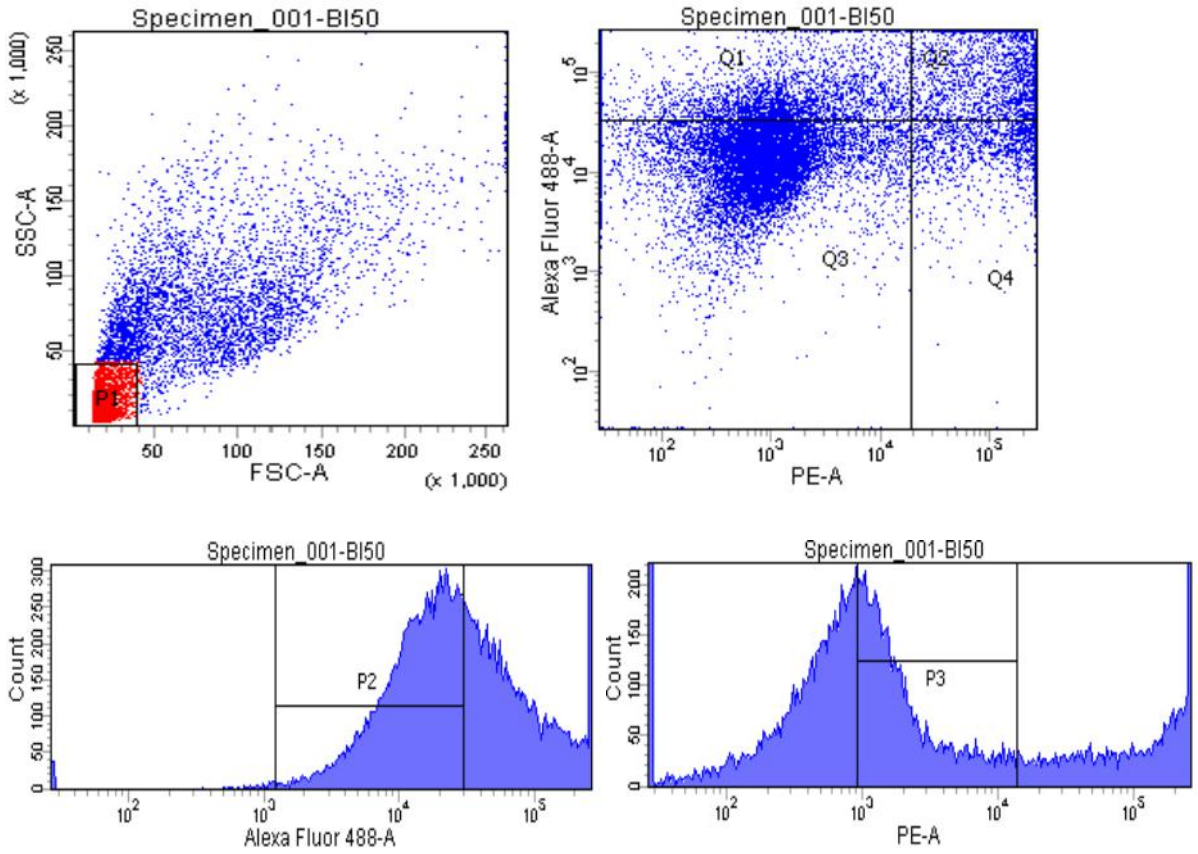

Figure 55: Annexin V assay of MiaPaCa-2 cells treated with 50nM BI 6727 for 24 hours, followed by 50nM BI 6727 and 5nM gemcitabine for 72 hours

A strong right shift is seen with the Annexin V histogram, which is not reflected with EthD-III. The result is the main cell population moving upwards on the scatter graph, suggesting that a significant number of these cells are in early apoptosis.

6) 0nM Gemcitabine 75nM BI 6727 (54 000 events)

For some reason, nearly twice the number of events was recorded under this condition compared to the other drug combinations and this warrants taking into consideration when visually comparing scatter plots. In comparison to the untreated control, the Annexin V histogram shows a definite right shift, similar to that seen with 25nM gemcitabine and 5nM BI 6727. In contrast the EthD-III histogram is identical in appearance to that seen under control conditions. The resulting scatter plot's most striking finding is that the main cell population has moved north on the y-axis, indicative of the increased Annexin V positivity suggesting early apoptosis.

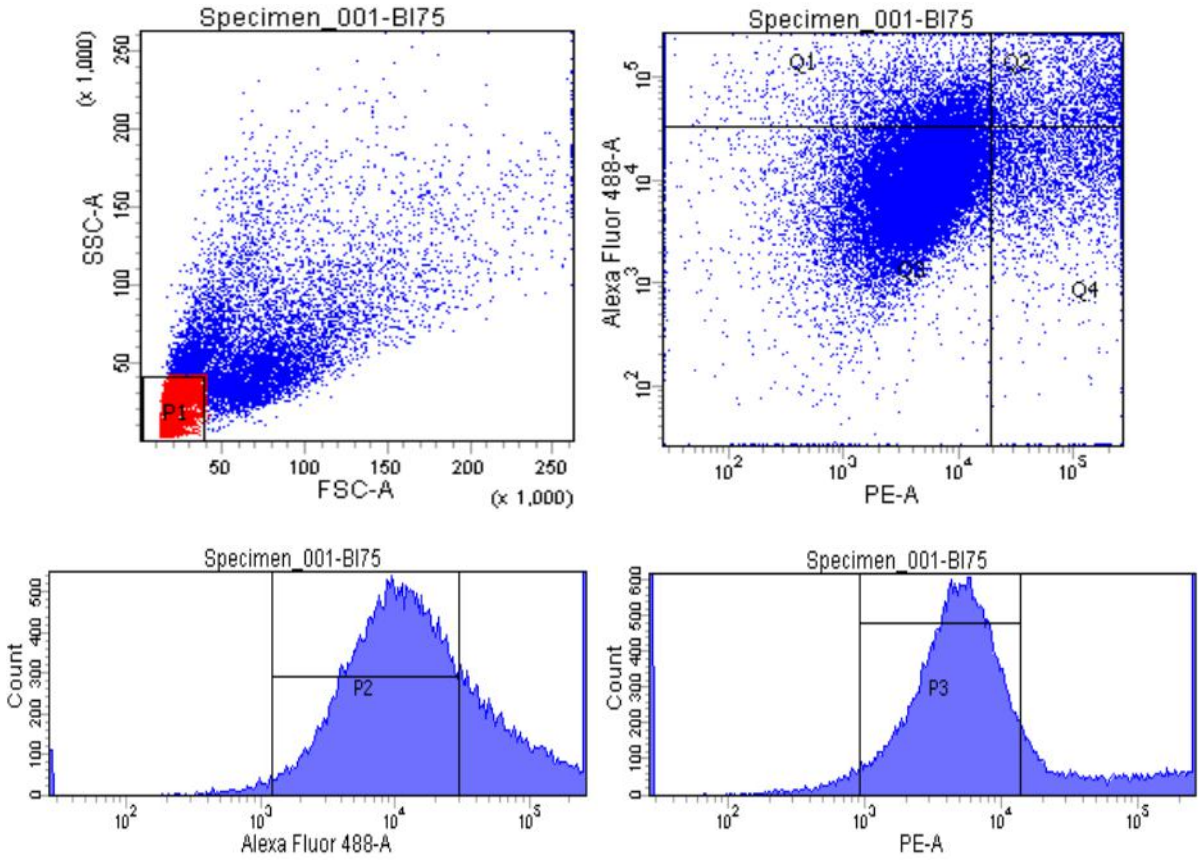

Figure 56: Annexin assay of MiaPaCa-2 cells treated with 75nM BI 6727 for 24 hours, followed by a further 75nM of BI 6727 for 72 hours

An increase is seen in positive Annexin V staining in comparison to untreated control, though this is not the case with EthD-III as evident on the histogram. This is reflected in the scatter graph's main cell population migrating upwards and not particularly rightwards, indicative ofearly apoptosis.

Table 19: Sectoral cell numbers for annexin apoptosis and necrosis assays displayed in Figure 50 to Figure 56

Condition	Total Events	Not P1 (%)	P2	P3	Q1 (%) Annexin V	Q2 (%) Dual	Q3 (%) Negative	Q4 (%) EthD-III
Untreated Control	30 000	21228 (70.8)	16567	15209	7.3	12.2	77	3.4
40nM Gemcitabine/0nM BI 6727	30 000	19771 (65.9)	13032	3707	9.8	18.2	43.4	28.6
25nM Gemcitabine/5nM BI 6727	30 000	19974 (66.6)	13656	4481	11.8	15.2	45.2	27.8
20nM Gemcitabine/10nM BI 6727	30 000	21045 (70.2)	14948	5626	10.4	10.8	55.3	23.5
10nM Gemcitabine/25nM BI 6727	30 000	22786 (76)	15618	9716	10.3	18.7	67.1	3.9
5nM Gemcitabine/50nM BI 6727	30 000	20490 (68.3)	11488	5718	24.2	16.5	50.8	8.5
0nM Gemcitabine/75nM BI 6727	54 000	39873 (72.8)	28688	25975	9.8	14.6	64.4	11.2

All quartiles (Q1-4) are expressed as percentage of total number of non-P1 cells. Q1 respresents Annexin V staining alone, Q4 Ethidium Homodimer III alone, Q3 gated as per control and Q2 as dual stained with both Annexin V and EthD-III.

Western Blotting for Cleaved Caspase-3

MiaPaCa-2 Cells Treated with Gemcitabine Monotherapy

The Western blot in Figure 57 shows that MiaPaCa-2 cells treated with the IC_{50} concentration of gemcitabine for 72 hours have caspase-3 cleavage indicative of apoptosis. Even though the signal is weak, this was achieved after a prolonged period of film exposure, with overnight exposure showing no improvement in band intensity. Though no cleaved caspase-3 is detected with cells treated at half the IC_{50} concentration of gemcitabine, this must be taken in the context of the very weak band seen at the IC_{50} concentration. Gemcitabine is widely acknowledged to induce apoptosis, and I would suggest that the evidence presented here is not strong enough to insist that 20nM of gemcitabine does not induce caspase-dependent apoptosis in MiaPaCa-2 cells.

Although it could be suggested that the beta-actin representative of the gemcitabine IC_{50} is overloaded I would argue that it is comparable to the BI 6727 IC_{50} equivalent and therefore it is sufficient to make a reasoned conclusion. I would concede that the untreated control actin is underloaded in comparison to the gemcitabine IC_{50}. However, a comparison between these two is also seen at the second experiment, from which I can confidently exclude any significant caspase-3 cleavage in untreated cells in comparison to those treated with 40nM of gemcitabine for 72 hours.

MiaPaCa-2 Cells Treated with BI 6727 Monotherapy

MiaPaCa-2 cells treated with concentrations of up to 75nM of BI 6727 for 72 hours show no evidence of caspase-3 cleavage, similar to the untreated control (Figure 57). BI 6727 has previously been described to induce polo-arrest and subsequently apoptosis in exposed cells with both cleaved caspase-3 and PARP documented as markers. Though the Western blot suggests the opposite, it must again be taken in the context of the very weak band attained by gemcitabine-treated cells, as the Western was run on the same gel, transferred, developed and exposed in the same experiment.

Cell proliferation evidence presented in Figure 25 shows that MiaPaCa-2 cell death is not definitively caused by BI 6727 at concentrations of under 250nM. At lower concentrations, a cytostatic effect is certainly evident, which may or may not be accompanied by apoptotic

cell death suggesting that caspase-3 cleavage may well not be occurring at the IC_{50} concentration and this western blot is an accurate representation of events.

Evidence to the contrary may be provided by the flow cytometry data in Table 17, which was undertaken with only adherent cells and therefore may be of limited use in helping dissect the result of this Western blot. However, it suggests that the induction of G2 arrest is most prominent within the first 8-24 hours of exposure, with the number of cells with abnormal DNA content peaking at 24-48 hours (Figure 31, Figure **32**, Figure **33** and Figure **34**). Therefore, there is definitive evidence of cell death, though there are two caveats to this – firstly, the cause of cell death is yet unproven and secondly, this predominantly occurs earlier than the 72 hour time point from which this Western blot is based. Whether the dead adherent cells seen at 24-48 hours during flow cytometry would be floating in the media at the 72 hour mark is unclear. Also unknown is whether caspase-3 was ever activated or moreso even peaked at this earlier time and has therefore been missed on the Western undertaken. These questions could potentially have been answered by including a high (>1000nM) concentration of BI 6727 in the experiment, in addition to including a greater variety of time points such as 8, 24 and 48 hours.

The other notable factor to consider from this experiment is that both adherent and floating cells were utilised to create the cell lysate. This may have a significant bearing on the conclusions drawn when comparing both monotherapies, as the ratio of live to dead cells may vary between the two drugs. As an MTS assay (utilised to determine the respective drug IC_{50}s) is based solely on determining an equal number of live cells, the number of dead cells may vary drastically between treatments. Therefore any disparity in the ratio of live to dead cells would clearly alter the cleaved caspase-3 band intensity when comparing an equal protein yield from their respective lysates. This potential deficiency could be overcome by utilising dead cells alone to formulate the lysates for this experiment.

MiaPaCa-2 Cells Pre-Treated with BI 6727 Followed by BI 6727 and Gemcitabine Combination Therapy

Isobolar analyses have previously shown that treating MiaPaCa-2 cells with BI 6727 for 24 hours prior to combination therapy with both BI 6727 and gemcitabine is synergistic (Figure 47). Annexin V apoptosis and necrosis data from multiple points on the curve of synergy

(Figure 48) has shown large quantities of cells staining positively for either Annexin V, EthD-III, or both, indicative of cell death.

Western blotting for cleaved caspsase-3 was undertaken with cell lysate obtained from those treated identically to that included in the Annexin V experiments. Compared to the Western blot undertaken with drug monotherapy, MiaPaCa-2 cells treated with 40nM of gemcitabine has this time produced a higher intensity band, despite undergoing the same experiment protocol. Taking into account the absence of a signal at 19kDa with untreated control, it can be concluded that exposing MiaPaCa-2 cells to gemcitabine monotherapy at the IC_{50} concentration will produce caspase-dependent apoptosis.

Moving from left to right, a comparatively very weak band is seen at 19kDa with the next drug combination of 5nM BI 6727 followed by its combination with 25nM of gemcitabine. When observing its equivalent Annexin V scatter plot (Figure 52), it can be argued that this comparatively major drop in band intensity does not equate to the rather lesser fall in the proportion of non-viable cells.

Further along to the right, where cells were treated with 25nM of BI 6727 followed by its combination with 10nM gemcitabine, there is a complete absence of any cleaved caspase-3 activity. Once again, by inspecting its related Annexin V scatter plot in Figure 54, it is difficult to comprehend how such an evidently large proportion of cells staining positively for both Annexin V and EthD-III could be undergoing caspase-dependent apoptosis yet not show any sign of cleaved caspase-3 on this Western blot. It must then be considered that the synergy demonstrated by combining the novel PLK1 inhibitor, BI 6727 with gemcitabine is not entirely due to caspase-dependent apoptosis and other lethal pathways may be in effect.

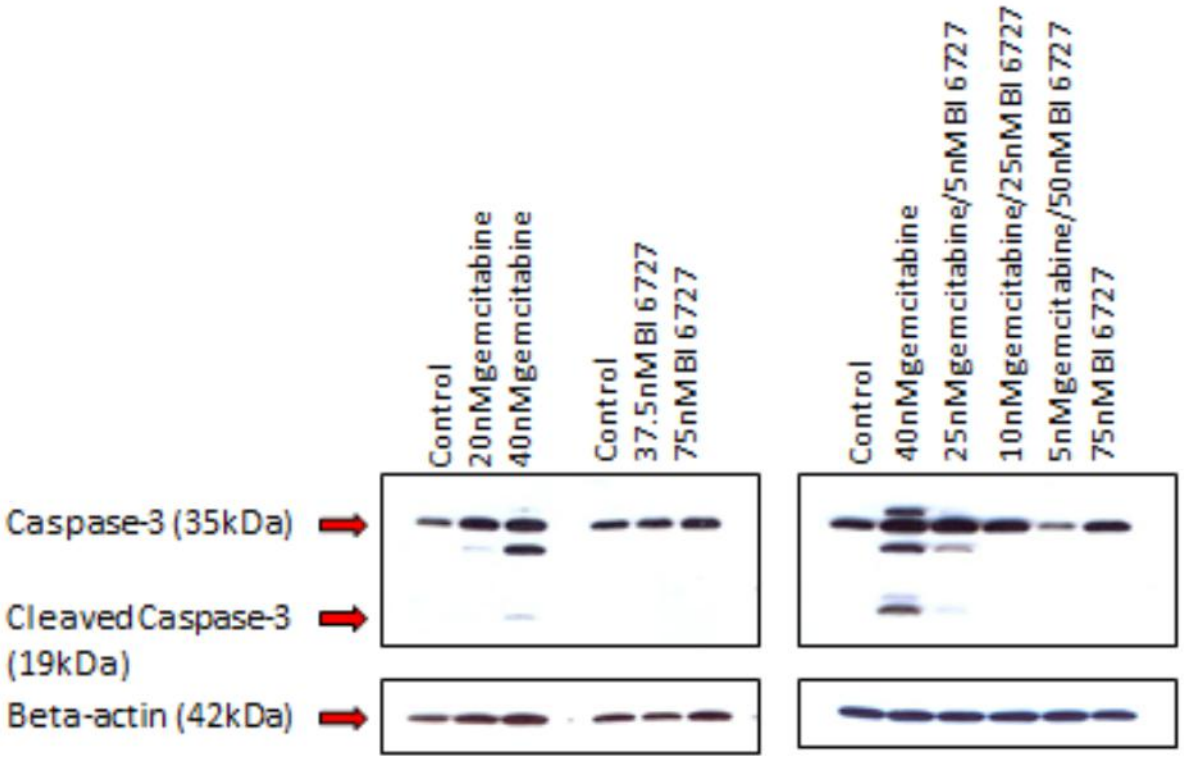

Figure 57: Western Blot for cleaved caspase-3 in MiaPaCa-2 cells treated with BI 6727 and gemcitabine monotherapy and in combination
Evidence of Caspase-3 cleavage, indicative of apoptosis is seen with gemcitabine but not BI 6727 monotherapy. When MiaPaCa-2 cells are treated with BI 6727 prior to combination therapy, which has previously been shown to be synergistic, cleaved caspases-3 is not seen, suggesting an alternative mode of cell death. Both experiments were independently performed and cannot therefore be used for direct comparative purposes.

Chapter 4 - Discussion

Summary of Main Findings

On commencing this project, there were specific objectives including establishing the IC_{50} concentrations of BI 6727 and gemcitabine in pancreatic cancer cell lines *in vitro.* The IC_{50} concentrations of both drugs were established across a range of pancreatic cell lines: Suit-2, MiaPaCa-2, Panc-1 and BxPC-3. Together, these cell lines carry the commonest known mutations in pancreatic cancer: including *KRAS, CDKN2A, TP53 and DPC4*.

Utilised as monotherapy, BI 6727 has been shown to be effective against a variety of pancreatic cancer cell lines at low nanomolar concentrations and reduces cell numbers as early as 24 hours in comparison to an untreated control. However, after 72 hours of exposure to lower concentrations (<50nM) of BI 6727, this response seems to be transient, with pancreatic cancer cells seeming to recover somewhat. Exposure to higher concentrations (>250nM), maintains viable pancreatic cell numbers at below 20% of that of untreated control.

Further proliferation assays with MiaPaCa-2 cells suggest that logarithmic cell division continues at the lower concentrations of BI 6727, though this is reduced in comparison to control. Flow cytometry of only adherent/viable MiaPaCa-2 cells treated with the IC_{50} concentration (75nM) demonstrated an increase in the proportion of G2/M cells, particularly during the first 24 hours of exposure. Further data support these cells maintaining the ability to duplicate their DNA but being unable to divide into two daughter cells, suggesting a mainly cytostatic mechanism. At concentrations of 100nM, viable cell numbers barely increase over 72 hours, with cell numbers falling with continued exposure to concentrations in excess of this. This is indicative of cytotoxicity, possibly as a result of polo arrest and apoptosis.

Gemcitabine monotherapy is already widely acknowledged to be effective against pancreatic cancer cells, which was reflected in this project's results with IC_{50} concentrations ranging 11-34nM. The nucleoside analogue's effects were limited within the first 24 hours due to its need to be incorporated in cellular DNA to be effective, with its toxic properties coming to prominence at later time points. This is demonstrated in a proliferation assay of

treated MiaPaCa-2 cells, with viable cell numbers diminishing over time at concentrations in excess of 50nM. Flow cytometry of treated adherent/viable MiaPaCa-2 cells showed their accumulation in S-phase, reflecting their inability to synthesise DNA. Evidence of cell death by apoptosis was later demonstrated by Western blotting.

The second objective was to establish an optimal drug sequencing and combination regime for BI 6727 and gemcitabine in pancreatic cancer cells *in vitro,* which was undertaken in MiaPaCa-2 cells. It was hypothesised that combining both a PLK1 inhibitor and gemcitabine would be antagonistic given that gemcitabine requires dividing cells to be at its most effective. However, an initial isobolar analysis demonstrated that combining these drugs resulted in an additive effect at worst.

This resulted in further isobolar experiments and by varying the addition of BI 6727 and gemcitabine, a hierarchy of sequential drug combination was clearly demonstrated. The preferred drug administration sequence, in order of superiority was shown to be:

1. Gemcitabine followed by more gemcitabine (most effective)
2. BI 6727 followed by gemcitabine
3. Gemcitabine followed by BI 6727
4. BI 6727 followed by more BI 6727 (least effective)

By taking this a step further MiaPaCa-2 cells were treated with BI 6727 or gemcitabine for 24 hours, followed by a combination of both drugs for 72 hours. Pretreatment with gemcitabine resulted in a isobolar graph similar to combination therapy alone (additive) with BI 6727 pretreatment showing strong evidence of synergy.

The final objective of this project was to identify the mode of cell death when BI 6727 and gemcitabine are utilised in this synergistic combination in pancreatic cancer cells. This process was undertaken with a combination of Annexin V apoptosis and necrosis assay and Western blotting. Annexin V assay of BI 6727-treated MiaPaCa-2 cells suggested an increase in the number of cells in early apoptosis, with Western blotting excluding the presence of cleaved caspase-3. With gemcitabine monotherapy, MiaPaCa-2 cells increasingly stained positively for Annexin V, EthD-III and both together. This indicates cell death by a combination of both primary necrosis and apoptosis, with the presence of cleaved caspase-3 confirmed with Western blotting.

When treating MiaPaCa-2 cells with various synergistic drug combinations, only one combination (25nM gemcitabine/5nM BI 6727) shows any evidence of cleaved caspase-3 with Western blotting. However, the level seems negligible in comparison with gemcitabine monotherapy.

When assessing all the combination therapy Annexin V assays, it is noticeable that increasing the BI 6727 concentration and a reducing the gemcitabine concentration generally seems to cause an increase in Annexin V staining. This is exemplified by a right shift on histograms and a north shift of the main cell population on the scatter plot. In contrast, by combining BI 6727 and gemcitabine, a fall in the latter's concentration, coupled with increasing PLK1 inhibition causes a left shift in the EthD-III histogram indicating a fall in positively stained cells. Coupled together, this alteration in the concentrations of combination therapy broadly causes a decrease in dual-stained cells and a global shift of the main cell population towards early apoptosis. Gemcitabine monotherapy, which exhibited the strong presence of cleaved caspase-3 has a large cellular population on the right side of its scatter plot, indicative of late apoptotic and necrotic cells. With combination therapy, the rather modest fall in cell numbers in this representative population seems disproportionate to the dramatic absence of cleaved-caspase-3 expression, suggesting an alternative method of cell death to caspase-dependent apoptosis.

Potential Mechanism of Action for Synergy

This work has identified evidence of synergy when utilising the ATP-competitive PLK1 inhibitor BI 6727 and the antimetabolite gemcitabine. Given that gemcitabine is a drug that incorporates its metabolites into a cell's DNA in S-phase, how can the drug work synergistically with a drug that arrests cells in G2/M? The experiments undertaken during this work merely shows the end result of combining both drugs and very little about the underlying mechanism and interaction between the two. For this reason, potential theories are speculative at best. What is useful however, is that evidence has been published which may help shed light on this conundrum.

Zhang *et al*[530] utilised DMTC, an alternative ATP-competitive PLK1 inhibitor in combination with gemcitabine. Interestingly, utilising low concentrations of both drugs resulted in synergy, with higher concentrations being antagonistic. It is already known that PKL1 is not essential for mitotic entry in the normal, healthy functioning cell. However, when the DNA

damage checkpoint is activated, as would be the case with gemcitabine-treated cells, its presence becomes crucial if mitosis is to be entered. Zhang suggests that as gemcitabine induces the DNA damage checkpoint, continued PKL1 inhibition by DMTC ensures that this checkpoint is not overcome. As these cells fail to enter mitosis they become apoptotic.

Li *et al*[531] used biochemical fractionation and RNA interference to show that PKL1 is required for both G1/S and G2/M phases. However the level of PLK1 required for G1/S transition was extremely low in comparison to the maximal activity necessary for cells to complete mitosis. In addition, it was also demonstrated that PLK1 inhibition significantly reduced the rate of DNA synthesis. Logically, it must be considered whether reducing the rate of DNA synthesis would either enhance the efficacy of gemcitabine by allowing more time for its metabolites to become incorporated, or disable its effects i.e. less DNA synthesis equating to less gemcitabine being incorporated. Interestingly, the ATP-competitive PKL1 inhibitor GSK461364A demonstrated synergy with gemcitabine, both *in vitro* in a variety of pancreatic cancer cells and *in vivo* in a Panc-1-derived orthotopic xenograft model.

Aurora A, along with Bora are the main activating kinases of PKL1. Zhou[532] observed an Aurora A kinase inhibitor in combination with gemcitabine in bladder cancer. Interestingly, concurrent therapy was additive/antagonistic, whereas sequential addition (Aurora A inhibitor first) became synergistic. It is suggested that the induction of spindle checkpoint dysfunction by Aurora A inhibition potentiates gemcitabine's ability to arrest the cell cycle. Given PKL1's critical role in mitosis and spindle assembly, it is of interest that the secondary effects of Aurora A inhibition, such as the downregulation of PLK1 activity, was not investigated. Could the lack of PLK1 activity be a factor in the synergy demonstrated?

As synergy is demonstrated between BI 6727 and gemcitabine, both drugs' mechanisms of action must cross paths. The question is does gemcitabine enhance the effects of PKL1 inhibition, vice versa, or a combination of the two? Does a tumour actively expressing PLK1 play a part in a pathway that eventually develops gemcitabine resistance? What effect does PLK1 have on thymidylate synthase, ribonucleotide reductase or DNA polymerase? The full effects of gemcitabine's effects on the subcellular localisation of PLK1 are also yet to be established, though it has been previously suggested that this could also be tumour dependent[531]. Gemcitabine metabolites could potentially increase the amount of a particular PBD ligand and therefore attract PKL1 to a particular cellular location at a particular phase of the cell cycle. Alternatively, gemcitabine metabolites may enhance BI

6727 in inhibiting PKL1, for example negatively regulating its cellular localisation, thereby preventing its presence in its most efficient location. It is certainly plausible that gemcitabine's downstream protein targets inhibit the PBD domain's binding capacity, or alternatively, inhibit the priming of its target ligands (for example CDK1, MAPKs and ATR), thereby rendering the kinase domain inactive. And even in the event of the PBD functioning, it is possible that gemcitabine may be responsible in negatively regulating proteins responsible for the phosphorylation of residues Thr210 or Ser137 and hence the eventual activation of the kinase domain.

Given that gemcitabine pretreatment prior to combination therapy is inferior to BI 6727 pretreatment, the underlying reason for this must also be considered and speculated upon. At the cessation of that first 24 hours of gemcitabine monotherapy, it is evident that viable cell numbers will be largely unaffected. However an underlying cellular process would have taken place rendering the subsequent combination therapy less effective than had they been pretreated with BI 6727. This is likely to be a result of a combination of the direct drug-dependent changes within the cell's microenvironment, in addition to the specific phase of the cell cycle that these cells will be present at the time of treatment with combination therapy. It must therefore be speculated that gemcitabine and BI 6727 are best added when cells are in G2/M phase as opposed to S-phase.

Interestingly, it has previously been reported that cells synchronised in S phase are more susceptible to gemcitabine toxicity[533]. It is suggested that a low initial dose of gemcitabine acts as a primer, synchronising cells is S phase and therefore increasing the efficacy of any subsequent dose. To the contrary, a high initial dose completely arrests the cell cycle, but without the lethality thereby decreasing the drug efficacy. This theory may explain the synergy shown in this research's isobolar analysis when utilising two consecutive doses of gemcitabine.

Evidence presented in this work suggests that over 50% cells will be in G2/M phase following 24 hours of treatment by BI 6727, the point at which further BI 6727 will be added alongside gemcitabine to demonstrate synergy. If we consider the 'priming' theory of gemcitabine described above, it would seem that the opposite applies to BI 6727 monotherapy with two consecutive doses being antagonistic. However, the inclusion of gemcitabine transforming this into synergy suggests that the lethal effects of gemcitabine become amplified in PKL1-inhibited G2/M-arrested cells. In my opinion, the mechanism of

synergy is multifactorial and may even differ considerably as the concentrations of both drugs are altered. For example, there may be elements of prolonged cellular stress due to the early effects of PKL1 inhibition and the later effects of gemcitabine. The inability of PKL1 inhibited cells to recover from gemcitabine induced DNA-damage checkpoint activation is almost certain to play a part. This may be in addition to PKL1-induced cytostasis and gemcitabine-induced caspase-dependent apoptosis. With regards to the mechanism of cell death in this research, there seems to be more than a single lethal pathway in play. Their exact nature cannot be fully explained, but it is reasonable to speculate that there may be a truncated form of apoptosis leading to necrotic cell death (a form of mitotic catastrophe).

Clinical Relevance of Main Findings

There is ample evidence to show that only rarely can pancreatic cancer be cured by resection alone and that adjuvant therapy provides a significant survival advantage. In the palliative setting, chemotherapy is shown to result in a small yet significant increase in life expectancy in comparison to best supportive care. Though significant advances have been made over the past quarter of a century, the long-term outlook for pancreatic cancer patients remains poor, particularly when compared with other gastrointestinal malignant diseases.

There are a multitude of tumour related factors that make pancreatic cancer such a formidable disease to overcome. Early undetectable micrometastases, the presence of a dense peri-tumoural stroma unlike other cancers and resistance to chemotherapy are just a few of those challenges. The fact that the majority of pancreatic tumours develop resistance to gemcitabine is a particular enigma for researchers developing appropriate alternative anti-cancer agents.

In addition to the factors listed above, the vast heterogeneity between tumours determines that it has become increasingly clear that ‘one size fits all’ chemotherapy is largely ineffective and in an ideal world, personalised therapy tailored to each individual tumour would be possible. However, this will not only require the identification of a biomarker for each cancer-triggering pathway and mutation, but also the development of a drug to counteract each facet. Even with the astonishing progress made in recent years, this will almost certainly remain a puzzle for the foreseeable future.

Developing novel drugs is a costly and laborious process, which more often than not ends in failure. Though it is essential that novel therapies are continually developed, instead of confining these 'failed' monotherapies to the well populated drug graveyard, their combination with current gold-standard drugs is an area of great potential for researchers. Only very recently, ESPAC-4 presented their findings on adjuvant combination therapy with gemcitabine and capecitabine following pancreatic cancer resection. Median and 5-year survival were shown to be significantly improved with combination therapy compared with gemcitabine monotherapy (Median survival 28 vs. 25.5 months, 5-year survival 28.8% vs. 16.3%)[534]. This supports the notion that combining drugs may be the way forward until further breakthroughs are made in developing novel and more targeted chemotherapeutic agents.

The main question that has arisen from this work is can PLK1 inhibition delay or avert gemcitabine resistance? Though the results from this work suggest this may be possible, it may be more credible to speculate that combining BI 6727 and gemcitabine will only be beneficial in a subset of patients with tumours that overexpress PLK1. Until pancreatic tumours are screened for PLK1 expression prior to the commencement of chemotherapy, its true potential may remain may remain undiscovered.

Limitations and Suggestions for Further Work

Be it academic or otherwise, the termination of any task or project provides an opportunity for reflection on what may have been done differently, or what any additional work could have been done. This work has demonstrated synergy between BI 6727 and gemcitabine in pancreatic cancer, though this must be taken within the context of its limitations.

Experiments demonstrating synergy between BI 6727 and gemcitabine were only undertaken in a single cell line. Given that MiaPaCa-2 possesses amongst the commonest mutations in pancreatic cancer, it could reasonably be argued that this synergy is potentially transferrable to other pancreatic cancer cell lines that overexpress PLK1, especially given that the IC_{50} concentrations of all experimented cell lines: MiaPaCa-2, Suit-2, BxPC-3 and Panc-1 were all very alike. Evidence in the literature states that MiaPaCa-2 cells significantly over-express PLK1, being 58-fold higher than that of a control cell line423423. A further

publication reports PLK1 mRNA expression in BxPC-3 and Panc-1 being >20-fold that of a control. It could therefore be argued that these cells should exhibit increased sensitivity to PLK1 inhibition than other pancreatic cell line expressing less PLK1, such as AsPC-1 or HPDE6.

In retrospect, defining PLK1 expression on both an mRNA and protein level via PCR and Western blot respectively should have been undertaken as the very first experiment of this project. The inclusion of a PLK1-control, such as AsPC-1 or HPDE6 pancreatic cancer cells should also have been considered, which may have resulted in a wider range of IC_{50} concentrations of BI 6727. The utilisation of a PLK1-inhibitor-resistant cell line may also have made a useful comparison to MiaPaCa-2, which displayed synergy with gemcitabine.

At present, limited evidence exists in the literature with regards to PLK1 expression, p53, KRAS status and their subsequent sensitivity to PLK1 inhibitors. PLK1 has previously been demonstrated to be expressed in three quarters of pancreatic cancers, but its extent was extremely variable423. Preserved p53 status has been associated with increased apoptosis when treated with PLK1 inhibitors, though this has been disputed by others. Mutant KRAS has also been claimed to increase sensitivity to PLK1 inhibition. It is this tumour heterogeneity that presents such a challenge to the pharmaceutical industry and oncologist alike. PLK1 inhibitors are clearly unlikely to be to be an effective chemotherapeutic treatment for all pancreatic cancers, meaning further work is required to identify the subset of patients whose tumour biology predisposes sensitivity to such drugs. Further *in vitro* work could include *TP53* or *KRAS* knockdown in pancreatic cancer cells prior to the inhibition of PLK1. It would be of interest to note whether the IC_{50} of BI 6727 is reduced after either.

The next step in assessing this drug combination's relevance to clinical practice could involve progressing to a human tumour xenograft model. Though successful results are no guarantee of the same in humans, a negative result is a strong indicator that any further research with this drug combination should be abandoned. For example, there is a possibility that a simple tolerability study in a murine model could demonstrate that this drug combination is too toxic and therefore not feasible in clinical practice.

This work raises the possibility that MiaPaCa-2 cell death by combining BI 6727 and gemcitabine may not be predominantly caspase-dependent, an alternative mode of cell death has not been demonstrated. Western blotting revealed an absence of cleaved caspase-3 with both BI 6727 and the majority of combination therapy-treated cells, though a strong presence when treated with gemcitabine alone. In retrospect, a stronger result could have been achieved by utilising dead cells in isolation as there remains a possibility that a dilution-effect may have been in-play. Separating these non-viable cells by FACS or alternatively by a Ficoll-Paque technique would give a far more accurate result and exclude the potential for a sampling error through dilution.

Another possibility for the absence of cleaved-caspase-3 is that these cells were harvested too early or too late to optimally demonstrate the presence of cleaved caspase-3. In some cell types, the half-life of some active caspase subunits can often be very short. In such cases a decrease in zymogen signal will be seen but a corresponding increase in the subunit signal will be absent[535]. This is certainly something to consider as an alternative to caspase-3 in future work. In addition, experimenting with dead cells at a greater variety of time points could also help eliminate this problem, as opposed to the single 72-hourpoint used in this research.

As previously mentioned, an even better marker of cellular or tumour response would be in a xenograft model. This would give the additional benefit of being able to measure tumour sizes and observing the histopathological appearance of the tumour's response to treatment. Immunohistochemistry for markers of cell death i.e. cleaved aspase-3 could also be undertaken, and is well documented in the literature.

In retrospect, an alternative experiment could have been undertaken to further distinguish between apoptosis and necrosis *in vitro*. Cells staining positively for both Annexin V and EthD-III are considered to be late apoptotic or secondary necrotic cells. This is due to the fact that *in vitro*, secondary necrosis, otherwise termed apoptotic necrosis will eventually follow apoptosis due to the absence of phagocytosis by macrophages[536]. Measured over time in a dynamic experiment, it should be possible to track these cells through the stages of apoptosis. In contrast, a single observation indicating that cells are both Annexin V and

EthD-III positive as undertaken in this work, reveals limited information about the process by which the cells underwent their downfall.

One of the most valuable suggestions for a dynamic experiment for future work is prolonged light microscopy. This would provide invaluable new information regarding proliferation, colony formation, cell phenotype and mode of cell death. Such an experiment could demonstrate whether combination-therapy treated cells still undergo the characteristic malformed spindle changes characteristic of PK1-inhibited cells. It would also be of interest to investigate how cells in S phase and G2/M differ when treated with combination therapy. Cells would need to be synchronised prior to any such experiment, with FACS or alternatively by chemical blockade with compounds such as hydroxyurea (S phase) and nocodazole (M phase) being tried and tested methods in this task. With regards to microscopy, fluorescence imaging could also be undertaken, which could define the subcellular location and expression of PLK1 in gemcitabine and combination-therapy treated cells.

Though observing cellular morphology would be of great interest, the information gathered in isolation may mask significant variations in biochemical and immunological heterogeneity. Due to the vast spectrum of routes in which cells can reach their demise[121], biochemical methods for assessing cell death do have advantages over morphological techniques in that they are quantitative, and therefore less prone to being misinterpreted by the operator. The absence of cleaved caspase-3 *in vitro* should in future lead to a variety of markers representing other cell death pathways such as mitotic catastrophe (caspase-2 activation) or necroptosis (RIP/RIP3 activation) amongst others.

Conclusion

The novel PLK1 inhibitor, BI 6727 is effective against a variety of pancreatic cancer cells *in vitro.* In MiaPaCa-2 cells, synergy has been demonstrated when BI 6727 is administered prior to combination therapy with gemcitabine, though the mode of cell death does not appear to be predominantly caspase-dependent.

References

[1] Agur AMR, Dalley AF. Grant's Atlas of Anatomy. 13th ed. Lippincott Williams and Wilkins; 2012.
[2] Gray H. Gray's anatomy – the classic first edition. 1st ed. Herron books; 1997.
[3] Sinnatamby CS. Last's anatomy. 12th ed. Churchill Livingstone; 2011
[4] Yu J, Turner MA, Fulcher AS, Halvorsen RA. Congenital Anomalies and Normal Variants of the Pancreaticobiliary Tract and the Pancreas in Adults: Pt 2, Pancreatic Duct and Pancreas. Am J Roent. 2006; 187: 1544-1553
[5] Santorini GD. Septendecim tabulae quas nunc primum edit atque explicat iisque alias addit de structura Parmensi universitate anatomes professor primaries, etc. 1775; Parmae ex regia typographia. Fol. (British Library 59.f.12; Wellcome Institute Hist. Med.)
[6] Kamisawa T, Okamoto A. Pancreatographic investigation of pancreatic duct system and pancreaticobiliary malformation. J Anat. 2008; 212(2): 125-34
[7] Turkvatan A, Erden A, Turkoglu MA, Yener O. Congenital variants and anomalies of the pancreas and pancreatic duct: imaging by magnetic resonance cholangiopancreaticography and multidetector computed tomography. Kor J Radiol 2013; 14(6): 905-913
[8] Schulte SJ. Embryology, normal variation, and congenital anomalies of the pancreas. In: Stevenson GW, Freeny PC, Margulis AR, Burhenne HJ, editors. Margulis' and Burhenne's alimentary tract radiology. 5th ed. St. Louis: Mosby; 1994
[9] Mandell J. Core Radiology. 1st ed. Cambridge University Press; 2013
[10] Vater A. Dissertatio anatomica qua novum bilis diverticulum circa orificum ductus cholodochi ut et valvulosam colli vesicae felleae constructionem…. 1720; Wittenbergae, Lit. Gerdesianus, 4to. (Wellcome Inst Hist Med A.I.f(20) 13298)
[11] Loukas M, Spentzouris G, Tubbs R, Kapos T, Curry B. Ruggero Ferdinando Antonio Guiseppe Vincenzo Oddi. World J Surg 2007; 31: 2260-2265
[12] Kern HF. Fine Structure of the Human Exocrine Pancreas. Chapter 2. In: The Pancreas: Biology, Pathobiology, and Disease, Second Edition, edited by Go VLW, et al. Raven Press Ltd., New York, pp. 9-19, 1993.
[13] Pandol SJ. The exocrine pancreas. 1st ed. Morgan and Claypool Life Sciences; 2010.
[14] Langerhans P. Beitrage zur mikroscopischen anatomie der bauchspeichel druse. Inaugural dissertation. Berlin: Gustav Lange. 1869.
[15] Williams JA, Goldfine ID. The insulin-acinar relationship. Chapter 41 In: The Pancreas: Biology, Pathobiology, and Disease, Second Edition, edited by Go VLW, et al. Raven Press Ltd., New York, pp.789-802, 1993
[16] Steiner DJ, Kim A, Miller K, Hara M. Pancreatic islet plasticity: interspecies comparison of islet architecture and composition. Islets 2010; 2(3): 135-145
[17] Jemal A, Bray F, Center MM, Ferlay J, Ward E, Forman D. Global cancer statistics. CA Cancer J Clin 2011; 61: 69–90
[18] Office for National Statistics. Cancer Statistics Registrations, England (Series MB1) , No. 42, 2011
[19] Cancer Research UK website
[20] AICR. World Cancer Research Fund/American Institute for Cancer Research. Food, nutrition, physical activity, and the prevention of cancer: a global perspective; 2007
[21] Jiao L, Berrington de Gonzalez A, Hartge P, Pfeiffer RM, Park Y, Freedman DM, Chow WH, Huang WY, Haynes RB, Hoppin JA, Ji B, Leitzmann MF, Linet MF, Meinhold CL, Schairer C, Schatzkin A, Virtamo J, Weinstein SJ, Zheng W, Stolzenberg-Solomon RZ. Body mass index, effect modifiers, and risk of pancreatic cancer: a pooled study of seven prospective cohorts. Can Causes Control 2010; 21(8): 1305-1314
[22] Genkinger JM, Spiegelman D, Anderson KE, Bernstein L, van den Brandt PA, Calle EE, English DR, Folsom AR, Freudenheim JL, Fuchs CS, Giles GG, Giovannucci E, Horn-Ross PL, Larsson SC, Leitzmann M, Männistö S, Marshall JR, Miller AB, Patel AV, Rohan TE, Stolzenberg-Solomon RZ, Verhage BA, Virtamo J, Willcox BJ, Wolk A, Ziegler RG, Smith-Warner SA. A pooled analysis of 14 cohort studies of anthropometric factors and pancreatic cancer risk. Int J Cancer. 2011; 129(7): 1708-17
[23] Licv D, Morris JS, Liu J, Hassan et al. Body mass index and risk, age of onset, and survival in patients with pancreatic cancer. JAMA 2009; 301: 2553-2562
[24] Iodice S, Gandini S, Maisonneuve P, Lowenfels AB. Tobacco and the risk of pancreatic cancer: a review and meta-analysis. Langenbecks Arch Surg 2008; 393: 535-545
[25] Duell EJ. Epidemiology and potential mechanisms of tobacco smoking and heavy alcohol consumption in pancreatic cancer. Mol Carcinog 2012; 51: 40-52

[26] Lynch SM, Vrieling A, Lubin JH, Kraft P, Mendelsohn JB, Hartge P, Canzian F, Steplowski E, Arslan AA, Gross M, Helzlsouer K, Jacobs EJ, LaCroix A, Petersen G, Zheng W, Albanes D, Amundadottir L, Bingham SA, Boffetta P, Boutron-Ruault MC, Chanock SJ, Clipp S, Hoover RN, Jacobs K, Johnson KC, Kooperberg C, Luo J, Messina C, Palli D, Patel AV, Riboli E, Shu XO, Rodriguez Suarez L, Thomas G, Tjønneland A, Tobias GS, Tong E, Trichopoulos D, Virtamo J, Ye W, Yu K, Zeleniuch-Jacquette A, Bueno-de-Mesquita HB, Stolzenberg-Solomon RZ. Cigarette smoking and pancreatic cancer: a pooled analysis from the pancreatic cancer cohort consortium. Am J Epidemiol. 2009; 170(4): 403-13

[27] Everhart J, Wright D. Diabetes mellitus as a risk factor for pancreatic cancer. A meta-analysis. JAMA 1995; 273(20): 1605-9

[28] Huxley R, Ansary-Moghaddam A, Berrington de Gonzalez A, Barzi F, Woodward M. Type-II diabetes and pancreatic cancer: a meta-analysis of 36 studies. Br J Cancer 2005; 92: 2076-2083

[29] Pannala R, Leirness JB, Bamlet WR, Basu A, Petersen GM, Chari ST. Prevalence and clinical profile of pancreatic cancer-associated diabetes mellitus. Gastroenterology. 2008; 134(4): 981-987

[30] Pannala R, Basu A, Petersen GM, Chari ST. New-onset diabetes: a potential clue to the early diagnosis of pancreatic cancer. Lancet Oncol. 2009; 10(1): 88-95

[31] Lucenteforte E, La Vecchia C, Silverman D, Petersen GM, Bracci PM, Ji BT, Bosetti C, Li D, Gallinger S, Miller AB, Bueno-de-Mesquita HB, Talamini R, Polesel J, Ghadirian P, Baghurst PA, Zatonski W, Fontham E, Bamlet WR, Holly EA, Gao YT, Negri E, Hassan M, Cotterchio M, Su J, Maisonneuve P, Boffetta P, Duell EJ. Alcohol consumption and pancreatic cancer: a pooled analysis in the International Pancreatic Cancer Case-Control Consortium (PanC4). Ann Oncol. 2012; 23(2): 374-82

[32] Pandol SJ, Raraty M. Pathobiology of alcoholic pancreatitis. Pancreatol 2007; 7: 105-114

[33] Grocock CJ, Rebours V, Delhaye MN, Andrén-Sandberg A, Weiss FU, Mountford R, Harcus MJ, Niemczyck E, Vitone LJ, Dodd S, Jørgensen MT, Ammann RW, Schaffalitzky de Muckadell O, Butler JV, Burgess P, Kerr B, Charnley R, Sutton R, Raraty MG, Devière J, Whitcomb DC, Neoptolemos JP, Lévy P, Lerch MM, Greenhalf W; European Registry of Hereditary Pancreatitis and Pancreatic Cancer.The variable phenotype of the p.A16V mutation of cationic trypsinogen (PRSS1) in pancreatitis families Gut. 2010; 59(3): 357-363

[34] Raimondi S, Lowenfels AB, Morselli-Labate AM, Maisonneuve P, Pezzilli R. Pancreatic cancer in chronic pancreatitis; aetiology, incidence, and early detection. Best Pract Res Clin Gastroenterol. 2010; 24(3): 349-358

[35] Lowenfels AB, Maisonneuve P, DiMagno EP, Elitsur Y, Gates Jr LK, Perrault J, Whitcomb DC. Hereditary pancreatitis and the risk of pancreatic cancer. J Natl Cancer Inst 1997; 89 (6): 442-446

[36] Lowenfels AB, Maisonneuve P, Whitcomb DC, Lerch MM, DiMagno EP. Cigarette smoking as a risk factor for pancreatic cancer in patients with hereditary pancreatitis. JAMA 2001; 286: 169-170

[37] Sheldon CD, Hodson ME, Carpenter LM, Swerdlow AJ. A cohort study of cystic fibrosis and malignancy. Br J Cancer. 1993; 68(5): 1025-1028.

[38] Neglia JP, FitzSimmons SC, Maisonneuve P, Schöni MH, Schöni-Affolter F, Corey M, Lowenfels AB. The risk of cancer among patients with cystic fibrosis. Cystic Fibrosis and Cancer Study Group. N Engl J Med. 1995; 332(8): 494-499.

[39] McWilliams RR, Petersen GM, Rabe KG, Holtegaard LM, Lynch PJ, Bishop MD, Highsmith WE Jr. Cystic fibrosis transmembrane conductance regulator (CFTR) gene mutations and risk for pancreatic adenocarcinoma. Cancer. 2010; 116(1): 203-209

[40] Brand RE, Lerch MM, Rubinstein WS, Neoptolemos JP, Whitcomb DC, Hruban RH, Brentnall TA, Lynch HT, Canto MI; Participants of the Fourth International Symposium of Inherited Diseases of the Pancreas. Advances in counselling and surveillance of patients at risk for pancreatic cancer. Gut 2007; 56: 1460-69

[41] Lynch HT, Lanspa SJ, Fitzgibbons RJ Jr, Smyrk T, Fitzsimmons ML, McClellan J. Familial pancreatic cancer (part 1): genetic pathology review. Nebr Med J 1989; 74: 109-112

[42] Klein AP, Brune KA, Petersen GM, Goggins M, Tersmette AC, Offerhaus GJ, Griffin C, Cameron JL, Yeo CJ, Kern S, Hruban RH. Prospective risk of pancreatic cancer in familial pancreatic cancer kindreds. Cancer Res. 2004; 64(7): 2634-8

[43] Applebaum SE, Kant JA, Whitcomb DC, Ellis IH. Genetic testing. Counselling, laboratory, and regulatory issues and the EUROPAC protocol for ethical research in multicentre studies of inherited pancreatic diseases. Med Clin North Am 2000; 84: 575-588

[44] Hruban RH, Petersen GM, Ha PK, Kern SE. Genetics of pancreatic cancer. From genes to families. Surg Oncol Clin North Am 1998; 7: 1-23

[45] Fendrich V, Langer P, Bartsch. Familial pancreatic cancer – status quo. Int J Colorectal Dis 2014; 29: 139-145

[46] Moldow RE, Connolly RR. Epidemiology of pancreatic cancer in Conneticut. Gastroenterology 1968; 55: 677-86

[47] O'Grady HL, Conlon KC. Pancreatic neuroendocrine tumours. EJSO 2008; 34: 324-332
[48] Thompson NW, Eckhauser FE. Malignant islet cell tumours of the pancreas. World J Surg 1984; 8: 940-51
[49] Halfdanarson TR, Rabe KG, Rubin J, Petersen GM. Pancreatic neuroendocrine tumours (PNETs): incidence, prognosis and recent trend toward improved survival. Ann Oncol 2008; 19: 1727-33
[50] Bellizzi AM, Frankel WL. Pancreatic pathology: a practical review. Lab Med 2009; 40(7): 417-26
[51] Hruban RH, Pitman MB, Klimstra DS. Ductal adenocarcinoma afip atlas of tumor pathology. Tumours of the pancreas. Am J Clin Pathol 2007; 6: 111-164
[52] Hidalgo M, Pancreatic cancer. N Engl J Med 2010; 362: 1605-17
[53] Longmore M, Wilkinson I, Baldwin A, Wallin E. Oxford handbook of clinical medicine (Oxford medical handbooks). 9th ed. Oxford University Press. 2014
[54] Klauss M, Mohr A, von Tengg-Kobligk H, Friess H, Singer R, Seidensticker P, Kauczor HU, Richter GM, Kauffmann GW, Grenacher L. A new invasion score for determining the resectability of pancreatic carcinomas with contrast-Enhanced multidetector computed tomography. Pancreatol 2008; 8(2): 204–210
[55] Miura F, Takada T, Amano H, Yoshida M, Furui S, Takeshita K. Diagnosis of pancreatic cancer. HPB 2006; 8: 337-42
[56] Dewitt J, Devereaux BM, Lehman GA, Sherman S, Imperiale TF. Comparison of endoscopic ultrasound and computed tomography for the preoperative evaluation of pancreatic cancer: a systematic review. Clin Gastroenterol Hepatol. 2006; 4(6): 717-25
[57] Kneuertz PJ, Cunningham SC, Cameron JL, Tapazoglou N, Herman JM, Makary MA, Eckhauser F, Wang J, Hirose K, Edil BH, Choti MA, Schulick RD, Wolfgang CJ, Pawlick TM. Palliative surgical management of patients with unresectable pancreatic adenocarcinoma: trends and lessons learned from a large, single institution experience. J Gastrointest Surg 2011; 15: 1917–1927
[58] Marinelli T, Filippone A, Tavano F, Fontana A, Pellegrini F, Köninger J, Richter GM, Bonomo L, Büchler MW, di Sebastiano P, di Mola FF.A tumour score with multidetector spiral CT for venous infiltration in pancreatic cancer: influence on borderline resectable. Radiol Med. 2014; 119(5): 334-42
[59] Callery MP, Chang KJ, Fishman EK, Talamonti MS, Traverso LW, Linehan DC. Pretreatment assessment of resectable and borderline resectable pancreatic cancer: expert consensus statement. Ann Surg Oncol 2009; 16: 1727-33
[60] Katz MH, Pisters PW, Lee JE, Fleming JB. Borderline resectable pancreatic cancer: what have we learned and where do we go from here? Ann Surg Oncol. 2011; 18(3): 608-10.
[61] Bockhorn M, Uzunoglu FG, Adham M, Imrie C, Milicevic M, Sandberg AA, Asbun HJ, Bassi C, Büchler M, Charnley RM, Conlon K, Cruz LF, Dervenis C, Fingerhutt A, Friess H, Gouma DJ, Hartwig W, Lillemoe KD, Montorsi M, Neoptolemos JP, Shrikhande SV, Takaori K, Traverso W, Vashist YK, Vollmer C, Yeo CJ, Izbicki JR; International Study Group of Pancreatic Surgery. Borderline resectable pancreatic cancer: a consensus statement by the International Study Group of Pancreatic Surgery (ISGPS). Surgery. 2014; 155(6): 977-988.
[62] Burnett AS, Calvert TJ, Chokshi RJ. Sensitivity of endoscopic retrograde cholangiopancreatography standard cytology: 10-y review of the literature. J Surg Res. 2013; 184(1): 304-11
[63] Asbun HJ, Conlon K, Fernandez-Cruz L, Friess H, Shrikhande SV, Adham M, Bassi C, Bockhorn M, Büchler M, Charnley RM, Dervenis C, Fingerhutt A, Gouma DJ, Hartwig W, Imrie C, Izbicki JR, Lillemoe KD, Milicevic M, Montorsi M, Neoptolemos JP, Sandberg AA, Sarr M, Vollmer C, Yeo CJ, Traverso LW; International Study Group of Pancreatic Surgery. When to perform a pancreatoduodenectomy in the absence of positive histology? A consensus statement by the International Study Group of Pancreatic Surgery. Surgery. 2014; 155(5): 887-92
[64] Sobin LH, Gospodarowicz MK, Wittekind Ch (eds). International Union Against Cancer TNM Classification of Malignant Tumours (7th edn). Wiley Blackwell, 2009.
[65] Taylor C, Munro AJ, Glynne-Jones R, Griffith C, Trevatt P, Richards M, Ramirez AJ. Multidisciplinary team working in cancer: what is the evidence? BMJ 2010; 340: c951
[66] Kausch W: Das Carcinom der Papilla duodeni und seine radikale Entfernung. Beitr Z Klin Chir 1912; 78: 439–486.
[67] Whipple AO: Observations on radical surgery for lesions of pancreas. Surg Gynecol Obstet 1946; 82: 623–631.
[68] Jones L, Russell C, Mosca F, Boggi U, Sutton R, Slavin J, Hartley M, Neoptolemos JP. Standard Kausch-Whipple pancreatoduodenectomy. Dig Surg 1999; 16(4): 297-304
[69] Barreto SG, Shukla PJ, Shrikhande SV. Tumors of the Pancreatic Body and Tail. World J Oncol 2010; 1(2): 52-65
[70] Artinyan A, Soriano PA, Prendergast C, Low T, Ellenhorn JD, Kim J. The anatomic location of pancreatic cancer is a prognostic factor for survival. HPB 2008; 10: 371-376

[71] Whipple AO. Present-day surgery of the pancreas. N Engl J Med 1942; 226: 515-526
[72] Trede M, Schwall G, Saeger HD. Survival after pancreatoduodenectomy. 118 consecutive resections without an operative mortality. Ann Surg 1990; 211: 447-458
[73] Cameron JL, Pitt HA, Yeo CJ, Lillemoe KD, Kaufman HS, Coleman J. One hundred and forty-five consecutive pancreatoduodenectomies without mortality. Ann Surg 1993; 217: 430-438
[74] National Cancer Action Team. National Manual of Cancer Services. London: Department of Health, 2004
[75] Allareddy V, Ward MW, Allareddy V, Konety B. Effect of meeting leapfrog volume thresholds on complication rates following complex surgical procedures. Ann Surg 2010; 251(2): 377-383
[76] The SH, Diggs BS, Deveney CW, Sheppard BC. Patient and hospital characteristics on the variance of perioperative outcomes for pancreatic resection in the United States. Arch Surg 2009; 144(8): 713-721
[77] Gagner M, Pomp A. Laparoscopic pylorus-preserving pancreatoduodenectomy. Surg Endosc 1994; 8: 408-410
[78] Melvin WS, Needleman BJ, Krause KR, Ellison EC. Robotic resection of pancreatic neuroendocrine tumor. J Laparoendosc Adv Surg Tech A 2003; 13: 33-36.
[79] Lei P, Wei B, Guo W, Wei H. Minimally invasive surgical approach compared with open pancreaticoduodenectomy: a systematic review and meta-analysis on the feasibility and safety. Surg Laparoscop Endosc Percutan Tech 2014; epub
[80] Nigri G, Petrucciani N, La Torre M, Magistri, Valabrega S, Aurello P, Ramacciato. Duodenopancreatectomy: open or minimally invasive approach? Surgeon 2014; 12: 227-234
[81] Correa-Gallego C, Dinkelspiel HE, Sulimanoff I, Fisher S, Vinuela EF, Kingham P, Fong Y, DeMatteo RP, D'Angelica MI, Jarnagin WR, Allen PJ. Minimally invasive vs open pancreaticoduodenectomy: systematic review and meta-analysis. 2014; 218(1): 129-139
[82] Lasse K, Coolsen MME, Slim K, Carli F, de Aguilar-Nascimento JE, Schafer M, Parks RW, Fearon KCH, Lobo DN, Demartines N, Braga M, Ljungqvist O, Dejong CHC. Guidelines for perioperative care for pancreaticoduodenectomy: Enhanced Recovery After Surgery (ERAS®) Society recommendations. Clin Nutrition 2012; 31: 817-830
[83] Coolsen MME, van Dam RM, van der Wilt AA, Slim K, Lassen K, Dejong CHC. Systematic review and meta-analysis of enhanced recovery after pancreatic surgery with particular emphasis on pancreaticoduodenectomies. World J Surg 2013; 37: 1909-1918
[84] Hruban RH, Adsay NZ, Albores-Saavedra J, Compton C, Garrett ES, Goodman SN, Kern SE, Klimstra DS, Klöppel G, Longnecker DS, Lüttges J, Offerhaus GJ. Pancreatic intraepithelial neoplasia: a new nomenclature and classification system for pancreatic duct lesions. Am J Surg Pathol. 2001; 25(5): 579-586
[85] Hruban RH, Takaori K, Klimstra DS, Adsay NV, Albores-Saavedra J, Biankin AV, Biankin SA, Compton C, Fukushima N, Furukawa T, Goggins M, Kato Y, Klöppel G, Longnecker DS, Lüttges J, Maitra A, Offerhaus GJ, Shimizu M, Yonezawa S. An illustrated consensus on the classification of pancreatic intraepithelial neoplasia and intraductal papillary mucinous neoplasms. Am J Surg Pathol. 2004; 28(8): 977-987
[86] Zamboni G, Hirabayashi K, Castelli P, Lennon AM. Precancerous lesions of the pancreas. Best Pract Res Clin Gastroenterol. 2013; 27(2): 299-322
[87] Distler M, Aust D, Weitz J, Pilarsky C, Grutzmann R. Precursor lesions for sporadic pancreatic cancer: PanIN, IPMN and MCN. Biomed Res Int. 2014;2014:474905
[88] Shammas MA. Telomeres, lifestyle, cancer, and ageing. Curr Opin Clin Nutr Metab Care 2011; 14(1): 28-34
[89] Valdes AM, Andrew T, Gardner JP, Kimura M, Oelsner E, Cherkas LF, Aviv A, Spector TD. Obesity, cigarette smoking, and telomere length in women. Lancet. 2005; 366(9486): 662-664
[90] Maitra A, Kern SE, Hruban RH. Molecular pathogenesis of pancreatic cancer. Best Pract Res Clin Gastroenterol 2006; 20(2): 211-226
[91] Matsuda Y, Ishiwata T, Izumiyama-Shimomura N, Hamayasu H, Fujiwara M, Tomita K, Hiraishi N, Nakamura K, Ishikawa N, Aida J, Takubo K, Arai T. Gradual telomere shortening and increasing chromosomal instability among PanIN grades and normal ductal epithelia with and without cancer in the pancreas. PLoS One. 2015; 10(2): e0117575
[92] van Heek NT, Meeker AK, Kern SE, Yeo CJ, Lillemoe KD, Cameron JL, Offerhaus GJ, Hicks JL, Wilentz RE, Goggins MG, De Marzo AM, Hruban RH, Maitra A. Telomere shortening is nearly universal in pancreatic intraepithelial neoplasia. Am J Pathol. 2002; 161(5): 1541-1547.
[93] Eser S Schnieke A, Schneider G, Saur D. Oncogenic KRAS signaling in pancreatic cancer. Br J Cancer 2014; 111: 817–822
[94] Furukawa. Impacts of activation of the mitogen-activated protein kinase pathway in pancreatic cancer. Front Oncol 2015; 5: 23

[95] Pylayeva-Gupta Y, Grabocka E, Bar-Sagi D. RAS oncogenes: weaving a tumorigenic web. Nat Rev Cancer 2011; 11: 761–774
[96] Lohr M, Kloppel, Maisonneuve P, Lowenfels AB, Luttges J. Frequency of K-ras mutations in pancreatic intraductal neoplasias associated with pancreatic ductal adenocarcinoma and chronic pancreatitis: a meta-analysis. Neoplasia 2005; 7(1): 17-23
[97] Kanda M, Matthaei H, Wu J, Hong SM, Yu J, Borges M, Hruban RH, Maitra A, Kinzler K, Vogelstein B, Goggins M. Presence of somatic mutations in most early-stage pancreatic intraepithelial neoplasia. *Gastroenterology* 2012**; 142**: 730–733
[98] Wilentz RE, Geradts J, Maynard R, Offerhaus GJ, Kang M, Goggins M, Yeo CJ, Kern SE, Hruban RH. Inactivation of the p16 (INK4A) tumor-suppressor gene in pancreatic duct lesions: loss of intranuclear expression. Cancer Res. 1998; 58(20): 4740-4744.
[99] Caldas C, Hahn SA, da Costa LT, Redston MS, Schutte M, Seymour AB, Weinstein CL, Hruban RH, Yeo CJ, Kern SE. Frequent somatic mutations and homozygous deletions of the p16 (MTS1) gene in pancreatic adenocarcinoma. Nat Genet. 1994; 8(1): 27-32.
[100] Sherr, C.J, Roberts JM. Living with or without cyclins and cyclin-dependent kinases. Genes Dev. 2004; 18: 2699–2711
[101] Sherr CJ. Cancer cell cycles. Science 1996; 274: 1672-1677
[102] Attri J, Srinivasan R, Majumdar S, Radotra BD, Wig J. Alterations of tumor suppressor gene p16INK4a in pancreatic ductal carcinoma. BMC Gastroenterol 2005; 5: 22
[103] Kern SE. p53: tumor suppression through control of the cell cycle. Gastroenterology 1994; 106: 1708–1711.
[104] Lane DP. Cancer. P53, guardian of the genome. Nature 1992; 358: 15-16
[105] Kandoth C, McLellan MD, Vandin F, Ye K, Niu B, Lu C, Xie M, Zhang Q, McMichael JF, Wyczalkowski MA, Leiserson MD, Miller CA, Welch JS, Walter MJ, Wendl MC, Ley TJ, Wilson RK, Raphael BJ, Ding L. Mutational landscape and significance across 12 major cancer types. Nature.2013; 502(7471): 333-339
[106] Morton JP, Timpson P, Karim SA, Ridgway RA, Athineos D, Doyle B, Jamieson NB, Oien KA, Lowy AM, Brunton VG, Frame MC, Evans TR, Sansom OJ. Mutant p53 drives metastasis and overcomes growth arrest/senescence in pancreatic cancer. Proc Natl Acad Sci U S A. 2010; 107(1): 246-251
[107] Green DR, Kroemer G. Cytoplasmic functions of the tumor suppressor p53. Nature 2009; 458(7242): 1127
[108] Koorsta JM, Feldman G, Habbe N, Maitra A. Morphogenesis of pancreatic cancer: role of pancreatic intraepithelial neoplasia (PanINs). Langenbecks Arch Surg 2008; 393(4): 561-570
[109] Maitra A, Adsay NV, Argani P, Iacobuzio-Donahue C, De Marzo A, Cameron JL, Yeo CJ, Hruban RH. Multicomponent analysis of the pancreatic adenocarcinoma progression model using a pancreatic intraepithelial neoplasia tissue microarray. Mod Pathol 2003; 16: 902–912.
[110] Hahn SA, Schutte M, Hoque AT, Moskaluk CA, da Costa LT, Rozenblum E, Weinstein CL, Fischer A, Yeo CJ, Hruban RH, Kern SE. DPC4, a candidate tumor suppressor gene at human chromosome 18q21.1. Science. 1996; 271(5247): 350-353
[111] Wilentz RE, Iacobuzio-Donahue CA, Argani P, McCarthy DM, Parsons JL, Yeo CJ, Kern SE, Hruban RH. Loss of expression of Dpc4 in pancreatic intraepithelial neoplasia: evidence that DPC4 inactivation occurs late in neoplastic progression. Cancer Res. 2000; 60(7): 2002-2006
[112] Sameer AS, Chowdri NA, Syeed N, Banday MZ, Shah ZA, Siddiqi MA. SMAD4 – Molecular gladiator of the TGF-β-signaling is trampled upon by mutational insufficiency in colorectal carcinoma of Kashmiri population: an analysis with relation to KRAS proto-oncogene. BMC Cancer 2010; 10: 300
[113] Massague J, Seoane J, Wotton D. Smad transcription factors. Genes Dev 2005; 19: 2783-2810
[114] Ringel J, Lohr M. The MUC gene family: their role in diagnosis and early detection of pancreatic cancer. Mol Cancer 2003; 2: 9
[115] Taylor-Papadimitriou J, Burchell JM, Plunkett T, Graham R, Correa I, Miles D, Smith M. MUC1 and the immunobiology of cancer. J Mammary Gland Biol Neoplasia. 2002; 7(2): 209-221
[116] Levi E, Klimstra DS, Adsay NV, Andea A, Basturk O. MUC1 and MUC2 in pancreatic neoplasia. J Clin Pathol 2004; 57: 456-462
[117] Yonezawa S, Higashi M, Yamada N, Goto M. Precursor lesions of pancreatic cancer. Gut Liver 2008; 2(3): 137-154
[118] Wilentz RE, Iacobuzio-Donahue CA, Argani P, McCarthy DM, Parsons JL, Yeo CJ, Kern SE, Hruban RH. Loss of expression of Dpc4 in pancreatic intraepithelial neoplasia: evidence that DPC4 inactivation occurs late in neoplastic progression. Cancer Res. 2000; 60(7): 2002-2006
[119] Hengartner MO. The biochemistry of apoptosis. Nature 2000; 407: 770-776

[120] Kerr JF, Wylie AH, Currie AR. Apoptosis: a basic biological phenomenon with wide-ranging implications in tissue kinetics. Br J Cancer 1972; 26: 239-257
[121] Galluzzi L, Vitale I, Abrams JM, Alnemri ES, Baehrecke EH, Blagosklonny MV, Dawson TM, Dawson VL, El-Deiry WS, Fulda S, Gottlieb E, Green DR, Hengartner MO, Kepp O, Knight RA, Kumar S, Lipton SA, Lu X, Madeo F, Malorni W, Mehlen P, Nuñez G, Peter ME, Piacentini M, Rubinsztein DC, Shi Y, Simon HU, Vandenabeele P, White E, Yuan J, Zhivotovsky B, Melino G, Kroemer G. Molecular definitions of cell death subroutines: recommendations of the Nomenclature Committee on Cell Death 2012. Cell Death Differ. 2012; 19(1): 107-120
[122] Tait SWG, Green DR. Mitochondria and cell death: outer membrane permeabilization and beyond. Nat Rev Mol Cell Biol 2010; 11: 621-632
[123] Walczak H, Krammer PH. The CD95 (APO-1/Fas) and the TRAIL (APO-2L) apoptosis systems. Exp Cell Res. 2000; 256(1): 58-66
[124] Kischkel FC, Hellbardt S, Behrmann I, Germer M, Pawlita M, Krammer PH, Peter ME. Cytotoxicity-dependent APO-1 (Fas/CD95)-associated proteins form a death-inducing signaling complex (DISC) with the receptor. EMBO J. 1995; 14(22): 5579-5588.
[125] Bamhart BC, Alappat EC, Peter ME. The CD95 type I/type II model. Semin Immunol 2003; 15: 185-193
[126] Scaffidi C, Fulda S, Srinivasan A, Friesen C, Li F, Tomaselli KJ, Debatin KM, Krammer PH, Peter ME. Two CD95 (APO-1/Fas) signaling pathways. EMBO J. 1998; 17(6): 1675-1687.
[127] Li H, Zhu H, Xu CJ, Yuan J. Cleavage of BID by caspase 8 mediates the mitochondrial damage in the Fas pathway of apoptosis. Cell 1998; 94: 491-501
[128] Luo X, Budihardjo I, Zou H, Slaughter C, Wang X. Bid, a Bcl2 interacting protein, mediates cytochrome c release from mitochondria in response to activation of cell surface death receptors. Cell 1998; 94: 481-490
[129] Lavrik IN, Golks A, Krammer PH. Caspases: pharmacological manipulation of cell death. J Clin Invest 2005; 115(10): 2665-2672
[130] Broker LE, Kruyt FAE, Giaccone G. Cell death independent of caspases: a review. Clin Cancer Res 2005; 11(9): 3155-3162
[131] Li P, Nijhawan D, Budihardjo I, Srinivasula SM, Ahmad M, Alnemri ES, Wang X. Cytochrome c and dATP-dependent formation of Apaf-1/caspase-9 complex initiates an apoptotic protease cascade. Cell 1997; 91: 479-489
[132] Zou H, Yang R, Hao J, Wang J, Sun C, Fesik SW, Wu JC, Tomaselli KJ, Armstrong RC. Regulation of the apaf-1/caspase-9 apoptosome by caspase-3 and XIAP. J Biol Chem 2003; 278(10): 8091-8098
[133] Mille F, Thibert C, Fombonne J, Rama N, Guix C, Hayashi H, Corset V, Reed JC, Mehlen P. The Patched dependence receptor triggers apoptosis through a DRAL-caspase-9 complex. Nat Cell Biol 2009; 11: 739-746
[134] Guenebeaud C, Goldschneider D, Castets M, Guix C, Chazot G, Delloye-Bourgeois C, Eisenberg-Lerner A, Shohat G, Zhang M, Laudet V, Kimchi A, Bernet A, Mehlen P. The dependence receptor UNC5H2/B triggers apoptosis via PP2A-mediated dephosphorylation of DAP kinase. Mol Cell 2010; 40: 863-876
[135] Clarke P, Tyler KL. Apoptosis in animal models of virus-induced disease. Nat Rev Micro 2009; 7: 144-155
[136] Saelens JK, FFestjens N, Walle LV, van Gurp M, van Loo G, Vandenabeele P. Toxic proteins released from mitochondria in cell death. Oncogene 2004; 23: 2861-2874
[137] Bakkevold KE, Arnesjø B, Dahl O, Kambestad B. Adjuvant combination chemotherapy (AMF) following radical resection of carcinoma of the pancreas and papilla of Vater--results of a controlled, prospective, randomised multicentre study. *Eur J Cancer* 1993; 29A: 698-703 [PMID: 8471327 DOI: 10.1016/S0959-8049(05)80349-1]
[138] Neoptolemos JP, Dunn JA, Stocken DD, Almond J, Link K, Beger H, Bassi C, Falconi M, Pederzoli P, Dervenis C, Fernandez-Cruz L, Lacaine F, Pap A, Spooner D, Kerr DJ, Friess H, Büchler MW. Adjuvant chemoradiotherapy and chemotherapy in resectable pancreatic cancer: a randomised controlled trial. *Lancet* 2001; 358: 1576-1585 [PMID: 11716884 DOI: 10.1016/S0140-6736(01)06651-X]
[139] Neoptolemos JP, Stocken DD, Friess H, Bassi C, Dunn JA, Hickey H, Beger H, Fernandez-Cruz L, Dervenis C, Lacaine F, Falconi M, Pederzoli P, Pap A, Spooner D, Kerr DJ, Büchler MW. A randomized trial of chemoradiotherapy and chemotherapy after resection of pancreatic cancer. *N Engl J Med* 2004; 350: 1200-1210 [PMID: 15028824 DOI: 10.1056/NEJMoa032295]
[140] Takada T, Amano H, Yasuda H, Nimura Y, Matsushiro T, Kato H, Nagakawa T, Nakayama T. Is postoperative adjuvant chemotherapy useful for gallbladder carcinoma? A phase III multicenter prospective randomized controlled trial in patients with resected pancreaticobiliary carcinoma. *Cancer* 2002; 95: 1685-1695 [PMID: 12365016 DOI: 10.1002/cncr.10831]

[141] Kosuge T, Kiuchi T, Mukai K, Kakizoe T. A multicenter randomized controlled trial to evaluate the effect of adjuvant cisplatin and 5-fluorouracil therapy after curative resection in cases of pancreatic cancer. *Jpn J Clin Oncol* 2006; 36: 159-165 [PMID: 16490736 DOI: 10.1093/jjco/hyi234]
[142] Burris HA, Moore MJ, Andersen J, Green MR, Rothenberg ML, Modiano MR, Cripps MC, Portenoy RK, Storniolo AM, Tarassoff P, Nelson R, Dorr FA, Stephens CD, Von Hoff DD. Improvements in survival and clinical benefit with gemcitabine as first-line therapy for patients with advanced pancreas cancer: a randomized trial. *J Clin Oncol* 1997; 15: 2403-2413 [PMID: 9196156]
[143] Oettle H, Post S, Neuhaus P, Gellert K, Langrehr J, Ridwelski K, Schramm H, Fahlke J, Zuelke C, Burkart C, Gutberlet K, Kettner E, Schmalenberg H, Weigang-Koehler K, Bechstein WO, Niedergethmann M, Schmidt-Wolf I, Roll L, Doerken B, Riess H. Adjuvant chemotherapy with gemcitabine vs observation in patients undergoing curative-intent resection of pancreatic cancer: a randomized controlled trial. *JAMA* 2007; 297: 267-277 [PMID: 17227978 DOI: 10.1001/jama.297.3.267]
[144] Neuhaus P, Riess H, Post S, Gellert K, Ridwelski K, Schramm H, Zuelke C, Fahlke J, Langrehr J, Oettle H. CONKO-001: Final results of the randomized, prospective, multicenter phase III trial of adjuvant chemotherapy with gemcitabine versus observation in patients with resected pancreatic cancer. J Clin Oncol 2008 ASCO Annual Meeting Proceedings (Post-Meeting Edition); 26(15S): LBA4504
[145] Ueno H, Kosuge T, Matsuyama Y, Yamamoto J, Nakao A, Egawa S, Doi R, Monden M, Hatori T, Tanaka M, Shimada M, Kanemitsu K. A randomised phase III trial comparing gemcitabine with surgery-only in patients with resected pancreatic cancer: Japanese Study Group of Adjuvant Therapy for Pancreatic Cancer. Br J Cancer 2009; 101: 908-915 [PMID: 19690548 DOI: 10.1038/sj.bjc.6605256]
[146] Neoptolemos JP, Stocken DD, Bassi C, Ghaneh P, Cunningham D, Goldstein D, Padbury R, Moore MJ, Gallinger S, Mariette C, Wente MN, Izbicki JR, Friess H, Lerch MM, Dervenis C, Oláh A, Butturini G, Doi R, Lind PA, Smith D, Valle JW, Palmer DH, Buckels JA, Thompson J, McKay CJ, Rawcliffe CL, Büchler MW. Adjuvant chemotherapy with fluorouracil plus folinic acid vs gemcitabine following pancreatic cancer resection: a randomized controlled trial. *JAMA* 2010; 304: 1073-1081 [PMID: 20823433 DOI: 10.1001/jama.2010.1275]
[147] Neoptolemos JP, Stocken DD, Tudur Smith C, Bassi C, Ghaneh P, Owen E, Moore M, Padbury R, Doi R, Smith D, Büchler MW. Adjuvant 5-fluorouracil and folinic acid vs observation for pancreatic cancer: composite data from the ESPAC-1 and -3(v1) trials. *Br J Cancer* 2009; 100: 246-250 [PMID: 19127260 DOI: 10.1038/sj.bjc.6604838]
[148] Maeda A, Boku N, Fukutomi A, Kondo S, Kinoshita T, Nagino M, Uesaka K. Randomized phase III trial of adjuvant chemotherapy with gemcitabine versus S-1 in patients with resected pancreatic cancer: Japan Adjuvant Study Group of Pancreatic Cancer (JASPAC-01). *Jpn J Clin Oncol* 2008; 38: 227-229 [PMID: 18272475 DOI: 10.1093/jjco/hym178]
[149] Fukutomi A, Uesaka K, Boku N, Kanemoto H, Konishi M, Matsumoto I, Kaneoka Y, Shimizu Y, Nakamori S, Sakamoto H, Morinaga S, Kainuma O, Imai K, Sata N, Hishinuma S, Nakamura S, Kanai M, Hirano S, Yoshikawa Y, Ohashi Y. JASPAC 01: Randomized phase III trial of adjuvant chemotherapy with gemcitabine versus S-1 for patients with resected pancreatic cancer. Journal of Clinical Oncology 2013 Gastrointestinal Cancers Symposium 2013; 31(4S): 145
[150] Antoniou G, Kountourakis P, Papadimitriou K, Vassiliou V, Papamichael D. Adjuvant therapy for resectable pancreatic adenocarcinoma: review of the current treatment approaches and future directions. Cancer Treat Rev 2014; 40: 78-85 [PMID: 23810287 DOI: 10.1016/j.ctrv.2013.05.008]
[151] Neoptolemos JP, Palmer DH, Ghaneh P, Psarelli EE, Valle JW, Halloran CM, Faluyi O, O'Reilly DA, Cunningham D, Wadsley J, Darby S, Meyer T, Gilmore R, Anthoney A, Lind P, Gilmelius B, Falk S, Izbicki JR, Middleton GW, Cummins S, Ross PJ, Wasan H, McDonald A, Crosby T, Ma YT, Patel K, Sherriff D, Soomal R, Borg D, Sothi S, Hammel P, Hackert T, Jackson R, Buchler MW. Comparison od adjuvant gemcitabine and capecitabine with gemcitabine monotherapy in patients with resected pancreatic cancer (ESPAC-4): a multicentre, open-label, randomised, phase 3 trial. Lancet 2017 doi: 10.1016/S0140-6736(16)32409-6. [Epub ahead of print]
[152] Jones OP, Melling JD, Ghaneh P. Adjuvant therapy in pancreatic cancer. World J Gastroenterol 2014; 20(40): 14733-14746
[153] Stocken DD, Büchler MW, Dervenis C, Bassi C, Jeekel H, Klinkenbijl JH, Bakkevold KE, Takada T, Amano H, Neoptolemos JP. Meta-analysis of randomised adjuvant therapy trials for pancreatic cancer. *Br J Cancer* 2005; 92: 1372-1381 [PMID: 15812554 DOI: 10.1038/sj.bjc.6602513]
[154] Klinkenbijl JH, Jeekel J, Sahmoud T, van Pel R, Couvreur ML, Veenhof CH, Arnaud JP, Gonzalez DG, de Wit LT, Hennipman A, Wils J. Adjuvant radiotherapy and 5-fluorouracil after curative resection of cancer of the

pancreas and periampullary region: phase III trial of the EORTC gastrointestinal tract cancer cooperative group. *Ann Surg* 1999; 230: 776-82; discussion 782-4 [PMID: 10615932]
[155] Kalser MH, Ellenberg SS. Pancreatic cancer. Adjuvant combined radiation and chemotherapy following curative resection. *Arch Surg* 1985; 120: 899-903 [PMID: 4015380 DOI: 10.1001/archsurg.1985.01390320023003]
[156] Further evidence of effective adjuvant combined radiation and chemotherapy following curative resection of pancreatic cancer. Gastrointestinal Tumor Study Group. *Cancer* 1987; 59: 2006-2010 [PMID: 3567862 DOI: 10.1002/1097-0142(19870615)59: 12<2006: : AID-CNCR2820591206>3.0.CO; 2-B]
[157] Boeck S, Ankerst DP, Heinemann V . The role of adjuvant chemotherapy for patients with resected pancreatic cancer: systematic review of randomised controlled trials and meta-analysis. Oncology 2007; 72: 314-21 [PMID:18187951 DOI: 10.1159/000113054]
[158] Butturini G, Stocken DD, Wente MN, Jeekel H, Klinkenbijl JH, Bakkevold KE, Takada T, Amano H, Dervenis C, Bassi C, Büchler MW, Neoptolemos JP. Influence of resection margins and treatment on survival in patients with pancreatic cancer: meta-analysis of randomized controlled trials. *Arch Surg* 2008; 143: 75-83; discussion 83 [PMID: 18209156 DOI: 10.1001/archsurg.2007.17]
[159] Liao WC, Chien KL, Lin YL, Wu MS, Lin JT, Wang HP, Tu YK. Adjuvant treatments for resected pancreatic adenocarcinoma: a systematic review and network meta-analysis. *Lancet Oncol* 2013; 14: 1095-1103 [PMID: 24035532 DOI: 10.1016/S1470-2045(13)70388-7]
[160] Haslam JB, Cavanaugh PJ, Stroup SL. Radiation therapy in the treatment of irresectable adenocarcinoma of the pancreas. *Cancer* 1973; 32: 1341-1345 [PMID: 4127980 DOI: 10.1002/1097-0142(197312)32: 6<1341: : AID-CNCR2820320609>3.0.CO; 2-A]
[161] Moertel CG, Childs DS, Reitemeier RJ, Colby MY, Holbrook MA. Combined 5-fluorouracil and supervoltage radiation therapy of locally unresectable gastrointestinal cancer. *Lancet* 1969; 2: 865-867 [PMID: 4186452]
[162] Wang F, Kumar P. The role of radiotherapy in management of pancreatic cancer. *J Gastrointest Oncol* 2011; 2: 157-167 [PMID: 22811846 DOI: 10.3978/j.issn.2078-6891.2011.032]
[163] Yeo CJ, Abrams RA, Grochow LB, Sohn TA, Ord SE, Hruban RH, Zahurak ML, Dooley WC, Coleman J, Sauter PK, Pitt HA, Lillemoe KD, Cameron JL. Pancreaticoduodenectomy for pancreatic adenocarcinoma: postoperative adjuvant chemoradiation improves survival. A prospective, single-institution experience. *Ann Surg* 1997; 225: 621-33; discussion 633-6 [PMID: 9193189 DOI: 10.1097/00000658-199705000-00018]
[164] Thomas A, Dajani K, Neoptolemos JP, Ghaneh P. Adjuvant therapy in pancreatic cancer. Dig Dis 2010; 28: 684-92 [PMID:21088421 DOI: 10.1159/000320099]
[165] Regine WF, Winter KA, Abrams RA, Safran H, Hoffman JP, Konski A, Benson AB, Macdonald JS, Kudrimoti MR, Fromm ML, Haddock MG, Schaefer P, Willett CG, Rich TA. Fluorouracil vs gemcitabine chemotherapy before and after fluorouracil-based chemoradiation following resection of pancreatic adenocarcinoma: a randomized controlled trial. *JAMA* 2008; 299: 1019-1026 [PMID: 18319412 DOI: 10.1001/jama.299.9.1019]
[166] Regine WF, Winter KA, Abrams R, Safran H, Hoffman JP, Konski A, Benson AB, Macdonald JS, Rich TA, Willett CG. Fluorouracil-based chemoradiation with either gemcitabine or fluorouracil chemotherapy after resection of pancreatic adenocarcinoma: 5-year analysis of the U.S. Intergroup/RTOG 9704 phase III trial. *Ann Surg Oncol* 2011; 18: 1319-1326 [PMID: 21499862 DOI: 10.1245/s10434-011-1630-6]
[167] Schmidt J, Abel U, Debus J, Harig S, Hoffmann K, Herrmann T, Bartsch D, Klein J, Mansmann U, Jäger D, Capussotti L, Kunz R, Büchler MW. Open-label, multicenter, randomized phase III trial of adjuvant chemoradiation plus interferon Alfa-2b versus fluorouracil and folinic acid for patients with resected pancreatic adenocarcinoma. *J Clin Oncol* 2012; 30: 4077-4083 [PMID: 23008325 DOI: 10.1200/JCO.2011.38.2960]
[168] Picozzi VJ, Kozarek RA, Traverso LW. Interferon-based adjuvant chemoradiation therapy after pancreaticoduodenectomy for pancreatic adenocarcinoma. *Am J Surg* 2003; 185: 476-480 [PMID: 12727570 DOI: 10.1016/S0002-9610(03)00051-5]
[169] Picozzi VJ, Abrams RA, Decker PA, Traverso W, O'Reilly EM, Greeno E, Martin RC, Wilfong LS, Rothenberg ML, Posner MC, Pisters PW. Multicenter phase II trial of adjuvant therapy for resected pancreatic cancer using cisplatin, 5-fluorouracil, and interferon-alfa-2b-based chemoradiation: ACOSOG Trial Z05031. *Ann Oncol* 2011; 22: 348-354 [PMID: 20670978 DOI: 10.1093/annonc/mdq384]
[170] Sultana A, Smith CT, Cunningham D, Starling N, Neoptolemos JP, Ghaneh P. Meta-analyses of chemotherapy for locally advanced and metastatic pancreatic cancer. J Clin Oncol. 2007; 25(18): 2607-2615.
[171] Moore MJ, Goldstein D, Hamm J, Figer A, Hecht JR, Gallinger S, Au HJ, Murawa P, Walde D, Wolff RA, Campos D, Lim R, Ding K, Clark G, Voskoglou-Nomikos T, Ptasynski M, Parulekar W; National Cancer Institute of Canada Clinical Trials Group. Erlotinib plus gemcitabine compared with gemcitabine alone in patients with

advanced pancreatic cancer: a phase III trial of the National Cancer Institute of Canada Clinical Trials Group. J Clin Oncol. 2007; 25(15): 1960-1966.

[172] Péron J, Roy P, Ding K, Parulekar WR, Roche L, Buyse M. Assessing the benefit-risk of new treatments using generalised pairwise comparisons: the case of erlotinib in pancreatic cancer. Br J Cancer. 2015 Feb 17. doi: 10.1038/bjc.2015.55. [Epub ahead of print]

[173] Vaccaro V, Bria E, Sperduti I, Gelibter A, Moscetti L, Mansueto G, Ruggeri EM, Gamucci T, Cognetti F, Milella M. First-line erlotinib and fixed dose-rate gemcitabine for advanced pancreatic cancer. World J Gastroenterol. 2013; 19(28): 4511-4519

[174] Van Cutsem E, Li CP, Nowara E, Aprile G, Moore M, Federowicz I, Van Laethem JL, Hsu C, Tham CK, Stemmer SM, Lipp R, Zeaiter A, Fittipaldo A, Csutor Z, Klughammer B, Meng X, Ciuleanu T. Dose escalation to rash for erlotinib plus gemcitabine for metastatic pancreatic cancer: the phase II RACHEL study. Br J Cancer. 2014; 111(11): 2067-2075

[175] Ychou M, Conroy T, Seitz JF, Gourgou S, Hua A, Mery-Mignard D, Kramar A. An open phase I study assessing the feasibility of the triple combination: oxaliplatin plus irinotecan plus leucovorin/ 5-fluorouracil every 2 weeks in patients with advanced solid tumors. Ann Oncol. 2003; 14(3): 481-489.

[176] Conroy T, Paillot B, François E, Bugat R, Jacob JH, Stein U, Nasca S, Metges JP, Rixe O, Michel P, Magherini E, Hua A, Deplanque G. Irinotecan plus oxaliplatin and leucovorin-modulated fluorouracil in advanced pancreatic cancer--a Groupe Tumeurs Digestives of the Federation Nationale des Centres de Lutte Contre le Cancer study. J Clin Oncol. 2005; 23(6): 1228-1236.

[177] Conroy T, Desseigne F, Ychou M, Bouché O, Guimbaud R, Bécouarn Y, Adenis A, Raoul JL, Gourgou-Bourgade S, de la Fouchardière C, Bennouna J, Bachet JB, Khemissa-Akouz F, Péré-Vergé D, Delbaldo C, Assenat E, Chauffert B, Michel P, Montoto-Grillot C, Ducreux M; Groupe Tumeurs Digestives of Unicancer; PRODIGE Intergroup. FOLFIRINOX versus gemcitabine for metastatic pancreatic cancer. N Engl J Med. 2011; 364(19): 1817-1825

[178] Gill S, Ho MY, Kennecke HF, Renouf DJ, Cheung WY, Lim HJ. Defining eligibility of FOLFIRINOX for first-line metastatic pancreatic adenocarcinoma (MPC) in the province of British Columbia: a population-based retrospective study. ASCO Meet Abstr. 2012; 30 (15 Suppl): e14588

[179] Faris J Blaszkowsky L, McDermott S, Guimaraes AR, Szymonifka J, Huynh MA, Ferrone CR, Wargo JA, Allen JN, Dias LE, Kwak EL, Lillemoe KD, Thayer SP, Murphy JE, Zhu AX, Sahani DV, Wo JY, Clark JW, Fernandez-del Castillo C, Ryan DP, Hong TS. FOLFIRINOX in locally advanced pancreatic cancer: the Massachusetts General Hospital Cancer Center experience. Oncologist 2013; 18(5): 543-548

[180] Goncalves PH, Ruch JM, Byer J, Shields AF, Choi M, Kim RD, Zalupski MM, Philip PA. Multi-institutional experience using 5-fluorouracil, leucovorin, irinotecan, and oxaliplatin (FOLFIRINOX) in patients with pancreatic cancer (PCA). ASCO Meet Abstr 2012; 30(15 Suppl): e14519

[181] Gourgou-Bourgade S, Bascoul-Mollevi C, Desseigne F, Ychou M, Bouche O, Guimbaud R, Bécouarn Y, Adenis A, Raoul JL, Boige V, Bérille J, Conroy T. Impact of FOLFIRINOX Compared With Gemcitabine on Quality of Life in Patients With Metastatic Pancreatic Cancer: Results From the PRODIGE 4/ACCORD 11 Randomized Trial. J Clin Oncol 2013; 31(1): 23-29

[182] Valsecchi ME, Diaz-Canton E, de la Vega M, Littman SJ. Recent treatment advances and novel therapies in pancreas cancer: a revire. J Gastrointest Canc 2014; 45: 190-201

[183] Kharofa J, Kelly TR, Ritch PS, George B, Wiebe LA, Thomas JP et al. 5-FU/levocovorin, irinotecan, oxaliplatin (FOLFIRINOX) induction followed by chemoXRT in borderline resectable pancreatic cancer. ASCO Meet Abstr 2012; 30(15 suppl): e14613

[184] Hosein PJ, Macintyre J, Kawamura C, Maldonado JC, Ernani V, Loaiza-Bonilla A, Narayanan G, Ribeiro A, Portelance L, Merchan JR, Levi JU, Rocha-Lima CM. A retrospective study of neoadjuvant FOLFIRINOX in unresectable or borderline-resectable locally advanced pancreatic adenocarcinoma. BMC Cancer 2012; 12: 199

[185] Boone B, Steve J, Krasinskas A, Zureikat A, Lembersky B, Gibson M, Stoller RG, Zeh HJ, Bahary N. Outcomes with FOLFIRINOX for borderline resectable and locally unresectable pancreatic cancer. J Surg Oncol. 2013; 108(4): 236-241

[186] Frese KK, Neesse A, Cook N, Bapiro TE, Lolkema MP, Jodrell DI, Tuveson DA. nab-Paclitaxel potentiates gemcitabine activity by reducing cytidine deaminase levels in a mouse model of pancreatic cancer. Cancer Discov 2012; 2(3): 260-269

[187] Von Hoff DD, Ramanathan RK, Borad MJ, Laheru DA, Smith LS, Wood TE, Korn RL, Desai N, Trieu V, Iglesias JL, Zhang H, Soon-Shiong P, Shi T, Rajeshkumar NV, Maitra A, Hidalgo M. Gemcitabine plus nab-paclitaxel is an active regimen in patients with advanced pancreatic cancer: a phase I/II trial. J Clin Oncol 2011; 29(34): 4548-4554.

[188] Von Hoff DD, Ervin T, Arena FP, Chiorean EG, Infante J, Moore M, Seay T, Tjulandin SA, Ma WW, Saleh MN, Harris M, Reni M, Dowden S, Laheru D, Bahary N, Ramanathan RK, Tabernero J, Hidalgo M, Goldstein D, Van Cutsem E, Wei X, Iglesias J, Renschler MF. Increased survival in pancreatic cancer with nab-paclitaxel plus gemcitabine. N Engl J Med 2013; 369(18): 1691-1703.
[189] Goldstein D, El-Maraghi RH, Hammel P, Heinemann V, Kunzmann V, Sastre J, Scheithauer W, Siena S, Tabernero J, Teixeira L, Tortora G, Van Laethem JL, Young R, Penenberg DN, Lu B, Romano A, Von Hoff DD. nab-Paclitaxel plus gemcitabine for metastatic pancreatic cancer: long-term survival from a phase III trial. J Natl Cancer Inst. 2015; 107(2). pii: dju413.
[190] Hoy SM. Albumin-bound paclitaxel: a review of its use for the first-line combination treatment of metastatic pancreatic cancer. Drugs. 2014; (15): 1757-1768
[191] Desai NV, Hughes S, Ivey A, Hochwald SN, Allegra CJ, Trevino JG, Dang LH, Behrns K, Lightsey JL, Zlotecki R, Liu C, Chauhan S, Zajac-Kaye M, Toro TZ, Hou W, George TJ. Gemcitabine with nab-paclitaxel in neoadjuvant treatment of pancreatic adenocarcinoma: GAIN-1 study. ASCO Meet Abstr 2012; 30(15 suppl): TPS4136
[192] Phase 2 Nab® -Paclitaxel (Abraxane®) Plus Gemcitabine in Subjects with Locally Advanced Pancreatic Cancer (LAPC) (LAPACT). Available from URL: https://clinicaltrials.gov/ct2/show/NCT02301143
[193] Alvarez-Gallego R, Cubillo A, Rodriguez-Pascual J, Quijano Y, Vicente ED, García L, López-Ríos F, Plaza C, García-García E, Morelli MP, Hidalgo M. Antitumor activity of nab-paclitaxel and gemcitabine in resectable pancreatic cancer. ASCO Meet Abstr 2012; 30(suppl 15): 4040
[194] Sawada N, Fujimoto-Ouchi K, Ishikawa T. Anti tumour activity of combination therapy with capecitabine plus vinorelbine, and capecitabine plus gemcitabine in human tumor xenograft models. Proc Am Assoc Cancer Res 2002; 43: 1088 (Abstract 5388)
[195] Cunningham D, Chau I, Stocken DD, Valle JW, Smith D, Steward W, Harper PG, Dunn J, Tudur-Smith C, West J, Falk S, Crellin A, Adab F, Thompson J, Leonard P, Ostrowski J, Eatock M, Scheithauer W, Herrmann R, Neoptolemos JP. Phase III randomized comparison of gemcitabine versus gemcitabine plus capecitabine in patients with advanced pancreatic cancer. J Clin Oncol. 2009; 27(33): 5513-5518
[196] Kindler HL, Niedzwiecki D, Hollis D, Sutherland S, Schrag D, Hurwitz H, Innocenti F, Mulcahy MF, O'Reilly E, Wozniak TF, Picus J, Bhargava P, Mayer RJ, Schilsky RL, Goldberg RM. Gemcitabine plus bevacizumab compared with gemcitabine plus placebo in patients with advanced pancreatic cancer: phase III trial of the Cancer and Leukemia Group B (CALGB 80303). J Clin Oncol. 2010; 28(22): 3617-3622
[197] Philip PA, Benedetti J, Corless CL, Wong R, O'Reilly EM, Flynn PJ, Rowland KM, Atkins JN, Mirtsching BC, Rivkin SE, Khorana AA, Goldman B, Fenoglio-Preiser CM, Abbruzzese JL, Blanke CD. Phase III study comparing gemcitabine plus cetuximab versus gemcitabine in patients with advanced pancreatic adenocarcinoma: Southwest Oncology Group-directed intergroup trial S0205. J Clin Oncol. 2010; 28(22): 3605-3610
[198] Kindler HL, Richards DA, Garbo LE, Garon EB, Stephenson JJ Jr, Rocha-Lima CM, Safran H, Chan D, Kocs DM, Galimi F, McGreivy J, Bray SL, Hei Y, Feigal EG, Loh E, Fuchs CS. A randomized, placebo-controlled phase 2 study of ganitumab (AMG 479) or conatumumab (AMG 655) in combination with gemcitabine in patients with metastatic pancreatic cancer. Ann Oncol. 2012; 23(11): 2834-2842
[199] Spano JP, Chodkiewicz C, Maurel J, Wong R, Wasan H, Barone C, Létourneau R, Bajetta E, Pithavala Y, Bycott P, Trask P, Liau K, Ricart AD, Kim S, Rixe O. Efficacy of gemcitabine plus axitinib compared with gemcitabine alone in patients with advanced pancreatic cancer: an open-label randomised phase II study. Lancet. 2008; 371(9630): 2101-2108
[200] Trial Comparing Adjuvant Chemotherapy with Gemcitabine Versus mFolfirinox to Treat Resected Pancreatic Adenocarcinoma. Available from URL: https://clinicaltrials.gov/ct2/show/NCT01526135
[201] Nab-paclitaxel and Gemcitabine vs Gemcitabine Alone as Adjuvant Therapy for Patients With Resected Pancreatic Cancer (the "Apact" Study). Avaiilable from URL: https://clinicaltrials.gov/ct2/show/NCT01964430?term=NCT01964430&rank=1
[202] Bao PQ, Ramanathan RK, Krasinkas A, Bahary N, Lembersky BC, Bartlett DL, Hughes SJ, Lee KK, Moser AJ, Zeh HJ 3rd. Phase II study of gemcitabine and erlotinib as adjuvant therapy for patients with resected pancreatic cancer. Ann Surg Oncol. 2011; 18(4): 1122-1129
[203] Herman JM, Fan KY, Wild AT, Hacker-Prietz A, Wood LD, Blackford AL, Ellsworth S, Zheng L, Le DT, De Jesus-Acosta A, Hidalgo M, Donehower RC, Schulick RD, Edil BH, Choti MA, Hruban RH, Pawlik TM, Cameron JL, Laheru DA, Wolfgang CL. Phase 2 study of erlotinib combined with adjuvant chemoradiation and chemotherapy in patients with resectable pancreatic cancer. Int J Radiat Oncol Biol Phys. 2013; 86(4): 678-685
[204] CONKO-005: Adjuvant Therapy in R0-resected Pancreatic Cancer Patients with Gemcitabine plus Erlotinib vs. Gemcitabine over 24 Weeks - a Prospective, Randomized Phase III Study. Available from URL: http://apps.who.int/trialsearch/trial.aspx?trialid=DRKS00000247

[205] Gemcitabine hydrochloride with or without erlotinib hydrochloride followed by the same chemotherapy regimen with or without radiation therapy and capecitabine or flurouracil in treating patients with pancreatic cancer that has been removed by surgery. Available from URL: http://clinicaltrials.gov/show/NCT01013649
[206] Heinrich S, Schafer M, Weber A, Hany TF, Bhure U, Pastalozzi BC, Clavien PA. Neoadjuvant chemotherapy generates a significant tumour response in resectable pancreatic cancer without increasing morbidity: results of a prospective phase II trial. Ann Surg 2008; 248(6): 1014-22
[207] Sahora K, Kuehrer I, Eisenhut A, Akan B, Koellblinger C, Goetzinger P, Teleky B, Jakesz R, Peck-Radosavljevic M, Ba'ssalamah A, Zielinski C, Gnant M. NeoGemOx: Gemcitabine and oxaliplatin as neoadjuvant treatment for locally advanced, nonmetastasized pancreatic cancer. Surgery 2011; 149(3): 311-320
[208] Hyperthermia European Adjuvant Trial (HEAT). Available at URL: https://clinicaltrials.gov/ct2/show/NCT01077427?term=NCT01077427&rank=1
[209] Issels RD. Hyperthermia adds to chemotherapy. Eur J Cancer 2008; **44**: 2546–2554
[210] Adachi S, Kokura S, Okayama T, Ishikawa T, Takagi T, Handa O, Naito Y, Yoshikawa T. Effect of hyperthermia combined with gemcitabine on apoptotic cell death in cultured human pancreatic cancer cell lines. Int J Hyperthermia 2009; **25**: 210–219
[211] Ishikawa T, Kokura S, Sakamoto N, Ando T, Imamoto E, Hattori T, Oyamada H, Yoshinami N, Sakamoto M, Kitagawa K, Okumura Y, Yoshida N, Kamada K, Katada K, Uchiyama K, Handa O, Takagi T, Yasuda H, Sakagami J, Konishi H, Yagi N, Naito Y, Yoshikawa T. Phase II trial of combined regional hyperthermia and gemcitabine for locally advanced or metastatic pancreatic cancer. Int J Hyperthermia 2012; **28**(7): 597-604
[212] Tschoep-Lechner K, Milani V, Berger F, Dieterle N, Abdel-Rahman S, Salat C, Issels RD. Gemcitabine and cisplatin combined with regional hyperthermia as second-line treatment in patients with gemcitabine-refractory advanced pancreatic cancer. Int. J. Hyperthermia 2013; **29**(1): 8–16
[213] Immunotherapy Study for Surgically Resected Pancreatic Cancer. Available at URL: https://clinicaltrials.gov/ct2/show/NCT01072981?term=NCT01072981&rank=1
[214] Hardacre JM, Mulcahy M, Small W, Talamonti M, Obel J, Krishnamurthi S, Rocha-Lima CS, Safran H, Lenz HJ, Chiorean EG. Addition of algenpantucel-L immunotherapy to standard adjuvant therapy for pancreatic cancer: a phase 2 study. J Gastrointest Surg. 2013; 17(1): 94-100
[215] Adjuvant Versus Neoadjuvant Plus Adjuvant Chemotherapy in Resectable Pancreatic Cancer. https://clinicaltrials.gov/ct2/show/NCT01314027?term=NCT01314027&rank=1
[216] Phase III FOLFIRINOX (mFFX) +/- SBRT in Locally Advanced Pancreatic Cancer. Available at URL: https://clinicaltrials.gov/ct2/show/NCT01926197?term=NCT01926197&rank=1
[217] Pancreatic Carcinoma: Chemoradiation Compared With Chemotherapy Alone After Induction Chemotherapy (CONKO-007). Available at URL: https://clinicaltrials.gov/ct2/show/NCT01827553?term=NCT01827553&rank=1
[218] Immunotherapy Study in Borderline Resectable or Locally Advanced Unresectable Pancreatic Cancer (PILLAR). Available at URL: https://clinicaltrials.gov/ct2/show/NCT01836432?term=NCT01836432&rank=1
[219] Jones S, Zhang X, Parsons DW, Lin JC, Leary RJ, Angenendt P, Mankoo P, Carter H, Kamiyama H, Jimeno A, Hong SM, Fu B, Lin MT, Calhoun ES, Kamiyama M, Walter K, Nikolskaya T, Nikolsky Y, Hartigan J, Smith DR, Hidalgo M, Leach SD, Klein AP, Jaffee EM, Goggins M, Maitra A, Iacobuzio-Donahue C, Eshleman JR, Kern SE, Hruban RH, Karchin R, Papadopoulos N, Parmigiani G, Vogelstein B, Velculescu VE, Kinzler KW. Core signalling pathways in human pancreatic cancers revealed by global genomis analyses. Science 2008; 321: 1801-1806
[220] Piccart-Gebhart MJ[1], Procter M, Leyland-Jones B, Goldhirsch A, Untch M, Smith I, Gianni L, Baselga J, Bell R, Jackisch C, Cameron D, Dowsett M, Barrios CH, Steger G, Huang CS, Andersson M, Inbar M, Lichinitser M, Láng I, Nitz U, Iwata H, Thomssen C, Lohrisch C, Suter TM, Rüschoff J, Suto T, Greatorex V, Ward C, Straehle C, McFadden E, Dolci MS, Gelber RD; Herceptin Adjuvant (HERA) Trial Study Team. Trastuzumab after Adjuvant Chemotherapyin HER2-Positive Breast Cancer. NEJM 2005; 353(16): 1659-72
[221] Costello E, Greenhalf W, Neoptolemos JP. New biomarkers and targets in pancreatic cancer and their application to treatment. Nat Rev Gastro Hepat 2012; 9: 435-444
[222] Hidalgo M, Plaza C, Musteanu M, Illei P, Brachmann CB, Heise C, Pierce D, Lopez-Casas PP, Menendez C, Tabernero J, Romano A, Wei X, Lopez-Rios F, Von Hoff DD. SPARC expression did not predict efficacy of nab-Paclitaxel plus gemcitabine or gemcitabine alone for metastatic pancreatic cancer in an exploratory analysis of the phase III MPACT trial. Clin Can Res 2015; 21: 4811-4818
[223] Greenhalf W, Ghaneh P, Neoptolemos JP, Palmer DH, Cox TF, Lamb RF, Garner E, Campbell F, Mackey JR, Costello E, Moore MJ, Valle JW, McDonald AC, Carter R, Tebbutt NC, Goldstein D, Shannon J, Dervenis C, Glimelius B, Deakin M, Charnley RM, Lacaine F, Scarfe AG, Middleton MR, Anthoney A, Halloran CM, Mayerle J, Olah A, Jackson R, Rawcliffe CL, Scarpa A, BassiC, Buchler MW. J Natl Cancer Inst 2014; 106: djt347

[224] Poplin E, Wasan H, Rolfe L, Raponi M, Ikdahl T, Bondarenko I, Davidenko I, Bondar V, Garin A, Boeck S, Ormanns S, Heinemann V, Bassi C, Jeffrey Evans TR, Andersson R, Hahn H, Picozzi V, Dicker A, Mann E, Voong C, Kaur P, Isaacson J, Allen A. Randomised, multicentre, phase II study of CO-101 versus gemcitabine in patients with metastatic pancreatic ductal adenocarcinoma: including a prospective evaluation of the role of hENT1 in gemcitabine or CO-101 sensitivity. J Clin Oncol 2013; 31(35): 4453-4461

[225] Sinn M, Riess H, Sinn BV, Pelzer U, Striefler JK, Oettle H, Bahra M, Denkert M, Blaker H, Lohneis P. Human equilibrative nucleoside transporter 1 expression analysed by the clone SP 120 rabbit antibody is not predictive in patients with pancreatic cancer treated with adjuvant gemcitabine – results from the CONKO-001 trial. Eur J Cancer 2015; 51: 1546-1554

[226] Fearon DT. The carcinoma-associated fibroblast expressing fibroblast activation protein and escape from immune surveillance. Cancer Immunol Res 2014; 2: 187-193

[227] Feig C, Jones JO, Kraman M, Wells RJ, Deonarnine A, Chan DS, Connell CM, Roberts EW, Zhao Q, Caballero OL, Teichmann SA, Janowitz T, Jodrell DI, Tuveson DA, Fearon DT. Targetting CXCL12 from FAP-expressing carcinoma-associated fibroblasts synergizes with anti-PD-L1 immunotherapy in pancreatic cancer. Proc Natl Acad USA 2013; 110: 20212-20217

[228] Hertel LW, Kroin JS, Misner JW, Tustin JM. Synthesis of 2'-deoxy-2'2'-difluoro-D-ribose and 2'-deoxy-2',2'-difluoro-D-ribofuranosyl nucleosides. J Org Chem 1988: 53(11): 2406-2409

[229] Griffith DA, Jarvis SM. Nucleoside and nucleobase transport systems of mammalian cells. Biochem Biophys Acta 1996; 1286: 153-181

[230] Ritzel MW, Ng AM, Yao SY, Graham K, Loewen SK, Smith KM, Hyde RJ, Karpinski E, Cas CE, Baldwin SA, Young JD .Recent molecular advances in studies of the concentrative Na^+-dependent nucleoside transporter (CNT) family: identification and characterization of novel human and mouse proteins (hCNT3andmCNT3) broadly selective for purine and pyrimidine nucleosides. Mol Memb Biol 2001; 18: 65-72

[231] Mackey JR, Mani RS, Selner M, Mowles D, Young JD, Belt CA,Crawford CR, Cass CE. Functional nucleoside transporters are required for gemcitabine influx and manifestation of toxicity in cancer cell lines. Cancer Res 1998; 58: 4349-4357

[232] Spratlin JL, Mackey JR. Human equilibrative nusleoside transporter 1 (hENT1) in pancreatic adenocarcinoma: towards individualized treatment decisions. Cancers 2010; 2: 2044-2054

[233] Van Rompay AR, Johansson M, Karlsson A. Phosphorylation of deoxycytidine analog monophosphates by UMP-CMP kinase: molecular characterization of the human enzyme. Mol Pharmacol 1999; 56: 562-569.

[234] Heinemann V, Hertel LW, Grindley GB et al. Comparison of the cellular pharmacokinetics and toxicity of 2',2'-difluorodeoxycytidine and 1-beta-D-arabinofuranosylcytosine. Cancer Res 1988; 48: 4024-4031

[235] Wong A, Soo RA, Yong WP, Innocenti F. Clinical pharmacology and pharmacogenetics of gemcitabine. Drug Metab Rev 2009; 41: 77–88

[236] Honeywell RJ, Ruiz van Haperen VW, Veerman G, Smid K, Peters GJ. Inhibition of thymidylate synthase by 2',2'-difluoro-2'-deoxycytidine (Gemcitabine) and its metabolite 2',2'-difluoro-2'-deoxyuridine. Int J Biochem Cell Biol. 2015; 60: 73-81

[237] Bergman AM, Giaccone G, van Moorsel CJ, Mauritz R, Noordhuis P, Pinedo HM, Peters GJ. Cross-resistance in the 2'2'-difluorodeoxycytidine (gemcitabine) -resistant human ovarian cancer cell line AG6000 to standard and investigational drugs. Eur J Cancer 2000; 36: 1974-1983

[238] Longley DB, Harkin DP, Johnston PG. 5-Fluorouracil: mechanisms of action and clinical strategies. Nat Rev Cancer 2003; 3: 330-338

[239] Veltkamp SA, Pluim D, van Eijndhoven MA, Bolijn MJ, Ong FH, Govindarajan R, Unadkat JD, Beijnen JH, Schellens JH. New insights into the pharmacology and cytotoxicity of gemcitabine and 2'2'-difluorodeoxyuridine. Mol Cancer Ther 2008; 7: 2415-2425

[240] Gandi V, Plunkett W. Modulatory activity of 2',2'-difluorodeoxycytidine on the phosphorylation and cytotoxicity of arabinosyl nucleosides. Cancer Res 1990; 50: 3675-3680

[241] Huang P, Chubb S, Hertel LW, Grindey GB, Plunkett W. Action of 2',2'-difluorodeoxycytidine on DNA synthesis. Cancer Res 1991; 51: 6110-6117

[242] Plunkett W, Huang P, Xu YZ, Heinemann V, Grunewald R, Gandhi V. Gemcitabine: metabolism, mechanisms of action, and self-potentiation. Semin Oncol. 1995; 22(4 Suppl 11): 3-10

[243] Mini E, Nobili S, Caciagli B, Landini I, Mazzei T. Cellular pharmacology of gemcitabine. Annal Oncol 2006; 17(supp 5): v7-12

[244] Heinemann V, Xu YZ, Chubb S, Sen A, Hertel LW, Grindey GB, Plunkett W. Inhibition of ribonucleotide reduction in CCRF-CEM cells by 2',2'-difluorodeoxycytidine. Mol Pharmacol 1990; 38: 567-572

[245] Ruiz van Haperen VW, Veerman G, Vermorken JB, Pinedo HM, Peters G. Regulation of phosphorylation of deoxycytidine and 2',2'-difluorodeoxycytidine (gemcitabine); effects of cytidine 5'-triphosphate and uridine 5'-triphosphate in relation to chemosensitivity for 2',2'-difluorodeoxycytidine. Biochem Pharmacol 1996; 51: 911-918

[246] Ewald B, Sampath D, Plunkett W. H2AX phosphorylation marks gemcitabine-induced stalled replication forks and their collapse upon S-phase checkpoint abrogation. Mol Cancer Ther 2007; 6: 1239-1248

[247] Bartek J, Lukas J. Chk1 and Chk2 kinases in checkpoint control and cancer. Cancer Cell 2003; 3: 421-429

[248] Zhou BB, Elledge SJ. The DNA damage response: putting checkpoints in perspective. Nature 2000; 408: 433-439

[249] Azorsa DO, Gonzales IM, Basu GD, Choudhary A, Arora S, Bisanz KM, Kiefer JA, Henderson MC, Tretnt JM, Von Hoff DD, Mousses S. Synthetic lethal RNAi screening identifies sensitizing targets for gemcitabine therapy in pancreatic cancer. J Transl Med 2009; 7: 43

[250] Hamed SS, Straubinger RM, Jusko WJ. Pharmacodynamic modelling of cell cycle and apoptotic effects of gemcitabine on pancreatic adenocarcinoma cells. Cancer Chemother Pharmacol 2013; 72(3): 553-563

[251] Carpenelli G, Bucci G, D'Agnano I, Canese R, Caroli F, Raus L, Brunetti E, Giannarelli E, Podo F, Carapella CM. Gemcitabine treatment of experimental C6 glioma: the effects on cell cycle and apoptotic rate. Antcancer Res 2006; 26: 3017-3024

[252] Pauwels B, Korst AE, Pattyn GG, Lambrechts HA, Van Bockstaele DR, Vermeulen K, Lenjou M, de Pooter CM, Vermorken JB, Lardon F. Cell cycle effect of gemcitabine and its role in radiosensitizing mechanism in virto. Int J Radiat Oncol Biol Phys 2003; 57: 1075-1083

[253] Hertel LW, Boder GB, Kroin JS, Rinzel SM, Poore GA, Todd GC, Grindey GB. Evaluation of the antitumor activity of gemcitabine (2',2'-difluoro-2'-deoxycytidine). Cancer Res 1990; 50: 4417-4422

[254] Rockwell S, Grindley GB. Effect of 2',2'-difluorodeoxycytidine on the viability and radiosensitivity of EMT6 cells in vitro. Oncol Res 1992; 4: 151-155

[255] Jiang PH, Motoo Y, Sawabu N, Minamoto T. Effect of gemcitabine on the expression of apoptosis-related genes in human pancreatic cancer cells. World J Gastroenterol 2006; 12(10): 1597-1602

[256] Chandler NM, Canete JJ, Callery MP. Caspase-3 drives apoptosis in pancreatic cancer cells after treatment with gemcitabine. J Gastrointest Surg. 2004; 8(8): 1072-1078.

[257] Schniewind B, Christgen M, Kurdow R, Haye S, Kremer B, Kalthoff H, Ungefroren H. Resistance of pancreatic cancer to gemcitabine treatment is dependent on mitochondria-mediated apoptosis. Int J Cancer 2004; 109(2): 182-188

[258] Habiro A, Tanno S, Koizumi K, Izawa T, Nakano Y, Osanai M, Mizukami Y, Okumura T, Kohgo Y. Involvement of p38 mitogen-activated protein kinase in gemcitabine-induced apoptosis in human pancreatic cancer cells. Biochem Biophys Res Commun 2004; 316: 71-77

[259] Cavalcante LS, Monteiro G. Gemcitabine: metabolism and molecular mechanisms of action, sensitivity and chemoresistance in pancreatic cancer. Eur J Pharmacol 2014; 741: 8-16

[260] Giovanetti E, Del Tacca M, Mey V, Funel N, Nannizzi S, Ricci S, Orlandini C, Boggi U, Campani D, Del Chiaro M, Iannopollo M, Bevilacqua G, Mosca F, Danesi R. Transcription analysis of human equilibrative nucleoside transporter-1 predicts survival in pancreas cancer parients treated with gemcitabine. Cancer Res 2006; 66: 3928-3935

[261] Skrypek N, Duchene B, Hebbar M, Leteutre E, van Seuningen I, Jonckheere N. The MUC4 mucin mediates gemcitabine resistance of human pancreatic cancer cells via the concentrative nucleoside transporter family. Oncogene 2013; 32: 1714-1723

[262] Ohhashi S, Ohuchida K, Mizumoto K, Fujita H, Egami T, Yu J, Toma H, Sadatomi S, Nagai E, Tanaka M. Downregulation of deoxycytidine kinase enhances acquired resistance to gemcitabine in pancreatic cancer. Anticancer Res 2008; 28: 2205-2212

[263] Nakano Y, Tanno S, Koizumi K, Nishikawa T, Nakamura K, Minoguchi M, Izawa Y, Mizukami Y, Okumura T, Kohgo Y. Gemcitabine chemoresistance and molecular markers associated with gemcitabine transport and metabolism in human pancreatic cancer cells. Br J Cancer 2007; 96: 457-463

[264] Duxbury MS, Ito H, Zinner MJ, Ashley SW, Whang EE. RNA interference targeting the M2 subunit of ribonucleotide reductase enhances pancreatic adenocarcinoma chemosensitivity to gemcitabine. Oncogene 2004; 23: 1539-1548

[265] Llamazares S, Moreira A, Tavares A et al. Polo encodes a protein kinase homolog required for mitosis in Drosophilia. Genes Dev 1991; 5(12A): 2153-65

[266] Sunkel CE, Glover DM. Polo, a mitotic mutant of Drosophila displaying abnormal spindle poles. J Cell Sci 1988; 89: 25-38

[267] Fode C, Motro B, Yousefi S, Heffernan M, Dennis JW. Sak, a murine protein-serine/threonine kinase that is related to the Drosophila polo kinase and involved in cell proliferation. Proceedings of the National Academy of Sciences of the United States of America 1994; 91(14): 6388-6392
[268] de Carcer G, Escobar B, Higuero AM, Garcia L, Anson A, Perez G, Mollejo M, Manning G, Melendez B, Abad-Rodriguez J, Malumbres M. Plk5, a polo box domain-only protein with specific roles in neuron differentiation and glioblastoma suppression. Mol Cell Biol 2011; 31(6): 1225-39
[269] Goto H, Kiyono T, Tomono Y, Kawajiri A, Urano T, Furukawa K, Nigg EA, Inagaki M. Complex formation of Plk1 and INCENP required for metaphase-anaphase transition. Nat Cell Biol 2006; 8: 180-187
[270] Nguyen HG, Ravid K. Tetraploidy/aneuploidy and stem cells in cancer promotion: the role of chromosome passenger proteins. J Cell Physiol 2006; 208: 12-22
[271] Lowery DM, Lim D, Yaffe MB. Structure and function of Polo-like kinases. Oncogene 2005; 24: 248-259
[272] Elia AE, Cantley LC, Yaffe MB. Proteomic screen finds pSer/pThr-binding domain localizing Plk1 to mitotic subtrates. Science 2003; 299(5610): 1228-1231
[273] Cheng KY, Lowe ED, Sinclair J, Nigg EA, Johnson LN. The crystal structure of the human polo-like kinase-1 polo box domain and its phosphopeptide complex. Embo J 2003; 22: 5757-68
[274] Hanks SK, Hunter T. Protein kinases 6. The eukaryotic protein kinase super family: kinase (catalytic) domain structure and classification. FASEB J 1995; 9(8): 576-596
[275] Weiβ L, Efferth T. Polo-like kinase 1 as a target for cancer therapy. Exp Hematol Oncol 2012; 14(1); 38-43
[276] Donohue PJ, Alberts GF, Guo Y, Winkles JA. Identification by targeted differential display of an immediate early gene encoding a putative serine/threonine kinase. J Biol Chem 1995; 270(17): 10351-10357
[277] Liu Y, Gray NS. Rational design of inhibitors that bind to inactive kinase conformations. Nat Chem Biol 2006; 2: 358-364
[278] Jani KS, Dalafave DS. Computational design of targeted inhibitors of polo-like kinase 1 (Plk1). Bioinform Biol Insights 2012; 6: 23-31
[279] Andrysik Z, Bernstein WZ, Deng L, Myer DL, Li YQ, Tischfield JA, Stambrook PJ, Bahassi el M. The novel mouse Polo-like kinase 5 responds to DNA damage and localizes in the nucleolus. Nucleic Acids Res 2010; 38(9): 2931-43
[280] Zitouni S, Nabais C, Jana SC, Guerrero A, Bettencourt-Dias M. Polo-like kinases: structural variations lead to multiple functions. Nat Rev 2014; 15: 433-452
[281] Barr FA, Sillje HHW, Nigg EA. Polo-like kinases and the orchestration of cell division. Nat Rev Mol Cell Biol. 2004; 5(6): 429-40
[282] Elia AE, Rellos P, Haire LF, Chao JW, Ivins FJ, Hoepker K, Mohammad D, Cantley LC, Smerdon SJ, Yaffe MB. The molecular basis for phosphodependent substrate targeting and regulation of Plks by the Polo-box domain. Cell 2003; 115(1): 83-95
[283] Sillibourne JE, Bornens. Polo-like kinase 4: the odd one out of the family. Cell Division 2010; 5: 25
[284] Leung GC, Hudson JW, Kozarova A, Davidson A, Dennis JW, Sicheri F. The Sak polo-ox comprises a structural domain sufficient for mitotic subcellular localization. Nat Struct Biol 2009; 9: 719-724
[285] Swallow CJ, Ko MA, Siddiqui NU, Hudson JW, Dennis JW. Sak/Plk4 and mitotic fidelity. Oncogene 2005; 24: 306-312
[286] Van de Weerdt BCM, Medema RH. Polo-like kinases, a team in control of the division. Cell Cycle 2006; 5(8): 853-864
[287] Mundt KE, Golsteyn RM, Lane HA, Nigg EA. On the regulation and function of human Polo-like kinase 1 (Plk1): effects of overexpression on cell cycle progression. Biochem Biophys Res Commun 1997; 239: 377-385
[288] Van Vugt MATM, Medema RH. Getting in and out of mitosis with Polo-like kinase-1. Oncogene 2005; 24: 2844-2859
[289] Song S, Grenfell TZ, Garfield S, Erikson RL, Lee KS. Essential function of the polo box of Cdc5 in the subcellular localization and induction of cytokinetic structures. Mol Cell Biol 2000; 20: 286-298
[290] Kothe M, Kohls D, Low S, Coli R, Cheng AC, Jaques SL, Johnson TL, Lewis C, Loh C, Nonomiya J, Sheils AL, Werdries KA, Wynn TA, Kuhn C, Ding YH. Structure of the catalytic domain of human polo-like kinase. Biochemistry 2007; 46: 5960-5971
[291] Nolen B, Taylor S, Ghosh G. Regulation of protein kinases: controlling activity through activation segment conformation. Mol Cell 2004; 15: 661-675
[292] Lee KS, Erikson RL. Plk is a functional homolog of Saccharomyces cerevisiae Cdc5, and elevated Plk activity induces multiple septation structures. Mol Cell Biol. 1997; 17(6): 3408-3417
[293] Schoffski P. Polo-like kinase (PLK) inhibitors in preclinical and early clinical development in oncology. The Oncologist 2009; 14: 559-570

[294] Jang YJ, Ma S, Terada Y, Erikson RL. Phosphorylation of threonine 210 and the role of serine 137 in the regulation of mammalian polo-like kinase. J Biol Chem 2002; 277(46): 44115-44120
[295] Smits VAJ, Klompmaker R, Arnaud L, Rijksen G, Nigg EA, Medema RH. Polo-like kinase-1 is a target of the DNA damage checkpoint. *Nature Cell Biology* 2000; **2**: 672 - 676
[296] Kelm O, Wind M, Lehmann WD, Nigg EA. Cell cycle-regulated phosphorylation of the Xenopus polo-like kinase Plx1. J Biol Chem 2002; 277: 25247-25256
[297] Tsvetkov L, Stern DF. Phosphorylation of Plk1 at S137 and T210 is inhibited in response to DNA damage. Cell Cycle 2005; 4(1): 166-171
[298] Xu J, Shen C, Wang T, Quan J. Structural basis for the inhibition of Polo-like kinase 1. Nature Struct Mol Biol 2013; 20: 1047-1053
[299] Archambault V, D'Avino PP, Deery MJ, Lilley KS, Glover DM. Sequestration of Polo kinase to microtubules by phosphopriming independent binding to Map205 is relieved by phosphorylation at CDK site in mitosis. Genes Dev 2008; 22: 2707-2720
[300] Bruinsma W, Raaijmakers JA, Medema RH. Switching polo-like kinase-1 on and off in time and space. Trends Biochem 2012; 37(12): 534-542
[301] Bruinsma W, Macurek L, Freire R, Lindqvist A, Medema RH. Bora and Aurora-A continue to activate Plk1 in mitosis. J Cell Sci 2014; 127: 801-811
[302] Chan EH, Santamaria A, Sillje HH, Nigg EA. Plk1 regulates mitotic Aurora A function through βTrCP-dependent degradation of hBora. Chromosoma 2008; 117: 457-469
[303] Seki A, Coppinger JA, Du H, Jang CY, Yates JR 3rd, Fang G. Plk1- and beta-TrCP-dependent degradation of Bora controls mitotic progression. J Cell Biol 2008; 181: 65-78
[304] Macurek L, Lindqvist A, Lim D, Lampson MA, Klopmaker R, Freire R, Clouin C, Taylor SS, Yaffe MB, Medema RH. Polo-like kinase-1 is activated by aurora A to promote checkpoint recovery. Nature 2008; 455: 119-123
[305] Kufer TA et al . Human TPX2 is required for targeting Aurora A kinase to the spindle. 2002 J Cell Biol 2002; 158: 617-623
[306] Macurek L, Lindqvist A, Lim D, Lampson MA, Klompmaker R, Freire R, Clouin C, Taylor SS, Yaffe MB, Medema RH. Polo-like kinase-1 is activated by aurora A to promote checkpoint recovery. Nature 2008; 455: 119-123
[307] Ellinger-Ziegelbauer H, Karasuyama H, Yamada E, Tsuijikawa K, Todokoro K, Nishida E. Ste20-like kinase (SLK), a regulatory kinase for polo-like kinase (Plk) during the G2/M transition in somatic cells. Genes Cells 2000; 5: 491-498
[308] Walter S.S, Cutler RE Jr, Martinex R, Gishizky M, Hill RJ. Stk10, a new member of the polo-like kinase kinase family highly expressed in haemopoetic tissue. J Biol Chem 2003; 278: 18221-18228
[309] Hu CK, Ozlu N, Coughlin M, Steen JJ, Mitchison TJ. Plk1 negatively regulates PRC1 to prevent premature midzone formation before cytokinesis. Mol Biol Cell 2012; 23: 2702-2711
[310] Yoo HY, Kumagai A, Shevchenko A, Dunphy WG. Adaptation of a DNA replication checkpoint response depends upon inactivation of Claspin by the Polo-like kinase. Cell 2004; 117(5): 575-588
[311] Santamaria A, Neef R, Eberspacher U, Eis K, Husemann M, Mumberg D, Prechtl S, Schulze V, Siemeister G, Wortmann L, Barr FA, Nigg EA. Use of the novel Plk1 inhibitor ZK-Thiavolidinone to eludicate functions of Plk1 in early and late stages of mitosis. Mol Biol Cell 2007; 18: 4024-4036
[312] Nakajima H, Toyoshima-Morimoto F, Taniguchi E, Nishida E. Identification of a consensus motif for Plk (Polo-like kinase) phosphorylation reveals Mut1 as a Plk1 substrate. J Biol Chem 2003; 278: 25277-25280
[313] Jackman M, Lindon C, Nigg EA, Pines J. Active cyclin B1-Cdk1 first appears on centrosomes in prophase. Nat Cell Biol. 2003; 5(2):143-148
[314] Yuan J, Eckerdt F, Bereiter-Hahn J, Kurunci-Csacsko E, Kaufmann M, Strebhardt K. Cooperative phosphorylation including the activity of polo-like kinase 1 regulates the subcellular localization of cyclin B1. Oncogene 2002; 21: 8282-8292
[315] Toyoshima-Morimoto F, Taniguchi E, Shinya N, Iwamatsu A, Nishida E. Polo-like kinase 1 phosphorylates cyclin B1 and targets it to the nucleus during prophase. Nature 2001; 410: 215-220
[316] Toyoshima-Morimoto F, Tanigushi E, Nishida E. Plk1 promotes nuclear translocation of human Cdc25C during prophase. EMBO Rep 2002; 3: 341-348
[317] Sakchaisri K, Asano S, Yu LR, Shulewitz MJ, Park CJ, Park JE, Cho YW, Veenstra TD, Thorner J, Lee KS. Coupling morphogenesis to mitotic entry. Proc Natl Acad Sci U S A. 2004; 101(12): 4124-4129
[318] Watanabe N, Arai H, Nishihara Y, Taniguchi M, Hunter T, Osada H. M-phase kinases induce phospho-dependent ubiquitination of somatic Wee1 by SCFbeta-TrCP. Proc Natl Acad Sci U S A. 2004;101(13):4419-4424

[319] Lin HR, Ting NS, Qin J, Lee WH. M phase-specific phosphorylation of BRCA2 by Polo-like kinase 1 correlates with the dissociation of the BRCA2-P/CAF complex. J Biol Chem 2003; 278: 35979-35987
[320] Nakajima H, Toyoshima-Morimoto F, Taniguchi E, Nishida E. Identification of a consensus motif for Plk (Polo-like kinase) phosphorylation reveals Myt1 as a Plk1 substrate. J Biol Chem. 2003; 278(28): 25277-25280
[321] Casenghi M, Meraldi P, Weinhart U, Duncan PI, Körner R, Nigg EA. Polo-like kinase 1 regulates Nlp, a centrosome protein involved ini microtubule nucleation. Dev Cell 2003; 5: 113-125
[322] Zhou T, Aumais JP, Liu X, Yu-Lee LY, Erikson RL. A role for PLK1 phosphorylation od NudC in cytokinesis. Dev Cell 2003; 5: 143-148
[323] Yarm FR.Plk phosphorylation regulates the microtubule-stabilizing protein TCTP. Mol Cell Biol 2002; 22: 6209-6221
[324] Lin CY, Madsen ML, Yarm FR, Jang YJ, Liu X, Erikson RL. Peripheral Golgi protein GRASP65 is a target of mitotic polo-like kinase (Plk) and Cdc2. Proc Natl Acad Sci U S A. 2000; 97(23): 12589-12594
[325] Sutterlin C, Lin CY, Feng Y, Ferris DK, Erikson RL, Malhotra V. Polo-like kinase is required for the fragmentation of pericentriolar Golgi stacks during mitosis. Proc Natl Acad Sci U S A. 2001; 98(16): 9128-9132
[326] Lee KS, Yuan YL, Kuriyama R, Erikson RL. Plk is an M-phase-specific protein kinase and interacts with a kinesin-like protein, CHO1/MKLP-1. Mol Cell Biol. 1995; 15(12): 7143-51
[327] Liu X, Zhou T, Kuriyama R, Erikson RL. Molecular interactions of Polo-like-kinase 1 with the mitotic kinesin-like protein CHO1/MKLP-1. J Cell Sci. 2004; 117(15): 3233-3246
[328] Neef R, Preisinger C, Sutcliffe J, Kopajtich R, Nigg EA, Mayer TU, Barr FA. Phosphorylation of mitotic kinesin-like protein 2 by polo-like kinase 1 is required for cytokinesis. J Cell Biol. 2003; 162(5): 863-875
[329] Bibi N, Parveen Z, Rashid S. Identification of potential Plk1 targets in a cell-cycle specific proteome through structural dynamics of kinase and polo box-mediated interactions. PLOS One 2013; 8(8): e70843
[330] Golsteyn RM, Mundt KE, Fry AM, Nigg EA. Cell cycle regulation of the activity and subcellular localization of Plk1, a human protein kinase implicated in mitotic spindle function. J Cell Biol 1995; 129(6): 1617-1628
[331] Lindon C, Pines J. Ordered proteolysis in anaphase inactivates PLK1 to contribute to proper mitotic exit in human cells. J Cell Biol 2004; 164(2): 233-241
[332] Piaggio G, Farina A, Perrotti D, Manni I, Fuschi P, Sacchi A, Gaetano C. Structure and growth-dependent regulation of the human cyclin B1 promoter. Exp Cell Res 1995; 216: 396-402
[333] Hagting A, Karlsson C, Clute P, Jackman M, Pines J. MPF localization is controlled by nuclear export. EMBO J. 1998; 17(14): 4127-38.
[334] Van Vugt MATM Medema RH. Getting in and out of mitosis. Oncogene 2005; 24: 2844-2859
[335] Trunnell NB, Poon AC, Kim SY, Ferrell JE Jr. Ultrasensitivity in the regulation of Cdc25C by Cdk1. Mol Cell. 2011; 41(3): 263-274.
[336] Atherton-Fessler S, Parker LL, Geahlen RL, Piwnica-Worms H. Mechanisms of p34cdc2 regulation. Mol Cell Biol 1993; 13: 1675-1685
[337] Booher RN, Holman PS, Fattaey A. Human Myt1 is a cell cycle-regulated kinase that inhibits Cdc2 but not Cdk2 activity. J Biol Chem 1997; 272: 22300-22306
[338] Millar JB, McGowan CH, Lenaers G, Jones R, Russell P. p80cdc25 mitotic inducer is the tyrosine phosphatase that activates p34cdc2 kinase in fission yeast. EMBO J. 1991; 10(13): 4301-4309.
[339] Strausfeld U, Labbé JC, Fesquet D, Cavadore JC, Picard A, Sadhu K, Russell P, Dorée M. Dephosphorylation and activation of a p34cdc2/cyclin B complex in vitro by human CDC25 protein. Nature. 1991; 351(6323): 242-245.
[340]Lammer C, Wagerer S, Saffrich R, Mertens D, Ansorge W, Hoffmann I. The cdc25B phosphatase is essential for the G2/M phase transition in human cells. J Cell Sci. 1998; 111(Part 16): 2445-2453.
[341]Fesquet D, Labbé JC, Derancourt J, Capony JP, Galas S, Girard F, Lorca T, Shuttleworth J, Dorée M, Cavadore JC. The MO15 gene encodes the catalytic subunit of a protein kinase that activates cdc2 and other cyclin-dependent kinases (CDKs) through phosphorylation of Thr161 and its homologues. EMBO J. 1993; 12(8): 3111-3121.
[342] Fisher RP, Morgan DO. A novel cyclin associates with MO15/CDK7 to form the CDK-activating kinase. Cell. 1994; 78(4): 713-724.
[343] Watanabe N, Arai H, Nishihara Y, Taniguchi M, Hunter T, Osada H. M-phase kinases induce phospho-dependent ubiquitination of somatic Wee1 by SCFbeta-TrCP. Proc Natl Acad Sci USA 2004; 101: 4419-4424
[344] Hoffman I, Clarke PR, Marcote MJ, Karsenti E, Draetta G. Phosphorylation and activation of human cdc25-C by cdc2--cyclin B and its involvement in the self-amplification of MPF at mitosis. EMBO J 1993; 12: 53-63
[345] Li J, Meyer AN, Donoghue DJ. Nuclear localization of cyclin B1 mediates its biological activity and is regulated by phosphorylation. Proc Natl Acad Sci USA 1997; 94: 502-507

[346] Heald R, McLoughlin M, McKeon F. Human wee1 maintains mitotic timing by protecting the nucleus from cytoplasmically activated Cdc2 kinase. Cell 1993; 74: 463-474
[347] Bassermann F, Frescas D, Guardavaccaro D, Busino L, Peschiaroli A, Pagano M. The Cdc14B-Cdh1-Plk1 axis controls the G2 DNA-damage-response checkpoint. Cell. 2008; 134(2): 256-267
[348] Elledge SJ. Cell cycle checkpoints: preventing an identity crisis. Science 1996; 274: 1664-1672
[349] Smits VA et al. Polo-like kinase-1 is a target of the DNA damage checkpoint. Nat Cell Biol 2000; 672-676
[350] Van Vugt MATM et al. Polo-like kinase-1 controls recovery from G2 DNA damage-induced arrest in mammalian cells. Mol Cell 2004; 15: 799-811
[351] Ciccia A, Elledge SJ. The DNA damage response: making it safe to play with knives. Mol Cell 2010; 40: 179-204
[352] Kumagai A, Dunphy WG. Claspin, a novel protein required for the activation of Chk1 during a DNA replication checkpoint response in Xenopus egg extracts. Mol Cell 2000; 6: 839-849
[353] Smits VA, Klompmaker R, Arnaud L, Rijksen G, Nigg EA, Medema RH. Polo-like kinase-1 is a target of the DNA damage checkpoint. Nat Cell Biol 2000; 2:672-676
[354] Mamely I, van Vugt MA, Smits VA, Semple JI, Lemmens B, Perrakis A, Medema RH, Freire R. Polo-like kinase-1 controls proteasome-dependent degradation of Claspin during checkpoint recovery. Curr Biol 2006; 16: 1950-1955
[355] Van Vugt MATM , Gardino AK, Linding R, Ostheimer GJ, Reinhardt HC, Ong SE, Tan CS, Miao H, Keezer SM, Li J, Pawson T, Lewis TA, Carr SA, Smerdon SJ, Brummelkamp TR, Yaffe MB. A mitotic phosphorylation feedback network connects Cdk1, Plk1, 53BP1 and Chk2 to inactivate the G(2)/M DNA damage checkpoint. PLoS Biol 2010; 8: e1000287
[356] Yata K, Lloyd J, Maslen S, Bleuyard JY, Skehel M, Smerdon SJ, Esashi F. Plk1 and CK2 act in concert to regulate Rad51 during DNA double strand break repair. Mol Cell 2012; 45: 371-383
[357] Esashi F, Yanagida M. Cdc2 phosphorylation of Crb2 is required for reestablishing cell cycle progression after the damage checkpoint. Mol Cell 1999; 4: 167-174
[358] Lane HA, Nigg EA. Antibody microinjection reveals an essential role for human polo-like kinase 1 (Plk1) in the functional maturation of centrosomes. J Cell Biol 1996; 135(6): 1701-1713
[359] Sankaran S, Parvin JD. Centrosome function in normal and tumor cells. J Cell Biochem. 2006; 99(5): 1240-1250
[360] Lee K, Rhee K, PLK1 phosphorylation of pericentrin initiates centrosome maturation at the onset of mitosis. J Cell Biol 2011; 195: 1093-1101
[361] Bahe S, Stierhof YD, Wilkinson CJ, Leis F, Nigg EA. Rootletin forms centriole-associated filaments and functions in centrosome cohesion. J Cell Biol 2005; 171: 27-33
[362] Mardin BR, Lange C, Baxter JE, Hardy T, Scholz SR, Fry AM, Schiebel E. Components of the Hippo pathway cooperate with Nek2 kinase to regulate centrosome disjunction. Nat Cell Biol 2010; 12: 1166-1176
[363] Mardin BR, Agircan FG, Lange C, Schiebel E. Plk1 controls the NEK2A-PP1γ antagonism in centrosome disjunction. Curr Biol 2011; 21: 1145-1151
[364] Bertran MT, Sdelci S, Regué L, Avruch J, Caelles C, Roig J. Nek9 is a Plk1-acivated kinase that controls early centrosome separation through Nek6/7 and Eg5. EMBO J 2011; 30: 2634-2647
[365] Smith E, Hégarat N, Vesely C, Roseboom I, Larch C, Streicher H, Straatman K, Flynn H, Skehel M, Hirota T, Kuriyama R, Hochegger H. Differential control of Eg5-dependent centrosome separation by Plk1 and Cdk1. EMBO J 2011; 30: 2233-2245
[366] Whitehead CM, Rattner JB. Expanding the role of HsEg5 within the mitotic anc post-mitotic phases of the cell cycle. J Cell Sci 1998; 111: 2551-2561
[367] Abe S, Nagasaka K, Hirayama Y, Kozuka-Hata H, Oyama M, Aoyagi Y, Obuse C, Hirota T. The initial phase of chromosome condensation requires CDK1-mediated phosphorylation of the CAP-D3 subunit of condensing II. Genes Dev 2011; 25: 863-874
[368] Zhang N, Panigrahi AK, Mao Q, Pati D. Interaction of soronin protein with polo-like kinase 1 mediates resolution of chromosomal arm cohesion. J Biol Chem 2011; 286: 41826-41837
[369] Archambault V, Glover DM. Polo-like kinases: conservation and divergence in their functions and regulation. Nat Rev Mol Cell Biol 2009; 10: 265-275
[370] Waizenegger IC, Hauf S, Meinke A, Peters JM. Two distinct pathways remove mammalian cohesin from chromosome arms in prophase and from centromeres in anaphase. Cell 2000; 103(3): 399-410
[371] Dai W, Wang X. The yin and yang of centromeric cohesion of sister chromatids: mitotic kinases meet protein phosphatase 2A. Cell Div 2006; 1: 9

[372] Kang YH et al. Self regulated Plk1 recruitment to kinetochores by the Plk1-PBIP1 interaction is critical for proper chromosome segregation. Mol Cell 2006; 24: 409-422
[373] Kang YH, Park JE, Yu LR, Soung NK, Yun SM, Bang JK, Seong YS, Yu H, Garfield S, Veenstra TD, Lee KS. Mammalian polo-like kinase 1-dependent regulation of the PBIP1-CENP-Q complex at kinetochores. J Biol Chem 2011; 286: 19744-19757
[374] Hauf S, Roitinger E, Koch B, Dittrich CM, Mechtler K, Peters JM. Dissociation of cohesin from chromosome arms and loss of arm cohesion during early mitosis depends on phosphorylation of SA2. PLoS Biol. 2005 Mar;3(3):e69. Epub 2005 Mar 1
[375] Beck J et al. Ubiquitation-dependent localization of PLK1 in mitosis. Nat Cell Biol 2013; 15: 430-439
[376] Hansen DV et al. Plk1 regulates activation of the anaphase promoting complex by phosphorylating and triggering SCFbetaTrCP-dependent destruction of the APC inhibitor Emi1. Mol Biol Cell 2004; 15: 5623-5634
[377] Di Fiore B, Pines J. Emil1 is needed to couple DNA replication with mitosis but does not regulate activation of the mitotic APC/C. J Cell Biol 2007; 177: 425-437
[378] Lenart P, Petronczki M, Steegmaier M, Di Fiore B, Lipp JJ, Hoffmann M, Rettig WJ, Kraut N, Peters JM. The small molecule inhibitor BI 2536 reveals novel insights into mitotic roles of polo-like kinase 1. Curr Biol 2007; 17: 304-315
[379] Goto H, Kiyono T, Tomono Y, Kawajiri A, Urano T, Furukawa K, Nigg EA, Inagaki M. Complex formation of Plk1 and INCENP required for metaphase-anaphase transition. Nat Cell Biol 2005; 8: 180-187
[380] Qi W. Phosphorylation and polo-box-dependent binding of Plk1 to Bub1 is required ffor the kinetochore localisation of Plk1. Mol Biol Cell 2006; 17: 3705-3716
[381] Elowe S et al Tension-sensitive Plk1 phosphorylation on BubR1 regulates the stability of kinetochore microtubule interactions. Genes Dev 2007; 21: 2205-2219
[382] Maia AR et al. CDK1 and Plk1 mediate a CLASP2 phospho-switch that stabilises kinetochore-microtubule attachments. J Cell Biol 2012; 199: 285-301
[383] Zhou L, Tian X, Zhu C, Wang F, Higgins JM. Polo-like kinase-1 triggers histone phosphorylation by Haspin in mitosis. EMBO Rep 2014; 15: 273-281
[384] Li H, Liu XS, Yang X, Wang Y, Wang Y, Turner JR, Liu X. Phosphorylation of CLIP-170 by Plk1 and CK2 promotes timely formation of kinetochore-microtubule attachments. EMBO J 2010; 29: 2953-2965
[385] Liu D, Davydenko O, Lampson MA. Polo-like kinase-1 regulates kinetochore-microtubule dynamics and spindle checkpoint silencing. J Cell Biol 2012; 198: 491-499
[386] Archambault V, Carmena M. Polo-like kinase-activating kinases: Aurora A, Aurora B and what else? Cell Cycle 2012; 11: 1490-1495
[387] Foley EA, Maldonado M, Kapoor TM. Formation of stable attachments between kinetochores and microtubules depends on the B56-PP2A phosphatase. Nat Cell Biol 2011; 13: 1265-1271
[388] Kruse et al Direct binding between BubR1 and B56-PP2A phosphatase complexes regulate mitotic progression. J Cell Sci 2013; 126: 1086-1092
[389] Golsteyn RM, Mundt KE, Fry AM, Nigg EA. J Cell Biol 1995; 129: 1617-1628
[390] Neef R, Gruneberg U, Kopajtich R, Li X, Nigg EA, Sillje H, Barr FA. Choice of Plk1 docking partners during mitosis and cytokinesis is controlled by the activation state of Cdk1. Nat Cell Biol 2007; 9: 436-444
[391] Hu CK, Ozlu N, Coughlin M, Steen JJ, Mitchson TJ. Plk1 negatively regulates PRC1 to prevent premature midzone formation before cytokinesis. Mol Biol Cell 2012; 23: 2702-2711
[392] Vasquez-Martin A, Oliveras-Ferraros C, Mendez JA. The active form of the metabolic sensor: AMP=activated protein kinase (AMPK) directly binds to the mitotic apparatus and travels from centrosomes to the spindle midzone during mitosis and cytokinesis. Cell Cycle 2009; 8: 2385-2398
[393] Vasquez-Martin A, Oliveras-Ferraros C, Cufi S, Menendez JA. Polo-like kinase 1 regulates activation of AMP-activated protein kinase (AMPK) at the mitotic apparatus. Cell Cycle 2011; 10(8): 1295-1302
[394] Banko MR, Allen JJ, Schaffer BE, Wilker EW, Tsou P, White JL, Villén J, Wang B, Kim SR, Sakamoto K, Gygi SP, Cantley LC, Yaffe MB, Shokat KM, Brunet A. Chemical genetic screen for AMPKα2 substrates uncovers a network of proteins involved in mitosis. Mol Cell 2011; 44(6): 878-892
[395] Scaglia N, Tyekucheva S, Zadra G, Photopoulos C, Loda M. De novo fatty acid synthesis at the mitotic exit is required to complete cellular division. Cell Cycle 2014; 13(5): 859-868
[396] Bates S, Vousden KH. Mechanisms of p53-mediated apoptosis. Cell Mol Life Sci 1999; 55: 28-37
[397] Levine AJ. The evolution of the p53 family of genes. Cell Cycle 2012; 11: 214-215
[398] Ando K, Ozaki T, Yamamoto H, Furuya K, Hosoda M, Hayashi S, Fukuzawa, Nakagawara A. Polo-like kinase 1 (Plk1) inhibits p53 function by physical interaction and phosphorylation. J Biol Chem 2004; 279: 25549-25561

[399] Liu X, Erikson RL. Polo-like kinase (Plk) 1 depletion induces apoptosis in cancer cells. Proc Natl Acad Sci USA 2003; 100: 5789-5794
[400] McKenzie L, King S, Marcar L, Nicol S, Dias SS, Schumm K, Robertson P, Bourdon JC, Perkins N, Fuller-Pace F, Meek DW. p53-dependent repression of polo-like kinase-1 (PLK1). Cell Cycle. 2010; 9(20): 4200-4212
[401] Chen J, Dai G, Wang YQ, Wang S, Pan FY, Xue B, Zhao DH, Li CJ. Polo-like kinase 1 regulates mitosic arrest after UV irradiation through dephosphorylation of p53 and inducing p53 degradation. FEBS Lett 2006; 580: 3624-3630
[402] Yang X, Li H, Zhou Z, Wang WH, Deng A, Andrisani O, Liu X. Plk1-mediated phosphorylation of Topors regulates p53 stability. J Biol Chem. 2009 ; 284(28): 18588-18592
[403] Liu XS, Li H, Song B, Liu X. Polo-like kinase 1 phosphorylation of G2 and S-phase-expressed 1 protein is essential for p53 inactivation during G2 checkpoint recovery. EMBO Rep 2010; 11(8): 626-632.
[404] Sanhaji M, Kreis NN, Zimmer B, Berg T, Louwen F, Yuan J. p53 is not directly relevant to the response of polo-like kinase1 inhibitors. Cell Cycle 2012; 11(3): 543-553
[405] Reindl W, Yuan J, Kramer A, Strebhardt K, Berg T. Inhibition of polo-like kinase 1 by blocking polo-box domain-dependent protein-protein interactions. Chem Biol 2008; 15: 459-4566
[406] Yuan J, Sanhaji M, Kramer A, Reindl W, Hofmann M, Kreis NN, Zimmer B, Berg T, Strebhardt K. Polo-box domain inhibitor poloxin activates the spindle assembly checkpoint and inhibits tumour growth in vivo. Am J Pathol 2011; 179: 2091-2099
[407] Liu X, Lei M, Erikson RL. Normal cells, but not cancer cells, survive severe Plk1 depletion. Mol Cell Biol 2006; 26: 2093-2108
[408] Guan R, Tapang P, Leverson JD, Albert D, Giranda VL, Luo Y. Small interfering RNA-mediatedd Polo-like kinase 1 depletion preferentially reduces the survival of p53-defective, oncogenic transformed cells and inhibits tumour growth in animals. Cancer Res 2005; 65: 2698-2704
[409] Degenhardt Y, Greshock J, Laquerre S, Gilmartin AG, Jing J, Richter M, Zhang X, Bleam M, Halsey W, Hughes A, Moy C, Liu-Sullivan N, Powers S, Bachman K, Jackson J, Weber B, Wooster R. Sensitivity of cancer cells to Plk1 inhibitor GSK461364A is associated with loss of p53 function and chromosome instability. Mol Cancer Ther 2010; 9: 2079-2089
[410] Sanhaji M, Louwen F, Zimmer B, Kreis NN, Roth S, Yuan J. Polo-like kinase 1 inhibitors, mitotic stress and the tumour suppressor p53. Cell Cycle 2013; 12(9): 1340-1351
[411] Lu B, Mahmud H, Maass AH, Yu B, van Gilst WH, de Boer RA, Sillje HH. The Plk1 inhibitor BI 2536 temporarily arrests primary cardiac fibroblasts in mitosis and generates aneuploidy in vitro. PLoS One 2010; 5: e12963
[412] King SI, Purdie CA, Bray SE, Quinlan PR, Jordan LB, Thompson AM, Meek DW. Immunohistochemical detection of Polo-like kinase-1 in primary breast cancer is associated with TP53 mutation and poor clinical outcome. Breast Cancer Res. 2012; 8;14(2): R40
[413] Sur S, Pagliarini R, Bunz F, Rago C, Diaz LA Jr, Kinzler KW, Vogelstein B, Papadopoulos N. A panel of isogenic human cancer cells suggests a therapeutic approach for cancers with inactivated p53. Proc Natl Acad Sci USA. 2009; 106(10): 3964-3969
[414] Collins MA et al. Oncogenic Kras is required for both the initiation and maintenance of pancreatic cancer in mice. J Clini Invest 2012; 122: 639-653
[415] Porzner M, Seufferlein T. Novel approaches to target pancreatic cancer. Curr Cancer Drug Targets 2011; 11: 698-713
[416] Costello E, Greenhalf W, Neoptolemos JP. New biomarkers and targets in pancreatic cancer and their application to treatment. Nat Rev Gastro Hepatol 2012; 9: 435-444
[417] Luo A genome-wide RNAi screen identifies multiple synthetic lethal interactions with the Ras oncogene. Cell 2009; 137: 835-848
[418] Yim. H. Current clinical trials with polo-like kinase 1 inhibitors in solid tumours. Anticanc Drug 2013; 24(10): 999-1006
[419] Eckerdt F, Yuan J, Stebhardt K. Polo-like kinases and oncogenesis. Oncogene 2005; 24: 267-276
[420] Takai N, Hamanaka R, Yoshimatsu J, Miyakawa I. Polo-like kinases (Plks) and cancer. Oncogene 2005; 24: 287-291
[421] Yamamoto Y, Matsuyama H, Kawauchi S et al. Overexpression of polo-like kinase 1 and chromosomal instability in bladder cancer. Oncology 2006; 70: 231-237
[422] Cogswell JP, Brown CE, Bisi JE, Neil SD. Dominant-negative polo-like kinase 1 induces mitotic catastrophe independent of cdc25C finction. Cell Growth Differ 2000; 11: 615-623

[423] Gray PJ, Bearss DJ, Han H, Nagle R, Tsao MS, Dean N, Von Hoff DD. Identification of human polo-like kinase 1 as a potential therapeutic target in pancreatic cancer. Mol Cancer Ther 2004; 3(5): 641-646
[424] He ZL, Zheng H, Lin H, Miao XY, Zhong DW. Overexpression of polo-like kinase 1 predicts a poor prognosis in heparocellular carcinoma patients. World J Gastroenterol 2009; 15: 4177-4182
[425] Yamada S, Ohira M, Horie H, Ando K, Takayasu H, Suzuki Y, Sugano S, Hirata T, Goto T, Matsunaga T, Hiyama E, Hayashi Y, Ando H, Suita S, Kaneko M, Sasaki F, Hashizume K, Ohnuma N, Nakagawara. Expression profiling and differential screening between hepatoblastomas and the corresponding normal livers: identification of high expression of the PLK1 oncogene as a poor prognostic indicator of hepatoblastomas. Oncogene 2004; 23: 5901-5911
[426] Tokumitsu Y, Mori M, Tanaka S, Akazawa K, Nakano S, Niho Y. Prognostic significance of polo-like kinase expression in esophageal carcinoma. Int J Oncol. 1999; 15(4): 687-692.
[427] Jang YJ, Kim YS, Kim WH. Oncogenic effect of polo-like kinase 1 expression in human gastric carcinomas. Int J Oncol 2006; 29: 589-594
[428] Kanaji S, Saito H, Tsujitani S, Matsumoto S, Tatebe S, Kondo A, Ozaki M, Ito H, Ikeguchi M. Expression of polo-like kinase 1 (PLK1) protein predicts the survival of patients with gastric carcinoma. Oncology 2006; 70: 126-133
[429] Weichert W, Ulrich A, Schmidt M, Gekeler V, Noske A, Niesporek S, Buckendahl AC, Dietel M, Denkert. Expression patterns of polo-like kinase 1 in human gastric cancer. Canceer Sci 2006; 97: 271-276
[430] Takahashi T, Sano B, Nagata T, Kato H, Sugiyama Y, Kunieda K, Kimura M, Okano Y, Saji S. Polo-like kinase 1 (PLK1) is overexpressed in primary colorectal cancers. Cancer Sci 2003; 94: 148-152
[431] Rodel F, Keppner S, Capalbo G, Bashary R, Kaufmann M, Rodel C, Strebhardt K, Spankuch B. Polo-like kinase 1 as a predictive marker and therapeutic target for radiotherapy in rectal cancer. Am J Pathol 2010; 177: 918-929
[432] Han DP, Zhu QL, Cui JT, Wang PX, Qu S, Cao QF, Zong YP, Feng B, Zheng MH, Lu AG, Polo-like kinase 1 is overexpressed in colorectal cancer and participates in the migration and invasion of colorectal cancer cells. Med Sci Monit 2012; 18: BR237-BR246
[433] Weichert W, Kristiansen G, Winzer KJ, Schmidt M, Gekeler V, Noske A, Muller BM, Niesporek S, Dietel M, Denkert C. Polo-like kinase isoforms in breast cancer: expression patterns and prognostic implications. Virchows Arch 2005; 446: 442-450
[434] Wolf G, Hildenbrand R, Schwar C, Grobholz R, Kaufmann M, Stutte HJ, Strebhardt K, Bleyl U. Polo-like kinase: a novel marker of proliferation: correlation with estrogen-receptor expression in human breast cancer. Pathol Res Pract 2000; 196: 753-759
[435] Weichert W, Schmidt M, Gekeler V, Denkert C, Stephan C, Jung K, Loening S, Dietel M, Kristiansen G. Polo-like kinase 1 is overexpressed in prostate cancer and linked to higher tumour grades. Prostate 2004; 60(3): 240-245
[436] Knecht R, Elez R, Oechler M, Solbach C, von Ilberg C, Strebhardt K. Prognostic significance of polo-like kinase (PLK) expression in squamous cell carcinomas of the head and neck. Cancer Res 1999; 59(12): 2794-2797
[437] Salvatore G, Nappi TC, Salerno P, Jiang Y, Garbi C, Ugolini C, Miccoli P, Basolo F, Castellone MD, Cirafici AM, Melillo RM, Fusco A, Bittner ML, Santoro M. A cell proliferation and chromosomal instability signature in anaplastic thyroid carcinoma. Cancer Res. 2007; 67(21): 10148-58.
[438] Dietzmann K, Kirches E, von Bossanyi P, Jachau K, Mawrin C. Increased human polo-like kinase-1 expression in gliomas. J Neurooncol 2001; 53: 1-11
[439] Wang ZX, Xue D, Lui ZL, Lu BB, Bian HB, Pan X, Yin YM. Overexpression of polo-like kinase 1 and its clinical significance in human non-small cell lung cancer. Int J Biochem Cell Biol 2012; 44: 200-210
[440] Strebhardt K, Kneisel L, Linart C, Bernd A, Kaufmann R. Prognostic value of polo-like kinase expression in melanomas. JAMA 2000; 283: 479-480
[441] Stutz N, Nihal M, Wood GS. Polo-like kinase 1 (Plk1) in cutaneous T-cell lymphoma. Br J Dermatol 2011; 164: 814-812
[442] Yamamoto Y, Matsuyama H, Kawauchi S, Matsumoto H, Nagao K, Ohmi C, Sakano S, Furuya T, Oga A, Naito K, Sasaki K. Overexpression of polo-like kinase 1 (PLK1) and chromosomal instability in bladder cancer. Oncology. 2006; 70(3): 231-237
[443] Wolf G, Elez R, Doermer A, Holtrich U, Ackermann H, Stutte HJ, Altmannsberger HM, Rubsamen-Waigmann H, Strebhardt K. Prognostic significance of polo-like kinase (PLK) expression in non-small cell lung cancer. Oncogene 1997; 14: 543-549

[444] Imai H, Sugimoto K, Isobe Y, Sasaki M, Yasuda H, Takeuchi K, Nakamura S, Kojima Y, Tomomatsu J, Oshimi K. Absence of tumour-specific over-expression of Polo-like kinase 1 (Plk1) in major non-Hodgkin lymphoma and relatively low expression of Plk1 in nasal NK/T cell lymphoma. Int J Hematol 2009; 89: 673-678
[445] Mito K, Kashima K, Kikuchi H, Daa T, Nakayama I, Yokoyama S. Expression of Polo-Like Kinase (PLK1) in non-Hodgkin's lymphomas. Leuk Lymphoma 2005; 46(2): 225-231
[446] Evans RP, Dueck G, Sidhu R, Ghosh S, Toman I, Loree J, Bahlis N, Klimowicz AC, Fung J, Jung M, Lai R, Pilarski LM, Belch AR, Reiman T. Expression, adverse prognostic significance and therapeutic small molecule inhibition of Polo-like kinase 1 in multiple myeloma. Leuk Res 2011; 35: 1637-1643
[447] Kneisel L, Strebhardt K, Bernd A, Wolter M, Binder A, Kaufmann R. Expression of polo=like kinase
[448] Takai N, Miyazaki T, Fujisawa K, Nasu K, Hamanaka R, Miyakawa I. Expression of polo-like kinase in ovarian cancer is associated with histological grade and clinical stage. Cancer Lett 2001; 164: 41-49
[449] Weichert W, Denkert C, Schmidt M, Gekeler V, Wolf G, Kobel M, Dietel M, Hauptmann S. Polo-like kinase isoform expression is a prognostic factor in ovarian carcinoma. Br J Cancer 2004; 90: 815-821
[450] Takai N, Miyazaki T, Fujisawa K, Nasu K, Hamanaka R, Miyakawa I. Polo-like kinase (PLK) expression in endometrial carcinoma. Cancer Lett 2001; 169: 1-49
[451] Zhang Y, Liu Y, Yang YX, Xia JH, Zhang HX, Li HB, Yu CZ. The expression of PLK-1 in cervical carcinoma: a possible target for enhancing chemosensitivity. J Expert Clin Cancer Res 2009; 28: 130
[452] Degenhardt Y, Lampkin T. Targeting polo-like kinase in cancer therapy. Clin Cancer Res 2010; 16(2): 384-389
[453] Smith MR, Wilson ML, Hamanaka R, Chase D, Kung H, Longo DL, Ferris DK. Malignant transformation of mammalian cells initiated by constitutive expression of the polo-like kinase. Biochem Biophys Res Commun 1997; 234: 397-405
[454] Rodel F, Keppner S, Capalbo G, Bashary R, Kaufmann M, Rödel C, Strebhardt K, Spänkuch B. Polo-like kinase 1 as a predictive marker and therapeutic target for radiotherapy in rectal cancer. Am J Pathol 2010; 177: 918-929
[455] Steegmaier M, Hoffman M, Baum A, Lenart P, Petronczki M, Krssak M, Gyrtler U, Garin-Chesa P, Lieb S, Quant J, Grauert M, Adolf GR, Kraut N, Peters JM, Rettig W. BI 2536, a potent and selective inhibitor of polo-like kinase 1, inhibits tumor growth in vivo. Curr Biol 2007; 17: 316-322
[456] Ju LY, Wood JL, Minter-Dykhouse K, Ye L, Saunders TL, Yu X, Chen J. Polo-like kinase 1 is essential for early embryonic development and tumour suppression. Mol Cell Biol 2008; 28: 6870-6876
[457] Guan R, Tapang P, Leverson JD, Albert, D, Giranda VL, Luo Y. Small interfering RNA-mediated polo-like kinase 1 depletion preferentially reduces the survival of p53-defective, oncogenic transformed cells and inhibits tumor growth in animals. Cancer Res 2005; 65(7): 2698–2704.
[458] Elez R, Piiper A, Kronenberger B, Kock M, Brendel M, Hermann E, Pliquett U, Neumann E, Zeuzem S. Tumor regression by combination antisense therapy against Plk1 and Bcl-2. Oncogene. 2003; 22(1): 69-80.
[459] Strebhardt K. Multifaceted polo-like kinases: drug targets and antitargets for cancer therapy. Nat Rev Drug Discovery 2010; 9: 643-660
[460] Matsumoto K, Nakamra T. NK4 gene therapy targeting HGF-Met and angiogenesis. Front Biosci 2008; 13: 1943-1951
[461] Johnson EF, Stewart KD, Woods KW, Granda VL, Luo Y. Pharmacological and functional comparison of the polo-like kinase family: insight into inhibitor and substrate specificity. Biochem 2007; 46: 9551-9563
[462] Kothe M, Kohls D, Low S, Coli R, Rennie GR, Feru F, Kuhn C, Ding YH. Selectivity-determining residues in PLK1. Chem Biol Drug Des 2007; 70: 540-546
[463] Hanks SK, Hunter T. Protein Kinases 6. The eukaryotic protein kinase superfamily: kinase (catalytic) domain structure and classification. FASEB J 1995; 9: 576-596
[464] Yuan J, Sanhaji M, Kramer A, Reindl W, Hofmann M, Kreis NN, Zimmer B, Berg T, Strebhardt K. Polo-box domain inhibitor poloxin activates the spindle assembly checkpoint and inhibits tumour growth in vivo. Am J Pathol 2011; 179: 2091-2099
[465] McInnes C, Estes K, Baxter M, Yang Z, Farag DB, Johnston P, Lazo JS, Wang J, Wyatt MD. Targetting subcellular localisation through the polo-box domain: non-ATP competitive inhibitors recapitulate a PLK1 phenotype. Mol Cancer Ther 2012; 11: 1683-1692
[466] Gumireddy K, Reddy MVR, Cosenza SC, Boominathan R, Baker SJ, Papathi N, Jiang J, Holland J, Reddy EP. ON01910, a non-ATP-competitive small molecule inhibitor of Plk1, is a potent anticancer agent. Cancer Cell. 2005; 7(3): 275-286.
[467] Jimeno A, Li J, Messersmith WA, Laheru D, Rudek MA, Maniar M, Hidalgo M, Baker SD, Donehower RC. Phase I study of ON 01910.Na, a novel modulator of the polo-like kinase 1 pathway, in adult patients with solid tumours. J Clin Oncol 2008; 26: 5504-5510

[468] Ohnuma T, Lehrer D, Ren C, Cho SY, Maniar M, Silverman L, Sung M, Gretz III FG, Benisovich V, Navada S, Akahoho E, Wilck E, Taft DR, Roboz J, Wilhelm F, Holland JF. Phase I study of intravenous rigosertib (ON 01910.Na), a novel benzyl styryl sulfone structure producing G2/M arrest and apoptosis, in adult patients with advanced cancer. Am J Res 2013; 3(3): 323-338

[469] Gilmartin AG, Bleam MR, Richter MC, Erskine SG, Kruger RG, Madden L, Hassler DF, Smith GK, Gontarek RR, Courtney MP, Sutton D, Diamond MA, Jackson JR, Laquerre SG. Distinct concentration-dependent effects of the polo-like kinase 1-specific inhibitor GSK461364A, including differential effect on apoptosis. Cancer Res 2009; 69: 6969-6977

[470] Laquerre S, Sung CM, Gilmartin A. A potent and selective Polo-like kinase 1 (Plk1) inhibitor (GSK461364) induces cell cycle arrest and growth inhibition of cancer cells. Presented at the 98th American Association for Cancer Research Annual Meeting, Los Angeles, CA, April 14-18 2007

[471] Emmitte KA et al Discovery of thiophene inhibitors of polo-like kinase. Bioorg. MedChem Lett 2009; 19: 1018-1021

[472] Degenhardt Y, Greshock J, Laquerre S, Gilmartin AG, Jing J, Richter M et al. Sensitivity of cancer cells to Plk1 inhibitor GSK461364A is associated with poss of p53 function and chromosome instability. Mol Cancer Ther 2010; 9: 2079-2089

[473] Erskine S, Madden L, Hassler D et al. Biochemical characterization of GSK461364: A novel, potent, adnd selective inhibitor of polo-like kinase-1 (Plk1). Presented at the 98th American Association for Cancer Research Annual Meeting, Los Angeles, CA, April 14-18 2007

[474] Sutton D, Diamond M, Faucette L. Efficacy of GSK461364, a selective Plk1 inhibitor, in human tumour xenograft models. Presented at the 98th American Association for Cancer Research Annual Meeting, Los Angeles, CA, April 14-18 2007

[475] Olmos D, Allred A, Sharma R, Brunetto AT, Yap TA, Taegtmeyer AB, Barriuso J, Medani H, Degenhardt YY, Allred AJ, Smith DA, Murray SC, Lampkin TA, Dar MM, Wilson R, de Bono JS, Blagden SP. Phase 1 study of the polo-like kinase 1 selective inhibitor GSK461364, a specific and competitive Polo-like kinase 1 inhibitor, in patients with advanced solid malignancies. Clin Cancer Res 2011; 17: 3420-3430

[476] Olmos D, Baker D, Sharma R, Brunetto AT, Yap TA, Taegtmeyer AB. Phase I study of GSK461364, in patients with advanced solid tumours. J Clin Oncol 2009; 27: abstract 3536

[477] Palmieri D, Hua E, Qian Y. Preclinical studies investigating the efficacy of GSK461364A, an inhibitor of Polo-like kinase-1, for the prevention of breast cancer brain metastases. Presented at the American Association for Cancer Research 2009 Annual Meeting, Denver, CO, April 18-22

[478] Garland LL, Taylor C, Pilkington DL, Cohen JL, Von Hoff DD. A phase I pharmacokinetic study of HMN-214, a novel oral stilbene derivative with polo-like kinase-1-interacting properties, in patients with advanced solid tumours. Clin Cancer Res 2006; 12: 5182-5189

[479] Takagi M, Honmura T, Wantanabe S, Yamaguchi R, Nogawa M, Nishimura I, Katoh F, Matsuda M, Hidaka H. In vivo antitumour activity of a novel sulphonamide, HNM-214, against human tumour xenografts in mice and the spectrum of cytotoxicity of its active metabolite, HMN-176. Invest New Drugs 2003; 21: 387-399

[480] Tanaka H, Ohshima N, Ikenoya M, Komori K, Katoh F, Hidaka H. HMN-176, an active metabolite of the synthetic antitumour agent HMN-124, restores chemosensitivity to multidrug resistant cells by targeting the transcription factor NF-Y. Cancer Res 2003; 63: 6942-6947

[481] Patnaik A, Forero L, Goetz A. HMN-214, a novel oral antimicrotubular agent and inhibitor of Polo-like and cyclin-dependent kinases: Clinical, pharmacokinetic (PK) and pharmacodynamics (PD) relationships observed in a phase I trial of a daily x5 schedule every 28 days [abstract]. Proc Am Soc Clin Oncol 2003; 22: 514

[482] Yim H. Current clinical trials with polo-like kinase 1 inhibitors in solid tumors. Anti-can Drugs 2013; 24(10): 999-1006

[483] Nie Z, Feher V, Natala S, McBride C, Kiryanov A, Jones B, Lam B, Liu Y, Kaldor S, Stafford J, Hikami K, Uchiyama N, Kawamoto T, Hikichi Y, Matsumoto S, Amano N, Zhang L, Hosfield D, Skene R, Zou H, Cao X, Ichikawa T. Discovery of TAK-960: an orally available small molecule inhibitor of polo-like kinase 1 (PLK1). Bioorg Med Chem Lett 2013; 23: 3662-3666

[484] Hikichi Y, Honda K, Hikami K , Miyashita H, Kaieda I, Murai S, Uchiyama N, Hasegawa M, Kawamoto T, Sato T, Ichikawa T, Cao S, Nie Z, Zhang L, Yang J, Kuida K, Kupperman E. TAK-60, a novel, orally available, selective inhibitor of polo-like kinase 1, shows broad-spectrum preclinical antitumour activity in multiple dosing regimens. Mol Cancer Ther 2012; 11: 700-709

[485] Study of Orally Administered TAK-960 in Patients With Advanced Nonhematologic Malignancies https://clinicaltrials.gov/ct2/show/results/NCT01179399?sect=X730156&term=tak-960&rank=1#outcome1

[486] Wiilliams R. Discontinued in 2013: oncology drugs. Expert Opin Investig Drugs. 2015; 24(1): 95-110

[487] Beria I, Bossi RT, Brasca MG, Caruso M, Ceccarelli W, Fachin G et al. NMS-P937, a 4,5-dihydro-1H-pyrazolo[4,3-h] quinazoline derivative as a potent and selective Polo-like kinase 1 inhibitor. Bioorg Med Chem Lett 2011; 21: 2969-2974

[488] Valsasina B, Beria I, Alli C, Alzani R, Avanzi N, Ballinari D et al. NMS-P937, an orally available, specific small-molecule polo-like kinase 1 inhibitor with antitumor activity in solid and hematologic malignancies. Mol Cancer Ther 2012; 11: 700-709

[489] Study of NMS-1286937 in Adult Patients With Advanced/Metastatic Solid Tumors. https://clinicaltrials.gov/show/NCT01014429

[490] Sumara I, Gimenez-Abian JF, Gerlilch D, Hirota T, Kraft C, de la Torre C, Ellenberg J, Peters JM . Roles of polo-like kinase 1 in the assembly of mitotic spindles. Curr Biol 2004; 14(19): 1712-22

[491] Hanisch A, Wehner A, Nigg EA, Sillje HH. Different PLK1 functions show distinct dependencies on Polo-box domain-mediated targeting. Mol Biol Cell 2006; 17: 448-459

[492] Van Vugt MA, van de Weerdt BC, Vader G, Janssen H, Calafat J, Klompmaker R, Wolthuis RM, Medema RH. Polo-like kinase-1 is required for bipolar spindle formation but is dispensable for anaphase promoting complex/cdc20 activation and initiation of cytokinesis. J Biol Chem 2004; 279(35): 36841-36854

[493] Lenart P, Petronczki M, Steegmaier M, Di Fiore B, Lipp JJ, Hoffmann M, Rettig WJ, Kraut N, Peters JM. The small-molecule inhibitor BI 2536 reveals novel insights into mitotic roles of polo-like kinase 1. Curr Biol 2007; 17: 304-315

[494] Frost A, Mross K, Steinbild S, Hedbom S, Inger C, Kaiser R, Trommeshauser D, Munzert G. Phase i study of the Plk1 inhibitor BI 2536 administered intravenously on three consecutive days in advanced solid tumours. Curr Oncol. 2012; 19(1): e28-35

[495]Sebastian M, Reck M, Waller CF, Kortsik C, Frickhofen N, Schuler M, Fritsch H, Gaschler-Markefski B, Hanft G, Munzert G, von Pawel J. The efiicacy and safety of BI 2536, a novel plk-1 inhibitor, in patients with stage IIIB/IV non-small cell lung cancer who had relapsed after, or failed, chemotherapy: results from an open-label, randomised phase II clinical trial. J Thorac Oncol 2010; 5: 1060-1067

[496] Schoffski P, Blay JY, De Greve J et al. Multicentric parallel phase II trial of the polo-like kinase 1 inhibitor BI 2536 in patients with advanced nead and neck cancer, breast cancer, ovarian cancer, soft tissue sarcoma and melanoma. The first protocol of the European Organisation for Research and Treatment Centre (EORTC) Network of Core Institutes (NOCI). Eur J Cancer 2010; 46: 2206-2015

[497] Hofheinz RD, Al-Batran SE, Hochhaus A, Jäger E, Reichardt VL, Fritsch H, Trommeshauser D, Munzert G. An open-label, phase I study of the polo-like kinase-1 inhibitor, BI 253, in patients with advanced solid tumours. Clin Cancer Res 2010; 16: 4666-4674

[498] Mross K, Frost A, Steinbild S, Hedbom S, Rentschler J, Kaiser R, Rouyrre N, Trommeshauser D, Hoesl CE, Munzert G. Phase I dose-escalation and pharmacokinetic study of BI 2536, a novel Polo-like kinase 1 inhibitor, in patients with advanced solid tumours. J Clin Oncol 2008; 26: 5511-5517

[499] Mross K, Dittrich C, Aulitzky WE, Struberg D, Schutte J, Schmid RM, Hollerbach S, Merger M, Munzert G, Fleischer F, Scheulen ME. A randomised phase II trial of the polo-like kinase inhibitor BI 2536 in chemo-naiive patients with unresectable exocrine adenocarcinoma of the pancreas – a study within the Central European Society Anticancer Drug Research (CESAR) collaborative network. Br J Cancer 2012; 107: 280-286

[500] Schoffski P, Awada A, Dumez H, Gil T, Bartholomeus S, Wolter P, Taton M, Fritsch H, Glomb P, Munzert G. A phase I, dose-escalation study of the novel Polo-like kinase inhibitor volasertib (BI 6727) in patients with advanced solid tumours. Eur J Cancer 2012; 48: 179-186

[501] Hong M, Ren M, Silva J, Kennedy T, Choi J, Cowell J, Hao Z. Sepatronium is a DNA damaging agent that synergises with PLK1 inhibitor volasertib. Am J Cancer Res 2014; 4(2): 135-147

[502] Rudolph D, Steegmaier M, Hoffmann M, Grauert M, Baum A, Quant J, Haslinger C, Garin-Chesa P, Adolf GR. BI 6727, a polo-like kinase inhibitor with improved pharmacokinetic profile and broad antitumor activity. Clin Cancer Res 2009; 15(9): 3094-3102

[503] Sanhaji M, Kreis NN, Zimmer B, Berg T, Louwen F, Yuan J. p53 is not directly relevant to the response of Polo-like kinase 1 inhibitors. Cell Cycle 2012; 11(3), 543-553

[504] Wissing MD, Mendonce J, Kortenhorst SQ, Kaelber NS, Gonzalez M, Kim E, Hammers H, van Diest PJ, Carducci MA, Kachhap SK. Targeting prostate cancer cell lines with polo-like kinase 1 inhibitors as a single agent and in combination with histone deacetylase inhibitors. FASEB J 2013; 27: 4279-93

[505] Gorlick R, Kolb EA, Keir ST, Maris JM, Reynolds CP, Kang MH, Carol H, Lock R, Billups CA, Kurmasheva RT, Houghton PJ, Smith MA. Initial testing (Stage 1) of the polo-like kinase inhibitor volasertib (BI 6727), by the pediatric preclinical testing program. Pediatr Blood Cancer 2014; 61: 158-164

[506] Gil T, Schoffski P, Awada A, Dumez H, Bartholomeus S, Selleslach J, Taton M, Fritsch H, Glomb P, Munzert GM. Final analysis of a phase 1 single dose-escalation study of the novel polo-like kinase 1 inhibitor BI 6727 in patients with advanced solid tumours. J Clin Oncol 2010; 28(15): Suppl 3061
[507] Lin CC, Su WC, Yen CJ, Hsu CH, Su WP, Yeh KH, Lu YS, Cheng AL, Huang DCL, Fritsch H, Voss F, Taube T, Yang JCH. A phase I study of two dosing schedules of volasertib (BI 6727), an intravenous polo=like kinase inhibitor, in patients with advanced solid malignancies. B J Cancer 2014; 110(10): 2434-40
[508] Stadler WM, Vaughn DJ, Sonpavde G, Vogelzang NJ, Tagawa ST, Petrylak DP, Rosen P, Lin CC, Mahoney J, Modi S, Lee P, Ernstoff MS, Su WC, Spira A, Pliz K, Vinisko R, Schloss C, Fritsch H, Zhao C, Carducci. An open-label, single-arm, phase 2 trial of the polo-like kinase inhibitor Volasertib (BI 6727) in patients with locally advanced or metastatic urothelial cancer. Cancer 2014; 120(7): 976-82
[509] Pujade-Lauraine E, Weber BE, Ray-Coquard I, Vergote I, Selle F, Del Campo JM, Sufliarsky J, Tschöpe I, Chesa PG, Nazabadioko S, Pilz K, Joly F. Phase II trial of volasertib (BI 6727) versus chemotherapy (CT) in platinum-resistant/refractory ovarian cancer (OC). J Clin Oncol 2013; 31(15): 5504
[510] Ellis PM, Leighl N, Hirsh V, Reaume MN, Blais N, Wierzbicki R *et al*. A randomised, open-label phase II trial of volasertib as monotherapy and in combination with standard dose pemetrexed compared with pemetrexed monotherapy in second-line non-small cell lung cancer (NSCLC). *J Thorac Oncol* 2013; **8**: 2307.
[511] Deleporte A, Dumez H, Awada A, Costermans J, Meeus M, Berghmans T et al. Phase I trial of volasertib *BI 6727), a polo-like kinase 1 inhibitor, in combination with cisplatin or carboplatin in patients with advanced solid tumors. J Clin Oncol 2011; 29: 3031
[512] Dumez H, Gombos A, Schoffski P, Gil T, Vulsteke C, Meeus MA et al. Phase I trial of the polo-like kinase 1 inhibitor volasertib (BI 6727) combined with cisplatin or carboplatin in patients with advanced solid tumors. J Clin Oncol 2012; 30: 3018
[513] Gjertsen BT, Schoffski P. Discovery and development of the Polo-like kinase inhibitor volasertib in cancer therapy. Leukemia 2015; 29: 11-19
[514] Peeters M, Machiels JP, Pilz K, De Smet M, Strelkowa N, Liu D. Phase I study of volasertib (BI 6727) combined with afatinib (BIBW 2992) in advanced solid tumours. J Clin Oncol 2013; 31: 2521
[515] De Braud FG, Cascinu S, Spitaleri G, Pilz K, Clementi L, Liu D et al. A phase 1 dose escalation study of volasertib (BI 6727) combined with nintedanib (BIBF 1120) in advanced solid tumours. J Clin Oncol 2013; 31: 2556
[516] Dohner H, Lubbert M, Fiedler W, Fouillard L, Haaland A, Brandwein JM, Lepretre S, Reman O, Turlure P, Ottoman OG, Muller-Tidow C, Kramer A, Raffoux E, Dohner K, Schlenk RF, Voss F, Taube T, Frisch H, Maertens J. Randomized, phase 2 trial comparing low-dose cytarabine with or without volasertib in AML patients not suitable for intensive induction therapy. Blood 2014; epub
[517] www.clinicaltrials.gov Search 'BI 6727' and 'Volasertib'. Accessed May 2015.
[518] Schulklenk U, Ashcroft R. International research ethics. Bioethics 2000; 14: 158-72
[519] Takimoto CH. Anticancer drug development at the US National Cancer Institute. Cancer Chemother Pharmacol 2003; 52 Suppl 1: S29–S33
[520] DiMasi JA, Reichert JM, Feldman L, Malins A. Clinical approval success rates for investigational cancer drugs. Clinical Pharmacology & Therapeutics 2013; **94**(3): 329–335
[521] DiMasi JA, Grabowski HG, Hansen RW. The cost of drug development. N Engl J Med. 2015; 372(20): 1972
[522] Pan C, Kumar C, Bohl S, Klingmueller U, Mann M. Comparative proteomic phenotyping of cell lines and primary cells to assess preservation of cell type-specific functions. Mol Cell Proteomics 2009; 8(3): 443-450
[523] Lu Y, Mahato RI (eds.). Pharmaceutical Perspectives of Cancer Therapeutics, 2009
[524] Veltkamp SA, Beijnen JH, Schellens. Prolonged versus standard gemcitabine infusion: translation of molecular pharmacology to new treatment strategy. Oncologist 2008; 13(3): 261-276
[525] Lieber M, Mazzetta J, Nelson-Rees W, Kaplan M, Todaro G. Establishment of a continuous tumor-cell line (PANC-1) from a human carcinoma of the exocrine pancreas. Int J Cancer 1975; 15(5): 741-747
[526] Iwamura T, Katsuki T, Ide K. Establishment and characterization of a human pancreatic cancer cell line (SUIT-2) producing carcinoembryonic antigen and carbohydrate antigen 19-9. Jpn J Cancer Res 1987; 78(1): 54-62.
[527] Yunis AA, Arimura GK, Russin DJ. Human pancreatic carcinoma (MIA PaCa-2) in continuous culture: sensitivity to asparaginase. Int J Cancer 1977; 19(1): 128-135
[528] https://www.dsmz.de/catalogues/details/culture/ACC-760.html
[529] Schoffski P, Awada A, Dumez H et al. A phase I single dose escalation study of the novel polo-like kinase 1 inhibitor BI 6727 in patients with advanced solid tumours. Eur J Cancer Suppl 2008; 6: 14-15

[530] Zhang C, Sun X, Ren Y, Lou Y, Zhou J, Liu M, Li D. Validation of Polo-like kinase 1 as a therapeutic target in pancreatic cancer cells. Cancer Biol Ther 2012; 13(10): 1214-1220
[531] Li J, Wang R, Schweickert PG, Karki A, Yang Y, Kong Y, Ahmad N, Konieczny SF, Liu X. Plk1 inhibition enhances the efficacy of gemcitabine in human pancreatic cancer. Cell Cycle 2016; 15(5): 711-719
[532] Zhou N, Singh K, Mir MC, Parker Y, Lindner D, Dreicer R, Ecsedy JA, Zhang Z, The BT, Almasan A, Hansel DE. The investigational Aurora kinase A inhibitor MLN8237 induces defects in cell viability and cell cycle progression in malignant bladder cancer cells in vitro and in vivo. Clin Cancer Res 2013; 19(7): 1717-1728
[533] Tonkinson JL, Worzalla JF, Tseng CH, Mendelsohn LG. Cell cycle modulation by a multitargeted antifolate, LY231514, increases the cytotoxicity and antitumor activity of gemcitabine in HT29 colon carcinoma. Cancer Res 1999; 59: 3671–3676
[534] Neoptolemos JP, Palmer D, Ghaneh P, ESPAC-4: a multicentre, international, open-label randomized controlled phase III trial of adjuvant combination chemotherapy of gemcitabine and capecitabine versus gemcitabine in patients with resected pancreatic ductal adenocarcinoma. ASCO 2016, June 3-7, 2016. Chicago.
[535] Brady HJM (Ed). 2004. Apoptosis methods and protocols. Humana Press
[536] Fink SL, Cookson BT. Apoptosis, pyroptosis, and necrosis: mechanistic description of dead and dying eukaryotic cells. J Infect Immunol 2005; 73(4): 1907-1916